Evaluating the therapeutic efficacy of synthetic enzyme inhibitors and complementary alternative medicines in restoring redox and immune imbalance during inflammatory bowel disease

Kangzhe Xie

B. Sci. (Adv.) (Hons)

A thesis submitted to fulfill the requirements for the degree of Doctor of Philosophy (Medicine)

School of Medical Sciences

Faculty of Medicine & Health

The University of Sydney

2025

Supervisor: Professor Paul Witting

Co-supervisor: Dr. Belal Chami

Table of Contents

Acknowledgements

Every PhD is unique in its own way, and I am deeply grateful to those who have supported me along the journey.

First and foremost, I would like to express my sincere gratitude to my supervisor, **Professor Paul Witting**, for his support throughout my degree. Thank you for giving me the opportunity to be part of your team and for introducing me to the field of redox. When I felt lost and defeated, you were always there to remind me that everything would be alright and that there is always light at the end of the tunnel. Your dedication to research and teaching has inspired me to strive for excellence in my work. Your patience, enthusiasm, and timely suggestions have been instrumental in advancing my research and the development of this thesis. Moreover, your extensive knowledge, insightful guidance, and constant encouragement have refined my critical thinking, bolstered my confidence, and nurtured my journey toward becoming an independent researcher. Thank you for being a constant source of support and encouragement. I am truly honoured to have had you as my supervisor. Words cannot fully express my emotions, but I am sincerely grateful for all you have done.

I would also like to extend my heartfelt thanks to my co-supervisor, **Dr. Belal Chami**: thank you for your invaluable support, guidance, and encouragement throughout my degree. It was a great pleasure working with you, and your mentorship has been instrumental in shaping this thesis.

To former post-doctoral researcher of the Redox Biology Group, **Dr. Tamara Ortiz-Cerda**: it was my greatest pleasure to work with you as both a colleague and a friend. Your extensive knowledge in redox, IBD, and animal work was paramount to the successful completion of this thesis. I will never forget the memories we created together (the Uruguay conference, mouse culling with a broken arm, staying until midnight for mass spec, aliquoting over 400 human stool samples, and many more…). Thank you for making my PhD journey special, and I wish you all the best in your new roles in Spain!

I would also like to thank **Associate Professor Paul Austin** for his constant support and guidance throughout my degree. Thank you for all the opportunities you provided, even years after I graduated with Honours from your lab. To **Dr. Xiaosuo Wang**: thank you for your support and guidance with the mass spectrometry experiments — this thesis would not have been possible without your help. To **Professor Luke Henderson**, **Professor Victoria Cogger**, **Professor Kevin Keay**, and **Associate Professor Andrew Hoy**: thank you for your support and guidance during my PhD. Lastly, to **Associate Professor Matthew Naylor**: thank you for taking me on as a PhD student, introducing me to the world of Higher Degree by Research, and looking after me even after you had decided to leave the university.

To past and present members of the **Redox Biology Group**, as well as the **Redox Inflammation Group**: Milna, Dhilan, Sanya, Yantong, Ella, Suehad, Nicolette, Bruno, Mary, Jordan, Aaron, Hannah, Mikaela, Sia, Alice, Tom, Milissa, Taylor, and Angie. Thank you for sharing your laughter with me. Your company in the office and the lab made my long PhD journey filled with fun and support. It was my pleasure to meet and work with you all.

To my friends from **CPC 4-West**: Bri, Jayden, Geroge, Michael, Emma, Karen, Jacinda, Jess, Jerry, Kenny and Dan, and my friends since undergrad: Brendon and Simone. I am grateful for your support and encouragement.

Thank you the **University of Sydney** for financially supporting me with the University Postgraduate Award. Also thank you to those not mentioned here but contributed to this thesis either directly or indirectly to make this journey possible.

Lastly, to my parents, thank you for all your support throughout my PhD journey. Your patience and support with all your love means the world to me.

Success is a way to say thank you for people who helped you along the way. The best thing is to celebrate it with the people who really cares and are here with you. This thesis is for you all.

Publications & Presentations

Peer review publications directly arising from this thesis:

1. **Research Article:** Xie, K., Hunter, J., Lee, A., Ahmad, G., Witting, P.K. & Ortiz-Cerda, T. (2024). The PAD4 inhibitor GSK484 diminishes neutrophil extracellular trap in the colon mucosa but fails to improve inflammatory biomarkers in experimental colitis *Biosci. Rep.* 45(6), 375-397. *(Chapter 3 of this thesis)*

2. **Research Article:** Xie, K., Abou Duhun, S., Ortiz-Cerda, T., Choi, H., Wang, X.S., O'Sullivan, J., Verley, E., Ghali, M., Kariyawasam, V., Mitrev, N., Chami, B. & Witting, P.K. (2025). Characterising short chain fatty acids profiles in stool specimens from patients diagnosed with inflammatory bowel disease. Joint first authorship with Abou Duhun, S. *Submitted for peer review at Redox Rep. (Chapter 4 of this thesis)*

3. **Research Article:** Xie, K., Ortiz-Cerda, T., Hoosen, L., Shiung, N., Chen, S., Ahmad, G., Lemos Wimmer, B., David, A., Wang, X.S., Tran, C., O'Sullivan, J., Don, A. & Witting, P.K. (2025). Herbal remedies curcumin, Hedyotis Diffusa and Amomum Villosum reduced colon inflammation by up-regulating the Nrf-2/HO-1 antioxidant signalling pathways in an animal model of ulcerative colitis. *Preparing for manuscript submission. (Joint first authorship with Ortiz-Cerda, T.; Chapter 5 of this thesis)*

Peer review publications where the candidate contributed as co-author during the candidacy but not directly arising from the current thesis:

4. **Research Article:** Baker, A.T., Ortiz-Cerda, T., Xie, K., Hunter, J., Dragutinovic, I., Morris, J.C., Vogt, L.I., George, G.N., Sokaras, D., Howard, D.L., Witting, P.K. & Harris, H.H. (2025). XFM and HERFD-XAS Studies of Selenium in Tissues and Whole Blood from Mice Supplemented with Potentially Therapeutic Selenocompounds. *Submitted for peer review at Chem. Sci.*

5. **Literature Review:** Shin, S., Chen, S., Xie, K., Abou Duhun, S. & Ortiz-Cerda, T. (2024). Evaluating the anti-inflammatory and antioxidant efficacy of complementary and alternative medicines (CAM) used for management of inflammatory bowel disease: a comprehensive review *Redox Rep.* 30(1), 2471737.

6. **Research Article:** Gao, A., Xie, K., Gupta, S., Ahmad, G., & Witting, P. K. (2024). Cyclic Nitroxide 4-Methoxy-Tempo May Decrease Serum Amyloid A-Mediated Renal Fibrosis and Reorganise Collagen Networks in Aortic Plaque. *Int. J. Mol. Sci.*, 25(14), 7863.

7. **Research Article:** Lau, A. A., Jin, K., Beard, H., Windram, T., Xie, K., O'Brien, J. A., Neumann, D., King, B. M., Snel, M. F., Trim, P. J., Mitrofanis, J., Hemsley, K.M., & Austin, P. J. (2024). Photobiomodulation in the infrared spectrum reverses the expansion of circulating natural killer cells and brain microglial activation in Sanfilippo mice. *J. Neurochem.*, 168(9), 2791-2813.

8. **Research Article:** Ortiz-Cerda, T., Argüelles-Arias, F., Macías-García, L., Vazquez-Roman, V., Tapia, G., Xie, K., García-García, M. D., Merinero, M., García-Montes, J. M., Alcudia, A., Witting, P. K., & De-Miguel, M. (2024). Effects of polyphenolic maqui (Aristotelia chilensis) extract on the inhibition of NLRP3 inflammasome and activation of mast cells in a mouse model of Crohn's disease-like colitis. *Front. Immunol.*, 14, 1229767.

9. **Response Letter:** Xie, K., Ortiz-Cerda, T., Schroder, A., Shiung, N., Lemos Wimmer, B., Chami, B., & Witting, P. K. (2023). Response to Low-density Granulocytes as Novel Biomarkers of Disease Activity in IBD. *Inflamm. Bowel. Dis.*, 29(8), e32-e32.

10. **Editorial:** Ortiz-Cerda, T., Xie, K., Mojadadi, A., & Witting, P. K. (2023). Myeloperoxidase in health and disease. *Int. J. Mol. Sci.*, 24(9), 7725. (Joint first authors)

11. **Systematic Review:** Xie, K., El Khoury, H., Mitrofanis, J., & Austin, P. J. (2023). A systematic review of the effect of photobiomodulation on the neuroinflammatory response in animal models of neurodegenerative diseases. *Rev. Neurosci.*, 34(4), 459-481. (Joint first authors)

12. **Literature Review:** Xie, K., Tan, K., & Naylor, M. J. (2022). Transcription factors as novel therapeutic targets and drivers of prostate cancer progression. *Front. Oncol.*, 12, 854151.

Presentations directly arising from this thesis:

1. **Regional Conference:** Xie, K., Abou Duhun, S., Ortiz-Cerda, T., Choi, H., Wang, X.S., O'Sullivan, J., Davis, T., Verley, E., Ghali, M., Kariyawasam, V., Mitrev, N., Chami, C. & Witting P.K. (2024). Characterising short chain fatty acid profiles in stool specimens from patients diagnosed with inflammatory bowel disease. 2024 SFRR-Australasia SFRR-Japan Joint Conference (**Invited oral presentation** – 10th December 2024; *this presentation was recognised with SFRR-Australasia Travel Award 2024*)

2. **Local Symposium:** Xie, K., Ortiz-Cerda, T., Lemos Wimmer, B. F., Shiung, N. C., & Witting, P. K. (2024) The effect of peptidyl arginine deiminase (PAD4) inhibition on extracellular traps (NETs) formation in DSS-induced mouse model of experimental colitis. USYD-UNSW Medical Science Symposium. (**Poster presentation** – 3rd July 2024)

3. **Regional Symposium:** Xie, K., Ortiz-Cerda, T., Lemos Wimmer, B. F., Shiung, N. C., & Witting, P. K. (2023) Inhibition of neutrophil extracellular traps formation with PAD4 inhibitor (GSK484) fails to ameliorate experimental IBD. SFRRA 2023 Research Symposium (**Invited oral presentation** –11th December 2023)

4. **International Conference:** Xie, K., Ortiz-Cerda, T., Lemos Wimmer, B. F., Shiung, N. C., & Witting, P. K. (2023) Neutrophil extracellular traps (NETs) inhibition in experimental colitis model of inflammatory bowel disease. 30th Annual Conference and Joint Meetings for SfRBM and SFRRI. (**Poster presentation** – 16th November 2023; *this poster presentation was recognised with SFRRI Travel Award 2023 and SfRBM Young Investigator Award 2023*).

5. **Local Seminar:** Xie, K., Ortiz-Cerda, T., & Witting, P.K. (2023) Investigating the role of neutrophil extracellular traps (NETs) in the pathogenesis of inflammatory bowel disease. The University of Sydney, Faculty of Medicine and Health, Molecular Biomedicine Theme Seminar. (**Oral presentation** – 22nd May 2023)

Presentations where the candidate contributed as co-author during the candidacy but not directly arising from the current thesis:

6. **Regional Conference:** Huang, G., Chami, B., Witting, P.K., Xie, K., Ortiz-Cerda, T. Stockdale, S. & Byrne, S. (2025) Topical Amomum Villosum extract attenuates experimental murine psoriasis. 2025 The Australasian College of Dermatologists 57th Annual Scientific Meeting. (**Figure contribution**, *poster was presented by Huang, G.*)

7. **Regional Conference:** Abou Duhun, S., Xie, K., Ortiz-Cerda, T., Choi, H., Wang, X.S., O'Sullivan, J., Davis, T., Verley, E., Ghali, M., Kariyawasam, V., Mitrev, N., Chami, B. & Witting, P.K. (2024) Optimisation of short chain fatty acid extraction in faecal samples of patients on a spectrum of inflammatory bowel disease severity. 2024 SFRR-Australasia SFRR-Japan Joint Conference. (**Figure contribution**, *poster was presented by Abou Duhun, S.*)

8. **International Conference:** Ortiz-Cerda, T., Hoosen, L., Xie, K., Chen, S., Ahmad, G., Chami, B., Wang, X.S., O'Sullivan, J. & Witting, P.K. (2023) Protective activity of natural products curcumin, Amomum Villosum and Aedyotis Diffusa in an animal model of inflammatory bowel disease. 30th Annual Conference and Joint Meetings for SfRBM and SFRRI. (**Figure contribution**, *poster was presented by Ortiz-Cerda, T.*)

9. **International Conference:** García-García, M.D., Xie, K., Ortiz-Cerda, T., Macías-García, L., Merinero, M., Tapia Opazo, G., Argüelles-Árias, F. and De-Miguel, M. (2023) Polyphenols from Maqui downregulate the NF-κB signalling pathway in epithelial and immune cells in TNBS-induced colitis model in mice. Congreso Sociedad Española de Patología Digestiva, Sevilla, Spain. (**Figure contribution,** *poster was presented by García-García, M.D.*).

10. **Local Seminar:** Xie, K., & Naylor, M.J. (2022) ETO: A novel regulator of prostate cancer. The University of Sydney, Faculty of Medicine and Health, Chronic Disease Theme Seminar. (**Oral presentation** – 6th July 2021)

Competitive Prizes & Awards

1. **Travel Award:** 2024 SFRR-Australasia Japan Joint Meeting Canberra, Australia. *($500 AUD).*

2. **Young Investigator Award:** 2023 SfRBM-SFRR-International 21st Biennial Meeting Punta del Este, Uruguay. *($500 USD + fee waiver for 2024 SfRBM Conference at Georgia, USA).*

3. **Travel Award:** 2023 SfRBM-SFRR-International 21st Biennial Meeting Punta del Este, Uruguay. *(£900 GBP).*

4. **The University of Sydney Postgraduate Award** *($37, 207 AUD p.a).*

Declaration – Statement of Originality

This is to certify that to the best of my knowledge, the content of this thesis is my own work. This thesis has not been submitted for any degree or other purposes.

I certify that the intellectual content of this thesis is the product of my own work and that all the assistance received in preparing this thesis and sources have been acknowledged.

Signed Dated: 28/02/2025

Kangzhe Xie
B. Sci. (Adv) (Hons)
PhD Candidate | Redox Biology Lab

The University of Sydney
School of Medical Sciences
Faculty of Medicine and Health
Level 4 West Charles Perkins Centre | The University of Sydney | NSW | 2006

Authorship Attribution Statement

In addition to the statements above, in cases where I am not the corresponding author of a published item or an item submitted for peer review for publication, permission to include the material has been granted by the corresponding author.

Signed Dated: 28/02/2025

Kangzhe Xie
B. Sci. (Adv) (Hons)
PhD Candidate | Redox Biology Lab

The University of Sydney
School of Medical Sciences
Faculty of Medicine and Health
Level 4 West Charles Perkins Centre | The University of Sydney | NSW | 2006

As supervisor for the candidature upon which this thesis is based, I can confirm that the authorship attribution statements above are correct.

Signed Dated: 28/02/2025

Paul Witting (PhD)
Professor, Redox Biology
School of Medical Sciences
Faculty of Medicine and Health
Charles Perkins Centre
Editor Redox Report

Rm 4212, D17 | The University of Sydney | NSW | 2006
+61 2 91140524
paul.witting@sydney.edu.au

BioRender Academic Publication License Statement

49 Spadina Ave. Suite 200
Toronto ON M5V 2J1 Canada
www.biorender.com

Confirmation of Publication and Licensing Rights - Open Access

August 29th, 2025

Subscription Type:	*Student Plan - Academic*
Agreement number:	*WM28OTO6U4*
Publisher Name:	*University of Sydney*
Figure Title:	*Evaluating the therapeutic efficacy of synthetic enzyme inhibitors and complementary alternative medicines in restoring redox and immune imbalance during inflammatory bowel disease*
Citation to Use:	*Created in BioRender. Xie, K. (2025) https://BioRender.com/krbi4ky*

To whom this may concern,

This document ("Confirmation") hereby confirms that Science Suite Inc. dba BioRender ("BioRender") has granted the following BioRender user: Kangzhe Xie ("User") a BioRender Academic Publication License in accordance with BioRender's Terms of Service and Academic License Terms ("License Terms") to permit such User to do the following on the condition that all requirements in this Confirmation are met:

1) publish their Completed Graphics created in the BioRender Services containing both User Content and BioRender Content (as both are defined in the License Terms) in publications (journals, textbooks, websites, etc.); and
2) sublicense such Completed Graphics under "open access" publication sublicensing models such as CC-BY 4.0 and more restrictive models, so long as the conditions set forth herein are fully met.

Requirements of User:

1) All Completed Graphics to be published in any publication (journals, textbooks, websites, etc.) must be accompanied by the following citation either as a caption, footnote or reference for each figure that includes a Completed Graphic:
   "Created in BioRender. Xie, K. (2025) https://BioRender.com/krbi4ky ".
2) All terms of the License Terms including all Prohibited Uses are fully complied with. E.g. For Academic License Users, no commercial uses (beyond publication in journals, textbooks or websites) are permitted without obtaining or switching to a BioRender Industry Plan.
3) A Reader (defined below) may request that the User allow their figure to be a public template for Readers to view, copy, and modify the figure. It is up to the User to determine what level of access to grant.

Open-Access Journal Readers:

Open-Access journal readers ("Reader") who wish to view and/or re-use a particular Completed Graphic in an Open-Access journal subject to CC-BY sublicensing may do so by clicking on the URL link in the applicable citation for the subject Completed Graphic.

The re-use/modification options below are available after the Reader requests the User to adapt their figure as a BioRender template and the User has granted such access.

1) View-Only/Free Plan Use: A Reader who wishes to only view the Completed Graphic may do so in the BioRender Services as either a BioRender Free Plan user or simply as a viewer. By becoming a BioRender Free Plan user, the Reader may view, modify and re-use the Completed Graphic as permitted under BioRender's Basic License Terms (e.g. personal use only, no publishing or commercial use permitted).
2) Re-Use/Publish with No Modifications: For any re-use and re-publication of a Completed Graphic with no modification(s) to the Completed Graphic made by the Reader, a Reader may do so by citing the original author using the citation noted above with the Completed Graphic. The Reader must also comply with the underlying License Terms which apply to the Completed Graphic as noted above (e.g. no commercial use for Academic License).
3) Re-Use/Publish with Modifications: For any re-use and re-publication of a Completed Graphic with a modification(s) made by the Reader, the Reader may do so by becoming a BioRender user themselves under either an Academic or Industry Plan, citing the original author using the citation noted above with the Completed Graphic and complying with the applicable License Terms.

For any questions regarding this document, or other questions about publishing with BioRender, please refer to our BioRender Publication Guide, or contact BioRender Support at support@biorender.com.

Abstract

Inflammatory bowel disease (IBD) is an umbrella term that describe a group of chronic autoimmune diseases that affects the gastrointestinal tract (GIT). These diseases include ulcerative colitis, Crohn's disease and indeterminate colitis. The clinical symptoms of IBD include abdominal pain, weight loss, chronic diarrhea, rectal bleeding, bloody stool, fever and anaemia, which all markedly decline the quality of life of the patients, compromises daily productivity and introduces significant economic and health care burden to the society. The exact cause of IBD is currently unknown. However, it is now appreciated that the complex interactions of genetic predisposition, altered gut microbiome and a range of environmental stimuli combine as potentiating factors for the disease. Specifically, IBD patients are characterised by excessive of neutrophil infiltration to the intestinal mucosa. This is accompanied with increased formation of neutrophil extracellular traps (NETs), a cellular process driven by enzymes myeloperoxidase (MPO), neutrophil elastase and peptidyl arginine deiminase IV (PAD4). Additionally, IBD patients also present with altered level of colon metabolites such as short chain fatty acids (SCFAs), increased oxidative stress and impaired antioxidant capacity in the inflamed colons. Collectively, these shifts from normal gut homeostatic balance are thought to create a sustained pro-inflammatory environment in the gut, leading the chronic perpetuation of inflammation observed in the case of IBD. Presently, there is no definitive cure for IBD and available treatments often perceived as ineffective and intolerable due to their high non-response rate and adverse side effects. As a result, IBD patients commonly seek alternative treatment options, particularly in the field of natural products and nutraceuticals.

The current thesis focuses on novel complementary and alternative medicines, investigating the therapeutic effects of synthetic compounds and natural products in reducing redox imbalances and alleviating gastric inflammation in the context of IBD.

Outcomes described here in

(i) **Chapter 1** summarised the physiology of the human GIT under both normal and pathological conditions, with a particular focus on IBD. This chapter detailed the potentiating factors of IBD pathogenesis, which include dysregulated immune response, altered gut microbiome and imbalanced redox environment, whilst currently available and emerging intervention approaches for the disease were also discussed.

(ii) **Chapter 2** provided detailed descriptions of ethics approval and experimental protocols that were not included or described in Chapters 3-5 due to adherence to strict publication guidelines.

(iii) **Chapter 3** is presented as a manuscript published at Bioscience Reports. This study investigated the effect of synthetic MPO and PAD4 inhibitors on mucosal NETs density in a dextran sodium sulfate (DSS)-induced murine model of experimental colitis.

(iv) **Chapter 4** is formulated into a second manuscript that was submitted to Redox Report for peer review. This study examined the level of SCFAs in stools of healthy individuals and IBD patients on a spectrum of disease severities. The correlative relationship between SCFA profiles and common inflammatory markers was also described in this manuscript.

(v) **Chapter 5** evaluated the effect of herbal remedies curcumin, *Hedyotis Diffusa* and *Amomum Villosum* in restoring redox imbalance and modulating colon lipid composition in a murine model of DSS-induced experimental colitis. Presently, this section of the thesis is being reviewed for future submission as a manuscript.

(vi) Lastly, **Chapter 6** provided general discussion of novel findings identified in the current thesis and detailed the importance of complimentary and alternated medicines for patients with IBD.

Overall, the data presented identify that GSK484, a synthetic inhibitor of the enzyme PAD4, was able to decrease the density of NETs in the colon mucosa in an animal model of colitis but this failed to inhibit the extent of experimental IBD in the same disease model. Our analysis of disease-stage-dependent change to SCFA levels from patient stool specimens revealed that butyrate increased markedly in patients that were categorised in remission, and that this peak in butyrate concentration diminished rapidly in patients to present with moderate and severe IBD judged by colonoscopy. Finally, an untargeted lipidomic analysis in colon tissues from mice with DSS-induced experimental colitis showed that the colon distribution of lipid underwent marked changes that were associated with disease pathology. Whereas treatments with natural products curcumin, and tonic teas derived from *Hedyotis Diffusa* and *Amomum Villosum* trended to differentially change the lipidome albeit this did not return the same distribution in the control colon. However, treatment with these natural remedies did restore the colon mucosa and decrease lesion in this animal model of colitis.

List of Abbreviations

Note: abbreviations from Chapter 3, 4 and 5 are not included here.

5-ASA	5-aminosalicyclic acid
8-OHdG	8-hydroxy-2'deoxyguanosine
ACE	Angiotensin converting enzyme
AIM2	Double-stranded DNA sensors absent in melanoma-2
ATP	Adenosine triphosphate
AUD	Australian dollar
BCA	Bicinchoninic acid assay
BSA	Bovine serum albumin
C2	Acetate
C3	Propionate
C4	Butyrate
C5	Valerate
CD	Crohn's disease
citH3	Citrullinated histone H3
COVID-19	Coronavirus Disease 2019
CRP	C-reactive protein
DAPI	4',6-diamidino-2-phenylindole
DC	Dendritic cell
DNA	Deoxyribonucleic acid
DSS	Dextran sodium sulfate
EIM	Extraintestinal manifestations
FMT	Faecal microbiota transplantation
GERD	Gastroesophageal reflux disease
GIT	Gastrointestinal tract
GPR	G-protein coupled receptor
H_2O_2	Hydrogen peroxide
HIER	Heat induced epitope retrieval
HIF	Hypoxia inducible factor
HO-1	Heme oxygenase-1
HOBr	Hypobromous acid
HOCl	Hypochlorous acid
HOSCN	Hypothiocyanous acid
IBD	Inflammatory bowel disease
IBS	Irritable bowel syndrome
IC	Indeterminate colitis
IFN-γ	Interferon gamma
Ig	Immunoglobulin
IL	Interleukin
ILC	Innate lymphoid cell
JAK	Janus kinase
JAM	Junction adhesion molecule
Keap1	Kelch-like ECH-associated protein 1
KO	Knockout
LAS	Laboratory Animal Service
LC-MS/MS	Liquid chromatography tandem mass spectrometry
MDA	Malondialdehyde
MMP	Matrix metalloproteinase
MPO	Myeloperoxidase
MyD88	Myeloid differentiation factor 88
NADPH	Nicotinamide adenine dinucleotide phosphate
NE	Neutrophil elastase
NET	Neutrophil extracellular trap
NFAT	Nuclear factor of activated T-cells
NF-κB	Nuclear factor kappa B
NLR	Nucleotide-binding domain and leucine-rich repeat receptors
NLR4	NLR family caspase recruitment domain-containing protein-4

NLRP	NLR pyrin domain-contacting family
NOX	NADPH oxidase
Nrf2	Nuclear factor erythroid 2-relataed factor 2
$O_2^{\cdot-}$	Superoxide anion radical
OAC	Oesophageal adenocarcinoma
$ONOO^-$	Peroxynitrite anion
OPA	Orthophosphoric acid
OSCC	Oesophageal squamous cell carcinoma
PAD4	Peptidyl arginine deiminase type IV
PARP	Poly adenosine diphosphate-ribose polymerases
PBS	Phosphate buffered-saline
PMN	Polymorphonuclear leukocyte
PPI	Proton pump inhibitor
Redox	Oxidation-reduction
ROS	Reactive oxygen species
SASP	Sulfasalazine
SCFA	Short chain fatty acid
SES-CD	Simple Endoscopic Score for Crohn's Disease
SOD	Superoxide dismutase
STAT	Signal transducer and activator of transcription
T-bet	T-cell specific T-box transcription factor
TBS	Tris-buffered saline
TBST	TBS with Tween 20
Tg	Transgenic
TGF-β	Transforming growth factor beta
Th	T-helper cell
TJ	Tight junction
TNBS	Trinitrobenzene sulfonic acid
TNF	Tumour necrosis factor
Treg	Regulatory T cell
UC	Ulcerative colitis
UCEIS	Ulcerative Colitis Endoscopic Index of Severity
WSLHD	Western Sydney Local Health District
ZO	Zona occludens

List of Figures

Note: figures from Chapter 3 are not included here, please see attached PDF for published manuscript.

List of Tables

Note: tables from Chapter 3 are not included here, please see attached PDF for published manuscript..

Chapter 1: Introduction

1.1 The human gastrointestinal tract (GIT)

The human gastrointestinal tract (GIT) is a complex and essential system responsible for digesting food, absorbing nutrients and eliminating waste products [1]. It comprises of several organs including the mouth, oesophagus, stomach, small intestine and the large intestine [2]. Anatomically, the GIT is divided into upper and lower sections. The upper GIT consists of the mouth, oesophagus, stomach and the three sections of the small intestine, duodenum, jejunum and the ileum [3]. On the other hand, the lower GIT includes the colon, rectum and the anus (Figure 1) [4]. The structure of the GIT is made up of several distinct layers (Figure 2), each contributing to its functionality [5]. The innermost mucosal layer contains specialised absorptive and secretory epithelial cells that regulate the intake of nutrients and secretion of enzymes and mucus involved in maintaining colon homeostasis [6]. Beneath this layer, the submucosa contains nerves, lymphatic vessels and connective tissues, which together provide structure and functional support [5]. A smooth muscle layer surrounds the submucosa, which is composed of circular and longitudinal muscles responsible for peristalsis [7]. The outmost serosal layer (serosa), made up of a continuous sheet of squamous epithelial cells, which as a protective barrier by secreting serous fluid to reduce friction from bowel movement within the peritoneal cavity [5].

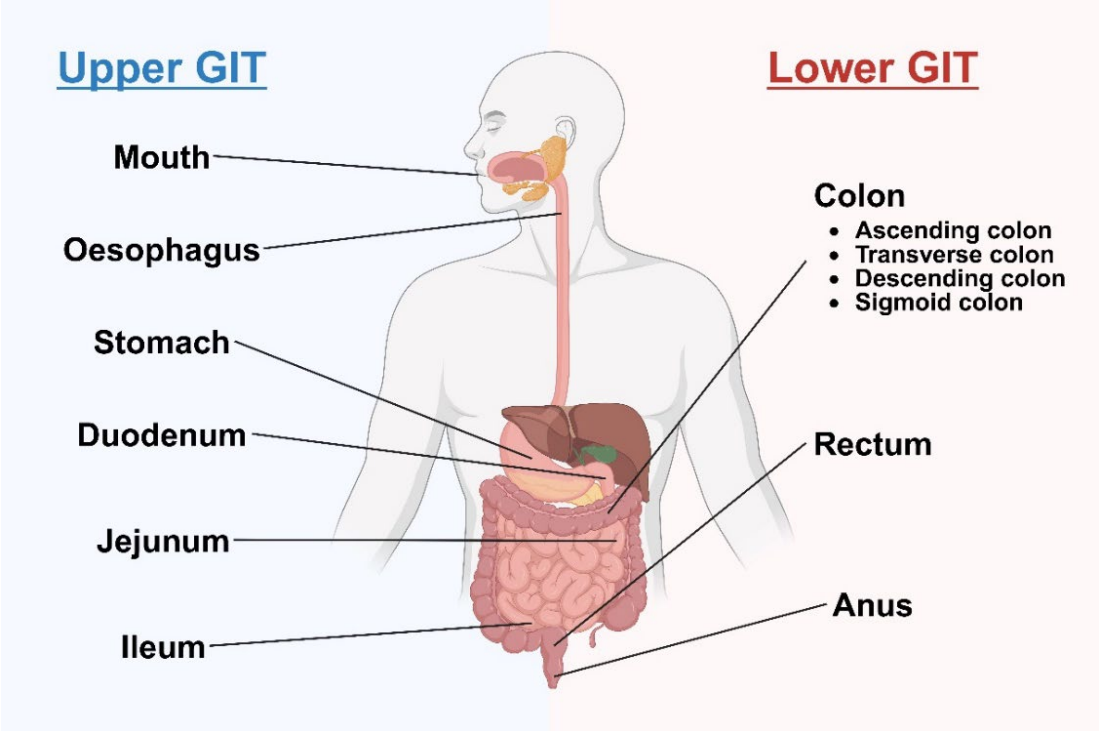

Figure 1.1. Schematic diagram of the human gastrointestinal tract (GIT). The upper human GIT includes the mouth, oesophagus, stomach and the small intestine, which then be further categorised anatomically as duodenum, jejunum and ileum. The lower human GIT consists of the colon, which can be further separated into ascending, transverse, descending and sigmoid colon, rectum and anus. Figure was generated in https://BioRender.com with appropriate permissions.

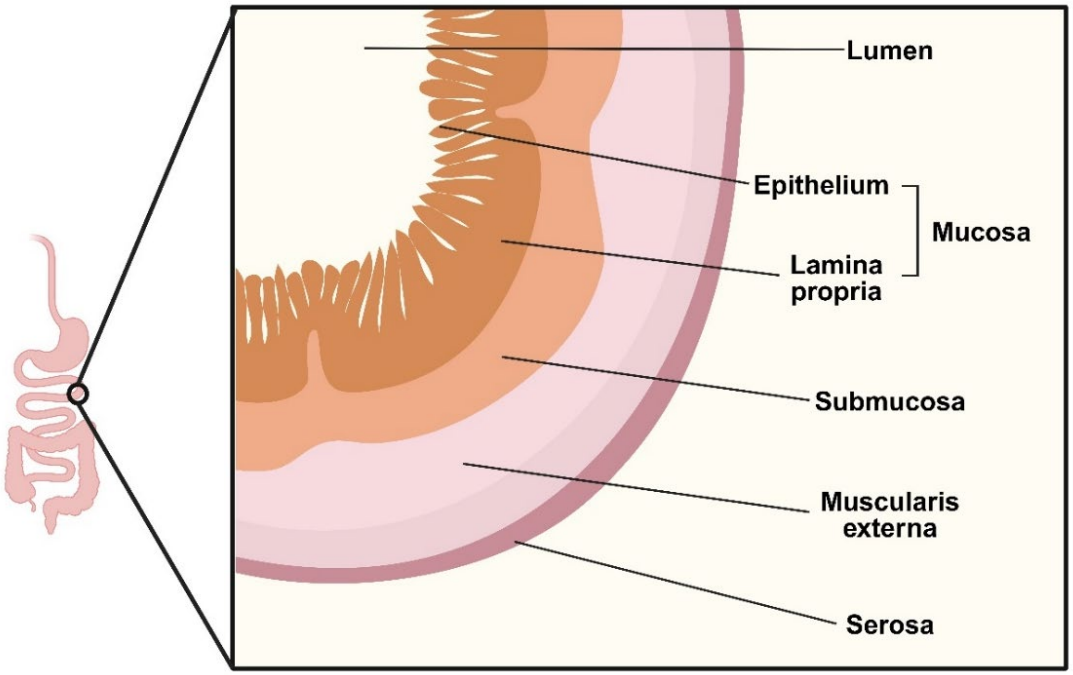

Figure 1.2. Schematic diagram of the layers of human GIT. The human GIT is comprised of 4 main layers: mucosa, submucosa, muscularis externa and serosa. Figure was generated in https://BioRender.com with appropriate permissions.

The primary role of the GIT is to convert ingested food into absorbable compounds that sustains bodily function. This process is facilitated through interactions with the vascular, lymphatic and the nervous systems, as well as through accessory organs such as the salivary glands, pancreas, liver and the gallbladder [5, 7]. After consumption, masticated food travels through the GIT via peristalsis, a coordinated, wave-like muscular contraction [8]. Along the way, the food bolus is mixed with gastric acids and digestive enzymes in the stomach to form chyme, which is then further processed along the digestive tract [9]. The stomach is the key site of digestion [10], where it is a glandular organ that houses gastric parietal cells that are responsible for the secretion of hydrochloric acids and intrinsic factors, the latter essential for vitamin B12 absorption [7, 11]. Chief cells, another type of secretory cells that are found in the stomach, produce enzyme precursor pepsinogen that breaks down proteins [12], while enteroendocrine cells release hormones such as gastrin, histamine, serotonin and somatostatin in the stomach to regulate digestive activities [13]. Most of the digestion and nutrient absorption process occurs in the small intestine, where digestive enzymes break food down into smaller molecules such as amino acids, fatty acids and simple sugars [7]. These nutrients are then absorbed through the intestinal mucosa and distributed to the body via dense blood vessels located in the mesentery and the lymphatic system. Remaining undigested content then enters the large intestine via the ileocecal valve, where water and water-soluble electrolytes re recovered and waste solidifies to form faeces [5].

In summary, the GIT functions as a highly organised system to process food, extract nutrients and eliminate wastes. Its intricate structure and physiological processes are critical in maintaining overall health and supporting the metabolic demands of the human body.

1.1.1 Gut homeostasis & barrier function

The maintenance of GIT structure and physiological functions, collectively referred to as gut homeostasis, relies on a complex system involving continuous secretion of biological agents that regulate microbial colonisation, monitoring of the intestinal microenvironment, detection of both beneficial and harmful microbes and the modulation of intestinal immune responses [14]. These processes are facilitated by interactions between the gut microbiota, intestinal epithelium and the host immune system. The key contributors to gut homeostatic balance are summarised in Figure 3 and will be discussed below.

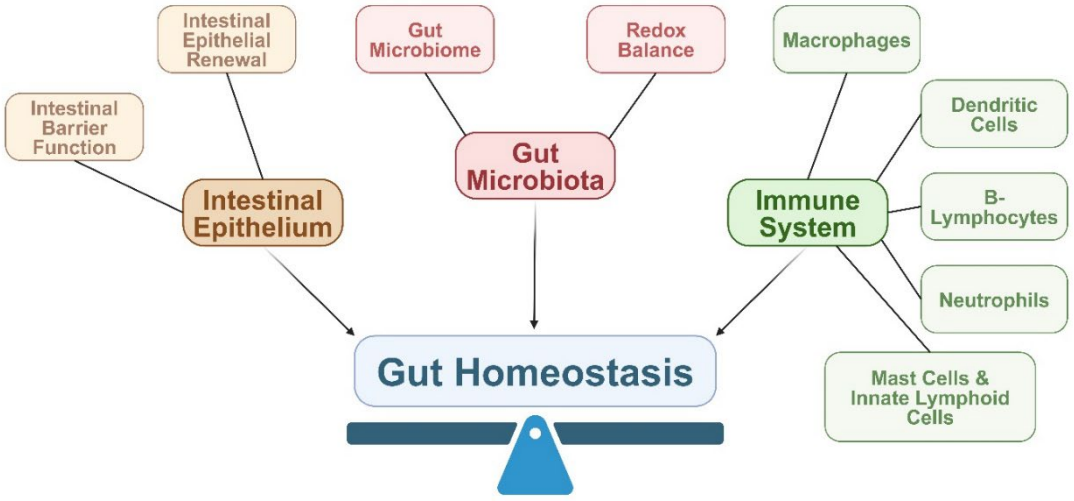

Figure 1.3. Contributors of gut homeostatic balance. The gut homeostatic balance is attributed to the balanced interactions between the factors of intestinal epithelium, gut microtia and the host immune system. Figure was generated in https://BioRender.com with appropriate permissions.

1.1.1.1 Intestinal barrier function

The intestinal epithelium serves as a critical interface between the internal and external environment, providing both a physical barrier and a selective gateway [15]. Covering an expansive surface area of approximately 30 m^2 [16], this layer is comprised of columnar epithelial cells that together form a physical defence against external insults such as invading pathogens and toxins [17]. Concurrently, selective passage of nutrients, electrolytes and other essential molecules are necessary for maintaining gut physiology and overall homeostasis [18]. The permeability of the intestinal epithelium varies along the GIT and is tightly regulated to balance protection and nutrient absorption. This regulation involves two main pathways: (i) paracellular permeability, where solutes and particulate matters cross the epithelium between adjacent cells; and (ii) transcellular permeability, where molecules are transported across the apical membrane of the intestinal epithelial cells [15].

Paracellular permeability is mediated by specialised protein complexes that form tight junctions (TJs), located near the apical surface of the adjoining epithelial cells, which allows the movement of ions, water and smaller compounds whilst simultaneously preventing the passage of large molecules [19]. As shown in Figure 4, the TJs are composed of transmembrane proteins including occludins, junction adhesion molecules and members of the claudin protein family[20]. These cell-surface proteins interact with intracellular scaffold proteins like Zonula occludens (ZO)-1, ZO-2 and ZO-3, which serve as anchors for the TJs to

cellular actin cytoskeleton, ensuring structural stability and functional regulation [21]. Beneath the TJs are additional cell-cell adhesion structures, including adherens junctions, desmosomes, and the gap junctions (Figure 5), which support intercellular adhesion and intracellular signalling [22-24]. The integration of these structures strengthens colon barrier function, whilst allowing dynamic responses to physiological needs in maintaining gut homeostatic balance.

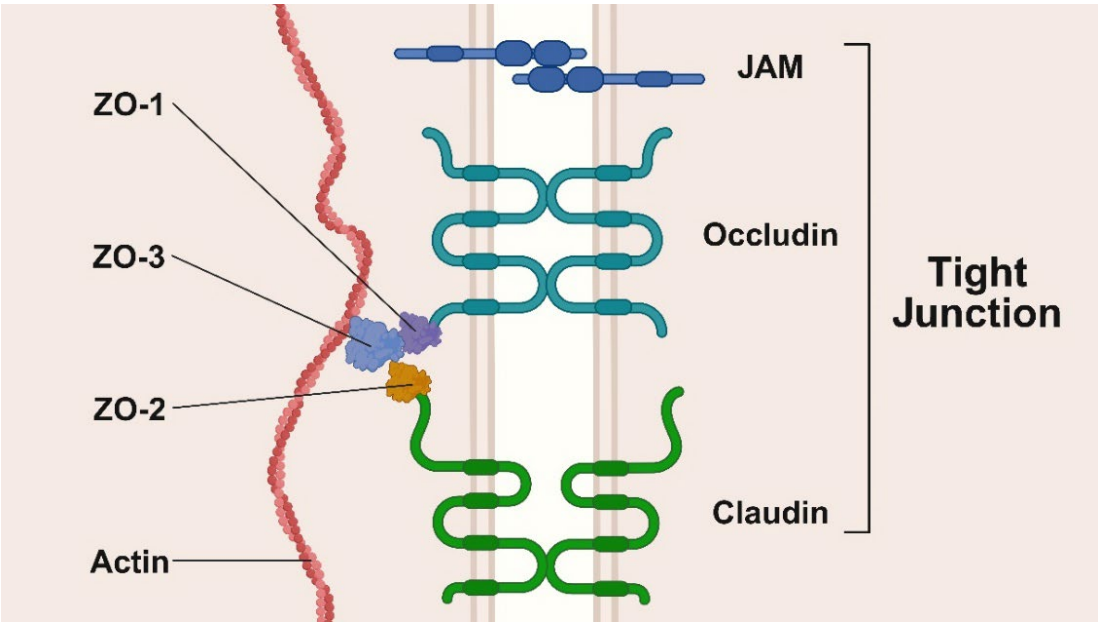

Figure 1.4. Schematic of tight junction structure. The tight junction is made up of junction adhesion molecules (JAM), Occludin and Claudin, which all are connected to the cellular actin cytoskeleton via intracellular scaffold proteins Zonula Occludens (ZO)-1, 2 and 3. Figure was created in https://BioRender.com with appropriate permissions.

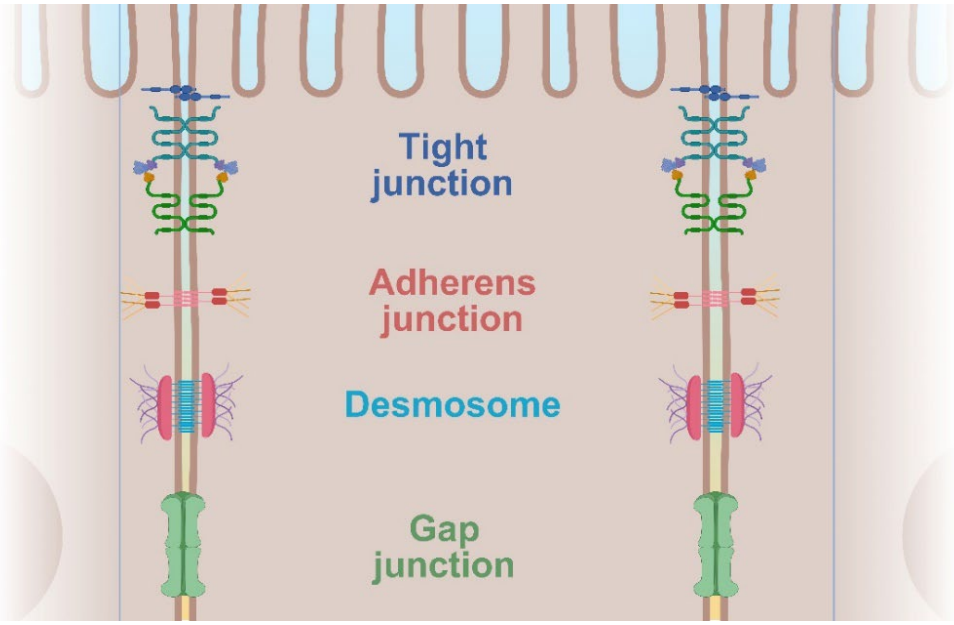

Figure 1.5. Schematic diagram of epithelial intercellular junctions. The human intestinal intracellular junctions include tight junctions, adherens junctions, desmosomes and gap junctions, which they collectively contribute to intercellular

adhesion and intracellular signalling. Figure was created in https://BioRender.com with appropriate permissions.

On the other hand, transport across the intestinal epithelial cells (transcellular permeability) encompasses multiple mechanisms to accommodate a diverse range of molecules. Passive permeability allows large hydrophilic compounds to diffuse across the barrier, whilst transcellular transport via the aqueous pores facilitates the movement of lipophilic and small hydrophilic molecules [7]. Active carrier-mediated transport is crucial for the absorption of nutrients and electrolytes, and the process of endocytosis, followed by transcytosis and exocytosis enables the uptake and movement of larger peptides, proteins and particles [25].

Together, these processes regulate the barrier integrity and permeability of the GIT. Which ensures a delicate balance between protection and absorption. Disruption in this balance, such as alterations in TJs composition or function, can result in increased intestinal permeability, a term often referred to as "leaky gut" [18]. This shift from homeostatic balance of the GIT is associated with various disorders, which will be discussed below.

1.1.1.2 The gut epithelium

The intestinal epithelium is turned over every 3 to 5 days in humans [26]. This high rate of renewal serves as a protective mechanism, which efficiently removes damaged or infected cells to facilitate homeostatic balance [27]. The intestinal epithelium is generally divided into two regions, the finger-like villi projections contain terminally differentiated cells, and crypts, the site for a small population of intestinal stem cells at the bottom of the cryptic structure [28]. These stem cells are vital for regenerating the epithelial cell layer, where they proliferate continuously to drive the upward migration of immature cells towards the villous tip [29]. During their migration, epithelial cells differentiate into specialised types including absorptive enterocytes, goblet cells and enteroendocrine cells [30]. Upon reaching the villous tip, the mature (functional) epithelial cells perform their respective physiological roles and eventually undergo cell death via apoptosis and are shed into the gut lumen [31]. Additionally, neighbouring immune cells such as macrophages also recognise and clear apoptotic cells through phagocytosis, preventing the accumulation of cellular debris [32]. Apoptosis, the process of programmed cell death, is critical in regulating epithelial turnover and is triggered by a wide variety of intrinsic and extrinsic factors such as deoxyribonucleic acid (DNA) damage, nutrient deficiency, stress or death receptor signalling [33].

The balance between epithelial cell renewal and apoptosis needs to be tightly regulated, as disruption to these two processes can lead to pathologies [34]. It is now widely appreciated that excessive cell death compromises epithelial barrier function, which promotes bacterial invasion and inflammation, whilst insufficient apoptosis has been linked to the abnormal accumulation of epithelial cells and the development of colonic polyps that increase the risk of colorectal cancer [35]. Thus, maintaining the balance is essential for epithelial integrity, barrier function and over gut health.

1.1.1.3 Immune cells in the gut

The GIT hosts a sophisticated mucosal immune system, encompassing both innate and adaptive immune components, in which resident cells synchronously monitor luminal content to distinguish between commensal microbiota and food antigens (tolerance) and invading pathogens that may potentially cause pathologies. Immune cells involved in gut homeostasis

include macrophages, dendritic cells and B-lymphocytes that are strategically located within the intestinal mucosa, mesenteric lymph nodes and Peyer's patches. Additionally, polymorphonuclear leukocytes (PMNs) such as neutrophils act as the first responder for the gut innate immune system, playing a crucial part in pathogen clearance and maintaining intestinal epithelial integrity, whilst mast cells and innate lymphoid cells further aid gut homeostasis through a myriad of cellular interactions and processes [36]. All these cells are critical for immune surveillance, pathogen elimination, and maintaining gut homeostasis and fostering a balanced immune response are summarised in Figure 6 and discussed below.

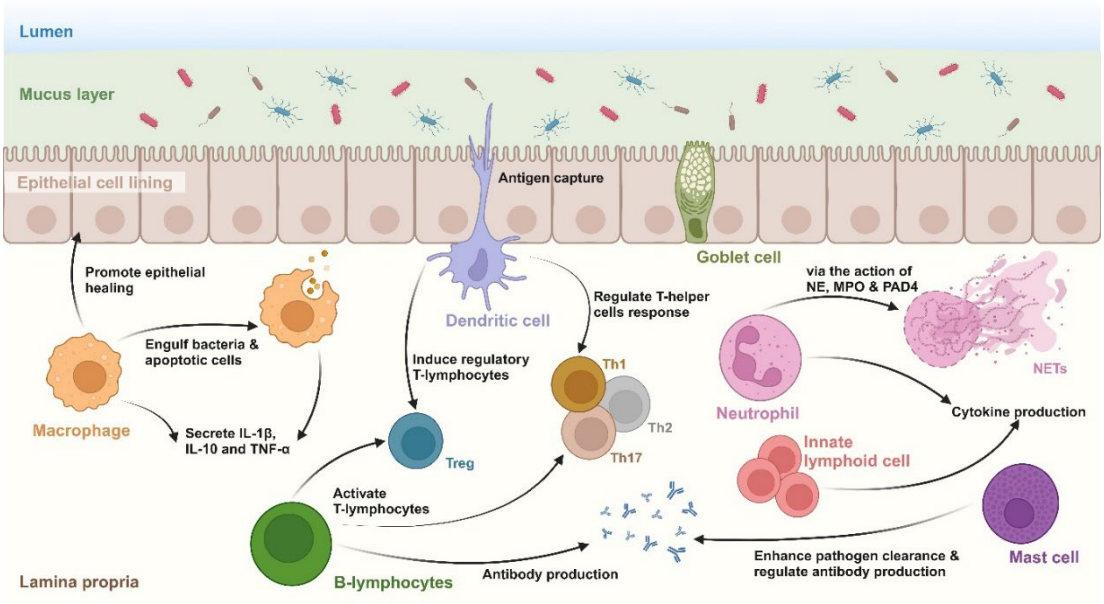

Figure 1.6. Schematic summary of gut homeostatic balance maintaining immune cells and their functions. Several types of immune cells in the gut are responsible for maintaining gut homeostatic balance. Macrophages engulf bacteria and apoptotic cells, secrete cytokines such as IL-1β, IL-10 and TNF-α, and promote epithelial healing. Dendritic cells capture antigens and regulate T-helper (Th) cell response and ultimately promote the induction of regulatory T-cells (Treg). B-lymphocytes are responsible for T-cells activation and antibody production whilst neutrophil contribute to bacterial clearance through phagocytosis, reactive oxygen species production and neutrophil extracellular traps (NETs) formation, mediated by neutrophil elastase (NE), myeloperoxidase (MPO) and peptidyl arginine deiminase type IV (PAD4). Innate lymphoid cells also secrete cytokines, supporting epithelial integrity and regulating antibody production. Mast cells enhance pathogen clearance via protease release, cytokine production and regulating IgA responses. Figure was generated in https://BioRender.com with appropriate permissions.

1.1.1.3.1 Macrophages

Macrophages are specialised phagocytes that play a crucial role in regulating gut homeostasis, being present throughout the GIT and across all layers of the gut wall. Characteristically these cells are identified by their expression markers CD11b [37], CD64 [38] and CD68 [39]. The anatomical positioning of macrophages within the gut wall highlights the phenotypes, and transcriptome of these cells. For instance, macrophages are more abundant in the colonic lamina propria and have higher expression of acid phosphatase 5 and complement

component 1q [39]. On the contrary, there are fewer macrophages within deeper gut layers, and they express higher levels of *LYVE1*, CD163 and *COLEC12* [39].

The functional difference between colonic macrophages and resident macrophages in other human organs remains elusive however, studies in murine models suggest that macrophages act as a first-line of defence in the gut, engulfing and destroying bacteria that breach the epithelial mucosal barrier [40]. It has also been shown that they are involved in efferocytosis [41], a process of clearing apoptotic epithelial cells to maintain gut health. Beyond their defensive roles in the gut, colonic macrophages can promote intestinal epithelial repair by providing trophic signals such as hepatocyte growth factor [42] and activating the Wnt signalling pathway [43]. Moreover, intestinal macrophages have been reported to constitutively secrete immunoregulatory cytokine interleukin (IL)-10 [44], which is essential in regulating $CD4^+$-mediated T-cell activities [45], signalling a decrease in inflammation and maintaining epithelial integrity. In addition, the macrophage-derived pro-inflammatory cytokine IL-1β has also been shown to maintain T-helper (Th)17 cells to promote mucosal immune protection [46], whilst the inflammatory mediator tumour necrosis factor (TNF)-alpha released by macrophages activates a range of down-stream pathways that strengthens epithelial integrity [47]. Together, the multi-functional role of macrophages in immune defence, intestinal epithelial turn-over and structural support underscores their importance in persevering gut homeostasis and ensuring physiological function of the GIT.

1.1.1.3.2 Dendritic cells

Dendritic cells (DCs) are essential antigen-presenting cells that can be found throughout the intestinal lamina propria, Peyer's patches, isolated lymphoid follicles and mesenteric lymph nodes in the gut [48]. They maintain gut homeostasis by balancing immune tolerance to commensal bacteria and self-antigens, whilst retaining immune protection against invading pathogens [49]. The subsets of intestinal DCs can be distinguished by their functions and markers. For example, $CD103^+$ DCs are primarily localised to the intestinal lamina propria and mesenteric lymph nodes, in which they are responsible for promoting the induction of $Foxp3^+$ regulatory T cells (Tregs) [50].

Induction of Foxp3+ Tregs is driven by retinoic acid, a vitamin A metabolite and transforming growth factor beta (TGF-β) [51], supporting immune tolerance and epithelial health under the steady state. In contrast, CD103- DCs, which express high levels of CX3CR1 [52], extend dendrites into the intestinal lumen to sample antigens from commensal microbes and apoptotic epithelial cells [53]. These cells form TJ-like structure with epithelial cells in a CX3CR1-myeldoid differentiation factor 88 (MyD88)-dependent manners to facilitate antigen update [54], and subsequently migrate to the mesenteric lymph nodes to present sampled antigens to naïve T cells and initiate the differentiation of Th17 cells [55]. In Peyer's patches, it has been shown that CD11b-$CD8\alpha^+$ subset of DCs produce IL-12 to drive Th1 immunity, whilst the subset of DCs that express CD11b and lacks CD8α expression secrete IL-10 to promote Th2 responses linked to the resolution of local inflammation [56]. The ability for DCs to orchestrate Th1, Th2, Th17 and Treg responses, implicates a pivotal role for these cells in preserving gut homeostasis and protecting again pathogens.

1.1.1.3.3 B-lymphocytes

B-lymphocytes act through various mechanisms to maintain gut homeostasis, including antibody production, antigen presentation to T-cells, immunomodulatory cytokine secretion, and supporting the development of secondary lymphoid organs. A key immune function of

gut-associated B-cells is the production of immunoglobulin (Ig) A, initiated during intestinal colonisation by bacteria shortly after birth [57]. This process involves the class switching production of IgM to IgA molecules, which is crucial for establishing immune tolerance and immune defence in the gut [58].

Distributed throughout the lamina propria of the intestinal villi, B-lymphocytes produce ~40-60 mg/kg/day of IgA [59, 60], which is transported across the intestinal epithelium and secreted into the gut lumen. Secretory IgA serves as a first line of defence by preventing pathogens and toxins from adhering to, or invading, the intestinal epithelium. This is achieved by blocking receptor-binding domains [61, 62], mediating immune exclusion through agglutination, entrapment and clearance [63] and the formation of protective biofilms [64].

It has been reported that about 45% of the gut bacteria were bound with secretory IgA in healthy humans [65], with IgA-bound bacteria gaining a selective advantage in forming stable biofilms in the gut [66] and maintaining appropriate metabolism of luminal contents such as carbohydrates [67]. On the contrary, the absence of IgA disrupts gut homeostasis as evidence from a study in AID-deficient mice, where the lack of IgA leads to a 100-fold increase in the number of anaerobic bacteria in the small intestine [68], effectively skewing the microbiome through shifting microbial diversity. Moreover, deficiencies in mature B-lymphocytes have been shown to exacerbate oxidative stress caused by commensal bacteria [69], which further highlights the integral role of B-cells in regulating gut commensal bacterial responses and maintaining the gut immune homeostasis.

1.1.1.3.4 Neutrophils

Neutrophils are a type of polymorphonuclear leukocyte that act as the first line of defence for the gut innate immune system, in which they possess strong capabilities to detect and eliminate infections with high efficiency [70, 71]. Notably, depletion of neutrophils in a mouse model of experimental colitis results in aggravated inflammation in the colonic mucosa [72], highlighting the importance of this immune cell-type in regulating gut immune responses. In response to noxious stimuli, circulating neutrophils initiate rapid infiltration into the affected tissues [73]. After tissue infiltration, neutrophils recognise and phagocytose pathogens, and produce reactive oxygen species (ROS) such as superoxide anion radical ($O_2^{\cdot-}$) and hydrogen peroxide (H_2O_2) through respiratory burst to deactivate invading bacteria [74]. They also release bactericidal enzymes such as myeloperoxidase (MPO) through degranulation; MPO utilises H_2O_2 to produce the powerful two-electron oxidant hypochlorous acid (HOCl) via the halogenation cycle to further facilitate the bacterial action (Figure 7) [75, 76]. Additionally, HOCL has been shown to react with heparan sulfate to generate polymer-derived *N*-chloro derivatives such as chloramines and chloramides [77], in which they retain their oxidising capacity and induce oxidative modifications at sites that are distant from the site of inflammation [76]. Whilst neutrophil-mediated ROS production provides efficient pathogen removal, excessive production of H_2O_2 and HOCl, and their secondary reactive species can lead to oxidative damage to host tissue, which has been proposed to be one of the major potentiating factors for inflammatory bowel disease (IBD, will be discussed further in Sections 1.3.1 and 1.3.5)

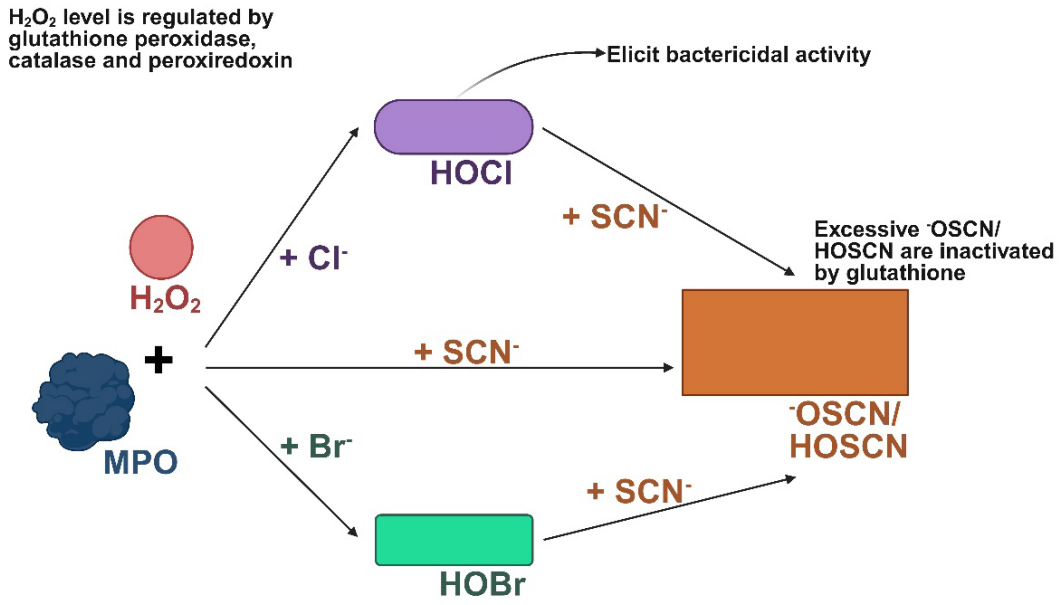

Figure 1.7. Halogenation activities of myeloperoxidase. The neutrophil enzyme myeloperoxidase (MPO) utilises hydrogen peroxide to catalyse the production of halogenated products hypochlorous acid (HOCl), hypobromous acid (HOBr) and hypothiocyanous acid (HOSCN). Of which, HOCl are known for their bactericidal activity in the gut, in which regulating immune responses through non-specific DNA damage. Figure was generated in https://BioRender.com with appropriate permissions.

Another key mechanism employed by neutrophils to eliminate invading bacteria is the formation of neutrophil extracellular traps (NETs) [78]. This process is known as NETosis, and it is initiated by ROS-induced nuclear translocation of NE, which results in nuclear chromatin decondensation [79]. The decondensed chromatins allow the conversion of histone arginine into citrulline (citH3) by the activity of peptidyl-arginine deiminase IV (PAD4) and the binding of MPO, which disassemble the nuclear envelope, leading to the subsequent rupture of the neutrophil membrane and the release of neutrophil contents into the extracellular space [79, 80]. This enables NETosis in the extracellular space allowing retention of MPO bactericidal actions, which extends the bacterial killing effects of neutrophils beyond their cell death [78] (see Figure 1.8 for molecular mechanism of NETosis).

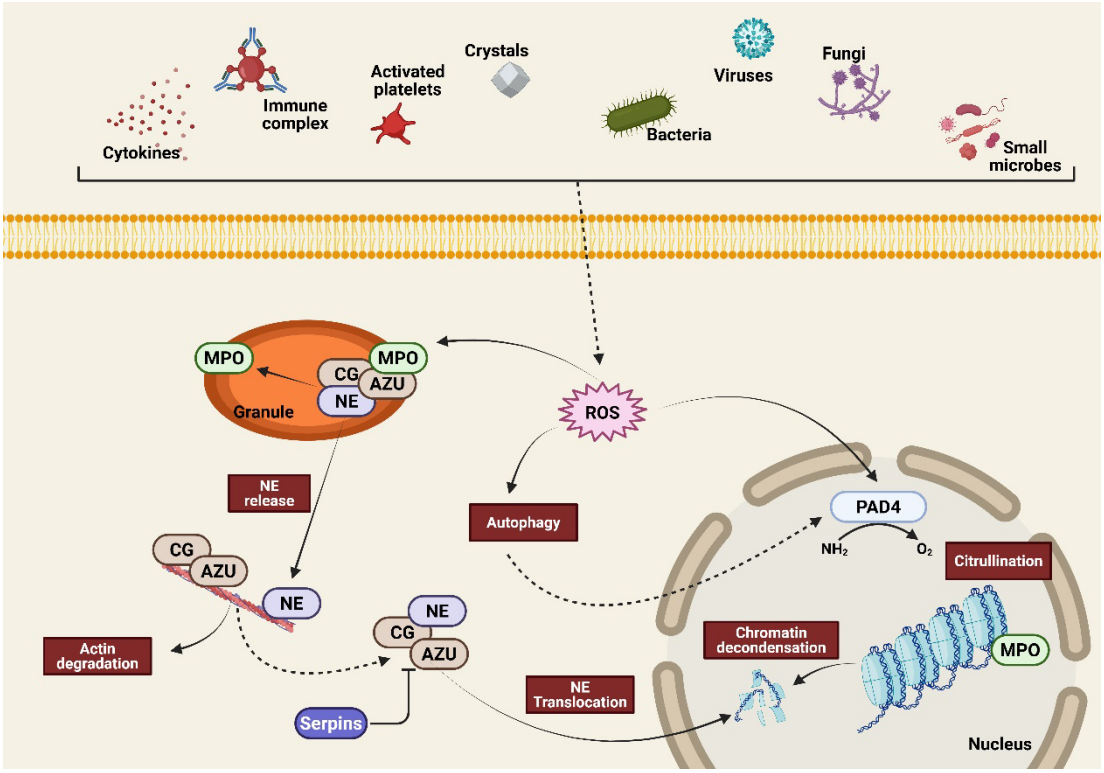

Figure 1.8. Molecular mechanism of NETosis. The formation of neutrophil extracellular traps (NETosis) can be triggered by various endogenous stimuli such as cytokines, immune complexes and activated platelets as well as exogenous factors such as crystals, bacteria, viruses, fungi and small microbes. These stimuli activate downstream signalling pathways to induce the generation of reactive oxygen species (ROS), which initiates the release of neutrophil elastase (NE) from the azurosome complex within the neutrophil granules, an essential process during NETosis. This results in the degradation of actin cytoskeleton and nuclear translocation of NE to drive chromatin decondensation. The process of chromatin decondensation can also be inducted by peptidyl arginine deiminase IV (PAD4)-mediated citrullination and myeloperoxidase (MPO) binding. Figure was adapted from [81, 82] and generated in https://BioRender.com with appropriate permissions.

Neutrophils have historically been regarded as a uniform group pf fully matured immune cells with limited functional diversity, characterised by expression of surface marker such as Ly6G in mice and CD66b in humans [83]. This perspective stems from their relatively short life-span, diminished transcriptional activity and inability to re-enter the vasculature once infiltrated into peripheral tissues [84]. However, growing evidence over the past few decades has revealed that neutrophils exhibit greater phenotypic diversity and functional adaptability than previous dogma. In addition to their anti-microbial activities, neutrophils also have a role in intestinal epithelial healing and resolving inflammation. For example, $CD177^{+}$ neutrophils have reduced production of pro-inflammatory cytokines IL-6, IL-17A and IFN-γ and elevated production of IL-22 and TGF-β [85], which are essential in promoting tissue repair [86]. Neutrophils also secrete vascular endothelial growth factors [87] and pro-resolving lipid mediators Protectin D1 and Resolvin E1 [88]. These molecules have been shown to reduce neutrophil recruitment [88, 89] and promote the macrophage-induced clearance of apoptotic neutrophils [90, 91], preventing the excessive aggregation of these destructive immune cells.

Together, neutrophils maintain gut homeostatic balance by balancing their pro-inflammatory action with mechanisms that promote mucosal healing through a complex pathway of protein secretion that facilitates the resolution of inflammation.

It has also been shown that neutrophils influence the metabolism and oxygen dynamics of the gut. Hypoxia inducible factor (HIF) is a global regulator of gene expression under low-oxygen conditions [92]. Stabilisation of HIF in the colonic mucosa has been shown to promote the expression of anti-microbial peptides such as β defensin-1 [93] and proteins essential for sustaining the mucosal barrier [94]. During acute inflammation, it has been reported that neutrophils increase oxygen consumption and alter the tissue microenvironments in ways that stabilise HIF. Additionally, the low oxygen environment created as a result of neutrophil-induced oxygen utilisation in the gut foster microbial production of short chain fatty acids (SCFAs), which further support the stabilisation of HIF and mucosal barrier integrity [94]. Overall, neutrophils serve as a critical mediator of gut homeostasis and dysregulated neutrophil actions and elevated formation of NETs has been associated with various GIT disorders such as inflammatory bowel disease (IBD), which will be discussed in greater details in this thesis.

1.1.1.3.5 Mast cells & Innate lymphoid cells

Mast cells are tissue-residence cells derived from haematopoietic origins and play a crucial role in maintaining mucosal homeostasis [95]. Firstly, mast cells support pathogen clearance by releasing proteases and increasing vascular permeability of the gut [96, 97], which facilitates the recruitment of neutrophils [98] and eosinophils to the site of inflammation or infection [97]. It has also been shown that mast cells regulate the production of IgA by facilitating the differentiation of B-cells into IgA-producing plasma cells in the intestinal environment through the secretion of IL-6 [99], and via CD40 ligand-CD-40-mediated cell-cell interactions [100], which are essential in establishing oral tolerance and immune defence in the gut (discussed above). Additionally, mast cell-derived chymase tightly regulate intestinal permeability, where mast cell and chymase deficient mice showed impaired epithelial migration and decreased epithelial barrier function [101], highlighting the important role of mast cells in maintaining gut epithelial integrity.

On the other hand, innate lymphoid cells (ILCs) are a group of innate immune cells derived from still poorly characterised lymphoid precursors, lacking the RAG-mediated recombined antigen receptors found in T- and B-lymphocytes [102]. There are three main categorised groups of ILCs, based on their secreted cytokine profiles. Group 1 ILCs produce Th1-like cytokines such as IFN-γ, Gorup 2 ILCs secrete Th2-associated cytokines, including IL-5 and IL-13, whilst Group 3 ILCs are key source of TH17-like cytokines such as IL-17A and IL-22 [103]. Of these ILCs, Group 3 ILCs have been found to play a pivotal role in maintaining intestinal homeostasis through the production of IL-22, a homeostatic cytokine essential for epithelial cell-mediated immune responses [104]. The cytokine IL-22 acts on IL-22 receptors located on intestinal epithelial cells, which stimulates the production of anti-microbial peptides such as RegIII-β and RegIII-γ [105], enabling the elimination of invading bacteria. Moreover, IL-22 deficient mice have been shown to exhibit increased crypt apoptosis, loss of epithelial integrity and elevated susceptibility to tissue damage [106], highlighting the role of ILC3-produced IL-22 in maintaining barrier function and its contribution to gut homeostasis. Together with other aforementioned immune cell types above, mast cells and ILCs combine

to maintain intestinal epithelial integrity and contribute to gut homeostatic balance through a myriad of intracellular and extracellular processes.

1.1.1.4 Gut microbiome

The gut microbiome is made up of a diverse community of microorganisms, including bacteria, archaea, fungi, viruses and bacteriophages [107, 108], all of which play a critical role in maintaining gut homeostasis. A healthy gut microbiome is predominantly composed of bacterial phyla such as *Firmicutes, Bacteroidetes, Actinobacteria* and *Proteobacteria* [109], with smaller contributions from phyla of *Verrucomicrobia*, *Fusobacteria*, *Tenericutes* and *Spirochetes* [110, 111]. Maintaining appropriate microbial bacterial distribution and density is crucial for gut health. A dense microbial community in the colon facilitates nutrient absorption and fermentation [112, 113], whereas a low-density microbial distribution in the small intestine is beneficial to avoid bacterial overgrowth [114]. Small intestinal bacterial overgrowth can lead to excessive bile salt deconjugation, malabsorption, diarrhoea and weight loss [114]. In addition to microbial density in the GIT, the metabolic products of these microbes profoundly influence host physiology, which also contribute substantially to maintaining physiological gut homeostasis.

The colonic microbial ecosystem harbours a microbial density approximately 100 times greater than any other sites in the body [115], with the intestinal microbes serve as a principal source of biologically active metabolites. In the colon, intestinal bacteria ferment undigested macronutrients, particularly plant polysaccharides into SCFAs that range between C2-C5 in carbon length and include acetate (C2), propionate (C3), butyrate (C4) and valerate (C5) [116]. These volatile metabolites provide energy support to the intestinal epithelial barrier and modulate immune responses. For example, SCFA acetate has been shown to resolves intestinal inflammation and prevent *Escherichia coli*-mediated enteropathogenic infection through G-protein coupled receptor (GPR) 43 [117, 118], whilst the production of another SCFA butyrate reported to strengthens barrier integrity [119] and have profound depressive effect on cytokine production in naïve Th cells [120]. Moreover, it has been demonstrated that the amount of dietary fibre can influence the concentrations of luminal SCFAs [121], which subsequently influence the composition of gut microbiota in a cyclic manner [122]. Therefore, the balance of gut microbiome and its interaction with host metabolism and immune system underscore its essential role in sustaining gut homeostasis and overall physiological immunity.

1.1.1.5 Redox balance in the gut

Oxidation-reduction (Redox) chemical reactions involve transfer of electrons between two species [123], and redox balance plays a crucial role in maintaining gut homeostasis by mediating microbial composition, immune responses and tissue repair. Locally formed ROS are central to this balance, with their production primarily driven by the enzyme nicotinamide adenine dinucleotide phosphate (NADPH) oxidases (NOX), as well as other sources like mitochondrial complex I, II and III, and enzymes xanthine oxidase, cyclooxygenase, lipoxygenase and myeloperoxidase [124].

In addition to the enzymic sources identified above, under normal physiological conditions, about 1-2% of molecular oxygen is converted into $O_2^{\cdot-}$ via mitochondrial electron transport chain leakage [125], establishing a basal electrophilic potential. Cellular $O_2^{\cdot-}$ are rapidly utilised by endogenous superoxide dismutase (SOD) to form H_2O_2, a more stable mediator of the gut's

electrophilic tone [126]. Thus ROS, including the parent $O_2^{\cdot-}$ species and derivatives such as H_2O_2, serve dual roles as anti-microbial agents and redox signalling molecules. Cellular ROS production is tightly regulated, as excessive ROS generation caused by factors like mitochondrial damage, hypoxia or increased metabolism can disrupt redox homeostasis [124, 127]. An imbalance in redox reactions may also lead to the formation of secondary oxidants such as peroxynitrite anions ($ONOO^-$, formed by the rapid reaction between $O_2^{\cdot-}$ and nitric oxide). Like myeloperoxidase-derived HOCl (discussed above), $ONOO^-$ is a potent two-electron oxidant that causes irreversible protein modification that can comprise tissue integrity [128].

During immune activation or tissue injury, a controlled elevation of electrophilic tone occurs in the gut, supporting wound healing and immune surveillance. Following pathogen clearance, the nucleophilic tone is restored by eliminating damaged tissues and re-establishing redox equilibrium. In addition to the establishment of electrophilic and nucleophilic tones in the gut, redox balance is also a key driver in bacterial community composition in the gut. The energy molecule adenosine triphosphate (ATP) is generated through redox reactions [129], where electron transfers from donors like glucose obtained from food nutrients to acceptors such as oxygen in the gut. Facultative anaerobes like *Lactobacillaceae* and *Enterobacteriaceae* in the oxygen-rich small intestine can utilise oxygen or nitrate as electron acceptors to produce ATP but switch to fermentation when acceptor molecules are absent or in low local concentration [130, 131]. In contrast, obligate anaerobes such as *Bacteroidia* and *Clostridia* dominate the oxygen-poor, densely populated large intestine [132, 133]. These microbiota fermenters reply on endogenous electron acceptors like pyruvate to produce ATP [134]. As ATP is essential for appropriate growth of bacteria [135], disruption to redox balance could result in alteration to GIT bacterial community alteration. Thus, efficient redox homeostasis safeguards the gut mucosa against unregulated ROS-induced damage and preserves the structural and functional integrity of the gut, ensuring microbial balance and supporting overall gut health.

1.1.2 Bowel disorders

Physiological GIT function is crucial for sustaining gut homeostasis, but when compromised, it can lead to pathological conditions including (but not limited to) general infection of the GIT, food allergy, gastroesophageal reflux disease (GERD), cancer, irritable bowel syndrome (IBS) and inflammatory bowel disease (IBD) [136]. These disorders often manifest as a range of symptoms including ulceration, inflammation, obstruction, diarrhoea, constipation and abdominal pain.

A key common factor in the development and progression of GIT disorders is increased intestinal permeability and abnormal barrier function, which disrupt normal gut homeostatic balance. The symptoms of many of these GIT disorders are often exacerbated during periods of stress, and negative emotions such as anxiety and depression [137]. The following section provides a brief description of the common GIT disorders and discuss how disrupted gut homeostasis may result in the development and progression of these conditions.

1.1.2.1 General infection in GIT (Gastroenteritis)

Gastroenteritis is a short-term illness characterised by infection and inflammation of the GIT, commonly caused by viruses, bacteria, parasites, chemicals or medications [138]. Acute

gastroenteritis affects individuals of all ages, with young children and elderly being particularly vulnerable to dehydration and severe complications [139].

Amongst infectious causes, enteric viruses are the leading contributors to gastroenteritis in the world [139]. Rotaviruses primarily affect young children [140], whilst noroviruses infect individuals across all age groups, accounting for approximately 20% of global cases of acute gastroenteritis [141]. Viral gastroenteritis presents with sudden onset of vomiting, watery diarrhoea, abdominal cramps and low-grade fever [142]. However, distinguishing viral from bacterial gastroenteritis based solely on clinical symptoms is challenging, necessitating laboratory testing for precise diagnosis [139]. Most cases of viral gastroenteritis resolve within 2-5 days [143], with treatment primarily focusing on maintaining adequate hydration [139]. It has been shown that rotaviruses target the intestinal villus enterocytes and enteroendocrine cells whilst sparing crypt cells, leading to enterocyte infections that cause absorptive cell destruction, enzyme downregulation and dysfunction of the TJs [144]. Conversely, the exact pathogenesis of norovirus-induced gastroenteritis remains unclear due to historical difficulties in cultivating the virus in laboratory settings [145]. Nonetheless, studies suggest norovirus infection is associated with epithelial barrier dysfunction [146], and viral antigens have been detected in villus enterocytes of immunocompromised patients with chronic infection [147].

On the other hand, bacterial gastroenteritis is frequently caused by *Campylobacter*, enteroaggregative *Escherichia coli*, non-O157 Shiga-toxin-producing *E. coli* and non-typhoidal *Salmonella* species [148], and it is the primary cause of traveller's diarrhoea [149]. The pathogenic mechanism of bacterial gastroenteritis involves toxin production and direct invasion of the intestinal mucosa, leading to dysentery in the GIT [150]. Like viral gastroenteritis, mortality from bacterial-induced gastroenteritis is often due to severe dehydration, particularly in vulnerable populations such as infants and the elderly [151]. Other common causes of gastroenteritis include *Giardiasis* [152] and C*ryptosporidium* infection [153].

1.1.2.2 Food allergy

Food allergy is a GIT disorder that arises due to a failure in oral tolerance, a natural immune response regulated by gut-associated lymphoid tissues and influenced by the gut microbiota [154]. The GIT serves as the primary exposure site to food allergens, leading to a range of symptoms including nausea, vomiting, diarrhoea, abdominal food, regurgitation and constipation [155]. These allergic reactions occur when the immune system mistakenly identifies certain food proteins as harmful, triggering a dysregulated inflammatory response.

Food allergy is most prevalent in infancy and early childhood, affecting about 6-8% of children [156]. This increased susceptibility is attributed to the immaturity of the gut barrier and immune system in these young individuals [157]. The most common food allergens, responsible for over 90% of food allergies in children worldwide [155], include dairy products such as milk, butter, cheese and cream, eggs, soybeans, wheats, peanuts, tree nuts such as almonds, hazelnuts and cashews, as well as seafood such as fish and shellfish [158]. Whilst many children outgrow allergies to dairy products, eggs, soybeans and wheats, studies indicated that allergies to peanuts, tree nuts and seafood often persist into adulthood [159]. Additionally, the worldwide prevalence of food allergies has increased over the last decade [160], like due to the global adoption to the Westernised lifestyles and diets [155].

Allergic food reactions can range from mild gastrointestinal symptoms to severe, life-threatening anaphylaxis [161]. The diagnosis of food allergy is based on clinical presentation, medical history and laboratory tests [162]. Initiation assessment involves the evaluation of symptoms onset, followed by investigation of potential co-factors that exacerbate reactions. These co-factors include exercise, alcohol and the use of non-steroidal anti-inflammatory and anti-histamine drugs [163]. The collected information then guides the appropriate selection of laboratory test to confirm the allergy diagnosis.

1.1.2.3 Gastroesophageal reflux disease (GERD)

Gastroesophageal reflux disease (GERD) is a chronic condition characterised by recurrent heartburn and acid regurgitation, often leading to complications such as oesophagitis, peptic strictures and Barrett oesophagus [164]. GERD is caused by the dysfunction of the oesophago-gastric junction, where the prolonged relaxation of lower oesophageal sphincter allows the gastric contents to be refluxed in the oesophagus [165]. In addition to recurrent acid regurgitation, GERD patients may also experience extra-oesophageal symptoms such as hoarseness, cough, wheezing and asthma, as gastric juices reach the pharynx, larynx and into the airways [166]. Figure 1.9 shows a representative macroscopic image of an oesophageal tissue obtained from a GERD patient, which illustrates the characteristic tissue damage (ulceration to the mucosa) associated with the condition as a result of acid reflux.

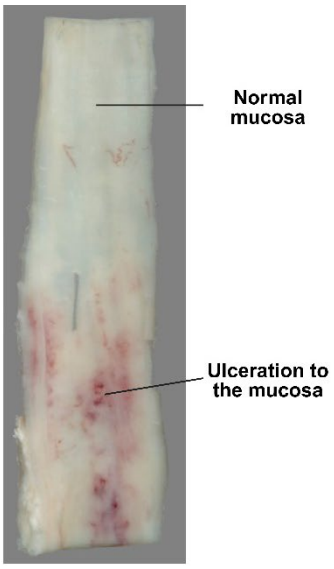

Figure 1.9. Representative macroscopic image of an oesophageal tissue with gastroesophageal reflux disease (GERD). The specimen is obtained from a male patient with GERD. The proximal oesophageal mucosa appears normal whilst a markedly dark colour with the presence of ulceration can be seen in the distal region, which are thought to cause by the reflux of gastric contents. The image was provided by The Ainsworth Interactive Collection of Medical Pathology, Faculty of Medicine & Health, The University of Sydney, specimen ID 33.2571.1.

GERD reportedly affects ~13.3% of adults globally, with high rates observed in South Asia, Central, South and North America, and Europe [167]. It has been shown that the prevalence of GERD increases with age, affecting 14% of individuals under the age of 50 and 17.3% of those who are 50-year-old and older [167]. GERD is also common in infants, with nearly 50%

of them experiencing daily regurgitation or vomiting, however, 90% of these cases spontaneously resolve by 1 year of age [168].

Complications of GERD include esophagitis, which occurs in 18-25% of symptomatic patients [169], and peptic strictures, which develops in 7-23% of those with untreated erosive oesophagitis [170]. A meta-analysis on over 26,000 GERD patients have found that the pool prevalence of Barrett oesophagus, a precursor lesion of oesophageal adenocarcinoma (OAC), is 7.2% [171]. The incidence of oesophageal cancer has increased rapidly over the last 40 years, averaging 1.1 cases per 100,000 persons in men and 0.3 per 100,000 persons in women [172].

Lifestyle modifications, such as weight loss, smoking cessation, bed elevation and dietary adjustments have been shown to effectively alleviate GERD symptoms [173-175]. Additionally, proton pump inhibitors (PPIs) are the most effective pharmacological intervention [176], and continuous PPIs treatment is recommended for patients with oesophagitis and Barrett oesophagus to prevent recurrent acid regurgitation and reduce cancer risk [177].

1.1.2.4 Cancers of the GIT

Cancers of the GIT are amongst the most prevalent forms of malignancy in human, arising from distinct tissues that make up the digestive system. The common types of GIT cancers include oesophageal cancer, stomach cancer and colorectal cancer.

1.1.2.4.1 Oesophageal cancer

Oesophageal cancer is a significant global health concern, ranking as the sixth leading cause of cancer-related deaths worldwide [178]. There are two major subtypes of oesophageal cancer: oesophageal squamous cell carcinoma (OSCC) and OAC. OSCC originates from the squamous epithelial cell lining of the oesophagus [179], accounts for nearly 90% of oesophageal cancer globally [180] (See Figure 1.10 for a macroscopic representative image illustrating the typical appearance of OSCC, highlighting the key pathological feature of cancer infiltration into the adjacent mucosa). Despite OSCC being the prominent subtype of oesophageal cancer in the world, its incidence is declining in many regions [181, 182]. Risk factors of OSCC include chronic chemical or physical damage to the oesophageal mucosa [183] and a low intake of fruits and vegetables [184]. In contrast, the incidence rates of OAC have been increased markedly over the recent years [185]. As discussed above, OAC develop from Barrett oesophagus, where the tumours are primarily localised to the distal oesophageal region with a glandular structure [186]. The main risk factor for OAC is prolonged reflux of gastric acids (often in the case of GERD) or bile [187]. The prognosis rate for patients with oesophageal cancer is poor, with the 5-year survival rate being less than 20% for both subtypes [188, 189]. However, both OSCC and OAC have detectable dysplastic precursor lesions, which can be identified though endoscopy [190] and treated with local ablation therapies [191, 192], which potentially avoids extensive surgical remove of the oesophagus.

Treatment strategies for OSCC and OAC heavily depends on tumour stages and patient fitness, where endoscopic resection is common for very-early-stage designated tumours (relatively small primary tumour size, no regional lymph node infiltration and absence of distal organ metastasis), whereas chemotherapy, chemoradiotherapy or a combined strategy of chemotherapy and oesophageal resection may be used for more advanced staged tumours [180].

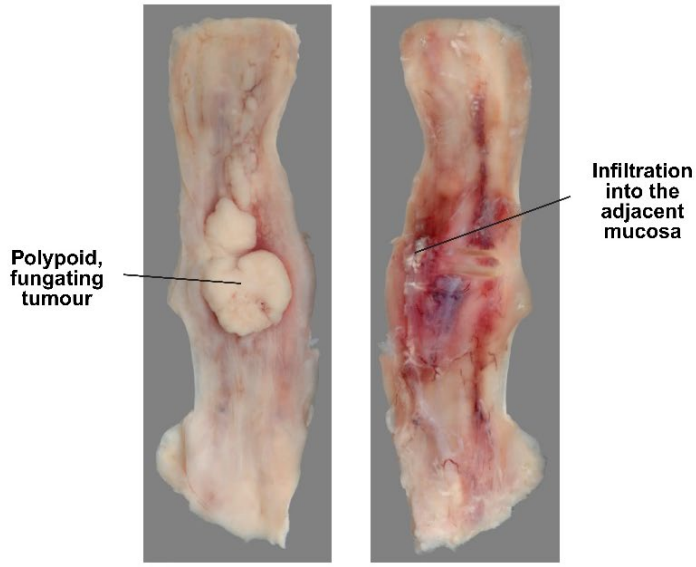

Figure 1.10. Representative macroscopic image of an oesophageal squamous cell carcinoma (OSCC) tissue with a fungating tumour. The fungating tumour can be observed in the middle of the oesophagus. There are signs of mucosa infiltration but the tumour has yet to penetrate the full thickness of the oesophageal wall. The specimen image was obtained from The Ainsworth Interactive Collection of Medical Pathology, Faculty of Medicine & Health, The University of Sydney, specimen ID 33.861.2.

1.1.2.4.2 Stomach cancer

Stomach cancer, also known as gastric cancer, is the fifth most common cancer and the third leading cause of cancer-related deaths in the world, with over 1 million new cases diagnosed annually [193]. It is anatomically classified into true gastric adenocarcinoma (non-cardia gastric cancer) and gastro-oesophageal junction adenocarcinoma (cardia gastric cancer), with the latter further categorised using the Siewert classification [194]. *Heliobacter pylori* infection is the most significant risk factor for sporadic gastric cancer [195], as chronic inflammation induced by the bacteria can lead to oncogenesis though altered cell proliferation, apoptosis and epigenetic modification of the stomach [196]. Epstein-Barr virus has also been shown to associate with the development of gastric cancer [197], particularly in cases with lymphoid stroma. However, the pathogenic mechanism of this virus in inducing gastric cancer development is currently unclear [198]. Additionally, it has been shown that approximately 10% of gastric malignancies occur within families [199], where genetic mutation in *CDH1* and *CTNNA1* has been observed in hereditary diffuse gastric cancer [200, 201], a common type of hereditary cancer syndrome. Early-stage gastric cancer is often asymptomatic [202], as a result, gastric cancer patients often received their diagnosis toward the later stage, which contributes the high mortality rate of this malignancy. Common symptoms of gastric cancer include anorexia, dyspepsia, weight loss and abdominal pain, with dysphagia also seen in tumours gastro-oesophageal junction [203]. The main treatment option for gastric cancer is adequate surgical resection of the carcinogenic area of the stomach [204].

1.1.2.4.3 Colorectal cancer

Colorectal cancer is the third most commonly diagnosed cancer and the second leading cause of cancer-related death worldwide [205, 206], with over 1.9 million new cases and

approximately 940, 000 deaths recorded in 2020 [207]. Its development is influenced by multiple factors, including genetic predisposition, family or personal history of colorectal cancer, polyps, IBD, diabetes mellitus, and previous cholecystectomy [208-213]. Lifestyle factors such as obesity, physical inactivity, smoking, alcohol consumption and poor diet also increase the risk [209, 214-217], alongside influences with gut microbiota and socioeconomic status [218, 219]. The carcinogenesis of colorectal cancer occurs in three stages [220], initiation, promotion and progression, where it starts with irreversible genetic damage, followed by abnormal cell proliferation and formation of benign precursor lesion, and ultimately transformation of benign precursor lesion into malignant tumours with aggressive features and metastatic potential. Adenomatous and serrate polyps are recognised as precursor carcinogenic lesion in most cases of colorectal cancer [221, 222].

Patients with colorectal cancer may present with rectal bleeding, abdominal pain, changes in bowel habits, unexplained weight loss and iron-deficiency anaemia [223]. Diagnosis of the disease primarily relies on endoscopic procedures such as colonoscopy, sigmoidoscopy and rectoscopy [216], which allow for tumour detection and tissue sampling. Currently, surgery remains the primary curative approach for non-metastatic colorectal cancer cases [224], with pre-operative or chemoradiotherapy recommended for advanced stage tumours to improve surgical outcomes [225]. Representative macroscopic image of colorectal cancer is highlighted in Figure 1.11a, where the tumour has infiltrated the full thickness of the intestinal wall. The tumour also resulted in dilation and muscle hypertrophy of the colon above the lesion and a complete obliteration of the intestinal lumen in the distal part of the colon. Figure 1.11b shows the representative microscopic image of the tissue section isolated from the same specimen, where a clear glandular pattern adenocarcinoma invading into the muscularis propria layer could be observed.

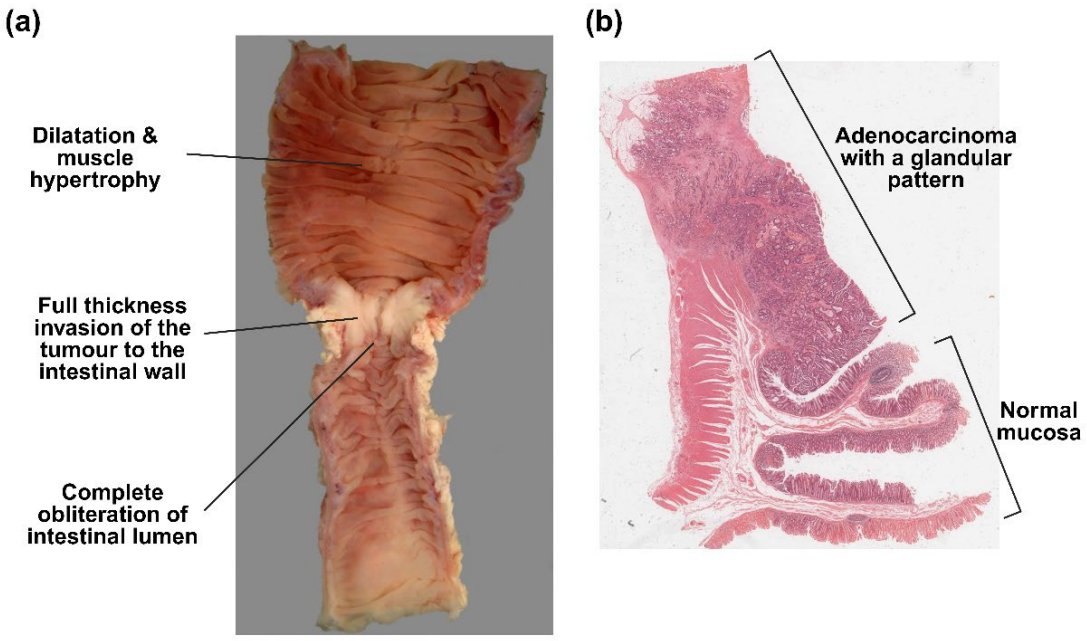

Figure 1.11. Representative macroscopic and microscopic images of colon adenocarcinoma. (a). Representative macroscopic image of a resected colon specimen. A white, annular, obstructing mass measuring 2.5 cm in length and 2 cm in diameter can be seen at the centre of the specimen. This lesion is located at the splenic flexure and has infiltrated the entire thickness of the intestinal wall. Proximal

to the lesion, the colon exhibits dilatation and muscular hypertrophy and the lumen appears almost completely occulted by the mass. The image of this specimen was obtained from The Ainsworth Interactive Collection of Medical Pathology, Faculty of Medicine & Health, The University of Sydney, specimen ID 354.863.4. (b). Representative microscopic image of the same specimen. The image was obtained from the Etaki virtual slide platform (Discipline of Pathology, Faculty of Medicine & Health, The University of Sydney).

1.1.2.5 Irritable bowel syndrome (IBS)

Irritable bowel syndrome (IBS) is a chronic functional disorder of the GIT characterised by altered bowel functions [226]. Patients with IBS often present with abdominal pain, diarrhoea, constipation, bloating and other functional gastrointestinal symptoms such as nausea, fullness and heartburn [227]. IBS has also been shown to associate with conditions such as fibromyalgia, chronic fatigue syndrome, GERD and psychiatric disorders [228-230], which significant impact the quality of life and work productivity of the patient. In the meta-analysis by Lovell *et al.*, it has been highlighted that IBD has the highest prevalence in South America, affecting approximately 21% of the population, the lowest prevalence can be found in Southeast Asia, which only affects 7% of the population [231].

In Australia, the prevalence of IBS has been reported to be 3.5%, and some individuals with IBD also experience IBS [232]. It has been shown that IBD is more common in women than men in North America, with women more frequently experiencing abdominal pain and constipation, while men report diarrhoea more often [233]. The exact cause of IBS is not well established, however, abnormalities in gut motility, visceral sensitivity, brain-gut axis and psychological factors are also linked to IBS pathogenesis [234]. Additionally, studies also reported that gut immune activation, increased intestinal permeability and microbiome dysbiosis are also implicated in the pathogenesis of IBS [235, 236]. Management strategies for IBS include dietary modifications, antidepressants, pharmacotherapy and probiotics [237-240]. Different to IBS, which is a functional disorder, another GIT disorder that possesses similar clinical manifestations, IBD, is a chronic inflammatory condition that damages the bowel and leading to ulcers and intestinal narrowing, which will be explored in greater details below as well as in later chapters of this thesis.

1.2 Inflammatory bowel disease (IBD)

IBD is a chronic recurrent inflammatory condition that mainly affects the GIT [241]. The two main clinical presentations of IBD include ulcerative colitis (UC) and Crohn's disease (CD). A less common clinical subtype, indeterminate colitis (IC), is diagnosed when clinical features are ambiguous and unequivocal and cannot definitively point to a UC and CD diagnosis [242]. Nevertheless, IBD patients diagnosed with UC, CD or IC share similar disease symptoms, including abdominal pain, diarrhoea, rectal bleeding and weight loss [243]. Patients typically experience alternating phases of active disease (classified as mild, moderate, or severe) and remission (a quiescent state) [244]. The current body of research described in this thesis focuses on IBD, where recent advances in the field of this debilitating condition and attempts in addressing current knowledge gaps in identifying new treatments will be discussed.

1.2.1 Ulcerative colitis

UC, first described in 1859 by Dr. Samuel Wilks in a 42-year-old woman with prolonged diarrhoea and fever [245]. This clinical presentation of IBD represents a chronic condition

characterised by acute mucosal inflammation that begins in the rectum and extends proximally through the colon in a continuous pattern [246]. This contiguous colon inflammation typically remains confined to the mucosal layer, causing superficial damage to the GIT wall (Figure 1.12). Although the exact pathophysiology of UC remains elusive, it is considered as an intestinal barrier disease, initiated by dysfunction in the epithelial cells or structural elements of the intestinal barrier [247].

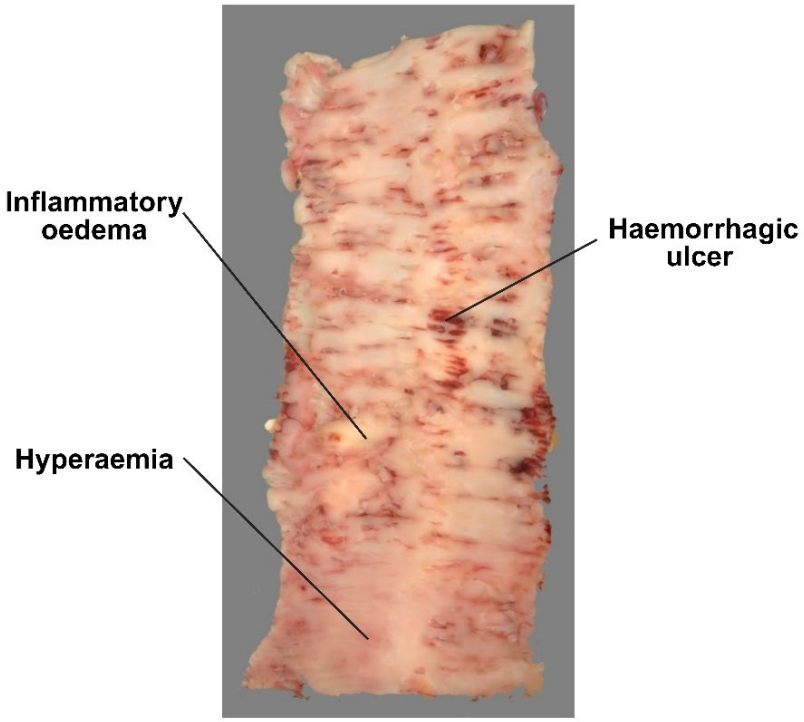

Figure 1.12. Macroscopic image of a human colon tissue from a patient with chronic ulcerative colitis. The colonic mucosa appears irregular, with multiple transverse mucosal defects. The ulcers vary in size, with many exhibiting signs of haemorrhage. In some regions, they have merged to form larger, irregular lesions. The edges of the specimen are eroded and the presence of inflammatory oedema and hyperaemia can be seen at the surrounding mucosa. The image was obtained from The Ainsworth Interactive Collection of Medical Pathology, Faculty of Medicine & Health, The University of Sydney, specimen ID 354.599.5.

As described above, disruption of epithelium function allows colonic bacteria to cross the barrier, resulting in macrophage activation, antigen presentation, which leads to chemokine expression and subsequent recruitment of neutrophils to the affected colon tissue [246]. Secondary immune responses include monocytes maturing into macrophages that produce cytokines such as TNF-α, IL-12, IL-23 and IL-6 [248, 249], which polarise Th1 cells. Additional contribution to barrier dysfunction come from IL-36γ, which inhibits Treg cells and induce Th9 cells polarisation [250]. It has also been shown that UC associates with a decreased gut microbiota diversity and a reduced concentration of SCFAs [251], alongside a diminished synthesis of colon mucin 2 [252], which further compromises the protective mucus layer and exacerbates barrier breaches. Continued unregulated inflammation also drives the formation of the inflammasome that signals a transition between acute and chronic responses [246].

1.2.2 Crohn's disease

Named after Dr. Burrill B. Crohn, CD is a chronic gastrointestinal disorder characterised by patches of inflammation interspersed with normal-appearing mucosa that can occur anywhere along the GIT [253]. Unlike UC, CD involves progressive, transmural lesions that can lead to complications such as fibrosis, strictures and fistulas [254]. Inflammatory processes in CD arise from epithelial barrier dysfunction, influenced by genetic factors such as polymorphism in NOD2 and nuclear factor kappa B (NF-κB) signalling pathway [254, 255]. This dysfunction allows luminal contents, including dietary components and gut microbiota to penetrate the lamina propria, which induces the activation of inflammatory T-lymphocytes including Th0, Th1, Th2 and Th17 cells by lamina propria residing dendritic cells [256]. The differentiation of these T cells results in the production of inflammatory cytokine such as interferon gamma (IFN-γ), TNF-α, IL-4, IL-6, IL-21 and IL-22. Concurrently, intestinal macrophage responds to luminal antigens and release IL-12 and IL-23 to activate natural killer cells, which further perpetuates the inflammatory cascade [257].

In addition to excessive colon inflammation, 21-47% of CD patients also present with systemic extraintestinal manifestations (EIMs) [258], which significantly impact the quality of life and can lead to long-term outcomes including the increased risk of hospitalisation and surgery. EIMs can involve various body systems, including the musculoskeletal system, the oral cavity, the eyes, and hepatobiliary system [259]. Additionally, the risk of developing colorectal cancer is increased in CD patients when compared to the general population [260]. Hence early diagnosis and correct treatment of CD is essential to limit the progression to colon cancer.

1.2.3 Diagnosis of IBD

The diagnosis of IBD requires a multidisciplinary approach, with clinical evaluation supported by endoscopic, histological and biochemical investigations, as no single gold-standard tool is available. Endoscopy is a cornerstone in diagnosing IBD, with proctosigmoidoscopy is often the initial examination [261]. However, this procedure is not sufficient for differentiating IBD from infectious colitis. A full diagnostic colonoscopy is essential to define IBD clinical subtypes (UC, CD or IC), with the intubation of the terminal ileum and systematic collection of biopsies from each segment of the colon and ileum are performed [261].

In terms of diagnosis following colonoscopy, UC patients are characterised by uniform continuous inflammation starting in the rectum and confined to the colon, whereas CD cases can affect any part of the GIT with skip transmural inflammation [246, 254]. Histological examination of biopsy samples plays a critical role in IBD diagnosis. In UC, inflamed mucosa typically shows diffuse chronic neutrophilic infiltration restricted to the colon, accompanied with mucus depletion, cryptitis, crypts abscesses and epithelial architectural distortion [262].

In contrast, CD histology reveals intact goblet cells with minimal mucosal layer disruption, along with a mononuclear immune cell infiltration dominated by T cells and macrophages [261]. CD patients also present with granulomas from their biopsy samples, which are observed in 40-60% of surgical specimens and 15-36% in biopsy samples [263]. Biomarkers are valuable adjuncts for IBD diagnosis, severity assessment and disease monitoring. The biomarker C-reactive protein (CRP) is produced by the liver [264]. Serum CRP level ranges from 5-200 mg/mL in IBD patients [265] and can be a useful marker for distinguishing active IBD patients from remission cases [266]. Faecal calprotectin is a highly sensitive marker for colonic inflammation and correlates more closely with disease activity in UC than CD [267].

Additional faecal markers include lactoferrin, polymorphonuclear neutrophil elastase, neopterin, and S100A12 can also be used to aid the diagnosis of IBD [268-271].

1.2.4 Prevalence& Incidence rate of IBD

The global burden of IBD has risen substantially in recent decades, with incidence rates varying widely by region, ranging from 0.1 to 58 cases per 100,000 persons annually [272]. The highest incidence rate of IBD is reported in North America, northern and western regions of Europe and in Oceania [254]. For instance, CD incidence ranges from 0 to 20.2 cases per 100,000 persons in North America and 0.3 to 12.7 per 100,000 persons in Europe [272]. The prevalence of CD is also prominent in Western countries, with Germany reporting 322 cases per 100,000 persons and Canada with 319 cases per 100,000, the top two IBD-bearing nations in the world [272]. Owing to the influence of Western lifestyle of diets and industrialisation [254], IBD incidence rates in developing regions of the world including Asia, Africa and South America has risen significantly since the early 21st century. Among these jurisdictions, India has the highest incidence rate of IBD of 9.31 cases per 100,000 persons and an UC incidence rate of 5.41 cases per 100,000 persons [273].

Although overall prevalence remains lower than in Western countries, CD incidence has grown more rapidly than UC in Asia. This is most notable in data from Taiwan, where CD prevalence rose from 0.6 cases per 100,000 persons in 2001 to 3.9 cases per 100,000 in 2015 [274]. Paediatric IBD is increasingly recognised, with Scandinavia and Canada reporting the highest rates in children under 16 years of age. The incidence of paediatric IBD is 10.6 cases per 100,000 children in Norway [275], 12.8 in Sweden [276] and 9.68 in Canada [277]. Gender differences are also evident, with CD being more prevalent in male during childhood but shifting to a female predominance in adulthood. In contrast, UC incidence is similar between sexes across all ages [278]. These trends underscore the rising global impact of IBD and highlight the need for ongoing research to identify innovative treatments that improve patient quality of life and relief burdens on the healthcare system.

1.2.5 Risk Factors of IBD

The exact cause of IBD remains unknown, but its development has been shown to associate with the interplay of genetic predisposition, gut microbiota dysbiosis and environmental influences. Whilst each factor contributes to disease risk, none of these documented factors alone is sufficient to trigger IBD, instead, complex interactions among these various elements are thought to drive the disease onset (Figure 1.13) and this may vary between individuals due the many variables involved.

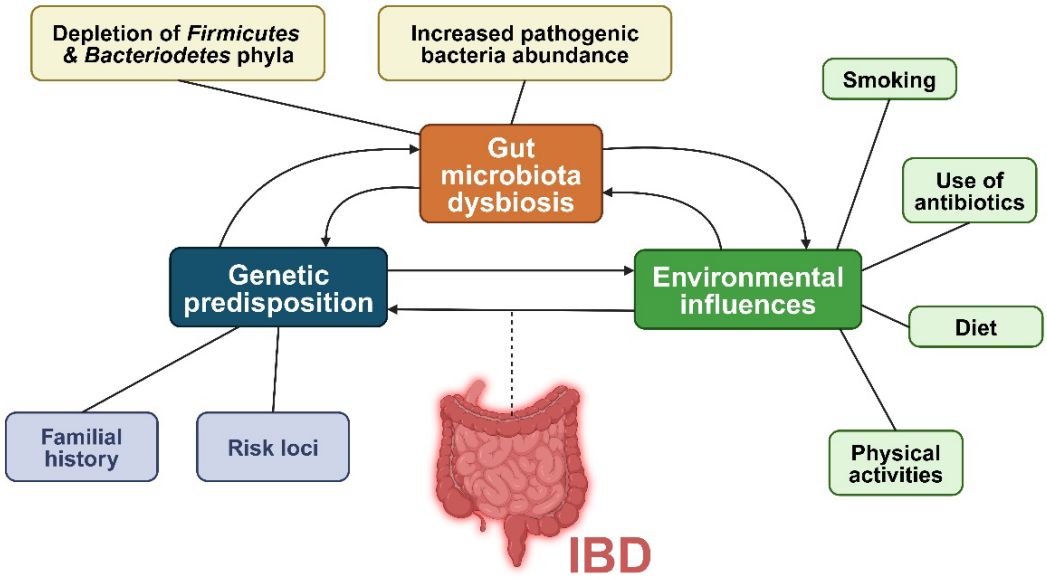

Figure 1.13. Risk factors of IBD. It has been appreciated that the development of IBD arises from the interplay of established risk factors, which includes genetic predisposition such as familial history and risk loci, gut microbiota dysbiosis (characterised by the depletion of Firmicutes and Bacteroidetes phyla) and increased abundance of pathogenic bacterial and environmental influences such as smoking, antibiotic use*, diets and physical activities. Figure was generated in https://BioRender.com with appropriate permissions.*

1.2.5.1 Genetic predisposition

Genetic predisposition is a significant risk factor for IBD, with family history being a common feature among patients. Approximately 2-14% of CD patients reported a family history of CD, of which a smaller proportion of them have a family history of UC. Similarly, 8-14% of UC patients report a family history of IBD [279]. The risk of developing IBD is higher for first-degree relatives, with an estimated relative risk of 5% for non-Jewish CD patients and 8% for Jewish CD patients. For CD, the corresponding risks are 1.6% for non-Jewish patients and 5.2% for individuals with a Jewish background [280]. Notably, the likelihood of an individual to develop IBD before the age of 30 is as high as one-third if both parents have established disease [279].

Genetic studies have identified more than 160 distinct risk *loci* of IBD [281], with about 30% of IBD-related genetic loci are shared between the CD and UC and has a similar direction of effects [282]. However, some loci, such as *NOD2* and *ATG16L1* are specially linked to the development of CD [283, 284]. It has been shown that homozygous bearing of the *NOD2 loci* increase the disease risk by approximately 20-fold, while heterozygosity confers a 2-6-fold elevated risk [285]. Despite these findings, the known genetic risk *loci* can only account for 16% and 23.2% of the heritability of UC and CD respectively [286, 287]. This suggests that environmental factors may play a significant contributing role in IBD pathogenesis, which will be further discussed below.

1.2.5.2 Gut microbiota dysbiosis

Dysbiosis of gut microbiota in IBD is characterised by significant alterations in the composition and diversity of intestinal bacteria. This dysbiosis in UC patients is characterised by reduced

species bacterial diversity, where the depletion of *Firmicutes* and *Bacteroidetes* phyla has been observed in surgical specimens [288]. In support of this finding, a twin study comparing mucosal biopsy samples from the sigmoid colon showed increased abundance of *Actinobacteria* and *Proteobacteria* and decreased *Bacteroidetes* compared to their healthy twins [289]. Temporal instability of dominant taxa has also been reported in UC patients. A year-long study of UC patients in remission found that only 23% of the dominant taxa persisted, contrasting sharply with the 78% similarity index observed in healthy individuals over the same period [290].

In CD patients, the dysbiosis pattern shares similarities with UC. Mucosal specimens from active CD patients undergoing surgery showed markedly reduced microbiota diversity compared to non-inflamed control specimens [291]. A microarray study that used 500 16S rDNA probes demonstrated a decreased in abundance of several *Firmicutes* species in CD patients [292]. Like UC patients, temporal instability of dominant species was also observed in CD. Additionally, altered expression of certain bacteria species, specifically an overexpression of aggressive disease-driving bacteria and a reduced expression of beneficial bacteria has been reported in both UC and CD. For example, there is an increased presence of gram-negative sulfate-reducing *Desulfovibrio* subspecies in UC patients [293], which may contribute to UC pathogenesis through sulphide production. On the other hand, high levels of *Escherichia coli* species have been consistently observed in mucosal and faecal samples of CD patients [294, 295]. *Faecalibacterium prausnitzii*, a major representative of the *Clostridium leptum* group that exert anti-inflammatory effects to the GIT is reduced in both active and remission states of IBD (both UC and CD) patients [296, 297].

1.2.5.3 Environmental influences

Environmental factors play a significant role in development and progression of IBD, with smoking being one of the most documented influences. Smoking doubles the risk of developing CD [298], and is associated with a more aggressive disease course, greater likelihood of requiring immunosuppressive therapies, high surgical rates and a high chance of recurrence after ileocecal resection [299-301]. Conversely, smoking appears to have a protective effect against UC, as current smokers experience a milder disease course, fewer flare ups, and a reduced need for immunosuppressive treatments [302, 303]. However, former smokers are at increased risk of developing UC [304], and disease flares are often triggered within a year of smoking cessation [303]. Early-life exposure to smoke, including passive smoking has been shown to have similar effects [305].

The use of antibiotics in early childhood also increases risk of IBD. It has been demonstrated by IBD cohort studies, paediatric IBD patients that were exposed to antibiotics in their first year of life have a stronger association for CD than UC [306], and a higher risk for those who used antibiotics in their first year of life compared to the ones who were exposed to later use [307], suggesting that early perturbation of the gut microbiota may disrupt immune development and increase susceptibility to IBD. Dietary factors also influence IBD risk. High dietary fibre intake, especially from fruits and vegetables, has been associated with a 40% reduction in CD risk [308]. This protective effect is thought to be mediated by enhanced production of SCFAs by intestinal bacteria, which help maintain epithelial barrier integrity and suppress pro-inflammatory mediator productions [309]. Whilst dietary fat has been linked to IBD pathogenesis in mouse model of IBD [310], human prospective cohort study has not confirmed this association [311]. Physical activity is another environmental factor that

influence IBD development. Sedentary lifestyles, linked to office or light manual work, are associated with a higher risk of IBD, while heavy manual labour appears to be protective [312]. In mice, voluntary exercise has been shown to alleviate colitis symptoms, while forced exercise can worsen inflammation likely due to increased physical and psychological stress [313]. In support of these findings, prospective cohort studies have shown that voluntary rigorous physical activity can reduce CD risk by 44% [314].

1.3 Immune dysregulation & Redox imbalance in IBD

This section further explores the pathophysiology of UC and CD, with a particular focus on immune dysregulation and redox imbalance. The potential therapeutic approach on targeting these immune dysregulations and on restoring redox equilibrium will also be discussed.

1.3.1 Neutrophils in IBD pathogenesis

Excessive neutrophil recruitment to the intestinal mucosa accompanied with disrupted intestinal epithelial barrier and altered crypts architecture is a hallmark of IBD [315]. The transepithelial migration of neutrophils induced by cytokines IL-8 and IL-33 [316, 317], and chemokines CXCL5, CXCL7, CXCL10 and CCL20 [318-321], whilst several IBD susceptible genes such as lymphocyte-specific protein 1 and hepatocyte growth factor active have been shown to promote neutrophil infiltration [322]. At the site of inflammation, neutrophil-derived proteases, including matrix metalloproteinase (MMP) and NE, degrade epithelial tight junctions [323-326], which deforms crypts and promote abscess formation. Additionally, neutrophil produce proinflammatory cytokines such as TNF and IL-1β [327, 328], which further recruit other immune cells such as macrophages, dendritic cells and T-lymphocytes to the site of inflammation [315, 329], which amplifies the inflammatory response. It has also been shown that α-defensins and calprotectin released by activated neutrophils recruits additional neutrophils to the inflamed sites [329, 330], creating a self-perpetuating cycle of inflammation, which further enhances the magnitude of immune response. Accumulated NETs have also been observed in colon tissue and blood of both UC and CD patients [330-334], which not only intensify immune responses, but also increase the risk of venous thromboembolism during active IBD [333] (See Figure 1.14 for potential contribution of NETs in IBD and the effect of inhibiting NETs in animal models of IBD will be further explored in Chapter 3 of this thesis).

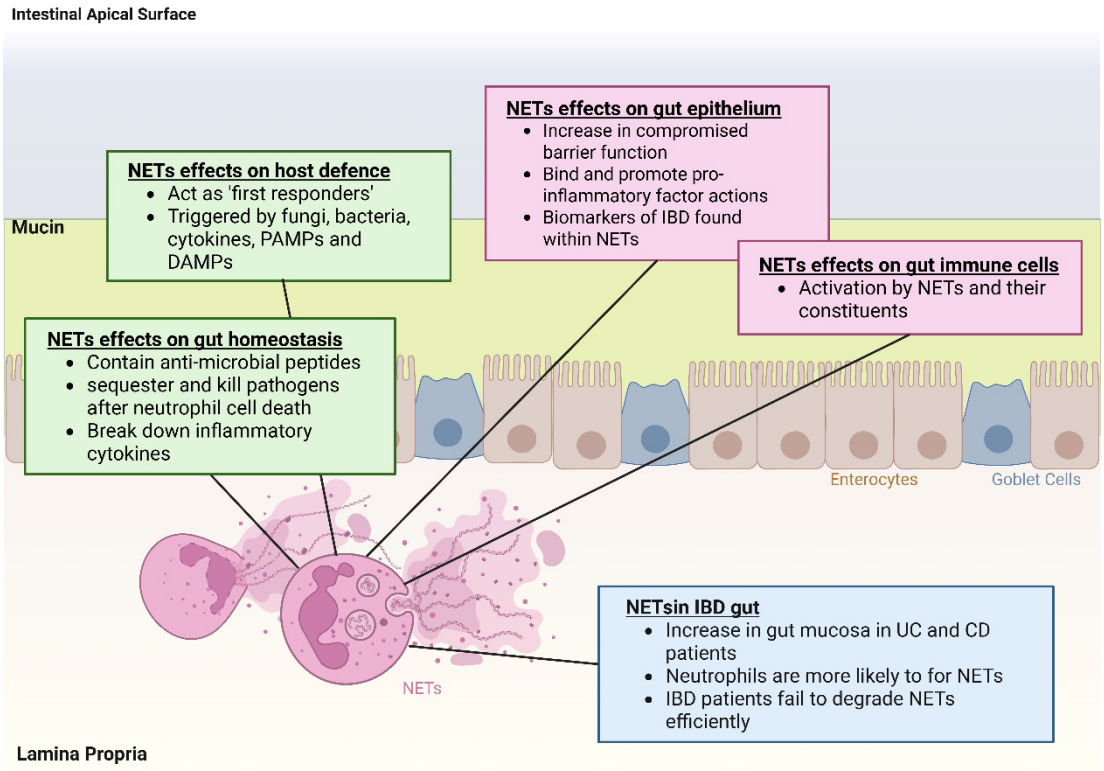

Figure 1.14. The potential contributions of NETs in IBD. Under physiological conditions, NETs act as a host defence system and maintain gut homeostasis. However, elevated level of NETs has been reported in gut mucosa of UC and CD patients. This is accompanied with higher tendency of NETs formation from neutrophils and the impaired degradation of these extracellular structures in IBD patients. It has been postulated that NETs are implicated in gut epithelium barrier functions and activate gut immune cells during the pathogenesis of IBD. Figure was adapted from [335] generated in https://BioRender.com with appropriate permissions.

Neutrophil dysregulation has been proposed to contribute differently to UC and CD [336]. In UC, neutrophil overactivation is central to disease pathogenesis, with increased neutrophil to lymphocyte ratios [337], elevated levels of neutrophil-derived proteases like NE and MMP-9 [338, 339] and elevated neutrophil infiltration in patients with therapeutic resistance to corticosteroids and cyclosporine A [340, 341], when compared to UC patients that are sensitive to these treatments have been reported. In CD, however, neutrophil dysfunction is thought to be a key factor, where an impaired recruitment [342], and reduced oxidative activity has been observed [343]. Additionally, delayed neutrophil-mediated bacterial clearance in CD results in persistent antigen presentation in the gut, which leads to the upregulation of adaptive immune responses and the formation of granuloma [344]. Therefore, therapeutic strategies aiming to reduce overaction of neutrophils while preserving their critical immune functions should be explored. Indeed, attempts in targeting neutrophils and neutrophil-derived contents has yielded various degree of success in animal models of experimental colitis, which will be discussed in detail in later sections.

1.3.2 Mast Cells in IBD pathogenesis

Mast cells are known for their involvement in IgE-mediated type I hypersensitivity [345], however, these cells are also capable of non-IgE driven autoimmune conditions and their role

in UC and CD has gained growing recognition [346]. Preclinical studies on animal models of experimental colitis strongly support the involvement of mast cells in IBD. For example, mast cell deficient $Kit^{w\text{-}sh/w\text{-}sh}$ mutant mice has been shown to be protective against intestinal inflammation whilst reconstitution of wildtype mast cells restores their susceptibility to develop experimental colitis [347]. Additionally, the study by Kurashima *et al.* demonstrated that inhibition of ATP receptor P2X7 reduced mast cell activation and simultaneously alleviated subsequent intestinal inflammation, highlighting the potential role of mast cells in IBD pathogenesis [347]. In further support of this notion, increased expression of P2X7 has been observed in the colonic mast cells of patients with active CD [348]. The accumulation of mast cells has also been reported in active CD patients, where increased number of mast cells has been observed in regions of mucosa, submucosa, muscularis propria and the surround fat tissues [349, 350]. This is accompanied by the elevated level of mast cell mediators in the colon mucosa [351, 352] and higher presence of N-methylhistamine, a metabolite of mast cell-secreted histamine [353], in the urine of the IBD patients, which further reinforces the potential pathogenic role of mast cells in IBD. Increased density of mast cells has also been reported in the colon of UC patients [354].

As mentioned above, stress is another factor linking the involvement of mast cells to IBD. A year-long population-based study involving 704 IBD patients have identified that perceived stress, negative mood and major life events are triggers for symptomatic IBD flare ups [355]. One possible mechanism potentially involves the activation of colonic mast cells. It has been shown that chronic psychological stress activates mast cells via substance P and eosinophil-secreted corticotrophin release hormones, which subsequently lead to barrier dysfunction [356]. Nevertheless, further investigation is warranted to confirm the pathogenic involvement of mast cells in human IBD.

1.3.3 Macrophages in IBD pathogenesis

In active IBD, macrophages accumulate in large numbers at the inflamed sites, producing vast amounts of pro-inflammatory cytokines such as TNF-α, IL-1β, IL-6 and IL-23 [357-360], which contribute to persistent inflammation and immune dysregulation characteristic of IBD. This is accompanied with the aggressive response of activated macrophages to commensal bacteria such as *Escherichia coli* and *Enterococcus faecalis* [359], which further exacerbate inflammation in the gut. One hallmark feature of CD is the formation of granulomas, which consist of aggregated macrophages and other inflammatory cells [361], highlighting the central role of macrophage in the disease progression of IBD. In support of the involvement of macrophages in IBD pathogenesis, genetic studies have identified several IBD susceptibility loci associated with monocytes and macrophage function [362-364], indicating that genetic alterations in these loci may result in dysfunctional macrophage activities and increased risk of IBD development.

Among these, mutations in NOD2 represent one of the strongest inheritable risk factors for IBD [365]. Loss-of-function mutation in NOD2 impairs macrophage function, leading to defective bacterial detection and clearance in the gut. This defect triggers constitutive activation of the inflammasomes and NF-κB signalling pathways [366], contributing to chronic inflammation. Moreover, NOD2 mutations have been linked to pathogenic activation of macrophages and fibroblasts in the peripheral blood of CD patients [362]. Deficiencies in other CD-risk genes, such as ATG16L1 and IRGM further highlight the role of impaired autophagy in macrophage dysfunction [364].

Furthermore, it has been demonstrated that macrophages with these genetic deficiencies exhibit defects in sensing intracellular microbial products and lysosome-mediated clearance [364], which results in exacerbated inflammation and tissue damage manifested in CD. Clinical evidence supports the correlation between aberrant macrophage activities and IBD disease severity, where IBD patients achieved clinical remission has been shown to correlate with a reduced pro-inflammatory macrophage activity [367, 368], suggesting that therapeutic strategies targeting macrophage dysregulation may be beneficial for IBD patients. However, a recent randomised, double-blind clinical trial on selective granulocyte and monocyte apheresis in 235 moderately or severely active CD and 215 UC patients with similar disease severities demonstrated no significant clinical benefits [369, 370].

1.3.4 T-Cells in IBD pathogenesis

Endogenous T-cells play a central role in mediating mucosal damage observed in IBD, including both UC and CD. Whilst there is no marked difference $CD8^+$ T-suppressor and $CD4^+$ Th cells population in the lamina propria and epithelium of IBD patients [371], an aggravated activation of these lymphocytes has been observed [372]. Activated T-cells release the pro-inflammatory cytokine IL-2 [373], which promotes the survival and proliferation of themselves through autocrine signalling via IL-2 receptors (CD25) [374]. In IBD, $CD25^+$ cells constitute more than 50% of the lamina propria mononuclear cells, with most being T-lymphocytes in the case of CD, and macrophages in UC [375].

Notably, $CD4^+$ T-cells that highly express the NKG2D receptors are a distinct subset of $CD4^+$ T-cells common in CD [376]. These cells exhibit cytotoxic activity and produce pro-inflammatory cytokines such as TNF-α, IFN- γ and IL-17A [376, 377], which leads to sustained mucosal inflammation. Additionally, Th1 cells induced by IL-12 and IL-18 from intestinal macrophages has also been shown to sustain mucosal inflammation in CD [378, 379]. Conversely, Th2 cells characterised by IL-13 secretion has been linked to impairing intestinal barrier function through epithelial apoptosis, tight junction disruption and reduced restitution velocity in UC [380]. It has also been shown that Th2 involved in UC development through the secretion of IL-5 [381], whilst IL-23 in the lamina propria drives the development of UC via IL-17 production [382].

In contrast, Tregs are implicated in IBD pathogenesis due to their dysfunctional suppressive function. In IBD patients, the number of peripheral Tregs has been shown to be reduced, whilst this is associated with an elevation of peripheral Th17 population [383]. In animal models of IBD, defective Treg function has been found to be associated with upregulation of T-cell specific T-box transcription factor (T-bet), phosphorylation of signal transducer and activator of transcription (STAT)-1 and activation of NF-κB, which contributes to intestinal inflammation and lesion development [384]. Attempts to target T-cells to dampen IBD-mediated intestinal inflammation as a novel treatment strategy have been reported in both experimental IBD models as well as in human trials.

1.3.5 Oxidative stress and redox imbalance in IBD pathogenesis

Chronically active inflammation in IBD is closely linked to the generation and release of ROS by immune cells [385]. Elevated oxidative stress is evidenced by increased biomarkers of lipid peroxidation and oxidative DNA. For instance, several studies have shown significantly higher levels of malondialdehyde (MDA) are present in the inflamed mucosa and blood of both UC and CD patients [386, 387], whilst a marked increase of 8-hydroxy-2'deoxyguanosine (8-

OHdG), a marker of oxidative DNA modification has been reported in isolated leukocytes from the blood of CD patients [388]. Furthermore, in patients diagnosed with UC, the study by Canbakan *et al*. has shown that severe inflammation correlates with higher MDA and MPO levels in intestinal tissues compared to controls or patients with moderate disease severity [389].

While it is clear that ROS function as essential signalling molecules in immunological processes, their continuous and unregulated formation during phases of active inflammation to the intestinal mucosa causes significant collateral damage [390]. This contributes to extensive cellular and molecular injuries, which perpetuates inflammation and exacerbates tissue damage/destruction. It has been shown that the presence of ROS activates redox-sensitive transcription factors like NF-κB, driving the expression of downstream inflammatory molecules, including components of the inflammasome pathway (Ref [391] and discussed below), which further amplifies intestinal inflammation.

In addition to increased oxidative stress, IBD patients also typically exhibit reduced antioxidant capacity. Studies utilising blood analyses have documented significantly decreased levels of the antioxidant enzyme glutathione peroxidase and its substrate reduced-glutathione in IBD patients [392, 393], reflecting a diminished capacity to neutralise ROS through thiol-dependent mechanisms. Supporting a role for anti-oxidation in IBD, the gut metabolic response to inflammation is critically regulated by master transcription factor nuclear factor erythroid 2-related factor 2 (Nrf2) and its inhibitor Kelch-like ECH-associated protein 1 (Keap1) [394]. Thus, it has been shown that activation of the Nrf2/Keap1 signalling pathways in animal models of experimental colitis increases antioxidant capacity through the production of down-stream antioxidant response elements, reduced intestinal inflammation and improvements in barrier function via maintenance of intestinal mucosa and epithelial integrity [395-397]. Together these outcomes highlight the potential for a dual role of Nrf2 in mitigating oxidative damage and suppressing inflammation in IBD. Interestingly, conflicting evidence of Nrf2 levels in IBD patients has been reported by published literature. For example, the study by Meyers *et al.*, a significantly lower level of Nrf2 has been observed in the blood of UC patients [398], whilst the study by Sabzevary-Ghahfarokhi *et al.* reported an increase of Nrf2 protein level in the inflamed colonic biopsy samples of UC patients [399]. These conflicting views highlight the need of further research to understand the role of this master 'antioxidant transcription regulator' in the pathogenesis of IBD.

Restoring redox balance by reducing oxidative stress and enhancing antioxidant capacity is a possible therapeutic strategy to alleviate IBD symptoms. Accordingly, nutraceuticals and natural products with robust antioxidant properties have shown promising effects in experimental models of IBD (discussed further below). These findings underscore the potential therapeutic value of targeting oxidative stress and redox imbalance in managing IBD, offering hope for improved outcomes in affected patients.

1.3.6 The inflammasome and IBD pathogenesis

The inflammasome is a biological conjugate formed from multiprotein complexes within the innate immune system that are responsible for the detection of harmful agents through pattern recognition receptors [400, 401]. Several inflammasome subtypes have been characterised including nucleotide-binding domain and leucine-rich repeat receptors (NLR) pyrin domain-contacting family (NLRP) [402-404], NLR family caspase recruitment domain-

containing protein-4 (NLRC4) [405] and double-stranded DNA sensors absent in melanoma-2 (AIM2) [406]. Their involvement in IBD pathogenesis has been extensively investigated in animal models of experimental colitis. Gut inflammasomes elicit protective effects against the development of IBD, where mice with deficiencies in specific inflammasomal components such as NLRC4, NLRPs, ASC, IL-1β and caspase-1 have all been shown to experience exacerbated colitis with more pronounced clinical symptoms reported [407-409]. Specifically, deficiency in NLRP3 expressions leads to lower levels of anti-inflammatory cytokine IL-10 and TGF-β [410], impaired neutrophil migration [411], and heightened intestinal inflammation [409], highlighting the essential role of NLRP3 in eliciting appropriate immune response.

Additionally, the NLRP6 inflammasome pathways could also play a role in IBD pathogenesis, where Nlrp6$^{-/-}$ mice exhibit crypt hyperplasia, enlarged Peyer's patches, reduced IL-18 production and alterations in gut microbiota [412], which impairs intestinal barrier function and facilitates intestinal inflammation. Additionally, these inflammasome component deficiencies have also reported to increase susceptibility to infections like *Citrobacter rodentium* and *Clostridium difficile* [413, 414], which together promote the colonisation of pathogenic bacteria such as *Akkermanisa muciniphila* [415]; the latter is indirectly linked to the promotion IBD pathogenesis in animal models.

Human studies corroborate these findings, revealing elevated NLRP3 activation in peripheral blood mononuclear cells from patients with CD [416], whilst upregulated expression of NLRP3, IL-1β and caspase-1 have also been identified in the colonic biopsy samples of patients diagnosed with UC and CD [417]. In direct support of the notion that inflammasome is involved in the pathogenesis of IBD, NLRP6 expression has found to be significantly increased in the ileal and colon samples of CD patients [418]. Moreover, enriched NLRC4 has been identified in patients with UC [419]. However, whether elevated inflammasome signalling pathways observed in IBD is responsible for driving disease pathogenesis or acting as a protective mechanism against intestinal inflammation is currently debated and warrants further investigations. Nonetheless, attempts to inhibit upstream and downstream signalling molecules and components of inflammasome pathways, including NRLP3 and its associated cytokines have shown promising results (discussed further below), highlight their potential as therapeutic targets for novel IBD interventions.

1.3.7 Role for SCFAs in IBD pathogenesis

As indicated above, SCFA, primarily acetate, propionate and butyrate are produced by the gut microbiota, with the phyla *Firmicutes* mainly responsible for the synthesis of butyrate and the phyla *Bacteroidetes* being the main producers of acetate and propionate [309]. SCFA serves as the primary energy source for colonic enterocytes through ATP production, while a small proportion that remains unabsorbed performs anti-inflammatory and immunomodulatory actions in the gut [420]. Since gut microbiota dysbiosis is an established risk factor for the development of IBD (discussed above), altered SCFA production may play a role in the pathogenesis and progression of the disease.

Altered SCFA levels in IBD patients have been reported as early as 1982, with Roediger *et al.* finding elevated faecal butyrate levels in active UC patients [421]. Similarly, van Nuenen *et al*. observed an increase in total SCFA (acetate, propionate and butyrate) levels in UC and CD patients [422], suggesting an impairment in SCFA utilisation in the IBD gut. However, these findings contrast with more recent studies. For example, Takaishi *et a*l. reported significant

reductions in propionate and butyrate in stool from patients diagnosed with UC and CD [423]. Likewise, the study by Machiels et al. demonstrated a reduced level of acetate, propionate and butyrate in IBD patients [251]. The discrepancies observed in these studies are likely influenced by IBD subtypes (UC versus. CD) as well as the presence of flares and the extent of colonoscopy activities as a measure of disease-stage severity. In a recent meta-analysis of SCFA levels in patients with IBD, Zhuang *et al*. highlighted that UC patients are characterised by a decrease in acetate, valerate and total SCFA levels, whilst CD patients have a more prominent reduction in acetate, butyrate and valerate concentrations when compared to the healthy controls [424]. However, these cumulative studies commonly show outcomes linked to groups of subjects designated with UC or CD or as a combined cohort with IBD, and the SCFA biomarkers are not stratified as a function of disease-stage severity.

Therefore, investigations on the levels of SCFA on a spectrum of IBD disease severities as well as identifying difference(s) in individual SCFA between UC and CD are warranted. To address this knowledge gap, Chapter 4 of the current thesis examined the level of SCFA acetate, propionate and butyrate on a spectrum of IBD disease severities as judged by colonoscopy activity index.

In the gut, SCFA, particularly butyrate regulates intestinal epithelial integrity and exerts anti-inflammatory effects through a plethora of cellular processes. Supplemented butyrate has been shown to increase transepithelial resistance *in vitro* [119], decrease gut permeability through the stabilisation of HIF [94], and suppress the activation of NF-κB via GPR109A signalling [425], highlighting the anti-inflammatory and barrier function protective roles of this SCFA. Thus, administration of SCFAs could efficiently dampen the extent of inflammation in IBD, presenting itself as a promising novel therapeutic target. Accordingly, successful attempts of SCFA supplementation on animal models of experimental colitis and on IBD patients have been reported and will be discussed in greater detail in this thesis chapter 4.

1.4 Currently available IBD treatment

1.4.1 Aminosalicylates

Aminosalicylates, including sulfasalazine (SASP) and other 5-aminosalicylic acid (5-ASA) preparations such as mesalamine and olsalazine are currently primary treatment options for IBD and have been for over 80 years [426]. The pro-drug SASP comprises 5-ASA linked to sulfapyridine via a labile diazo bond that prevents early absorption of the drug by the stomach and the small intestine, allowing bacteria-derived azoreductase to release the active 5-ASA in the colon (locally) [427], which provides the therapeutic effect, whilst the sulfapyridine component serves primarily as a carrier. The exact mechanism of actions for SASP and 5-ASAs are currently unknown [428]. However, it has been shown that these drugs interfere with arachidonic acid metabolism by cyclo-oxygenase enzymes [429], which prevents the formation of biologically active prostaglandin and leukotrienes mediators [430], scavenges ROS from the site of inflammation [431], and suppresses the production of pro-inflammatory cytokines such as TNF-α and IL-1β [432, 433]. Additionally, 5-ASA has been reported to promote Treg-induction in the colon via the aryl hydrocarbon receptor pathway, leading to TGF-β activation and down-regulation of the inflammatory state in colon tissue [434].

The clinical efficacy of 5-ASA has been reported in mild-to-moderate UC patients, with a primary response rate of 60-80% of compliant patients [435]. This is supported by findings from Eaden *et al*., where long term 5-ASA maintenance therapy was found to reduce

colorectal cancer risk by 75% in UC patients [436]. On the contrary, the therapeutic efficacy of 5-ASA in CD patients remains debated. It has been shown that more than 1 year of 5-ASA therapy reduced hospitalisation and surgery rates in patients diagnosed with CD [437], and 5-ASA is effective in maintaining CD remission after surgery [438]. However, a Cochrane systematic review by Akobeng *et al.* identified that oral 5-ASA drugs present no significant advantage in preventing relapse in patients with CD suggesting that the benefits are limited and do not represent a suitable long-term management strategy for these patients [439].

Although nephrotoxicity can occur in some patients after one year of 5-ASA treatment [440], the off-target effects of 5-ASA are typically mild, including nausea, abdominal pain, diarrhoea and headache [441]. On the other hand, in addition to the gastrointestinal discomforts identified with 5-ASA administration, SASP also possesses more severe side effects such as promoting male infertility, haemolytic anaemia and hepatotoxicity [442]. Therefore, the challenge for clinicians is to develop strategies for individuals that maintain the therapeutic benefits of 5-ASAs while minimising the side-effects of SASP. To assist in this goal several second-generation aminosalicylates have been developed primarily targeting the replacement of linked sulfapyridine with an inert compound, or an addition of pH-sensitive coating to adjust release rates of the active component [427].

1.4.2 Corticosteroids

Corticosteroids have played a significant role in the treatment of IBD since their clinical effectiveness was first recognised in the 1950s [443]. Commonly used corticosteroids, including hydrocortisone, prednisone, methylprednisolone, dexamethasone and budesonide, are primarily administered orally or intravenously to IBD patients [444]. Their anti-inflammatory effects are mediated through specific corticosteroid receptors, where corticosteroids bind to their responsive-elements in the nucleus, leading to the suppression of pro-inflammatory transcription factor such as NF-κB and activator protein 1 [445, 446]. It has been well appreciated that corticosteroids modulate inflammatory responses through the inhibition of vasodilation, leukocyte infiltration, cytokine release, fibroblast activation and vascular proliferation thereby providing a multi-faceted mechanism of action [444].

Oral corticosteroids are effective in inducing remission during flare-ups, particularly in patients who do not respond to mesalamine within 2-4 weeks, and in those with mild-to-moderate CD [447]. The clinical efficacy of orally administered corticosteroids in UC has been recently highlighted by a meta-analysis by Ford *et al.*, in which their superiority over placebo was confirmed in inducing remission amongst IBD patients [448]. Similarly, an overall response rate of 67% was achieved when administering corticosteroids in severe acute colitis [449]. Despite their remarkable clinical efficacy, short-term complications have been reported by nearly 50% of drug-compliant patients receiving corticosteroid therapies [448]. These adverse effects include insomnia, acne, increased appetite, weight gain, hypertension, hyperglycaemia and mood disturbance [448, 450]. Prolonged use of corticosteroids has also been shown to associated with increased risk of venous thromboembolism, bone fractures and opportunistic infections [451], once again indicating the limitations of these current therapeutic options for patients with IBD.

To improve safety and tolerability, second-generation corticosteroid therapy such as budesonide MMX has been introduced as a management option for UC. Budesonide MMX uses a multi-matrix system that enables targeted colonic drug release [452], which minimises

systemic absorption of the drug and reduces adverse side effects. This has been demonstrated in a pooled analysis of over 900 UC patients [453], where budesonide MMX did not impair adrenocorticoid function nor increase the risk of corticosteroid-associated adverse effects. It has also been shown that 9 mg/day of budesonide MMX significantly improves clinical and endoscopic remission rates while promoting histological healing of the colon in over 500 mild-to-moderate UC patients [454], suggesting that budesonide MMX is well tolerated in UC patients and offers enhanced performance over other conventional corticosteroid preparations.

Whilst it has been well established that corticosteroids can effectively induce remission during flare-ups, numerous studies have demonstrated that corticosteroids offer no significant reduction in relapse rates for UC and CD when used beyond three months [455-457], which again limits the overall therapeutic benefit and questions the longer-term use of this therapeutic approach.

1.4.3 Immunomodulators

Immunomodulators for IBD include thiopurines, methotrexate and calcineurin inhibitors offer option for long-term control of intestinal inflammation, with all of which exert immunosuppressive effects on T-lymphocytes. Thiopurine-based treatments, including azathioprine, 6-mercaptopurine and 6-thioguanine are commonly used in IBD treatment [458]. They work by inhibiting T-lymphocyte proliferation and activation through interference with DNA synthesis and binding to Rac1 [459], thereby blocking Rac1 activation in T-cells, which leads to the diminution of T-cell survival and function. Azathioprine has demonstrated similar therapeutic effects in both UC and CD, which significantly reduces hospitalisation and surgery rates amongst IBD patients [460, 461]. The clinical effectiveness of thiopurine treatments was further supported by the meta-analysis conducted by Yamada *et al.,* where a 7-year remission maintenance rate of 43.9% and a colectomy-free survival rate of 88% has been observed in UC patients following treatment with immunomodulators [462]. However, it should be noted that thiopurines were associated with several adverse side-effects, including bone marrow suppression and liver injury amongst the cohort studied [463, 464]. Furthermore, compliance is a major issue with his form of treatment as it has been shown that up to 39% of IBD patients discontinue thiopurine therapies within the first three months of treatment due to the severity of their adverse reactions [460].

Another available IBD immunomodulator is methotrexate, a folate antagonist that inhibits DNA synthesis and downregulates inflammatory cytokines production at low dose [465-467]. By suppressing T-lymphocytes proliferation and inducing activated T-cell apoptosis [468-470], methotrexate is particularly effective in treating CD, where 72% of active CD patients achieve clinical remission three months after methotrexate treatment [471]. However, its efficacy in UC has not been well established and as a result prescription of methotrexate among this cohort is not common [472]. Like other immune-modulators there are some severe side-effects of methotrexate, including peritoneal abscess, hypoalbuminemia and atypical pneumonia [472], which again limits its long-term use in some patients.

Calcineurin inhibitors include Cyclosporine and Tacrolimus have been used as pharmacological interventions for IBD. These drugs target the nuclear factor of activated T-cells (NFAT) [473], which prevents its translocation to the nucleus and thereby regulates the transcription of inflammatory cytokines such as TNF-α and IL-2 [473, 474]. The clinical trial

conducted by Lichtiger *et al*. have demonstrated that more than 80% of patients with severe acuate refractory UC respond to Cyclosporine A [475]. However, the study by Stange *et al*. showed that long-term treatment with Cyclosporine A combined with low-dose corticosteroids did not provide additional beneficial effects over corticosteroids treatments alone in active CD patients [476]. In addition to the immunosuppressive effect on T cells, Tacrolimus has also been shown to inhibit macrophage activation as well as promote the apoptotic process of these monocytes [477]. Accordingly, Tacrolimus has been found to be 10-20-fold more potent *in vivo* and 30-100-fold *in vitro* [426, 478]. This is also reflected in clinical outcomes where 68.4% of refractory UC patients showed significant improvement in disease biomarkers two-weeks after oral Tacrolimus treatment, compared to only 10% in the corresponding the control group [479]. Despite its efficacy, Tacrolimus-treated patients often experience adverse effects, including tremors, renal dysfunctions, hyperkalaemia and headaches [480].

1.4.4 Biologic agents

Biologic agents have revolutionised the treatment of IBD, particularly for patients with moderate-to-severe disease index who do not respond well to conventional therapies such as corticosteroids and immunomodulators [426]. Amongst these, anti-TNF agents are the most widely used, given the central role of this inflammatory molecule in driving intestinal inflammation and mediating tissue damage in IBD (discussed above – refer to Section 1.3 Immune dysregulation & Redox imbalance in IBD). Infliximab, the first commercially available anti-TNF agent approved for IBD treatment, is a genetically engineered IgG1 monoclonal antibody composed of 75% human and 25% murine proteins [481]. Infliximab provides rapid symptom relief and is particularly valuable as a rescue therapy for severe acute UC [482], where its efficacy can be shown within 2 weeks post treatment [483]. Additionally, it has been demonstrated that colonic fistula closure can occur within 3 months in CD patients who received Infliximab [483]. A randomised controlled trial on Infliximab in moderate-to-severe UC patients reported a 7% reduction in colectomy rates after 54 weeks, alongside a decrease in UC-related hospitalisation and surgery [484], highlighting the therapeutic efficacy of this agent. Similar findings were reported by Present *et al*., where intravenous administration of Infliximab at 5 mg/kg led to a 79% positive clinical response rate in CD patients, with a 55% of patients simultaneously reporting a complete fistula healing rate [483].

Adalimumab and Golimumab are fully humanised anti-TNF monoclonal antibodies designed for subcutaneous administration [485, 486]. Adalimumab is approved for both UC and CD, whilst Golimumab can be used on moderate-to-severe UC patients that repeatedly show unresponsive to conventional therapies [482]. Although anti-TNF therapies provide effective relief for IBD symptoms, up to 40% of patients do not respond initially, with an additional 23-46% of patients experiencing secondary loss of response to the drug within a year [487]. Long-term remission can be maintained through dosage adjustment, increased infusion frequency, or combining anti-TNF agents with conventional therapies once the degree of colonic inflammation is controlled [488]. Furthermore, anti-TNF agents also present with several adverse reactions due to systemic cytokine blockage. These include infusion reactions, blood disorders such as neutropenia, opportunistic infections, autoimmune disorders such as anti-TNF-induced lupus, complication to the heart and the nervous system [489-494], as well as an increased risk of nonmelanoma skin cancer [495]. Other biologic options for IBD treatment include anti-IL-12/23 and anti-integrin therapies [496-498].

1.4.5 Surgery and other interventions

Over the last decade, the number of hospitalised IBD patients has increased, however, surgical rates for both UC and CD cases have slightly declined. Nevertheless, surgical intervention remains a crucial treatment option for IBD [499]. Surgery is primarily indicated in UC patients with life-threatening complications such as excessive colonic bleeding, intestinal perforation, or suspected carcinogenesis [500]. In cases where patients with severe UC or toxic megacolon failed to respond to medical therapy, surgical intervention is also recommended. Additionally, patients experiencing poor treatment response or severe adverse drug reactions, which results in substantially impacted quality of life may also be considered as candidates for surgery.

In CD, surgery is typically reserved for patients with localised ileocecal disease who have recurring flares or failed medical therapies, or those who preferred surgery over long-term continuous drug treatments [500]. Postoperative recurrence is a major concern in CD, where a study by Rutgeerts *et al*. showed the symptomatic recurrence occurs in 20% and 34% of patients 1- and 3- years after ileo-colectomy respectively, with the number even higher for endoscopically verified recurrence rates at 73% and 85% for 1- and 3-years post-operation, respectively [501].

Overall, it is now clear that the available treatment options described in this section are not all-encompassing, and beyond the scope of the current thesis. Other intervention options relevant for IBD treatment have been summarised elsewhere (See comprehensive reviews by Cai *et al*. Ref [426] and Sokic-Multinovic and Milosavljevic Ref [482]). *However, it is noteworthy that there is currently no cure for IBD, where all of the available treatments typically aim to dampen intestinal inflammation and relieve symptoms. Thus, research into novel therapeutic targets and alternative medicine is highly essential for the disease, which is also a main goal of the current thesis.*

1.5 Patient outcomes

As indicated, there is no cure for IBD, and available treatments focuses on managing symptoms to achieve and maintain remission rather than eradicating the disease. Patients with UC often experience debilitating digestive symptoms with over 30% also developing EIMs [246], significantly impacting their psychological, social, familial and professional well-beings. Similarly, disabling digestive symptoms of abdominal pain, diarrhoea, rectal bleeding and weight loss can also be seen in CD patients [254], with about 43% also reporting EIMs [259]. Unregulated IBD can lead to severe complications, including colorectal cancer and toxic megacolon. It has been shown that IBD patients are 2-6 times more likely to develop colorectal cancer [211], a life-threatening malignancy with poor patient prognosis (as discussed in earlier sections).

On the other hand, toxic megacolon is characterised by excessive colonic distension and systemic toxicity [502], with a potentially fatal outcome. The incidence of toxic megacolon in IBD patients is estimated to be 1-6.3% [503], with study reporting its presence in 10% of UC hospital admissions and 2.3% of CD admissions [504]. The symptoms of toxic megacolon include abdominal distension, constipation, fever, tachycardia and hypotension [502, 505], with a potentially fatal outcome. The incidence of toxic megacolon in IBD patients is estimated to be 1-6.3% [503], with study reporting its presence in 10% of UC hospital admissions and 2.3% of CD admissions [504]. The symptoms of toxic megacolon include abdominal distension,

constipation, fever, tachycardia and hypotension [502, 505]. However, IBD-associated gastrointestinal symptoms may also present during the onset of the disease [502]. Treatment of mega toxic colons requires a combination of medical and surgical interventions, with immunomodulatory drugs and antibiotics being the first-line therapy [506]. Severe cases of mega toxic colon may necessitate surgical resection of the colon, with some patients requiring an external colostomy [506]. As a result, there is an urgent need for the development of novel treatments for IBD patients, allowing better management of the gastrointestinal symptoms and EIMs and minimising the development of serious complications such as toxic megacolon and colorectal cancer.

1.6 Animal models of IBD

Animal models, particularly mouse models, have become increasingly invaluable tools for investigating the pathogenesis of IBD [507]. The following section highlights the common animal models of UC and CD and discuss how these experimental colitis models provide crucial insights into the underlying pathophysiology of IBD and serve as effective platforms for evaluating the therapeutic potential of novel treatments.

1.6.1 Animal models of UC

Animal models of UC are widely used to study the disease pathophysiology and test potential treatment approaches. UC-like phenotypes can be induced in animals using chemical agents, bacterial infections or genetic modifications. Chemically induced UC-like colitis is commonly performed on mice but has also been tested in other species such as drosophila, zebrafish, rats and pigs [508]. Dextran sodium sulfate (DSS) is a commonly used chemical agent that causes epithelial injury, exposing the lamina propria and submucosal compartments to luminal agents and bacteria, which triggers inflammation [509]. DSS-induced colitis is characterised by colonic crypt disruption and excessive immune infiltrations primarily concentrating in the colon mucosa and sub-mucosa [510].

Other chemical methods include intrarectal administration of oxazolone with ethanol, which induces a Th2-mediated immune responses, or diluted acetic acid, which mimics UC with transient ulceration and crypt abnormalities [511]. Alternatively, UC-like colitis can be induced via bacterial infections using gram-negative bacteria *Salmonella typhimurium* or commensal adherent-invasive *Escherichia coli* strains isolated from Crohn's disease patients [508]. Transgenic (Tg) and gene knockout (KO) models offer another approach, targeting specific immune responses or signalling pathways. For example, the IL-7 Tg, T-cell receptor α KO, Wiskott-Aldrich syndrome protein KO and IL-2 KO models all exhibit a prominent T-cell mediated UC-like pathologies [512-515], guanine nucleotide-binding protein G(i) subunit α-2 KO model can be used to investigate T- and B-lymphocyte biology ultimately inducing a UC-like condition [508].

1.6.2 Animal models of CD

Similar to models of UC, CD-like experimental colitis can be induced using chemical agents or genetic modifications. Trinitrobenzene sulfonic acid (TNBS) is a common chemical inducer in rodents, leading to mucosal barrier destruction, granuloma formation, and infiltration of inflammatory cells in all layers of the intestine [516]. TNBS induction has been shown to trigger a Th1-type immune response, characterised by production of inflammatory IL-12 by activated macrophages and IFN-γ and IL-2 by lymphocytes, making it a suitable model for CD

[517]. Indomethacin is another chemical agent that induces small intestinal and colonic ulceration in a dose-dependent manner by inhibiting prostaglandin E_1 and E_2 and prostacyclin synthesis, which facilitates bacterial penetration and inflammation to generate a CD-like phenotype [508, 518].

A CD-like phenotype can also be stimulated through genetic manipulation in animals. For example, the SAMP1/Yit model, developed through sibling mating of senescence-accelerated mouse lines, spontaneously develop ileitis at 20 weeks age without additional genetic or immunological manipulation. This model closely mirrors human CD, with pathophysiological features including segmental inflammation, transmural lesions, granuloma formations and structural changes in epithelial and neural tissues [519].

The TNF-ΔARE mouse is another model of experimental CD that involves genetic modification of the AU-rich motif in the 3' untranslated region of the TNF gene [520]. Homozygous ($TNF^{\Delta ARE/\Delta ARE}$) and heterozygous ($TNF^{\Delta ARE/+}$) mice can develop chronic transmural ileitis resembling varying extents of CD, with inflammation localised primarily to the terminal ileum and proximal colon [521]. Together, these models offer value platforms to study the underlying mechanisms and investigate the therapeutic potential of novel treatment targets of CD.

1.7 Alternative medicines & Novel treatment approaches

Due to the chronic nature of IBD, its unpredictable disease relapse and irregular flare ups that are difficult to predict, the absence of a definitive cure, and numerous adverse side effects associated with the current treatment options, are all driving a profound interest in developing new therapies that provides superior clinical efficacy and offers fewer side-effects. *The following section and the remaining body of the thesis comment on current advancement of alternative medicines and novel treatment approaches in both animal models and human patients of IBD, with particular emphasis on synthetic inhibitors, diet and gut microbiome modulation and the utilisation of nutraceuticals.*

1.7.1 Synthetic inhibitors

1.7.1.1 Janus kinase targeting inhibitors

The Janus kinase (JAK)/STAT pathway plays a crucial role in cell growth, immune regulation, and inflammation, and genome-wide association studies have highlighted its involvement in the pathogenesis of IBD, making it a promising target for IBD. Accordingly, several JAK inhibitors, previously approved for other inflammatory conditions such as rheumatoid arthritis, have demonstrated promising results in various phases of IBD human trials. For example, Tofacitinib, an orally available small-molecule JAK1/JAK3 inhibitor has shown efficacy in a Phase III clinical trials of over 1,500 UC patients, where 18.5% of UC patients receiving 10 mg of Tofacitinib achieved clinical remission 8 weeks after treatment initiation, and remission was maintained in 34.3% and 40.6% of patients after 1 year when administered 5 and 10 mg of Tofacitinib, respectively [522].

Similar beneficial results were also observed in a Phase II trial of UC patient using Filgotinib, a JAK1 specific inhibitor originally designed for rheumatoid arthritis treatment [523], with 200 mg of Filgotinib demonstrated good tolerance in patients and efficacious in inducing and maintaining clinical remission in comparison to the control group [524]. Additionally, it has also been shown that 47% of patients achieved clinical remission at week 10 compared to

23% on placebo in another Phase II trial of CD patients [525], highlighting the therapeutic potential of inhibiting JAK/STAT pathway as a novel IBD treatment approach. Similarly, another JAK1 selective inhibitor, Upadacitinib, showed promising results in a Phase II study for CD, with significant improvement in clinical response and endoscopic remission [526]. Collectively, these findings suggests that JAK inhibitors offer a novel and effective therapeutic approach for IBD, potentially improving patient outcomes and proving an alternative option to conventional treatments.

1.7.1.2 Angiotensin converting enzyme targeting inhibitors

Although angiotensin converting enzymes (ACE) are primarily known for regulating blood pressure, their increased presence in the gastrointestinal mucosa during intestinal injury and colitis in both animal models and humans suggest a potential role in IBD pathogenesis [527, 528]. Captopril, an oral ACE inhibitor, was the first drug studied for its potential beneficial effect on intestinal inflammation. Wengrower et al. reported ACE inhibition resulted in improved colitis symptoms and reduced colonic fibrosis in TNBS-induced rats of experimental colitis [529]. Subsequent research confirmed its ability to mitigate inflammation, oxidative stress and collagen deposition in the same model of experimental colitis [530].

Another ACE inhibitor Losartan has been shown to alleviate colitis severity by reducing pro-inflammatory cytokines such as TNF-α, IFN-γ and IL-1β in TNBS-stimulated mice [531]. Furthermore, the therapeutic potential of ACE inhibition was further highlighted by ACE inhibitor Enalaprilat, with significantly reduced pro-inflammatory cytokine profile and improved intestinal barrier function documented in a murine IL-10 deficient model of experimental colitis [532]. However, retrospective studies on CD patients taking ACE inhibitors over a 10-year period has yielded mixed findings. Whilst these patients experienced a more severe overall disease course, evident in higher imaging and endoscopic procedures, they have a reduced need for corticosteroids [533], suggesting a potential long-term benefits and highlight the need for further large-scale studies to understand to therapeutic efficacy of ACE inhibition as an IBD treatment.

1.7.1.3 Inflammasome targeting inhibitors

Given the potential involvement of inflammasomes in IBD pathogenesis (discussed in earlier section), inhibition of this inflammatory pathway could improve IBD symptoms. Presently, attempts to target the inflammasome pathway are largely focusing on inhibiting the canonical and non-canonical activation of NLRP3 inflammasome. MCC950, a selective NLRP3 inhibitor, has shown efficacy in experimental colitis models by preventing ASC oligomerisation and reducing pro-inflammatory cytokines such as IL-1β and IL-18 [534]. Additionally, combining MCC950 with metformin significantly alleviated DSS-induced colitis in mice by inhibiting toll-like receptor 4/NF-κB signalling [535], which further highlights targeting of the inflammasome as a potential IBD treatment. Notably, a rheumatoid arthritis Phase II trial for MCC950 has been suspended due to elevation in liver enzymes, suggesting a potential adverse impact on liver hepatocytes [536].

Lastly, another promising compound, OLT177, is an orally active β-sulfonyl nitrile molecule that specifically inhibit NLRP3, which leads to reduction of IL-1β and dampened caspase-1 activity in human neutrophils [537]. Meanwhile, Tranilast, an anti-allergic drug, has been identified as a direct NLRP3 inhibitor, showing effectiveness in treatment NLRP3-related autoinflammatory conditions such as gouty arthritis and Type 2 diabetes [538]. However, the

clinical efficacy of OLT177 and Tranilast for IBD remains to be tested. Whilst promising results have been reported by animal studies, further research and clinical trials are needed to determine the therapeutic potential of NLRP3 inhibitors as novel treatment options for IBD.

1.7.1.4 NETs targeting inhibitors

As discussed in earlier sections of this chapter, excessive neutrophil infiltration into the colonic mucosa, accompanied with increased formation of NETs is a hallmark feature of IBD. As a result, reducing the amount of NETs in the IBD colon could serve as a novel strategy to improve IBD patient outcomes. Accordingly, the therapeutic effect of inhibiting enzymes involved in the process of NETs formation has been reported in the literature. The neutrophil enzymes NE and MPO have critical roles in the formation of NETs, where MPO triggers the activation and nuclear translocation of NE in the presence of ROS, whilst NE is responsible for the proteolytic process to disrupt chromatin packaging in the histone [79].

In the study by Morohoshi *et al*., the synthetic NE inhibitor ONO-5046 significantly reduced body weight loss and histological score in DSS-induced experimental colitis in mice, highlighting the therapeutic potential of NE inhibition as a the treatment of IBD [539]. On the other hand, Ahmad et al. demonstrated the therapeutic potential of MPO inhibition, showing that the synthetic MPO inhibitor AZD3241 alleviated experimental colitis symptoms whilst activating the heme oxygenase-1 (HO-1)/Nrf2 signalling pathways [540]. More recent attempts to inhibit PAD4, the vital enzyme involved in the citrullination process of NETs formation has been reported, where inhibition of this enzyme by pan-PADs inhibitor Cl-amidine as well as PAD4 specific inhibitor GSK484 have shown to reduce NETs formation in murine model of experimental colitis, and significantly improved colitis symptoms and dampened intestinal inflammation by lowering pro-inflammatory cytokine productions [541, 542].

One shortcoming of these latter studies is the mode of identifying NETs in the colon tissues with only one component of the three characteristic biomarkers (NE, MPO and Cit3) consistently being used as the readout for colonic NET formation, which may lead to ambiguous assignment of NETs. *Based on these collective positive outcomes, the therapeutic efficacy of PAD4 enzyme inhibitor GSK484 was examined further in Chapter 3 of this thesis with implementation of multiplex (simultaneous) imaging of NE, MPO and Cit3 extending these previous studies to provide definitive (unequivocal) identification of colonic NETs.*

1.7.2 Gut microbiome modulation

1.7.2.1 Faecal microbiota transplantation (FMT)

Faecal microbiota transplantation (FMT) is an innovative therapeutic approach aimed to restore gut microbiota balance by introducing donor microbiota into the GIT of the recipient [543]. Historically, FMT dates back to fourth-century China, where it was known as the “yellow soup”, and was used to treat severe diarrhoea [544]. The process of contemporary FMT at the present days involves donor selection, faecal material collection, processing, storage and ultimately administration through various route [545, 546].

The introduction of beneficial microbiota is known to restore SCFA such as butyrate levels in the gut [547], which plays a crucial role in maintaining gut barrier integrity and immune regulations (discussed in Sections 1.1.1.4, 1.2.5.2 and 1.3.7 of this chapter). Studies have shown that FMT leads to higher clinical remission and endoscopic improvement rates in both

UC patients and animal models of UC-like colitis [548-550]. These positive findings were reinforced by the meta-analysis by El Hage Chehade et al., where multiple administrations of FMT correlates with better clinical outcomes in UC [551].

In CD, a recent randomised controlled trial demonstrated significantly higher remission rates at 10- and 20-weeks post FMT treatment when compared to the controls [552]. It has also been shown that patients who received FMT treatment have improved endoscopic activity [552], suggesting a restoration of the intestinal balance. Furthermore, FMT has been deemed a generally safe option for CD patients, with no severe adverse effects reported [553]. Despite the promising results, the regulatory and safety challenges for FMT should not be overlooked, necessitating further large-scale clinical trials to establish its long-term efficacy and safety as an IBD treatment.

1.7.2.2 SCFA supplementation

In the gut, SCFA particularly butyrate has been shown to maintain intestinal epithelial integrity and exert anti-inflammatory effect via a plethora of cellular processes (discussed in Section 1.3.7 of this chapter). Thus, supplementation of SCFA may provide improvement against IBD symptoms. However, studies with SCFA supplementation have yielded mixed results in IBD patients. A study by Luhrs et al., demonstrated that administering 100mM of butyrate via enema for 4-8 weeks inhibited macrophage NF-κB activation in the lamina propria of UC patients, which results in significantly improved disease activity [554], highlighting the therapeutic potential of butyrate supplementation in IBD. In contrast, Facchin *et al*. performed a double-blind, placebo-controlled pilot study that failed to show any clinical benefits in UC and CD patients, despite the combination of oral sodium butyrate supplementation in with conventional therapies yielding elevated levels of SCFA-producing bacteria and butyrate-producing bacteria in UC and CD patients, respectively [555].

Similarly, Hamer *et al*. reported that butyrate enemas led to minor improvement in gut inflammation in UC patients in remission [556], suggesting that elevated butyrate levels may only encourage a shift towards remission, but offer limited disease-modifying benefits for IBD patients. Additionally, sodium propionate supplementation has been shown to reduced inflammatory markers in end-stage renal disease patients [557], however, its role in IBD remains unexplored. Together, these results suggests that further research is needed to fully determine the therapeutic potential of SCFA supplement in IBD.

1.7.3 Nutraceuticals

Conventional IBD treatments often come with significant side effects and lacks a definitive cure (as discussed in Section 1.4 of this chapter). As a result, nutraceuticals, which are food-derived substances with medicinal benefits, have emerged as a promising alternative or adjuncts to conventional IBD therapies. Several plant-based compounds have demonstrated therapeutic efficacy in both experimental IBD models and humans. In addition to the synthetic NLRP3 inhibitors mentioned above, plant-based NLRP3 inhibitors also showed therapeutic efficacy in experimental IBD. For example, Oridonin, a plant derived covalent inhibitor of NLRP3 [558], attenuated TNBS-induced CD-like colitis and reduced TNF-α and IFN-γ levels [559]. Therapeutic potential for nutraceuticals was also highlight in a study that I was involved in during my candidacy, where polyphenol extract from a native Chilean berry also alleviated experimental colitis and reduced pro-inflammatory mediators NF-κB and IL-1β expressions through the inhibition of NLRP3 inflammasome [560]. Furthermore, aloe

vera gel has also been investigated for its medicinal properties, with a study showing that oral administration resulted in clinical improvement in UC patients, despite having no significant endoscopic or histological recovery [561].

Curcumin, the active compound of turmeric, has been extensively studied for its anti-inflammatory effects, primarily through NF-κB inhibition and suppression of TNF-α, IL-2 and IL-2 productions [562]. Clinical trials have demonstrated its effectiveness in inducing and maintaining remission in UC patients, with oral and enema formulations showing promising results [563-565]. Additionally, traditional Chinese herbal medicines have also contributed to potential nutraceutical treatments. *Hedyotis diffusa* has demonstrated anti-inflammatory [566], antioxidant [567] and immuno modulating properties [568], improving clinical scores and reducing pro-inflammatory cytokine release in animal models of experimental colitis [569].

Amomum villosum, a Chinese herb from the ginger family, has been found to strengthen the intestinal mucosal barrier and reduce inflammation by upregulating the HO-1/Nrf2 pathway [570]. Whilst these findings suggests that nutraceuticals offer a natural, well-tolerated approach to IBD management, the underlying mechanism of action of most of these nutraceuticals remains unknown. *Hence, in Chapter 5 of this study, the therapeutic efficacy and mechanism of action of nutraceuticals curcumin, Hedyotis diffusa and Amomum villosum were investigated.*

1.8 Aims & Hypotheses

Presently, the exact cause of IBD is unknown and there is no definitive cure for this debilitating disease. Contemporary IBD treatments carry severe adverse side-effects and commonly poor primary response and compliance rates have been reported in substantial portion of IBD patients prescribed the available treatments. As a result, there is an urgent need to explore novel treatment targets and strategies to develop next-generation IBD interventions. As highlighted in the introductory chapter, the utilisation of synthetic inhibitors, modulation of gut microbiome as well as the administration of nutraceuticals have reported positive clinical effects in both experimental animal models of IBD and in human IBD patients.

Therefore, it is ***hypothesised*** that simultaneously investigating novel synthetic inhibitors, factors that influence gut microbiome composition and whole-of-body lipidomic changes (lipidome) as well as the mechanism of actions of various nutraceuticals could provide valuable insights into IBD pathogenesis and potentially identify novel pathways that aid the development of innovative IBD treatments.

The current thesis encompasses ***three main aims***:

1. To investigate the clinical efficacy of synthetic PAD4 inhibitor in a DSS-induced animal model of experiment colitis (Chapter 3);

2. To characterise SCFA profiles in stool specimens from patients on a spectrum of IBD disease severity (Chapter 4); and

3. To evaluate the therapeutic efficacy of curcumin powder, and Hedyotis diffusa and Amomum villosum herbal tonics in a mouse model of experimental colitis (Chapter 5).

Chapter 2: Methods

2.1 Ethics

In the current thesis, Chapter 3 and Chapter 5 involves experimental procedures performed on mice, whilst Chapter 4 utilised human plasma and stool samples obtained from various hospital within the Western Sydney Local Health District (WSLHD).

All experimental procedures involving mice were conducted within the Laboratory Animal Service (LAS) facility at the University of Sydney (Charles Perkins Centre) and followed the approved protocol (#2019/1496 for Chapter 3 and Chapter 5) reviewed by the University of Sydney Animal Ethics Committee.

All procedures involving human samples in the current thesis have strictly adhered to the Declaration of Helsinki ethical principles regarding human experimentation and the study was approved by the WSLHD ethics committee (ethics approval number 2021/PID#03593). Informed consent was obtained from each participating subject before study enrolment and where circumstances changed, and consent was withdrawn (n=1 instance), the patient data was eliminated from the data set. All data was coded and reviewed in blinded fashion until decloaking was required to assign different treatment groupings.

2.2 Equipment

Table 2.1. List of equipment used in the current thesis.

Equipment	Model	Manufacture
General Equipment		
Bio-safety cabinet	SAFE-2020	Thermo Scientific
Centrifuge	12011919 Mini Centrifuge	Bio-Rad
Centrifuge	Heraeus Pico 21	Thermo Fisher Scientific
Centrifuge	Heraeus Megafuge 16R	Thermo Scientific
Centrifuge	5425R	Eppendorf
Dry heat bath	AccuBlock	Labnet International Inc.
Freezer	MDF-U731M	SANYO
Fridge	MPR-1412-PE	PHCBI
Fume cupboard	1500	Dynaflow
Magnetic stirrer	MS-20A	WiseStir
Microbalance	PIONEER	OHAUS
Microbalance	PR series	OHAUS
Microbalance	BM 20	A&D
Micropipettes	-	Bio-Rad/Eppendorf
Microwave	EM134AL7	Midea
Orbital shaker	E0M5	RATEK
pH meter	SevenDirect SD20	Mettler Toledo
Tube roller mixer	BTR5	RATEK
Ultralow temperature freezer	Salvum Ultimate	Haier Biomedical
Ultrapure water system	H2OPRO-VF-D	Sartorius
Vortex	G560E	Scientific Industries

Absorbance Reading		
In vivo Imaging chamber	IVIS® Spectrum CT	Perkin Elmer
Microplate reader	SPARK(r)	Tecan
Microplate reader	Infinite M200-Pro	Tecan
Microscopy		
Decloaking chamber	ARC	Biocare Medical
Inverted microscope	Vert.A1	ZEISS
Microscope imaging camera	AxioCam ICm1	ZEISS
Microscope imaging camera	AxioCam 105 Color	ZEISS
Upright microscope	Scope.A1	ZEISS
Upright microscope	Lab.A1	ZEISS
Tissue Processing		
Homogeniser	RW 20 D	IKA
Rotary microtome	Shandon Finesse 325	Thermo Scientific
Teflon coated tube	5mL-Glass	Wheaton Glassware
Western Blot		
Electrophoresis chamber	Mini-PROTEAN Tera system	Bio-Rad
Membrane imager	ChemiDoc MP Touch imaging system	Bio-Rad
Power Source	PowerPac Basic	Bio-Rad
Transfer machine	Trans-blot Turbo	Bio-Rad
Mass Spectrometry		
High-throughput mass spectrometer	QTRAP 6500+	SCIEX
Orbitrap mass spectrometer	Q Exactive HF-X	Thermo Scientific
Property Analysis		
Liquid chromatographer	AKTA pure	Cytiva
Multi-angle light scattering detector	miniDAWN TREOS	Wyatt Technology
Polarimeter	341	Perkin Elmer
Refractive index detector	Optilab T-rEX	Wyatt Technology

2.3 Reagents

Table 2.2. List of reagents used in the current thesis.

Reagents	Catalogue Number	Supplier
General Reagents		
BCA protein assay kit	23225	Thermo Scientific
Ethanol	459844	Sigma Aldrich
Hydrochloric acid	320331	Sigma Aldrich
Methanol	179337	Sigma Aldrich
Phosphate buffered saline tablet	P4417	Sigma Aldrich
Sodium chloride	AJA-465	Ajax Finechem
Sodium hydroxide	567530	Sigma Aldrich
Tris-base	A1379	AppliChem
Tween 20	663684B	VWR Chemicals

Enzyme Linked Immunosorbent Assay (ELISA)		
Human IL-10 ELISA kit	BMS215-2	Invitrogen
Human IL-1β ELISA kit	BMS224-2	Invitrogen
Human IL-6 ELISA kit	EH2IL6	Invitrogen
Mouse calprotectin ELISA kit	Ab263885	Abcam
Mouse GM-CSF ELISA kit	0010	ELISAkit.com
Mouse IFN-γ ELISA kit	EK00002	ELISAkit.com
Mouse IL-10 ELISA kit	BMS614	Invitrogen
Mouse IL-1β ELISA kit	BMS6002	Invitrogen
Mouse IL-4 ELISA kit	BMS613	Invitrogen
Enzyme Activity Assay & Other Assay Kits		
Catalase colorimetric activity kit	EIACATC	Invitrogen
Lipolysis (3T3-L1) colorimetric assay kit	MAK211	Sigma Aldrich
Superoxide dismutase activity assay kit	ab65354	Abcam
Immunohistochemical & Immunofluorescence Staining		
0.5% alcoholic eosin Y-solution	1.02439	Sigma Aldrich
10x antigen retrieval buffer pH 6.0	S2369	DAKO
10x antigen retrieval buffer pH 9.0	S2367	DAKO
30% hydrogen peroxide	H3410	Sigma Aldrich
Alcian blue 8GX powder	A5268	Sigma Aldrich
Bovine serum albumin	A7906	Sigma Aldrich
DAB substrate kit	K3468	DAKO
Disodium 5-amino-2,3-dihydro-1,4-phthalazinedion	A4685	Sigma Aldrich
DPX medium	06522	Sigma Aldrich
Fluorescence mounting medium	S3023	DAKO
Formalin solution, neutral buffered, 105	HT501640	Sigma Aldrich
Harris hematoxylin solution	HHS32	Sigma Aldrich
Histolene	H2779	Sigma Aldrich
Opal 7-color IHC kit	NEL811001KT	AKOYA Biosciences
Safranin O	S2255	Sigma Aldrich
Scott's Tap Water Substitute Concentrate	S5134	Sigma Aldrich
Serum-free protein block	X0909	DAKO
Triton X-100	270733	Sigma Aldrich
Tissue Homogenisation		
2,6-Di-tert-butyl-4-methylphenol	112990010	ACROS
cOmplete protease inhibitor cocktail	CO-RO	Roche
DNase	DN25	Sigma Aldrich
Ethylenediamine-tetra-acetic acid	E6758	Sigma Aldrich
PhosSTOP	PHOSS-RO	Roche
Sodium azide	S2002	Sigma Aldrich

Western Blot		
4-15% Mini-PROTEAN TGX precast protein gels – 15-well	4561086	Bio-Rad
Clarity Western ECL substrate	1705060	Bio-Rad
Glycine	AJA1083	Ajax Finechem
Ponceau S solution	A40000279	Thermo Fisher
Precision Plus Protein Kaleidoscope ladder	1610375	Bio-Rad
Skim milk powder	-	Coles
Sodium dodecyl sulfate	428023	Calbiochem
Trans-Blot Turbo Midi 0.2 μm PVDF transfer packs	1704157	Bio-Rad
Liquid Chromatograph & Mass Spectrometry		
Acetic acid	695092	Sigma Aldrich
Acetic acid-d_4	151785	Sigma Aldrich
Acetonitrile	FSBA955-4	Thermo Fisher
Butyric acid-1,2-$^{13}C_2$	491993	Sigma Aldrich
Formic acid	5.33002	Supelco
Hexanoic acid	153745	Sigma Aldrich
Hexanoic acid-6,6,6-d_3	489727	Sigma Aldrich
Methanol	1.06035	Supelco
Methyl tert-butyl ether	34875	Sigma Aldrich
Orthophosphoric acid	5.43828	Supelco
Propionic acid-1-^{13}C	282448	Sigma Aldrich
Sodium butyrate	B5887	Sigma Aldrich
Sodium propionate	P1880	Sigma Aldrich
Splash Lipidomix mass spectrometry standards	330707-1EA	Avanti Polar Lipids
Valeric acid	240376	Sigma Aldrich
Water (LC-MS Grade)	1.15333.2500	Supelco
Antibodies		
β-Actin	4967S	Cell Signaling Technology
4HNE	BS-6313R	Bioss
Anti-mouse IgG HRP	Ab205719	Abcam
Anti-rabbit IgG HRP	A6154	Sigma Aldrich
citH3	Ab219407	abcam
GPx4	Ab125066	Abcam
HO-1	AB5700731	Sigma Aldrich
MPO	PA5-16672	Invitrogen
NE	PA5-115648	Invitrogen
Nrf2	PA5-88084	Invitrogen
Nrf2	Ab137550	Abcam
SOD1	SAB5200083	Sigma Aldrich
Drugs		
Amomum villosum	110001-1	Beijing Tongrentang Sydney
AZD3241	-	Pharmaxis Ltd.

AZD3241	HY-17646	MedChemExpress
Curcumin	110001-2	Beijing Tongrentang Sydney
Dextran sodium sulfate	160110	MP Biomedicals
GSK484	Ab223598	Abcam
Hedyotis diffusa	110001-3	Beijing Tongrentang Sydney
Peanut butter	-	Bega

2.4 Consumables

Table 2.3. List of consumables used in the current thesis.

Consumable	Catalogue Number	Supplier
1.5 mL Eppendorf tube	EPPE0030120.086	Eppendorf
15 mL falcon tube	CLS430790	Corning
2 mL Eppendorf tube	EPPE0030120.094	Eppendorf
50 mL falcon tube	CLS430290	Corning
500 µL Eppendorf tube	EPPE0030121.023	Eppendorf
96-well clear flatbottom microplate	650001	Greiner Bio-One
Menzel-Glaser cover slips	22 x 50mm No.1	Thermo Scientific
Micropipette tips	-	Sarstedt
Plain disposable soda lime 6mL tube	KIML60BM12	Bio Strategy Pty Limited
Superfrost plus microscope slides	25 x 75 x 1.0 mm	Thermo Scientific

2.5 Software

Table 2.4. List of software used in the current thesis.

Software	Version	Sources
BioRender	-	Biorender.com
GraphPad Prism	10.1.0	GraphPad Software
ImageJ	1.54d	National Institute of Health
LipidSearch	5.0	Thermo Fisher Scientific
Living Image®	4.8.2	Perkin Elmer
MetaboAnalyst	6.0	Xia Lab
MetScape	3.10.3	Cytoscape Consortium
Microsoft Excel	2308	Microsoft
Zen Blue	3.11	ZEISS

2.6 General methodologies

This section covers general methodologies that are not specific to any of the experimental procedures described in Chapter 3, 4 and 5, but were essential for optimising a workflow or protocol and adhering to good laboratory practices.

2.6.1 Buffer preparation

2.6.1.1 Tissue lysis buffer preparation

Colon and faecal samples investigated in the current thesis were homogenised in a tissue lysis buffer that was prepared in bulk and used within 1-week of preparation. This buffer was

stored at 4℃ until required. Briefly, 1 tablet of commercially available phosphate-buffered saline (PBS) was dissolved into 30 mL of Mili-Q water, followed by the addition of 400 µL 100 mM ethylenediaminetetraacetic acid, 4 µL of 100 mM butylated hydroxytoluene, 1 tablet each of commercial multi-protease and phosphatase inhibitors before the addition of 200 µL of 10 mM sodium azide solution. All reagents were mixed thoroughly using a magnetic stirrer until fully dissolved. The pH of this buffer was then adjusted to 7.4 before topping up to 40 mL (the required final volume).

2.6.1.2 Tris-buffered saline (TBS) and TBS with Tween 20 (TBST) preparation

A concentrated tris-buffered saline (TBS) solution was prepared using 24 g of tris-base and 88 g of sodium chloride into 750 mL of Mili-Q water in a Schott bottle with constant stirring. Once all salts were completely dissolved, the pH was gradually adjusted to 7.6 by adding 2 mM hydrochloric acid in a dropwise fashion. After the desired pH was achieved the solution was brought up to 1 L (final volume). Similarly, a concentrated TBS with Tween 20 (TBST) solution was prepared using the same method. After adjusting the pH to 7.6, 10 mL of Tween 20 was added, before the volume was adjusted to 1 L (final volume). Concentrated TBS and TBST solutions were stored at 4℃ in a convenient walk-in cold room until required. For experimental use, TBS and TBST working solutions were prepared by diluting 100 mL of concentrated TBS/TBST solution with 900 mL of Mili-Q water. The pH of TBS/TBST working solution was monitored using the pH probe after the dilution.

2.6.1.3 Phosphate-buffered saline (PBS) preparation

PBS was prepared and used for immunochemical and immunofluorescence studies described throughout the current thesis. Briefly, 5 tables of commercially sourced PBS were added into a 1 L Mili-Q water in a Schott bottle with rigorous magnetic stirring to aid the dissolving process. Once the tablets were fully dissolved, PBS solutions were stored at 4℃ in the dark until required.

2.6.2 Protein analyses using the bicinchoninic acid assay (BCA)

Total protein concentration was determined in colon and faecal homogenates using a commercially available bicinchoninic acid assay (BCA) kit. To ensure data reproducibility, standards and samples were analysed in duplicates with factory recommended protocols followed. Briefly, serial dilutions were performed to create a standardised protein concentration gradient of bovine serum albumin (BSA), ranging from 2000 µg/mL to 25 µg/mL in Mili-Q water. Next, 10 µL of pre-diluted BSA standards were loaded onto a 96-well clear flat-bottom polystyrene plate. This step was followed by loading of 10 µL diluted colon homogenate or faecal tissue lysate at 1:10 and 1:4 (v/v), respectively in Mili-Q water onto the 96-well plate. Once the standards and samples were loaded, 190 µL of a freshly prepared 4% v/v $CuSO_4$ BCA solution was loaded onto each of the analysing wells. The plate was mixed vigorously by placing onto an orbital shaker at maximum speed before incubation in a dry oven at 37℃ for 30 ± 2 min. After incubation, the absorbance was measured at 562 nm using a plate reader. Calculation of total protein was conducted using Microsoft Excel and a standard curve was generated. The linear equation and correlation coefficient (R^2) were evaluated to confirm an acceptable linear regression and then protein concentrations were deduced from the absorbance readings for each of the samples by interpolation against the standard curve.

2.7 Specific methodologies

The following sections include relevant methodologies and protocols of specific experiments that were either not described or briefly summarised in the following chapters to adhere to strict publication word limits.

2.7.1 Methodologies specific to Chapter 3

2.7.1.1 Triple-plex immunofluorescence labelling of NETs

The presence and density of NETs in the colon tissues was visualised by using the Opal 7-Color IHC Kit (NEL811001KT; AKOYA Biosciences). All staining steps were completed at room temperature (~22℃) in an opaque humidity chamber unless specified otherwise and following the manufacture's recommended protocol. After slide dewaxing and rehydrating, heat induced epitope retrieval (HIER) was performed by placing with the slides into an opaque Coplin jar with pH 6.0 citrate HIER buffer (S2369, DAKO) to expose the antigens for NETs markers: NE, MPO and citH3. The device settings used for the HIER process were summarised in Table 5. After HIAR, slides were washed with tris-buffer saline with 0.1% v/v Tween® 20 (TBST) and PBS to fully remove the HIER buffer. This is followed by incubation with 5% v/v H_2O_2 for 30min to remove endogenous peroxidase activities and serum-free protein block (X0909, DAKO) for 30min to reduce non-specific antibody binding.

Next, the slides were then incubated with primary antibody anti-NE (1:500 v/v; PA5-115648; Invitrogen) in antibody dilution buffer (1% w/v bovine serum albumin and 0.5% v/v Triton-X100 in TBST) at 4℃ overnight. The following day, primary antibodies were flicked off and washed with TBST and PBS before incubating with Opal Polymer HRP Ms+Rb secondary antibodies provided by the detection kit for 45min. Subsequently, colonic sections were incubated with Opal fluorophore (Opal 520) for 10min in the dark. The HIER, primary antibody, secondary antibody and fluorophore incubation process was then repeated with the use of anti-MPO (1:100 v/v; PA5-16672; Invitrogen) with Opal 570 fluorophores and anti-citH3 (1:200 v/v; ab219407; abcam) with Opal 690 fluorophores. Lastly, triple labelled colon slides were stained with 4',6-diamidino-2-phenylindole (DAPI) to visualise cell nuclei and coverslipped with fluorescence mounting medium (S3023, DAKO). Immunofluorescence images were captured using an upright microscope (Axio Scope.A1, ZEISS) equipped with an AxioCam-ICm1 camera (ZEISS) at 10x magnifications. Refer to Table 6 for the settings for immunofluorescence imaging and their corresponding fluorophores employed with the different antibodies identified here.

Table 2.5. Devices and settings used for heat-induced antigen retrieval.

Antigen	Heat Induction Device	Retrieval Settings
Myeloperoxidase (MPO)	Decloaking Chamber (Biocare Medical)	Pre-heat at 80℃ for 30sec and heat induced retrieval at 125℃ for 30sec; followed by cooling fan on at 95℃ and fan off at 90℃.
Neutrophil Elastase (NE)	Microwave (Media)	1100W for 2min followed by 220W for 20min.
Citrullinated Histone H3 (CitH3)	Microwave (Media)	1100W for 2min followed by 220W for 20min.

Table 2.6. Imaging settings for neutrophil extracellular trap markers.

Antigen	Opal Fluorophore	ZEISS Camera Filter Set	Beam Splitter	Excitation/Emission Wavelength
Myeloperoxidase (MPO)	Opal 570	Filter set 43	FT570	550/570nm
Neutrophil Elastase (NE)	Opal 520	Filter set 44	FT500	494/525nm
Citrullinated Histone H3 (CitH3)	Opal 690	Filter set 50	FT660	676/694nm
-	4',6-diamidino-2-phenylindole (DAPI)	Filter set 49	FT395	358/461nm

2.7.1.2 NETs immunofluorescence intensity and density analysis

The immunofluorescence staining intensity of each NETs marker (MPO, NE and CitH3) was analysed using the ImageJ Software (v.1.54d, National Institute of Health, USA). Briefly, multi-plex immunofluorescence images were converted and channel separated using the Bio-Formats Plugin (v.7.3.0) (Figure 13a). Next, areas of the colon tissue as well as their corresponding cryptic areas were selected using the "Freehand Selections" tool in the ROI Manager (Figure 13b & c). After area selection, staining intensity of each marker was then measured using the "Multi Measure" function in the ROI Manager tool (see Figure 13d).

The co-localisation of MPO and NE as well as the process of histone citrullination by PAD4 is essential for NET formation. Thus, the overlapping staining of all three immune markers is indicative of NETs presence. The density and number of such overlap was measured using the ImageJ software (v.1.54d, National Institute of Health, USA) with the Trainable Weka Segmentation Plugin (v.3.3.4). To summarise, three multi-plex immunofluorescence images (with heavy, medium and light/no immunofluorescence) were used to "train" the plugin to accurately identify the presence of NETs (Figure 14). After the serial training was judged to be sufficiently accurate by comparison with assignments made by human eyes, the same NETs selection criteria were applied to all images and isolated NETs from each image file was created in a new greyscale 8-bit image (Figure 15). The area of colon/crypts was highlighted using the "Freehand Selections" tool and stored in ROI manager and the number of NETs presence was determined using the "Analyze Particles" function.

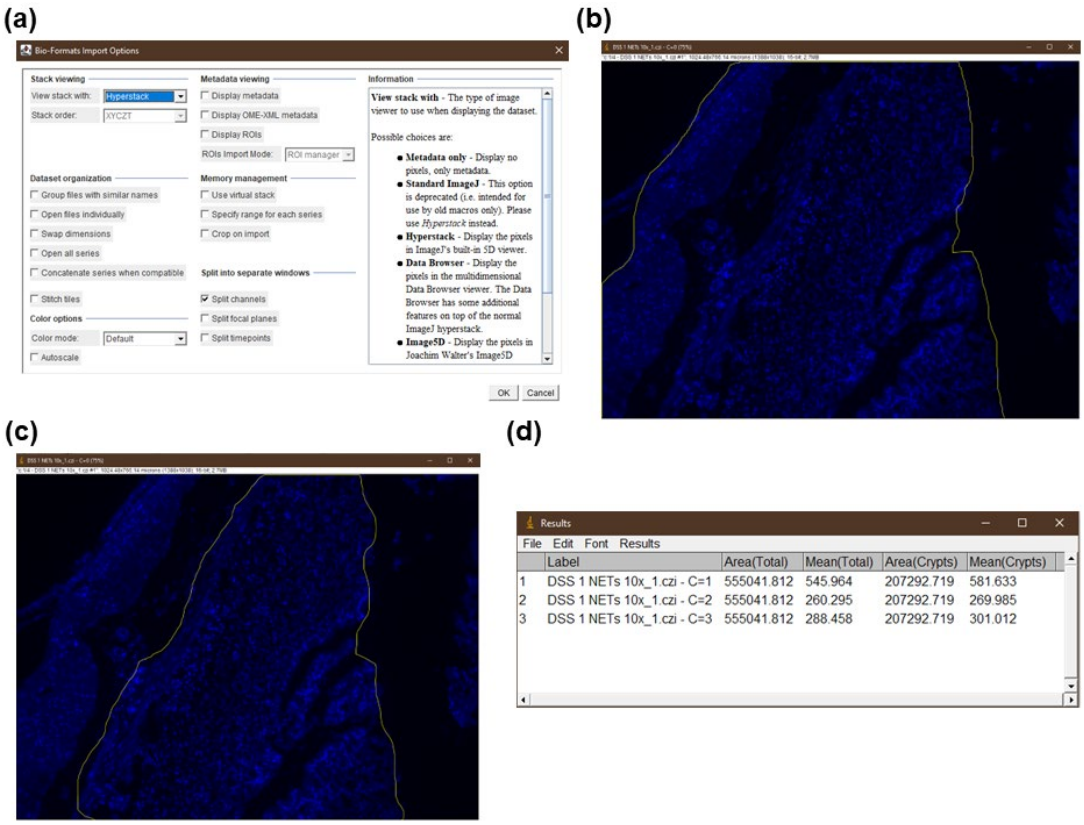

Figure 2.1. Illustration of steps involved for NETs immunofluorescence intensity analysis. (a). Settings for Bio-Formats Plugin. (b). Areal selection of total colon tissue. (c). Areal selection of cryptic area of the colon tissue. (d). Staining intensity results of the analysis, C = 1: NE, C = 2: MPO and C = 3: citH3.

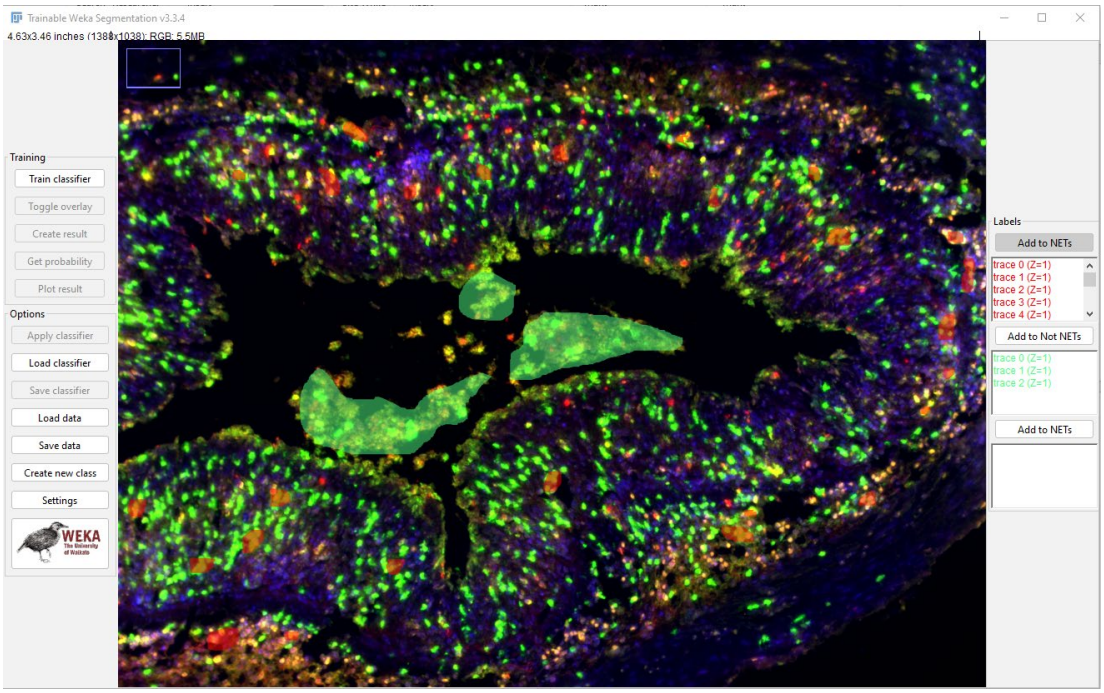

Figure 2.2. Settings of "Trainable Weka Segmentation" in the available software plugin. Red shading: training examples of NETs. Green shading: example of training the artificial intelligence system to exclude histological structures that are not NETs.

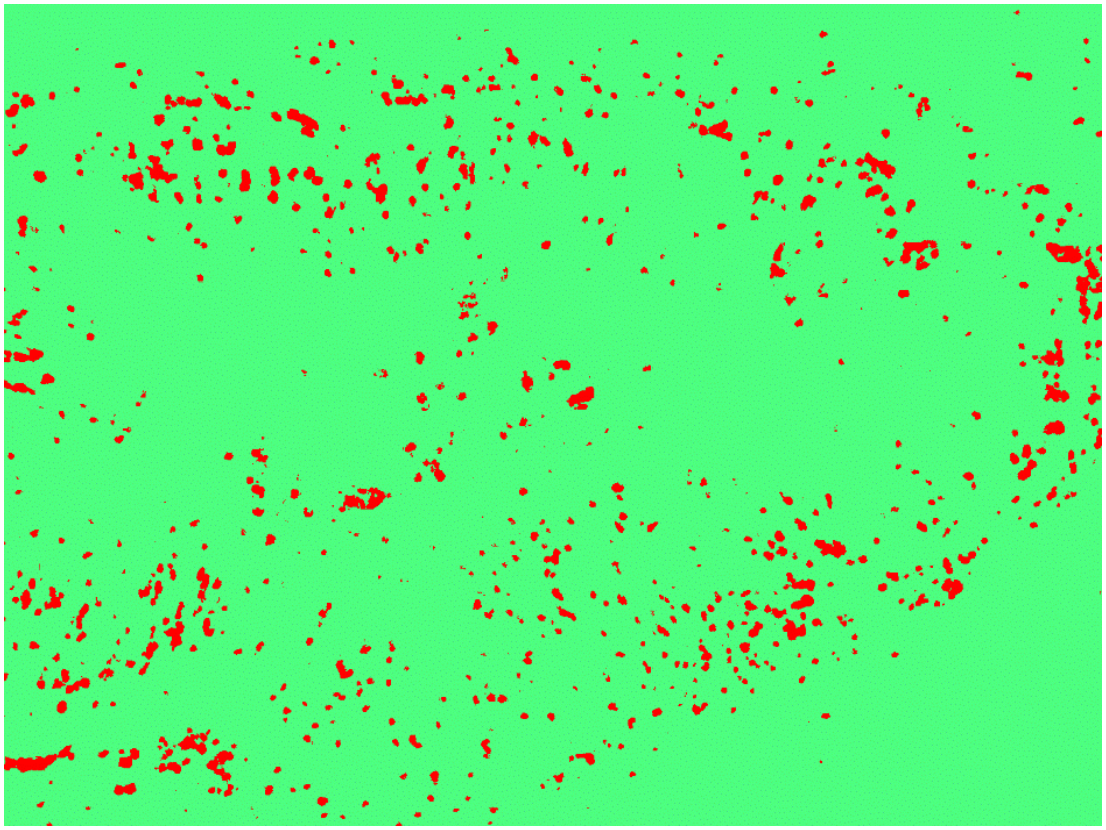

Figure 2.3. Representative 8-bit image of isolated NETs that were identified in the colon tissue following the process described above.

2.7.2 Methodologies specific to Chapter 4

2.7.2.1 Optimisation of SCFA extraction

A series of optimisation studies were performed to evaluate the efficiency of stool SCFA extraction prior to the analyses of bulk patient specimens and subsequent liquid chromatography tandem mass spectrometry (LC-MS/MS) with auto sampling. These studies compared extraction methods using organic solution of 30% v/v acetonitrile/water and aqueous solution (0.5% v/v orthophosphoric acid (OPA)/water) to isolate the analytes of interest and were essential to demonstrate a reliable and robust extraction method that would be used for all available human stool samples.

As shown in Figure 16a, extraction with the aqueous solution resulted in the detection of clear and distinct peaks with no signs of impurities. The clear symmetrical peaks have been consistently detected for all SCFA of interest, with retention time near identical to those of the corresponding authentic SCFA standards. In contrast, inorganic extraction of SCFA with 30% v/v acetonitrile/water largely resulted in responses displaying markedly larger peak width with a generally broader chromatogram (Figure 16b). Additionally, multiple split-peak responses, suggesting contaminating impurities, were often present with this method of extraction. Together the broadened split peaks obscured the appropriate SCFA peak response and subsequently the evaluation of SCFA concentrations was non-rigorous and not reproducible, hence this method was not taken further. As a result, aqueous extraction of SCFA with 0.5% v/v OPA/water on stool specimens was selected as the desired methodologies for SCFA analysis reported in Chapter 4 of the current thesis.

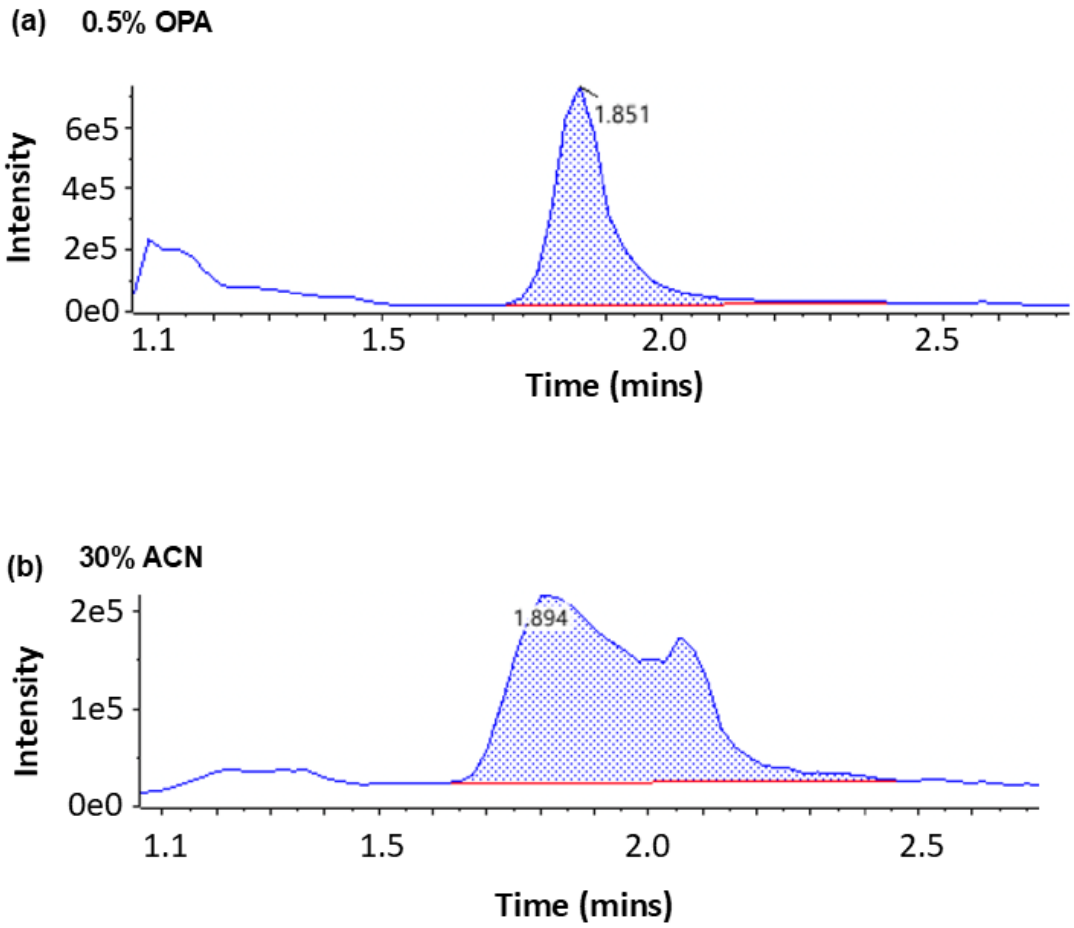

Figure 2.4. Representative chromatograms of SCFA extraction optimisation study. Panel (a). Representative chromatogram of stool specimens extracted with 0.5% v/v OPA/water, which resulted in distinct m/z peaks with optimal sensitivity. Panel (b). Representative chromatogram of stool samples extracted with 30% v/v acetonitrile/water organic solution showing significant peak broadening and likely peak contamination in the region of interest.

Chapter 3: Synthetic enzyme inhibitor as a potential IBD treatment

Below find the validation of submitted work indicating the contribution from the higher degree candidate as verified by the senior author for this manuscript.

Authorship contribution statement:

Kangzhe Xie (K.X): Investigation, validation, formal analysis, data curation, and writing – original draft. **Jordan Hunter (J.H);** Investigation and validation. **Aaron Lee (A.L):** Investigation and validation. **Gulfam Ahmad (G.A.):** Conceptualization and methodology. **Paul K. Witting (P.K.W.):** Conceptualization, methodology, project administration, supervision and review & editing of the manuscript. **Tamara Ortiz-Cerda (T.O.C.):** Investigation, validation, formal analysis, supervision, and writing – original draft and review & editing.

Confirmation from the senior authors:

I confirm that Mr Kangzhe (Steven) Xie was an active contributor and collaborator for this study now published to the journal Bioscience Reports as a "Research Paper". The authorship statement above accurately describes Steven's contribution and justifies his position as first author for this manuscript.

Signed

Dated: 17/02/2025

Dr Tamara Ortiz Cerda
Redox Biology Group
School of Medical Sciences
Faculty of Medicine & Health
Charles Perkins Centre
The University of Sydney, NSW 2006 Australia

&

Departmento de Citología e Histología Normal y patológica
Facultad de Medicina
Universidad de Sevilla, Spain. Avda. Sánchez-Pizjuán s/n
41009 Sevilla, Spain

Signed

Dated: 28/02/2025

Paul Witting (PhD)
Professor, Redox Biology
School of Medical Sciences
Faculty of Medicine and Health
Charles Perkins Centre
Editor Redox Report

Rm 4212, D17 | The University of Sydney | NSW | 2006
+61 2 91140524
paul.witting@sydney.edu.au

Bioscience Reports (2025) **45** 375–397
https://doi.org/10.1042/BSR20253205

Research Article

The PAD4 inhibitor GSK484 diminishes neutrophil extracellular trap in the colon mucosa but fails to improve inflammatory biomarkers in experimental colitis

Kangzhe Xie[1,2], Jordan Hunter[1,2,3], Aaron Lee[1,2], Gulfam Ahmad[1,4], Paul K. Witting[1,2] and Tamara Ortiz-Cerda[1,2,5]

[1]Redox Biology Group, School of Medical Sciences, Faculty of Medicine & Health, The University of Sydney, Sydney, New South Wales 2006, Australia; [2]Charles Perkins Centre, School of Medical Sciences, Faculty of Medicine & Health, The University of Sydney, Sydney, New South Wales 2006, Australia; [3]Department of Biological Sciences, Purdue University, West Lafayette, Indiana, U.S.A.; [4]Andrology Department, Royal Women's and Children's Pathology, Carlton, Victoria 3053, Australia; [5]Departmento de Citología e Histología Normal y patológica, Facultad de Medicina, Universidad de Sevilla, Avda. Sánchez-Pizjuán s/n Sevilla, Seville 41009, Spain

Correspondence: Paul K. Witting (paul.witting@sydney.edu.au) and Tamara Ortiz-Cerda (tortiz@us.es)

Inflammatory bowel disease (IBD) is a gastrointestinal disorder characterised by elevated colonic neutrophil extracellular traps (NETs), which are associated with disease severity. Formation of NETs is primarily driven by peptidyl arginine deaminase IV (PAD4) and other enzymes including myeloperoxidase (MPO) and neutrophil elastase. The present study evaluated the effect of MPO and PAD4 inhibition in dextran sodium sulfate (DSS)-induced colitis. Experimental colitis was induced in male C57BL/6 mice by 2% w/v DSS in drinking water ad libitum. Treatment groups received daily oral administration of MPO inhibitor (AZD3241; 30 mg/kg) and/or intraperitoneal injection of PAD4 inhibitor (GSK484; 4 mg/kg) 4 times over 9 days. Inhibition of PAD4 significantly diminished NET density in the colonic mucosa of mice insulted with DSS, reaching levels similar to that detected in control mice. Both inhibitors offered limited improvement in disease-activity-index, a scoring system that considers the extent of weight loss, stool consistency and rectal bleeding. Histology showed that MPO and/or PAD4 inhibition did not recover DSS-induced colon histoarchitectural damage whilst Alcian blue staining demonstrated that PAD4 failed to reduce goblet cell loss. The selected dosage of PAD4 inhibition also yielded no effect on inflammatory markers and antioxidant protein levels. These data sets suggest that other mechanisms may be involved in the pathogenesis of IBD, and the appropriate dosage of GSK484 requires thorough investigation.

Introduction

Inflammatory bowel disease (IBD) is an umbrella term that encapsulates Crohn's disease (CD) and ulcerative colitis (UC). These chronic autoimmune conditions manifest as severe gastrointestinal disorders, predominantly confined in the colon in UC or affecting any part of the digestive tract in CD [1]. The general clinical symptoms of IBD include abdominal pain, weight loss, diarrhoea, rectal bleeding, fever and anaemia [2,3]; all factors that affect lifestyle and clinical outcomes in patients diagnosed with IBD [4]. Currently, there is no cure for IBD and contemporary treatments such as 5-aminosalicylates, corticosteroids, immunomodulators and biologic therapies (e.g. anti-tumour necrosis factor alpha [TNF-α]) [5] all address symptoms. However, patients often experience disease relapse with adverse side effects such as nausea, vomiting and compromised immune systems [6].

The cause of IBD is largely unknown; however, risk factors such as age, familial history, ethnicity and environmental factors (e.g. diet and smoking), use of antibiotics and non-steroidal anti-inflammatory drugs are all linked to IBD pathogenesis [7]. Specifically, UC is characterised by immune cell infiltration, namely mast cells (MC) and neutrophils into the colon epithelium. This characteristic immune infiltration correlates with an elevation of calprotectin (CP; from activated neutrophils) level in the stool [8]. However, the underlying mechanism driving immune recruitment remains elusive. The current dogma identifies invading pathogenic bacteria, erosion of the colon epithelium and formation of colonic lesions in the presence of reactive oxygen species (ROS) as potentiating factors [9].

Increased MC infiltration and activation in the ileum and colon of IBD patients has been demonstrated [10–12]. Similarly, MC infiltration and activation is also described in animal models of UC and CD

Received: 19 February 2025
Revised: 12 May 2025
Accepted: 17 May 2025

Version of Record Published: 23 June 2025

Bioscience Reports (2025) **45** 375–397
https://doi.org/10.1042/BSR20253205

[13,14]. Upon activation by interleukin (IL)-18, tissue-resident MC degranulate to release inflammatory mediators including histamine and serine proteases [15]. In parallel, activated MCs interact with dendritic cells to secrete pro-inflammatory cytokines interferon (IFN)-γ and IL-17, which together promote T cell differentiation to yield Th1 and Th17 phenotypes [16]. Activated neutrophils have been reported to cross-talk with the IL-18/IL-18 receptor (IL-18R)-Th1 polarisation signalling pathway, where IL-18R stimulation on natural killer and Th1 cells results in neutrophil recruitment to the site of inflammation [17]. Furthermore, the G-protein-coupled receptor GPR35 contributes to efficient recruitment of neutrophils *in vivo*, where the MC-derived serotonin metabolite, 5-hydroxyindoleacetic acid (5-HIAA), acts as ligand for this receptor [18], suggesting a direct interplay between MCs and neutrophils during the inflammatory response.

Myeloperoxidase (MPO) is a heme enzyme that is abundantly found in the lysosomal azurophilic granules of neutrophils, comprising ~5% of the neutrophil dry mass [19]. Enzymic MPO utilises hydrogen peroxide (H_2O_2) and chloride anions (Cl^-) as substrates, catalysing the production of hypochlorous acid (HOCl) [20]. The potent cytotoxic oxidant HOCl elicits bactericidal actions and eliminates invading pathogens by inducing non-specific DNA damage [21]. However, the release of neutrophil MPO into the extracellular space can also cause host tissue damage. Together, infiltrating immune cells and host tissue damage become central to IBD pathogenesis that results in further pathogenic bacterial invasion and cyclic recruitment of immune cells to the inflamed colon.

The immune system tightly regulates the action of neutrophils via degranulation, phagocytosis and the formation of neutrophil extracellular traps (NETs) [22], which are extracellular structures that contain cytosolic and granule proteins (including MPO) [23]. Formation of NETs (NETosis) is initiated by nuclear chromatin decondensation, where ROS drive the translocation of neutrophil elastase (NE) to the nucleus, disrupting the chromatin structure [24]. This nuclear disruption is followed by the binding of MPO to chromatin and the conversion of arginine residues into citrullinated histone 3 (citH3) by peptidyl-arginine deiminase IV (PAD4), stimulating the disassembly of the nuclear envelope [23,25]. Nuclear envelope disassembly initiates the rupturing of the neutrophil membrane, releasing the cytosolic and granule contents into the extracellular space, which enables sustained bactericidal effects to be observed after cell death [26].

The dysregulation of NETs has been identified in various chronic inflammatory conditions. For example, increased NET density is detected in the synovial fluid of patients with rheumatoid arthritis [27], and patients diagnosed with chronic obstructive pulmonary disease or small vessel vasculitis [28]. Recently, the association of dysregulated NETs formation and IBD has been established [29–31], whereby elevated NETs density was observed in patients with CD and UC when compared with healthy controls. Furthermore, through the utilisation of multiplex imaging of NE, MPO and citH3, Schroder et al. showed that an increasing colonic NET density correlates with greater disease severity in CD [32], highlighting the potential involvement of NETs in the pathogenesis of IBD.

Pharmacological inhibition of MPO by synthetic inhibitor AZD3241 has shown to improve experimental colitis symptoms and activate the heme oxygenase-1 (HO-1)/nuclear factor erythroid factor 2-related factor 2 (Nrf2) signalling pathways [33], whilst the inhibition of PAD4 by the pan-PAD inhibitor Cl-Amidine ameliorated experimental colitis and up-regulated glutathione peroxidase 1 (GPx1) and superoxide dismutase 1 (SOD1) expression [34,35]. However, the exact involvement of NETs in experimental IBD pathogenesis remains to be fully defined, as the spatial co-localisation of essential markers of NETs: MPO, NE and citH3 was not examined. Herein, we examined the therapeutic potential of two selective enzyme inhibitors: AZD3241 (inhibiting MPO) and GSK484 (inhibiting PAD4) in ameliorating dextran sodium sulphate (DSS)-induced experimental colitis.

Results

Electrospray of MedChemExpress supplied AZD3241 contains impurities

Electrospray mass spectrometry analysis of sourced AZD3241 (M = 253.32 g/mol) obtained from Pharmaxis and MedChemExpress showed a high abundance peak at 254.09 m/z, indicating the detection of parent ion $M + 1$ (M + H) under positive ion mode. Compared with authentic AZD3241 supplied by Pharmaxis, the peak response at 254.09 m/z for the compound obtained from MedChemExpress was substantially lower. Additionally, a weak complex peak response was observed at 74.06 m/z (Supplementary

Figure S1a-c), which suggests that AZD3241 sourced from MedChemExpress contained low-molecular weight contaminants (likely inorganic salts). Ratio difference calculation between the two MPO inhibitors showed that AZD3241 from MedChemExpress contained ~42% of the compound of interest relative to the same weight of inhibitor supplied by Pharmaxis. Thus, a compensatory dosage equivalent to 30 mg/kg for AZD3241 sourced from MedChemExpress was prepared prior to administration to mice in the current study.

Administered MPO and/or PAD4 inhibitor failed to improve DSS-induced weight loss, disease activity index, nor alleviate macroscopic colon damage

DSS is a water-soluble polysaccharide that promotes gut epithelial monolayer damage when administered orally, which results in a loss of body weight and intestinal inflammation that mimics a UC-like condition in rodents [36]. Here, mice supplemented with DSS progressively lost weight from day 5, whilst control mice (absence of DSS or drug intervention) continued to increase body weight throughout the monitoring period (Figure 1a). At day 8 (day of sacrifice), mice insulted with DSS recorded a significant reduction in body weight when compared with the control (P=0.0066, Figure 1b). However, pharmacological inhibition with AZD, GSK or the combination of drugs (AZD+GSK group) was unable to mitigate DSS-induced weight loss. In mice supplemented with DSS, the disease activity index (DAI) scores increased markedly after day 4, yielding an average score of 4.5 at the end of monitoring (Figure 1c). By contrast, the DAI scores remained negligible in the control group over the same period. At the day of sacrifice, the DAI score from mice challenged with DSS was significantly greater than the corresponding control group (P=0.0087). In mice insulted with DSS in the presence of AZD3241 and/or GSK484, both inhibitors failed to ameliorate the DAI score (Figure 1d).

Next, we evaluated colon length and colon weight/length ratio as markers of macroscopic colon damage. As shown in Figure 1e and f, mice in the control group recorded a significantly longer colon length (P<0.0001) and lower colon weight/length ratio (P<0.0001) when compared with isolated colons from the DSS-insult group, whilst MPO and/or PAD4 inhibition did not improve these DSS-induced criteria. Representative images shown in Figure 1g demonstrated the dark-red colour of stool and reddened appearance of colons from DSS-insulted mice indicative of intestinal hyperaemia and colon inflammation, which was largely unaffected by any of the drug interventions. Indeed, determination of stool haemoglobin content demonstrated that DSS significantly increased faecal haemoglobin levels (P=0.0008) whilst MPO and PAD4 inhibitions had no effect (P>0.05, Supplementary Figure S2). Collectively, these outcomes demonstrate that insult with DSS resulted in extensive colon damage with parallel decline in colon function, whilst pharmacological inhibition of the enzymes MPO and/or PAD4 offered negligible protection to the colon.

Pharmacologic inhibition of MPO and/or PAD4 did not reduce biomarkers of colonic inflammation

CP is a calcium-binding protein primarily produced by neutrophils, and elevated faecal CP (FCP) level directly reflects the extent of neutrophil infiltration in patients with IBD [37,38]. In the present study, significantly higher CP levels were observed in colon homogenates and stool samples from the mice that received DSS supplementation in their drinking water (P=0.0032 and P=0.038 respectively, Supplementary Figure S3a and b). The administration of AZD3241 or GSK484 failed to alleviate the elevated CP level in both colon tissue and faeces, suggesting that MPO or PAD4 inhibition did not reduce the extent of neutrophil recruitment to the inflamed colon.

Colon damage elicited by DSS is not abrogated by MPO and/or PAD4 inhibition

The histoarchitecture of the isolated colons was visualised with H&E staining with a focus on surface epithelium loss, crypt loss and the extent of neutrophil infiltration. When compared with the control group, mice insulted with DSS exhibited significantly greater extent of surface epithelium loss, commonly showing severe erosion of the brush epithelial border (P=0.006, red arrows in Figure 2a(i,ii) and b). These tissue changes were accompanied by the presence of extensive colon ulceration, disruption of

Bioscience Reports (2025) **45** 375–397
https://doi.org/10.1042/BSR20253205

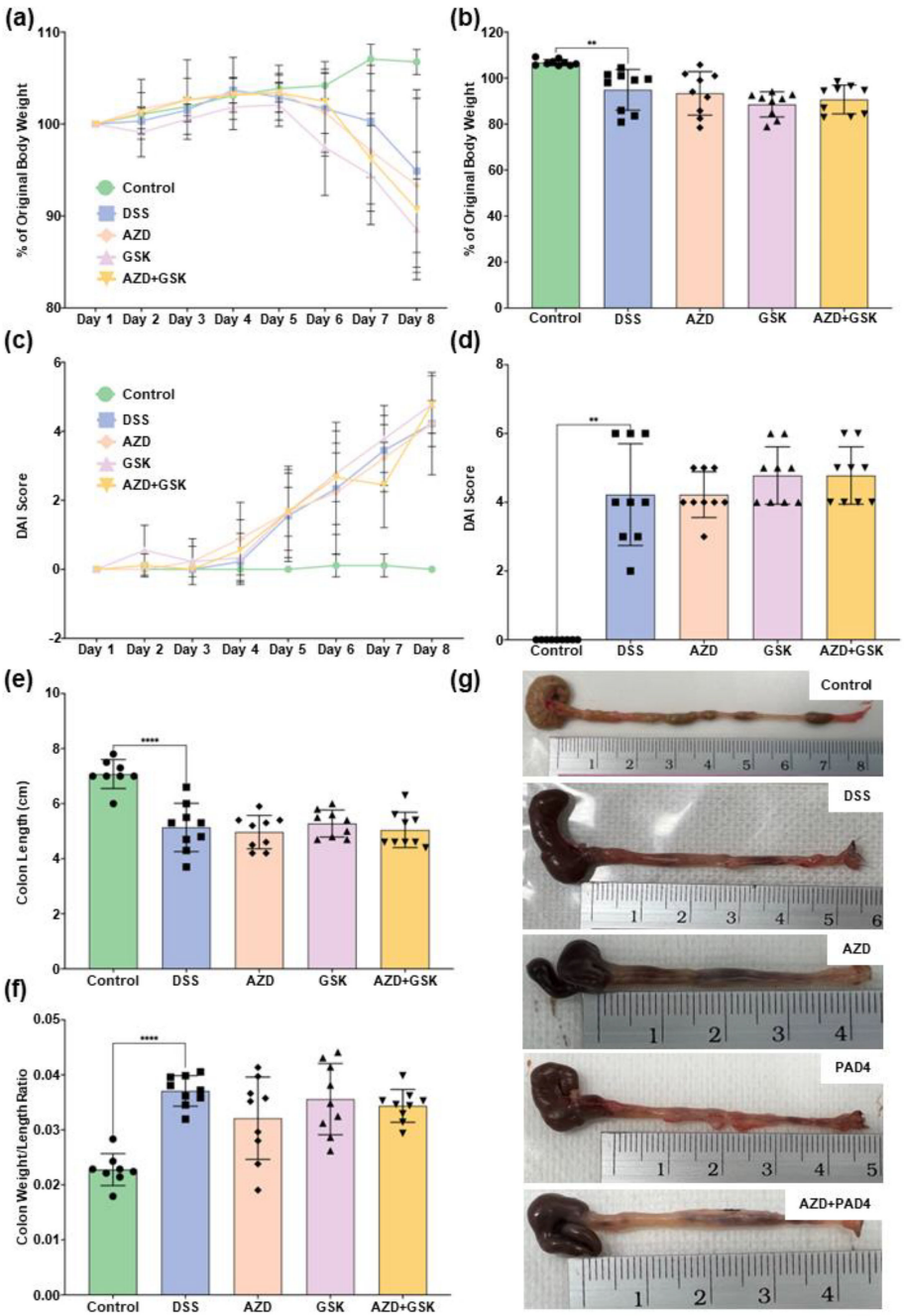

Figure 1: Effect of MPO and/or PAD4 inhibition on clinical outcomes and macroscopic colon damage in mice following eight days of DSS insult.

(**a**) Percentage of the original weight from the start of the experiment to the day of sacrifice. (**b**) Percentage of original weight at the day of sacrifice. (**c**) DAI score recorded throughout the experiment period. (**d**) DAI score recorded at the day of sacrifice. (**e**) Isolated colon length at the day of sacrifice. (**f**) Isolated colon weight/length ratio recorded at the day of sacrifice. (**g**) Representative images of isolated colon from different experimental groups. Graphical values represent mean ± SD with $n = 9$ mice per group. Normalcy of the collected data was analysed using Shapiro–Wilk test, group difference was analysed by one way ANOVA with Tukey's multiple comparison for parametric data and Kruskal–Wallis test with Dunn's multiple comparison test was used for non-parametric data. *$P \leq 0.05$, ** $P \leq 0.01$, ***$P \leq 0.001$ and ****$P \leq 0.0001$. DAI, disease activity index; DSS, dextran sodium sulphate; MPO, myeloperoxidase; PAD4, peptidyl arginine deaminase IV.

crypt histoarchitecture (P=0.0062, yellow arrows in Figure 2a(i,ii) and c) and pronounced oedema and neutrophil infiltration into the colon mucosa and submucosa (P<0.0001, green arrows in Figure 2a(i,ii) and d). Mice that received MPO and/or PAD4 inhibitors showed similar histopathologic characteristics in which AZD3241 and/or GSK484 administration failed to preserve colon histoarchitecture and reduce immune infiltration (Figure 2a(iii-v) and b-d).

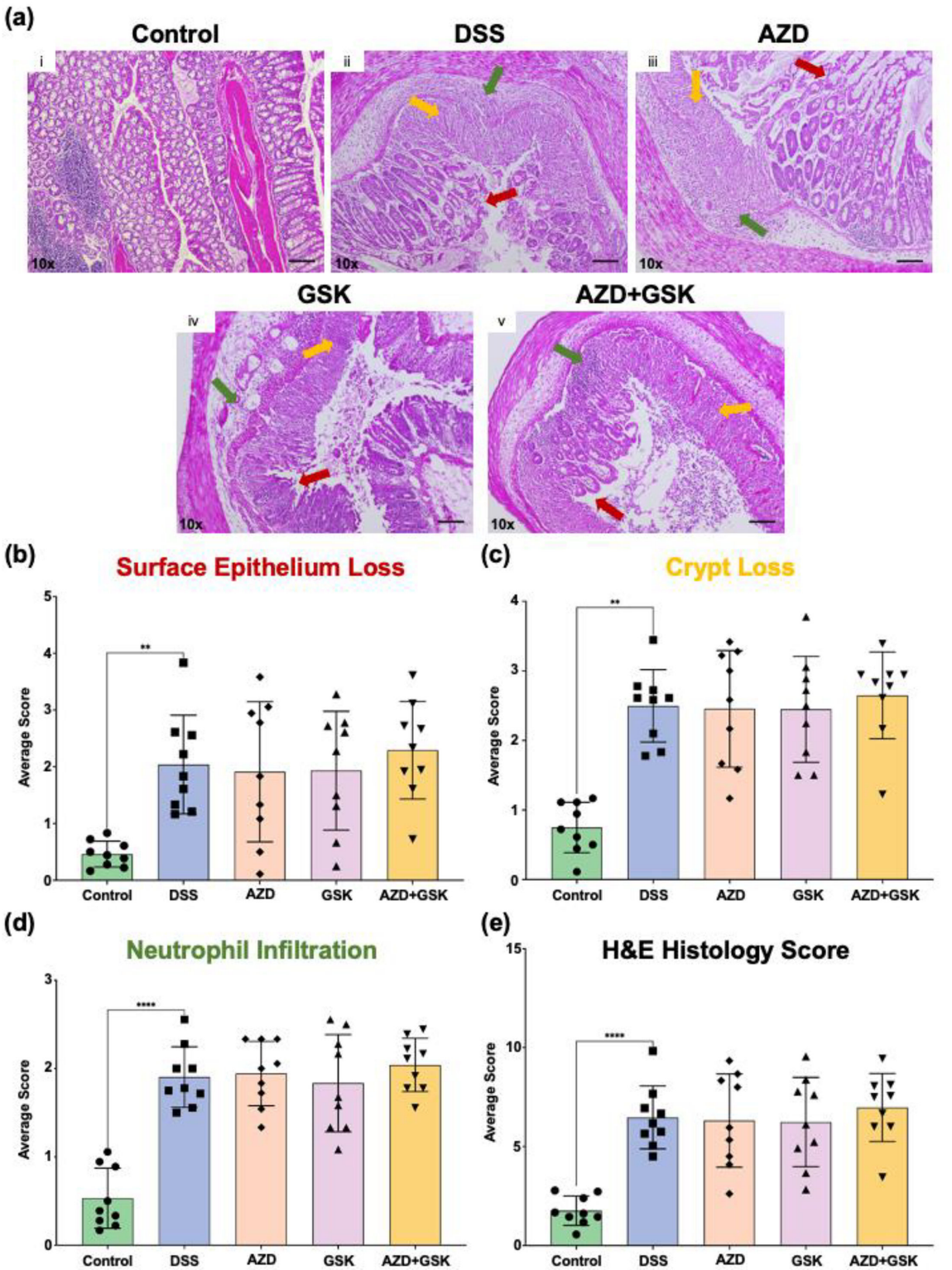

Figure 2: Haematoxylin and eosin (H&E) staining of isolated mouse colons and histopathological evaluation.

(**a**) Representative colon images from different groups were captured from Axio Lab.A1 light microscope with a Axiocam 105 Color camera at 10 x magnification. (i–v) The type and location of histoarchitectural damage was highlighted: surface epithelium loss (red arrows), crypt loss (yellow arrows) and neutrophil infiltrations (green arrows). Scale bar = 100 µm. Histology score for (**b**) surface epithelium loss, (**c**) crypt loss, (**d**) neutrophil infiltration and (**e**) total histology score. Graphical values represent mean ± SD with n = 9 mice per group. Normalcy of the collect data was analysed using Shapiro–Wilk test, group difference was analysed by one way ANOVA with Tukey's multiple comparison for parametric data and Kruskal–Wallis test with Dunn's multiple comparison test was used for non-parametric data. *$P \leq 0.05$, ** $P \leq 0.01$, ***$P \leq 0.001$ and **** $P \leq 0.0001$.

Bioscience Reports (2025) **45** 375–397
https://doi.org/10.1042/BSR20253205

As anticipated, combining the histological scoring showed that DSS insult caused extensive colon histoarchitectural disruption and immune infiltration, whereas pharmacological inhibition of MPO and/or PAD4 (either separately or in combination) was unable to ameliorate this DSS-induced colon damage (P<0.0001, Figure 2e).

MPO and/or PAD4 inhibition did not prevent goblet cell loss nor mitigate mucin production

We next utilised Alcian blue and Safranin-O stains to investigate the impact of different treatments on mucus-secreting cells from isolated colons. Goblet cells synthesise and secrete mucin to form a protective colonic mucus layer [39]. Along with the extensive inflammatory damage observed in the colons from the DSS group, weak staining of Alcian blue suggested a loss of goblet cell mucin secretion in response to the DSS insults (green arrows in Figure 3a(i-v)). This outcome is further supported by the quantitative

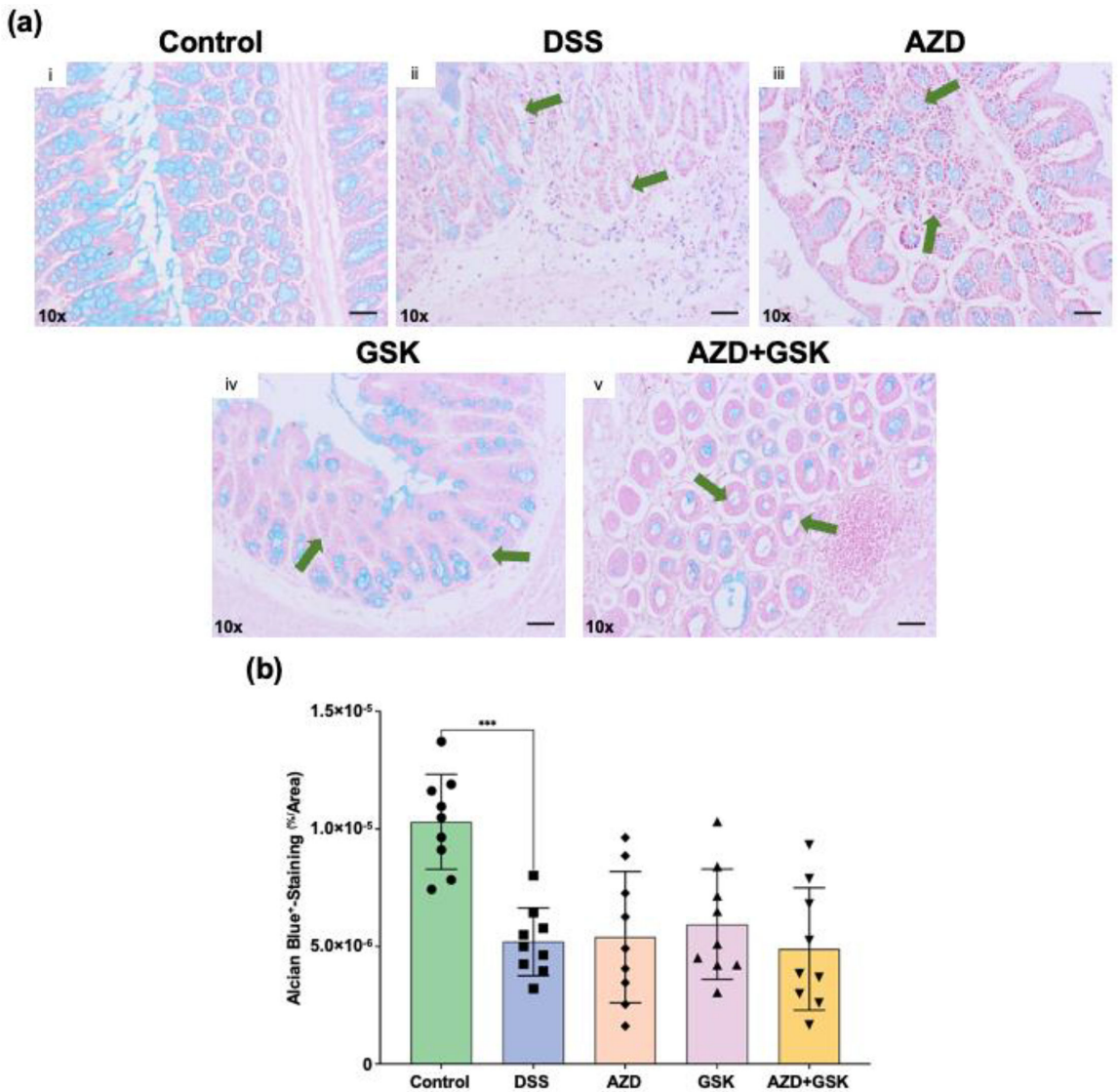

Figure 3: Alcian blue and Safranin O staining for goblet cells and mucin in mouse colons.

(**a**) Representative colon images from different experimental groups were captured from Axio Lab.A1 light microscope with a Axiocam 105 Color camera at 20x magnification. (i–v) The area of goblet cell death and mucin loss was highlighted with green arrows. Scale bar = 50 µm. (**b**) Quantification of positive staining for alcian blue is expressed as % of positive stain vs. colon area. Graphical values represent mean ± SD with n = 9 mice per group. Normalcy of the collect data was analysed using Shapiro–Wilk test, group difference was analysed by one way ANOVA with Tukey's multiple comparison as a post hoc test. *P≤0.05, **P≤0.01, ***P≤0.001 and ****P≤0.0001.

analysis of Alcian blue$^+$ staining, where significant reduction of Alcian blue was observed in colons taken from the same DSS-insulted mice compared with the control (P=0.0003, Figure 3b). In mice treated with pharmacological inhibitors (either separately or in combination), the loss of mucin was persistent and was not recovered to control levels. Percentage (%) of alcian blue$^+$ staining from all three treatment groups was not significantly different compared with the DSS group (P>0.05), which suggests that MPO and/or PAD4 inhibition did not prevent goblet cell loss and neither mitigated mucin loss nor improved the mucus physical protective layer.

MPO inhibition potentially facilitates mast cell migration and activation, whilst PAD4 inhibition dampened such mast cell response

Infiltrating MCs are characteristic of the inflammatory response of IBD and experimental colitis [10,14]. Here, Toluidine blue staining of mouse colon tissues was used to identify MCs. In the control group, few MCs were detected in the connective tissue with little evidence of MC degranulation (Figure 4a(i), respectively). Colons from mice exposed to DSS insult were characterised by substantial MC degranulation in the lamina propria, submucosa and muscularis externa layers (Figure 4a(ii)). Additionally, MCs were identified in blood vessels and in colon adventitia layers (Figure 4a(ii) and b), consistent with MC infiltration and subsequent activation in the colon tissue. Compared with the control, a significant increase in MC number was identified in the colons of mice allocated to the DSS group (P=0.0278, Figure 4b). Similar to the DSS group, a pronounced MC response was also observed in mice from the AZD group, where MC count from mice that received the MPO inhibitor was significantly higher than control (P<0.0001 Figure 4b). However, most of the MCs were not activated (as judged by an absence of non-degranulated) (Figure 4a(iii) and c). As shown in Figure 4a(iv,v), a notable decrease in MC density was determined when mice were treated with PAD4 or AZD + PAD4 inhibitors. However, these differences were not statistically significant (P>0.05, Figure 4b). Together, these results showed the potential involvement of MC in the inflamed colon that paralleled neutrophil recruitment, thereby implicating the possibility of immune-crosstalk with the neutrophil inflammatory pathway.

PAD4 inhibition diminishes the density of NETs in mucosal crypts evaluated by triple-labelled immunofluorescence

To further investigate the relationship between MC and neutrophils in DSS-induced colitis in the presence of MPO and/or PAD4 inhibition, we next examined the extent of colon NETosis. Chromatin decondensation promoted by MPO and NE and concomitant citrullination of the histone proteins by PAD4 are processes essential for NETosis [23,24]. The current study utilised multiplex immunofluorescence (IF) labelling of these three key markers: MPO, NE and citH3 to confirm spatial co-localisation of these proteins in the extracellular domain (Supplementary Figure S4) and to visualise/quantify NETs in colon tissues. As shown in Figure 5a, a noticeable increase in the colon expression of MPO and NE was detected in mice from the DSS-insult group, whereas little expression of these two immune$^+$ biomarkers was detected in the healthy controls. Importantly, pharmacological inhibition of MPO and/or PAD4 enzymes resulted in decreased MPO and NE accumulation in the DSS-injured colon. Also, the level of histone citrullination, detected as citH3$^+$ immune signal, was relatively higher in the same colon tissue, whilst colons from the healthy controls, AZD, GSK and AZD+GSK treatment groups all displayed similar levels of immune$^+$ fluorescence. However, semiquantitative analysis of the IF images showed that none of these visible changes reached statistical significance (Supplementary Figure S5a-f, P>0.05).

The current study also attempted to quantify NETs density in colon tissues by examining the degree of overlapping staining of all three immune markers. Importantly, when investigating NETs density specifically in the mucosal (epithelial) region of the colon, it was noted that NETosis increased significantly in DSS-treated colons (P=0.0092), whereas pharmacological inhibition of PAD4 with GSK484 significantly lowered NETs density in the same colon region (P=0.0294, Figure 5b and c). The administration of AZD3241 (alone) and AZD3241+GSK484 (combined) also lowered mucosal NETs formation, albeit this did not reach statistical significance (P>0.05). Thus, inhibition of PAD4 with GSK484 showed different regional effects, and reduction in NETs was limited to the colon mucosa.

Bioscience Reports (2025) **45** 375–397
https://doi.org/10.1042/BSR20253205

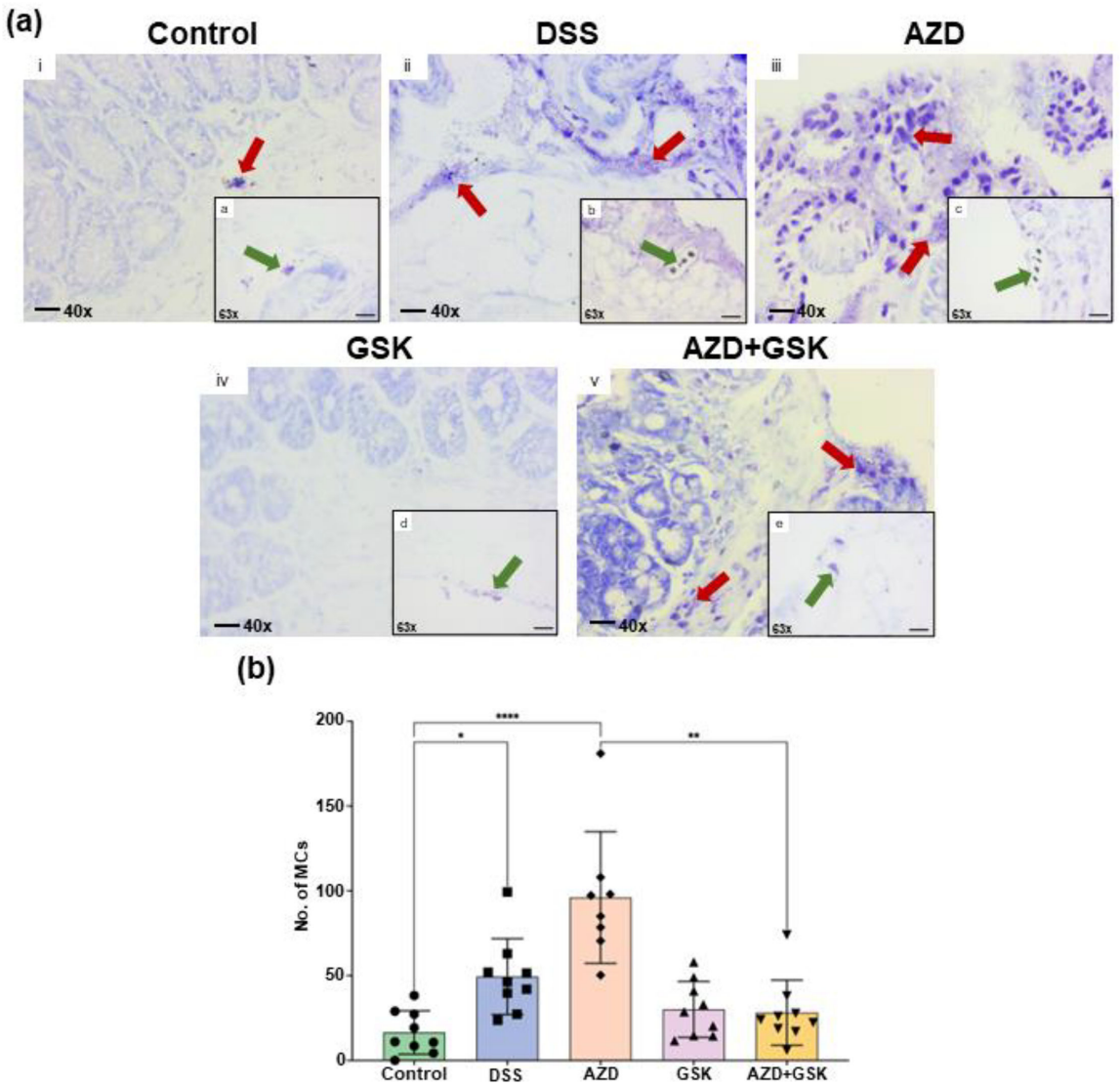

Figure 4: Toluidine Blue staining for mast cells (MC) in colon tissues.

(**a**) Representative colon images from different experimental groups. Images were captured from Axio Lab.A1 light microscope with a Axiocam 105 Color camera at 40x and 63x magnifications as indicated on the figure. Scale bar = 20 µm. (**i**) Red arrow showed a single MC in the connective tissue of submucosa and (**i.a**) MC granule was highlighted by the green arrow. (**ii**) Red arrows indicated extensive degranulation of MC in the submucosa and lamina propria layers, (**iii**) but MCs were not degranulated in the AZD group (**ii.b and iii.c**) green arrows displayed the presence of MCs in blood vessels. (**iv**) Absence of submucosal MC was observed in GSK484-treated mouse colons and (**iv.d**) presence of degranulated MC in the muscularis externa layer (green arrow). (**v**) Red arrows showed submucosal connective tissue MC and (**v.e**) presence of an inactive MC was indicated by green arrow. (**b**) Quantification of positive staining for Toluidine blue throughout the entire section. Graphical values represent mean ± SD with $n = 9$ mice per group. Normalcy of the collect data was analysed using Shapiro–Wilk test, group difference was analysed by one way ANOVA with Tukey's multiple comparison as a post hoc test. *$P \leq 0.05$, **$P \leq 0.01$, ***$P \leq 0.001$ and ****$P \leq 0.0001$.

MPO and/or PAD4 inhibition marginally alters antioxidant signalling proteins without affecting colonic lipid peroxidation

Previously published studies have reported redox state dysregulation in both IBD patients and animal models of experimental colitis [40–42]. Next, we investigated the effect of pharmacological inhibition of MPO and PAD4 on transcription factors and enzymes that are involved in the antioxidant signalling pathway. As shown in Figure 6a, DSS supplementation in drinking water did not change the colonic expression of Nrf2, and administration of PAD4 inhibitor showed a non-significant trend to increase Nrf2 expression compared with the control group (P>0.05). As indicated in Figure 6b, protein expression of GPx4, a downstream antioxidant enzyme regulated by Nrf-2 transcriptional activation [43], trended to

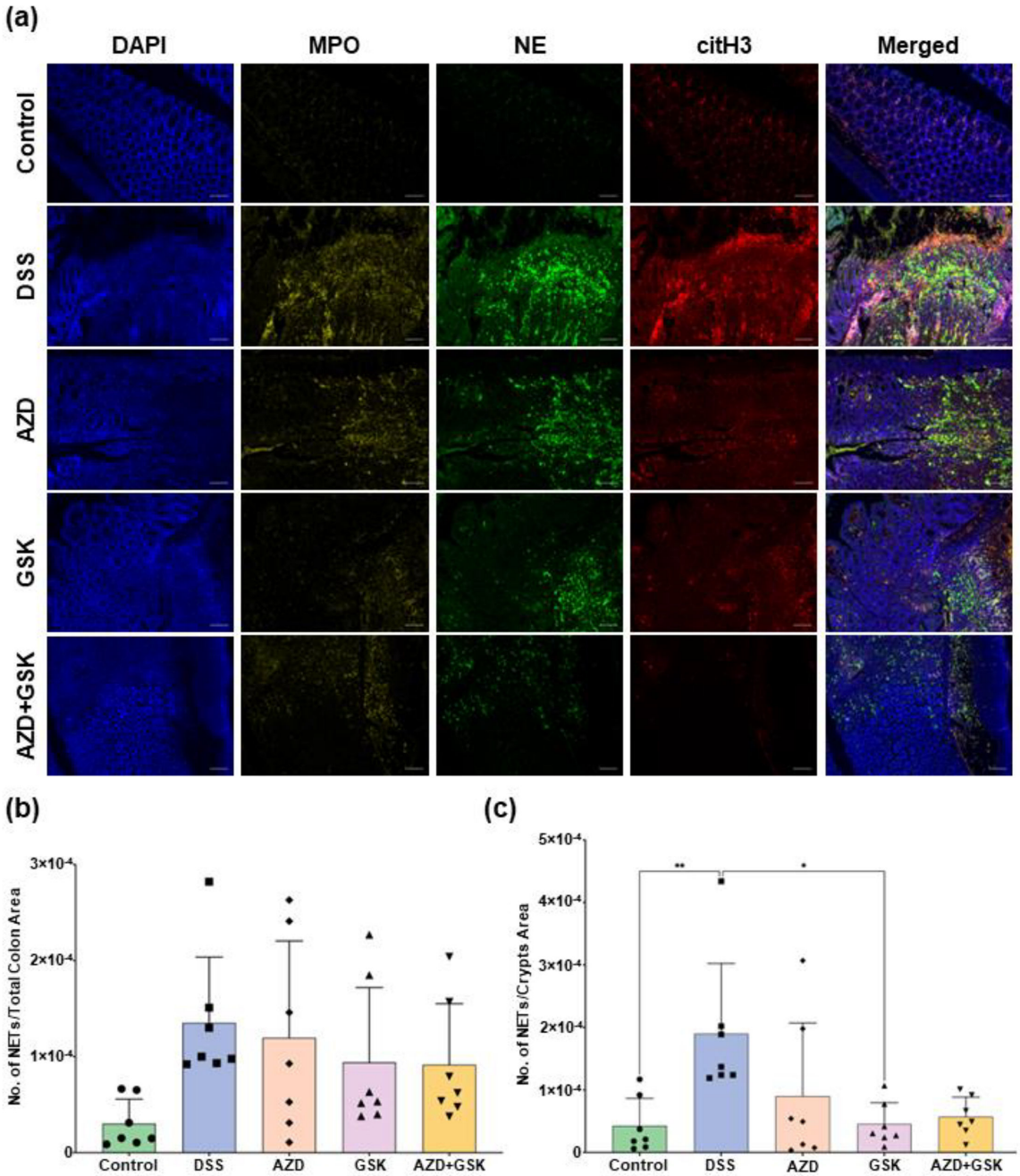

Figure 5: The effect of pharmacological inhibition of MPO and/or PAD4 on the number of NETs in DSS-insulted colons.

(**a**) Representative images of triple-plex immunofluorescence images of colons from different experimental groups were captured from Axio Scope.A1 fluorescence microscope with a AxioCam-ICm1 camera at 10x magnification. Scale bar = 100 µm. (**b**) Number of NETs per total colon area. (**c**) Number of NETs per cryptic area in the colon. Statistical outliers were identified and removed using the ROUT method (Q = 1%) and data normality was tested using the Shapiro–Wilk test. Graphical values represent mean ± SD with $n = 7$ mice per group after outlier removal. Kruskal–Wallis test with Dunn's multiple comparison as a post hoc were performed for non-parametric data. *$P \leq 0.05$, **$P \leq 0.01$, ***$P \leq 0.001$ and ****$P \leq 0.0001$. DSS, dextran sodium sulphate; MPO, myeloperoxidase; NETs, neutrophil extracellular traps; PAD4, peptidyl arginine deaminase IV.

increase in the AZD group, although this was not significantly different to all groups ($P>0.05$). SOD1 is an antioxidant enzyme with profuse expression in the gut, in which it modulates intestinal redox homeostasis under physiological conditions [44]. Despite not reaching statistical significance, Figure 6c showed that DSS insults resulted in a trend to decreased expression of colonic SOD1 ($P>0.05$).

By contrast, the inhibition of MPO or PAD4 mitigated this trend of reduction in SOD1 expression in the colon. However, this difference was not statistically significant when compared with mice treated

Bioscience Reports (2025) **45** 375–397
https://doi.org/10.1042/BSR20253205

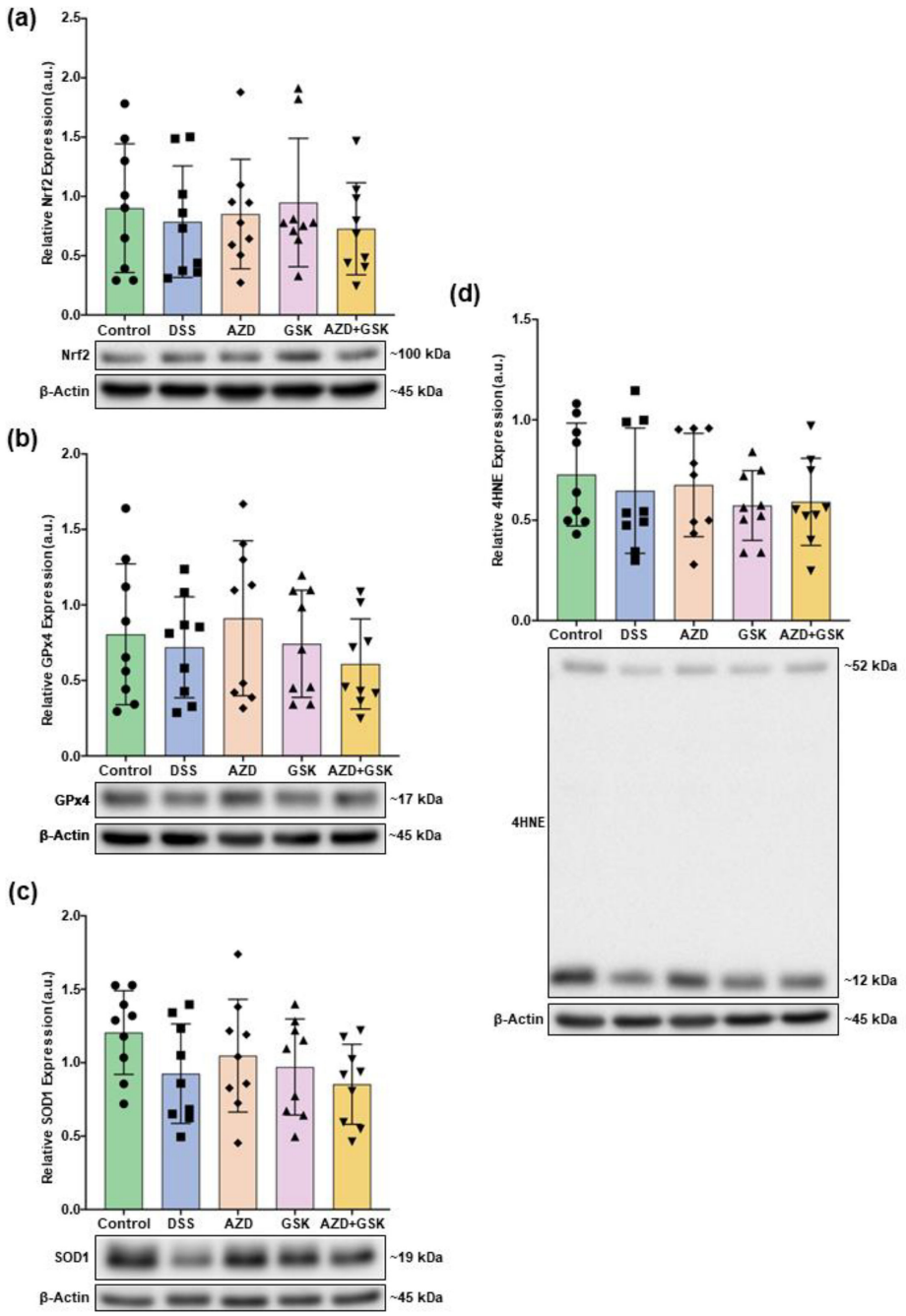

Figure 6: The effect of pharmacological inhibition of MPO and/or PAD4 on antioxidant signalling protein expressions and lipid peroxidation in colon tissue.

Representative western blots bands with densiometric quantification graphs of (**a**) Nrf2, Nuclear factor erythroid 2-related factor 2. (**b**) GPx4, glutathione peroxidase 4; (**c**) SOD1, superoxide dismutase-1; and (**d**) 4HNE, 4-hydroxynonenal. Relative expression (densiometric value) was quantified as an intensity ratio of protein of interest/β-actin. Graphical values represent mean ± SD with $n = 9$ mice per group. Normalcy of the collect data was analysed using Shapiro–Wilk test, group difference was analysed by one way ANOVA with Tukey's multiple comparison for parametric data and Kruskal–Wallis test with Dunn's multiple comparison test was used for non-parametric data distributions. MPO, myeloperoxidase; PAD4, peptidyl arginine deaminase IV; SOD, superoxide dismutase.

with DSS alone (P>0.05). In addition to the antioxidant signalling proteins, we investigated the effect of MPO and/or PAD4 inhibition on lipid peroxidation by using 4HNE as a marker. Group-wise comparison demonstrated that the difference across all experimental groups was not statistically significant (P>0.05, Figure 6d). Overall, western blot studies on antioxidant proteins and oxidative stress markers suggest that MPO and/or PAD4 inhibition had minimal influence on the redox protein expression in the DSS-insulted

colons. Contrary with previous studies that reported altered redox protein expressions in the model of DSS-induced experimental colitis, the utilisation of total colon tissue (which encompasses inflamed as well as non-inflamed areas) as well as acute induction of the disease may account for this negligible change.

PAD4 inhibition reduced total SOD activity in colons but had no effect on catalase activity

To further explore colonic SOD1 expression in the DSS-supplemented mice (refer to Figure 6c), total SOD activity assay was determined in the same colon tissue. As shown in Figure 7a, total SOD activity was maintained in the colon when compared with the controls, suggesting a potential up-regulation of SOD enzymatic activities as a compensatory mechanism for the reduction in its expression. However, in the mice that received PAD4 inhibitor or MPO and PAD4 inhibitors simultaneously, a significantly lower SOD activity was observed (P=0.0104 and P=0.0168 respectively). A similar trend to lower total SOD activity was observed in mice supplemented with the MPO inhibitor, albeit this did not reach statistical significance (P>0.05). These results suggest that NET inhibition by PAD4 (refer to Figure 5) could potentially diminish total SOD activities in the colitis colons. As SOD catalyses the dismutation of superoxide radicals into oxygen and hydrogen peroxide [45], total catalase activity was evaluated to understand the colon capacity to neutralise ROS in response to NETs inhibition by PAD4. Overall, no difference in catalase activity was observed across all experimental groups (Figure 7b).

MPO and/or PAD4 inhibition has minimal effect on IL-1β level in DSS-stimulated colons

Finally, we investigated the effect of MPO and/or PAD4 inhibition on the change in immunological profiles by examining the balance of pro-inflammatory (IL-1β) and anti-inflammatory (IL-4 and IL-10) cytokines in isolated colon. A trend to increased colon IL-1β was observed in the mice that were challenged with DSS. However, this was not statistically significant when compared with the healthy controls (P>0.05). Contrastingly, treatment with MPO and/or PAD4 inhibitors appeared to diminish the marginal increase in IL-1β level in the colon (P>0.05. Figure 8a). DSS supplementation has shown to drastically dampen the anti-inflammatory profiles in the colon tissue. Overall, IL-10 was significantly downregulated (P<0.0001, Supplementary Figure S6), whilst a substantial decrease in colon IL-4 level was also observed, albeit not statistically significant when compared with the DSS group (P>0.05, Figure 8b). No difference in colon IL-4 and IL-10 levels was detected between the DSS and mice co-supplemented with MPO and/or PAD4

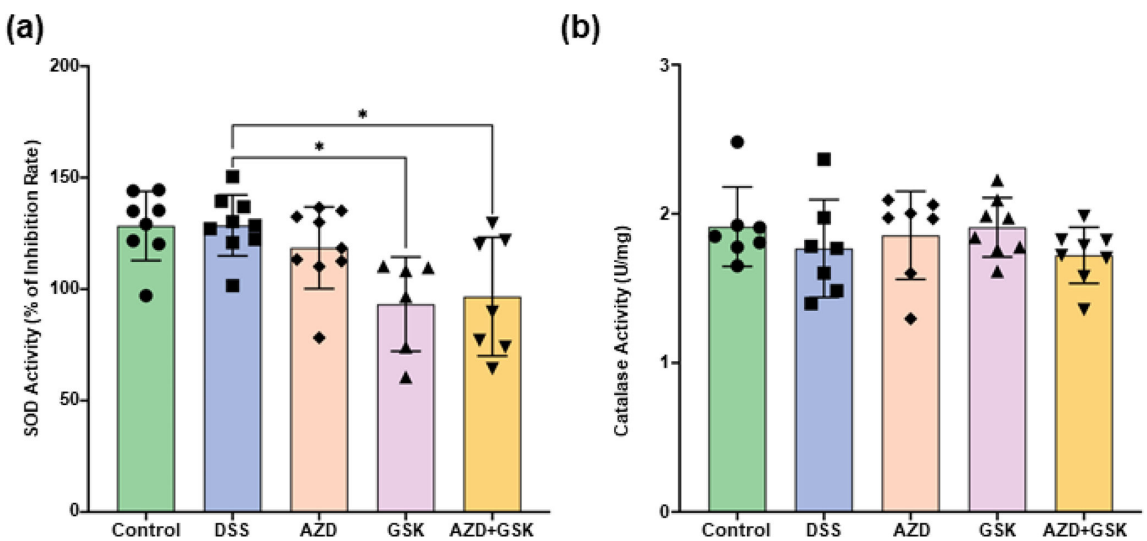

Figure 7: The effect of MPO and/or PAD4 inhibition on antioxidant enzyme activities.

(**a**) Total superoxide dismutase (SOD) activity. (**b**) Total catalase activity. Graphical values represent mean ± SD with $n = 6–9$ mice per group after standard curve interpolation. Normalcy of the collect data was analysed using Shapiro–Wilk test, group difference was analysed by one way ANOVA with Tukey's multiple comparison as a post hoc test. *P≤0.05, **P≤0.01, ***P≤0.001 and ****P≤0.0001. MPO, myeloperoxidase; PAD4, peptidyl arginine deaminase IV.

Bioscience Reports (2025) **45** 375–397
https://doi.org/10.1042/BSR20253205

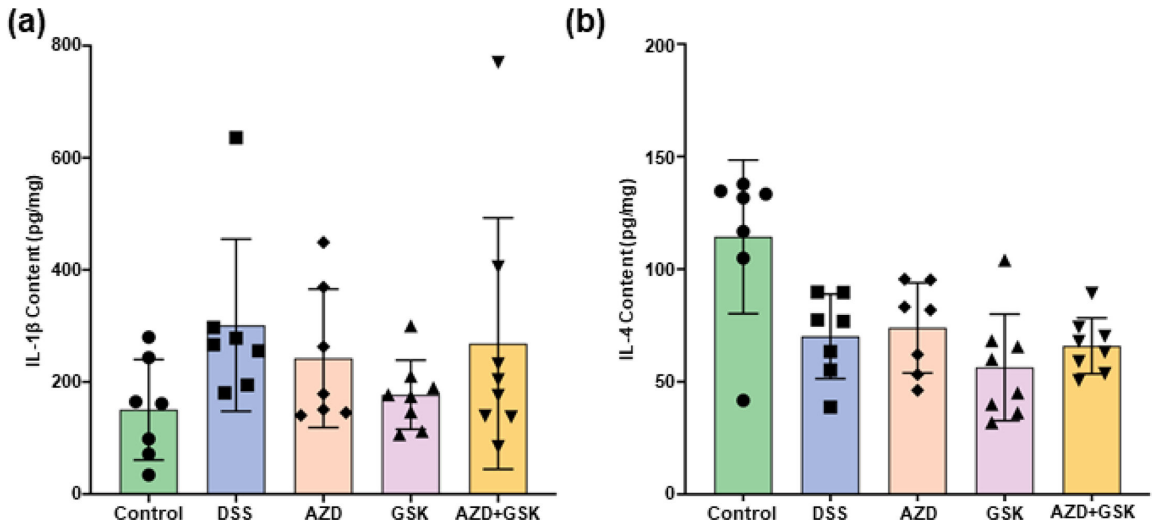

Figure 8: The effect of MPO and/or PAD4 inhibition on inflammatory markers.

(**a**) Interleukin (IL)-1β. (**b**) IL-4. Graphical values represent mean ± SD with $n = 7–8$ mice per group after standard curve interpolation. Normalcy of the collect data was analysed using Shapiro–Wilk test, group difference was analysed by one way ANOVA with Tukey's multiple comparison for parametric data and Kruskal–Wallis test with Dunn's multiple comparison test was used for non-parametric data. MPO, myeloperoxidase; PAD4, peptidyl arginine deaminase IV.

inhibitors ($P>0.05$), suggesting that AZD3241 and GSK484 have no effect on IL-4 and IL-10 molecular pathways.

Discussion

Whilst current evidence supports the notion that excessive neutrophil infiltration and dysregulated immune responses are linked to IBD disease pathogenesis, the precise mechanism remains unclear. In the context of UC, the formation of NETs can be considered a process that maintains the DNA-damage activity by trapping MPO released from neutrophils within the extracellular matrix, effectively prolonging MPO activity and sustaining inflammation in the colon [26]. Accordingly, elevated NET formation and parallel enhancement of inflammation have been reported in the colon mucosa of patients with UC [29]. Therefore, the inhibition of extracellular MPO activity and/or decreased NET formation can potentially represent a therapeutic approach to improve tissue damage observed in the pathogenesis of UC. This current study was the first to highlight the spatial co-localisation of 3 essential NETosis enzymes: MPO, NE and citH3 in the colon tissue using multi-plex IF imaging, further reinforcing the involvement of NETs during the pathogenesis of DSS-induced experimental colitis. As anticipated, DSS insult elevated NET density in colon tissue, yielding a significant increase in the colonic crypts, indicating that NET formation occurs primarily in the mucosa layer during acute inflammation in UC. Similarly, *Citrobacter rodentium* – a murine pathogen that mimics *Escherichia coli* infection – has also been shown to elicit NET formation in specific experimental mouse strains. For instance, *Citrobacter rodentium*-infected C3H mice display similarities clinical and histological features similar to those observed in UC. A study by Sanchez-Garrido et al. demonstrated that a greater number of neutrophils was evident in the lumen of C57 mice, whereas an extensive accumulation of neutrophils and a marked elevation of NETs and citrullinated histone H3 were observed in *C. rodentium*-infected C3H mice, specifically trapped within the colon mucosa and submucosa [46]. These findings are consistent with our results, where DSS-induced chemical colitis also led to acute inflammation, elevated faecal CP and triggered NET formation in the colonic mucosa. We also showed that administration of GSK484 (inhibiting PAD4) at 4 mg/kg administered four times over 9 days (total drug provided to each mouse ~400 µg) significantly reduced mucosal NETs. Meanwhile, the treatment with either AZD (MPO inhibitor) or GSK484+AZD trended to decrease mucosal NET formation, although this was not significantly different to mice stimulated with DSS alone. Despite GSK484 reducing mucosal NET density, the extent of UC-like experimental colitis remained unchanged as judged by several measures of colon inflammation, suggesting a local effect without affecting disease pathogenesis.

AZD3241 is a synthetic MPO inhibitor developed by AstraZeneca, in which it completely blocks MPO-mediated oxidation at 2 µM and elicits minimal effects on the oxidation activities of other

peroxidases such as thyroid peroxidases and lactoperoxidases [47]. Despite a compensated dose being administered, the colon protective activity of AZD3241 (inhibiting extracellular MPO) was not recapitulated in the current study, evident in the lack of improvement in experimental colitis symptoms and persistent intestinal inflammation after the mice were co-supplemented with DSS and AZD3241. This may be attributed to the presence of low-molecular weight contaminants in the newly acquired compound, interfering with previously reported AZD3241 bioactivity [33]. Despite adjusting the dosage of AZD3241 to closely match dosing used previously [33], a potential limitation is the low purity of the compound used in this study, which may restrict the anti-inflammatory action of this inhibitor or elicit unwanted pro-inflammatory activity in colon tissues from low-molecular weight contaminants. The effect of AZD3241 on NET formation has been studied in the context of experimental UC. Interestingly, a markedly lower number of NETs was observed in the mice that received AZD3241 treatment, suggesting that the MPO inhibitor reduces NETosis via a pathway that is PAD4-independent, possibly via reduced oxidative stress in the colon mucosa. Indeed, AZD3241 has shown to reduce oxidative stress in the brain of Parkinsonian patients [48]. This is further supported by the critical roles of ROS in NETosis, where MPO-derived ROS are documented to stimulate neutrophil elastase translocation to the nucleus via the MEK-extracellular-signal-regulated kinase (ERK) signalling pathway [49,50]. Nevertheless, additional research is required to fully understand the effect of inhibiting MPO activity on NETs formation in IBD.

On the other hand, GSK484 is a selective inhibitor against the PAD4 enzyme, and it has been shown to have negligible off-target activities against a panel of 50 unrelated proteins [51]. Previous reports have demonstrated that the administration of PAD4 inhibitors like GSK484 at the same dose of our study (4 mg/kg) but delivered daily for one week suppressed NETosis in mice with cancer-associated kidney injury [52]. Meanwhile, an intraperitoneal injection of GSK484 at a higher concentration (10 mg/kg body weight) in a murine model of myocardial infarction resulted in profound inhibition of NETosis and significantly improved clinical parameters with no adverse side effects [53]. These successful experimental interventions may be due to GSK484 being tested under different dosing regimens (daily administration vs. every second day in the current study), suggesting that a greater extent of PAD4/NETs inhibition is required to achieve a threshold level of NETs inhibition and consequently a therapeutic effect. Additionally, the pharmacokinetics of GSK484 display a low-moderate clearance rate yielding a half-life (T1/2 h) of 3.8 ± 1.5 h and blood clearance (Clb) over 19 ± 3 ml/min/kg in mice [51,54], showing that daily administration could be beneficial to achieve optimal pharmacological activity. Nevertheless, the dose tested here was able to limit NETosis in the colon mucosa, although this focal inhibition failed to ameliorate disease progression.

It is notable that the therapeutic potential of NETs inhibition by limiting PAD4 activities should be examined with caution, as the available literature reports conflicting results on the role of NETosis in IBD development. In the study by Dragoni et al., NETs were identified to be a potential pathological stimulus for fibroblast activation, and depletion of PAD4 in neutrophils reduced NET formation and limited fibroblast activation, implying a stimulatory role of PAD4 in mediating fibrogenesis in IBD [55]. In contrast, Leppkes et al. reported that PAD4-deficient mice were associated with exacerbated DSS-induced colitis and more severe rectal bleeding, suggesting a vital role for PAD4 and NETs in minimising immuno-thrombosis and rectal bleeding [56]. These outcomes conflict with the data reporting PAD4 inhibition with a pan-inhibitor can ameliorate experimental colitis [34, 35]. Together, these findings suggest that the therapeutic potential of PAD4-dependent NETs inhibition in IBD remains unclear and warrants further investigation. Certainly, more research is required to unambiguously demonstrate that inhibiting NETosis is an appropriate therapy for treating IBD and to establish the optimal dosage of PAD4-specific inhibitors such as GSK484 without generating associated risks like opportunistic infection.

The role of MC is not fully clear in the pathogenesis of IBD. Inflammatory and oxidative stimuli can act in concert to recruit MC and stimulate neutrophils to perpetuate a continuous cycle of inflammatory immune cell infiltration and driving the chronicity of the disease [57], particularly in the colon mucosa. Interestingly, production of the potent MPO-oxidant HOCl chlorinates the primary amino group of histamine derived from MC to form chloramine-histamines [58], thereby potentially limiting HOCl-mediated oxidation [59] in the colon mucosa. In this study, mice simulated with DSS insult showed concomitant increases in NETs and MC in the colon. This result highlights that MC migration/degranulation occurs in parallel with active recruitment of neutrophils during the pathogenesis of DSS-mediated colon inflammation, suggesting that MC mediators and downstream histamine-modification by HOCl could be a potential protective compensatory mechanism to prevent indiscriminate HOCl-mediated colon damage. This notion is supported by a study in an IL-10-deficient mouse model of IBD, where

Bioscience Reports (2025) **45** 375–397
https://doi.org/10.1042/BSR20253205

colonic MCs were found to enhance intestinal epithelial barrier function and protect the colon mucosa [60]. Notably, accompanying a reduction in NETosis in the colon mucosa, treatment with GSK484 simultaneously and significantly reduced the number and degranulation status of MC in the same colon region, with levels diminished to be similar to controls. This outcome may explain the lack of improvement in symptoms and biomarkers of experimental colitis in the presence of the PAD4 inhibitor. Therefore, this current study shows for the first time another potential pathway in the non-allergic regulatory role of MC, suggesting that GSK484 failed to resolve intestinal inflammation and colitis symptoms, likely due to the inhibition of MC activation. This is further supported by previous studies that have shown the immunomodulatory and protective role of MC in attenuating injury and inflammation [61,62].

Furthermore, the close relationship between MC and neutrophils has been recently reported in chronic allergic inflammation. Interestingly, MC degranulation can reroute neutrophil migration, leading them to invade MC and initiating a process where neutrophils become trapped by MC and form 'cell-in-cell' structures, where neutrophils can remain viable up to 48 h post encapsulation inside the MC. This newly described phenomenon called MC intracellular trap (MIT) by Mihlan et al. [63], which suggests that MC can prolong neutrophil survival in tissues and may play a relevant role in the inflammatory process that involves the innate immune response; although it remains to be determined whether the PAD4 inhibitor (GSK) not only reduced NET formation but also inhibited MC migration and activation, which in turn affects MIT structures. In contrast, the study by Kurashima et al. demonstrated that MC activation promotes DSS-induced experimental colitis via P2X7 receptors [64], whilst Okayama et al. showed that neutrophils promote intestinal inflammation via MC infiltration and activation in a rat model of indomethacin-induced enteritis [65]. However, these outcomes were observed in a period of 24 hours after inflammation induction. The current study observed a significant increase in MC when mice were treated with AZD3241, suggesting that neutrophils may potentially activate MC through other pro-inflammatory cytokines such as IL-18 [66], which has been previously demonstrated to be critical for MC activation and degranulation in inflamed tissues *via* IL-18R [17]. Thus, further work is warranted to elucidate the potential interplay between non-allergic function of MC and neutrophils to achieve a comprehensive understanding of the interplay between these cell types in the setting of IBD.

Nrf2 governs the transcription of numerous genes involved in the antioxidant defence system to maintain physiological redox balance. For instance, Nrf2 promotes the expression of thioredoxin and thioredoxin reductase to facilitate the removal of oxidised thiols and peroxides [67,68] whilst regulating the expressions of glutamate cysteine ligase and GPx to allow glutathione production and ROS detoxification [69,70]. However, this redox balance was disrupted in UC, where impaired activities of SOD, GPx and CAT in UC all contribute to chronic inflammation in the gut [71]. Additionally, oxidative stress is also closely interrelated with NETs formation, where NADPH oxidase-generated ROS is required for the nuclear translocation of NE during the process of NETosis [24]. Interestingly, this current study showed that the administration of AZD3241 and/or GSK484 lowered the total SOD activities in the homogenised colon tissues, suggesting that reduced colon mucosa NETs formation is associated with lowered ROS detoxifying power in the gut. However, a major limitation in the current study is the lack of examination on ROS content, where the levels of H_2O_2 and MPO-derived HOCl were not directly evaluated. As a result, the link between intestinal NETs reduction and diminished SOD activities in the context of DSS-induced experimental colitis requires further investigations where the potential synergistic effects of quenching ROS as well as administration of NETosis-associated enzyme inhibitors should also be explored.

To conclude, the current study highlighted the involvement of NETs in the DSS-induced model of experimental colitis via multi-plex IF imaging, whilst the administration of AZD3241 (inhibiting MPO) and GSK484 (inhibiting PAD4) both reduced NET mucosa formation and reduced MC migration and activation, which are closely related to the pathophysiology of the neutrophil immune response. Overall, the off-target effects of these drugs yielding changes in MC responses may explain why inhibiting PAD4 activity and reducing mucosal NETosis failed to improve clinical symptoms nor reduce intestinal inflammation.

Methods

Animals

All experimental procedures involving mice were conducted within the Laboratory Animal Service (LAS) facility at the University of Sydney and followed the approved protocol by the University of Sydney Animal

Ethics Committee (Approval #2019/1496). Male C57BL/6 mice (six weeks of age) were purchased from Animal Resource Centre (Perth, Australia) and housed in environmentally enriched ventilated cages at the LAS facility located at the Charles Perkin Centre (CPC) at the University of Sydney, Australia, under a 12-h light–dark cycle at 22°C with standard chow diet and tap water provided *ad libitum*. All mice were acclimated for seven days prior to the start of experiments, and each mouse was tail marked for individual identification.

Drug administration

Molecular grade DSS (molecular weight range: 36–50 kDa) was purchased from MP Biomedicals (CAS# 9011–18-1). Acute experimental colitis was induced with 2% w/v DSS in the drinking water as previously described by our group [33]. Water consumption was monitored daily, and fresh DSS-water mixture was replaced every 3 days with the same dosage maintained throughout the duration of the study. The synthetic MPO inhibitor, AZD3241 (also known as Verdiperstat), was purchased from MedChemExpress (Cat# HY-17646), whilst PAD4 inhibitor, GSK484, was acquired from a commercial source (Abcam, Sydney Australia, Cat# ab223598; purity > 98%).

The doses and administration routes for MPO and PAD4 inhibitors were selected based on previously published studies [33,72], taking into consideration the need to avoid toxic effects and high doses that could lead to consequences of infections, since MPO activity/NETosis is associated with the bactericidal action of MPO. A stock solution of GSK484 (25 mg/ml) was prepared in 100% ethanol and stored at −30°C. Where required, this PAD inhibitor was diluted with sterile saline using an insulin syringe (Thermo) and administered via *i.p.* injection to achieve a final dose of 4 mg/kg body weight. Additionally, mice were trained to accept approximately 0.1 g of peanut butter (PB) via oral intake during their acclimation period to avoid invasive oral gavage of AZD3241 and hence reduce animal handling-associated stress.

Electrospray mass spectrometry analysis of AZD3241

Recently, the colon protective activity of the MPO inhibitor AZD3241 (obtained as a gift from Pharmaxis Ltd, Frenchs Forrest, Sydney) was demonstrated in an experimental colitis [33]. Due to a change in supplier, and to validate the purity of the MPO inhibitor supplied by MedChemExpress, electrospray ionisation mass spectrometry was conducted on both original and newly sourced AZD3241 using a Q Exactive HF-X Orbitrap System (Thermo Scientific). Both inhibitors were analysed at 5 µg/mL in 50% v/v methanol, and the Q Exactive HF-X Tune Software (Thermo Scientific) was used to operate the orbitrap system in positive ion mode with a HILIC column. Data accumulation parameters were as follows: scan range: 50.0–750.0 m/z, mass resolution 120,000, spray voltage: 4 kV, capillary temperature: 320°C and Funnel RF level: 50. Both synthetic drugs were diluted 1:200 v/v in H_2O: MeOH = 1:1 v/v (final concentration ~5 µg/mL). Analysis was performed in triplicate and peak intensities were averaged and compared. The amount of MedChemExpress-supplied AZD3241 administered to the mice was then normalised through relative comparison to the authentic AZD3241 supplied by Pharmaxis to achieve an equivalent dose.

Experimental design

The experimental design has been outlined schematically in Figure 9. At seven weeks of age, mice were randomly allocated into five groups (n = 9 per group) as follows:

1. *Control Group*: 0.1 g of PB daily + standard chow diet and drinking water *ad libitum*.
2. *DSS Group*: 0.1 g of peanut butter daily + standard chow diet and 2% w/v DSS in drinking water *ad libitum*.
3. *AZD3241 Group*: 30 mg/kg body weight in 0.1 g of PB daily + standard chow diet and 2% w/v DSS in drinking water *ad libitum*.
4. *GSK484 Group*: 4 mg/kg injected *i.p.* every second day +0.1 g of PB daily + standard chow diet and 2% w/v DSS in drinking water *ad libitum*.
5. *AZD3241+GSK484 Group*: 4 mg/kg of GSK484 injected *i.p.* every second day+30 mg/kg body weight of AZD3241 in 0.1 g of PB daily + standard chow diet and 2% w/v DSS in drinking water *ad libitum*.

Bioscience Reports (2025) **45** 375–397
https://doi.org/10.1042/BSR20253205

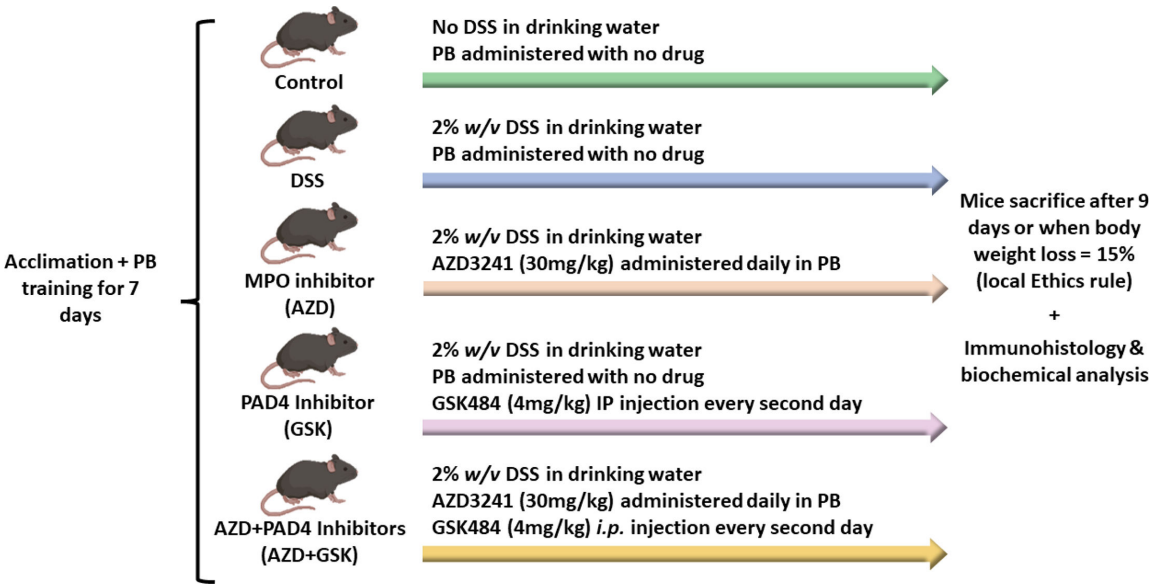

Figure 9: Overview of the experimental timeline and group allocations.

(i) Control group; (ii) DDS group, dextran sodium sulphate (DSS) at 2% w/v was administered to induce colitis; (iii) AZD group, myeloperoxidase (MPO) inhibitor AZD3241 at 30 mg/kg was provided to mice daily in peanut butter (PB) through the experiment; (iv) GSK group, peptidyl-arginine deiminase IV (PAD4) inhibitor GSK484 at 4 m/kg was injected via i.p. every second day. (v) AZD+GSK inhibitors group, both treatments were administered following the conditions mentioned above.

Mice were terminated at the loss of 15% of their body weight measured at day 0 or eight days after DSS induction according to the approved Ethics protocol. At the end of the experiment, blood was collected via cardiac puncture from mice under full anaesthesia (4% v/v inhaled isoflurane). Subsequently, cervical dislocation was performed, and colon tissue and faecal material were harvested.

Clinical features and disease activity index

Monitoring progression of experimental colitis throughout the duration of the study was achieved by evaluating an individual mouse DAI using criteria previously described [33]. To capture gross disease progression, the average total DAI score for each allocated group was determined at the end of the experiment. The DAI score involved four clinical markers summarised in Table 1 and took into consideration stool appearance, the presence of rectal prolapse, grooming and the percentage of weight loss with scores ranging from 0 to 2. Following organ harvest, the length and colon weight were recorded.

Tissue fixation, embedding and sectioning

Isolated colons were processed initially by overnight fixation in 70% v/v ethanol, followed by embedding in paraffin wax. Next, colons were sectioned at 5 μm thickness with a rotary microtome (Shandon Finesse 325, Thermo), and sections were then mounted onto Superfrost™ Plus Microscope Slides (Fisher Scientific). Mounted slides were dried in an oven (60°C, 2 h). After drying, slides were assigned randomly generated codes to blind the treatment conditions throughout the duration of subsequent staining and image analysis.

Histopathological studies

Where required, slides were dewaxed and rehydrated in xylene (2 × 10 min) and graded alcohols (2 × 2 min 100% ethanol, 2 × 2 min 95% ethanol and 1 × 2 min 70% ethanol) before commencing staining described below. Histological images were captured by using the Axio Lab.A1 light microscope (ZEISS) with the Axiocam 105 Color Camera (ZEISS). Two imaging fields per section (6 images per slide) were generated at 20× magnifications to conduct histology scoring (H&E and Alcian Blue/ Safranin O staining). Quantitation of MC in Toluidine Blue-stained sections was performed by screening the complete colon

Table 1: Disease activity index (DAI) scoring criteria.

Clinical markers	Score	Description
Stool appearance	0	Normal
	1	Soft
	2	Watery/Presence of blood
% of weight loss	0	< 1%
	1	1–10%
	2	> 10%
Rectal prolapse	0	No prolapse
	1	Prolapse present
Grooming	0	No hunched posture, bristle fur, or skin lesions
	1	Presence of hunched posture, bristle fur and skin lesions

section with representative images captured using 40× and 63× objectives by three different experienced researchers (K.X, T.O.C, and J.H) unless specified otherwise.

Haematoxylin and eosin staining

Colon histoarchitectural and histopathological changes were assessed using haematoxylin and eosin (H&E)-stained colon sections. Briefly, colon sections (10 μm) were immersed in filtered Harris Haematoxylin solution for 2 min to visualise the cell nuclei, washed thoroughly with tap water, then submerged in Scott's blue solution for 30 s and another 10 s in acid alcohol. Subsequently, the slides were placed into eosin for 30 s. Next, slides were exposed to 10 s of 95% v/v ethanol and 2 × 10 s of 100% ethanol. After this dehydration step, colon sections were cleared in xylene and mounted with Dibutylphthalate plasticiser xylene (DPX) mounting medium. The criteria for histoarchitecture examination included visualisation of crypt inflammation and loss, degree of neutrophil infiltration and loss of surface epithelium, which were scored manually from 0 to 3, with this scale corresponding to an absence of the criteria to severe damage (refer to Table 2 for scoring summary).

Alcian Blue with Safranin O staining

Alcian Blue and Safranin O stains were used to examine the presence of mucin secreted from goblet cells in the colon mucosa. Briefly, slides were immersed in 0.1% w/v Alcian Blue pH 2.5 solution for 30 min before rinsing with distilled water for 5 min. Then, slides were counterstained in 0.1% w/v acetic Safranin O solution for 10 min, followed by another 5 min of distilled water wash to visualise the colon epithelial histoarchitecture. Then, the slides were air-dried completely under a fume cupboard for 4 h before immersing in xylene for 2 × 10 min and coverslipped with DPX medium. The staining intensity of Alcian blue was quantified by two different researchers (K.X and T.O.C) using the 'Color Threshold' function in the ImageJ software (v.1.54d, National Institute of Health, U.S.A.).

Toluidine Blue staining

Toluidine Blue staining was utilised to determine the presence of resident MC due to their metachromatic properties after staining. The staining procedure was modified from a previously published protocol [13]. Briefly, colon sections were stained with Toluidine Blue working solution (0.5% w/v Toluidine Blue and 1% v/v glacial acetic acid in distilled water) for 90 s. Next, the slides were immersed in visualising solution (5% w/v ammonium molybdate in distilled water) for 5 min to minimise dye removal, rinsed with tap water for 5 min then rapidly dehydrated through graded alcohols (1 × 1 min in 90%, 95% and 100% v/v ethanol with gentle agitation). After 2 × 5 min of clearing with xylene, stained sections were then coverslipped with DPX mounting medium. Since matured MCs often reside in lamina propria, submucosa, smooth muscle or near blood vessels of the gastrointestinal tract [73], the current study focused on the transient MC populations restricted to connective tissue. Furthermore, mucosa and brush border MC staining were excluded due to the non-specific metachromasia of the Toluidine blue dye that interacts with mucin-derived sulphated glycoproteins in this region.

Bioscience Reports (2025) **45** 375–397
https://doi.org/10.1042/BSR20253205

Table 2: Haematoxylin and eosin (H&E) histoarchitectural evaluation criteria.

Score	0	1	2	3	4
Pathologies					
Crypt loss	Intact crypts	Disoriented crypts	Variable crypt diameter	Atrophied crypts	Mucosa devoid of crypts
Neutrophil infiltration	No infiltration	Mucosal/lamina propria infiltration	Mucosal and submucosal infiltration	Moderate cryptitis/infiltration to crypts	Severe cryptitis
Loss of surface epithelium	Intact surface epithelium	Sloughing off epithelial surface	Patchy loss of surface epithelium	Moderate loss of surface epithelium	Severe loss/erosion of surface epithelium

IF staining: three-plex immuno-labelling and fluorescent imaging and analysis

The presence and density of NETs in colon tissue was visualised by using the Opal 6-Plex Detection Kit (NEL811001KT; AKOYA Biosciences) and simultaneously identifying MPO, CitH3 and NE in the same colon tissues using a multiplex imaging approach. All staining steps were completed at 22°C in an opaque humidity chamber unless specified otherwise and following the manufacturer recommended protocol. After slide dewaxing and rehydrating, heat-induced epitope retrieval (HIER) was performed by placing the slides into an opaque Coplin jar with pH 6.0 citrate HIER buffer (S2369, DAKO) to expose the NETs antigens: MPO, NE and citH3. The device settings used for the HIER process and final dilutions were summarised in Supplementary Table S1. After HIER processing, slides were washed three times with tris-buffer saline (TBS) with 0.1% v/v Tween® 20 (TBST) and one time with PBS to fully remove the HIER buffer. This was followed by incubation with 5% v/v H_2O_2 for 30 min to inhibit endogenous peroxidase activity and blocking with serum-free protein (X0909, DAKO) for 30 min to reduce non-specific antibody binding.

Next, slides were incubated with anti-NE primary antibody in antibody dilution buffer [1% w/v bovine serum albumin (BSA) and 0.5% v/v Triton-X100 in TBST) at 4°C overnight. The following day, primary antibodies were removed by washing with 3 × 2 min TBST and 1 × 2 min PBS before incubating with Opal Polymer HRP Ms + Rb secondary antibodies for 45 min. Subsequently, colonic sections were incubated with Opal fluorophore (Opal 520) for 10 min in the dark. The HIER, primary antibody, secondary antibody and fluorophore incubation process was then repeated sequentially using anti-MPO and anti-citH3 antibodies with their respective fluorophores. Finally, triple-labelled colon slides were stained with 4′,6-diamidino-2-phenylindole (DAPI) to visualise cell nuclei and coverslipped with fluorescence mounting medium (S3023, DAKO). IF images were captured using an upright microscope (Axio Scope.A1, ZEISS) equipped with an AxioCam-ICm1 camera (ZEISS) at 10× objective. The imaging settings for different antibodies and their corresponding fluorophores are summarised in Supplementary Table S2.

The IF staining intensity of each NETs marker (MPO, NE and citH3) was analysed using the ImageJ Software (v.1.54d, National Institute of Health, U.S.A.). Briefly, multi-plex IF images were converted and channel separated using the Bio-Formats Plugin (v.7.3.0). Next, areas of the colon tissue as well as their corresponding cryptic areas were selected using the Freehand Selections tool in the ROI Manager. After area selection, staining intensity of each marker was then measured using the Multi Measure function in the ROI Manager tool (see Appendix S1 in Supplementary information). Overlap of the three immune markers, to identify NET density, was measured using ImageJ software (v.1.54d, National Institute of Health, U.S.A.) with the Trainable Weka Segmentation Plugin (v.3.3.4). To summarise, three representative images (with heavy, medium and light/no IF) were used to 'train' the AI plugin to accurately identify the presence of NETs. After verifying selectivity, the NETs selection criteria were applied to all images, and isolated NETs from each image file were identified in a new greyscale 8-bit image. The area of colon/crypts was highlighted using the Freehand Selections tool and stored in ROI manager, and the number of NETs was then determined using the Analyze Particles function (see Appendix S2 in Supplementary information).

Tissue homogenisation for molecular and biochemical analysis

Isolated colon and faecal samples were homogenised to enable further molecular and biochemical analysis. Briefly, colon tissues or stool samples were snap frozen in liquid nitrogen then grounded into a fine powder with a mortar and pestle before resuspending with complete lysis buffer [50 mM phosphate buffer saline pH 7.4, 1 mM ethylenediaminetetraacetic acid, 10 μM butylated hydroxytoluene, 0.05 mM sodium azide, one tablet of cOmplete™ Protease Inhibitor Cocktail (Roche) and one tablet of PhosSTOP™ Phosphatase Inhibitor Cocktail (Roche)] in a 5 ml Teflon-coated tube (Wheaton Glassware). Next, the gross suspension was homogenised with a rotating piston matched to the Teflon-coated tube at 600 r.p.m. for 5 min whilst submerging in an ice bath, before centrifugation at 15,000x g for 15 min at 4°C. Clarified supernatants were collected, stored at −80°C and total protein concentration was determined using the Pierce™ bicinchoninic acid (BCA) Protein Assay Kit (Thermo Scientific) by following the manufacturer recommended protocol.

Western blot assay

Western blot was used to visualise separated proteins in homogenised colon tissues using Precision Plus Protein™ Kaleidoscope™ (1610375, BioRad) ladder for molecular weight determination. Where required, 20 μg protein homogenised sample (except for 4-hydroxynonenal [4HNE], a marker of lipid oxidation that used 30 μg protein) was mixed with sodium dodecyl sulfate (SDS)-loading buffer (final concentration: 50 mM Tris-HCl pH 6.8, 2% w/v SDS, 6% v/v glycerol and 0.004% w/v bromophenol blue) and heat reduced at 95°C for 5 min. After heating, samples were resolved on 12% w/v Mini-PROTEAN® hand-cast gels (BioRad) in running buffer (containing: 25 mM Tris pH 8.3, 192 mM glycine and 0.1% w/v SDS) at 35 mA for 45 min using the Mini-PROTEAN® chamber (BioRad).

Gels were then transferred onto 0.2 μm polyvinylidene fluoride (PVDF) membranes in transfer buffer (25 mM Tris pH 8.3, 192 mM glycine and 20% v/v methanol) using the Trans-Blot Turbo System (BioRad). After protein transfer, PVDF membranes were blocked with 5% w/v skim milk/TBST (1 h, 22°C) to minimise non-specific antibody binding. This is followed by the incubation with primary antibody anti-Nrf2, anti-GPx4, anti-SOD1 and anti-4HNE in antibody diluent buffer (5% w/v BSA, 0.05% w/v sodium azide in TBS) at 4°C overnight. Anti-β actin visualisation of total β actin was used as a loading control. Subsequently, PVDF membranes were incubated with HRP-conjugated secondary antibodies [anti-rabbit HRP or anti-mouse HRP in 5% w/v skim milk in TBST for 2 h at 22°C (see Supplementary Table S3 for all antibodies dilutions). Protein bands of interest were visualised with Clarity™ Western ECL Substrate (1705060, BioRad) for 5 min at 22°C in the dark after the membrane was washed 3 × 5 min with TBST and 1 × 5 min with TBS and images were captured using the ChemiDoc™ Touch Gel/Membrane Imaging System (BioRad). The densiometric intensity of the protein bands was analysed and normalised using the Image Lab software (v6.1, BioRad).

Enzyme linked immunosorbent assays and enzymatic activity assays

The following commercially available enzyme linked immunosorbent assay (ELISA) were purchased: Mouse IL-1β, IL-4, IL-10 and Calprotectin SimpleStep ELISA kit. Colorimetric enzymatic activity assay kits for colorimetric Activity Kit and SOD Activity Assay Kit were also obtained. The recommended protocols for manufacture were followed and clarified Colon or faecal homogenates were diluted with Mili-Q water to fit absorbance changes within the standard curve. The colorimetric absorbance of each sample was collected by using a microplate reader (Infinite M200-Pro, Tecan) (see Supplementary Table S3 for all sample dilution and microplate reader settings).

Statistical analysis

All data collected in the current study were made available publicly via Mendely Data repository [74] and were subjected to heterogeneity (parametric) testing prior to group-wise comparison using GraphPad® Prism software (v.10.1.0, La Jolla, U.S.A.). To minimise machine-introduced errors during the triple-plex IF analysis, statistical outliers were identified using the ROUT Method (Q = 1%) before normalcy testing and pair-wise comparisons were conducted. The heterogeneity and normality of the collected data were examined using the Shapiro–Wilk test with alpha (α) error = 0.05. For parametric data sets, one-way analysis of variance (ANOVA) test with Tukey's multiple comparison as a post hoc analysis was conducted. The Kruskal–Wallis test with Dunn's multiple comparison post hoc was used to identify any statistical

Bioscience Reports (2025) **45** 375–397
https://doi.org/10.1042/BSR20253205

differences between the treatment groups for non-parametrically distributed data sets. The statistical significance threshold between treatment groups was set as $P<0.05$, and all graphical data were represented as means ± standard deviation (SD).

Data Availability

All data generated from this work are included in the manuscript and its supplementary files. All datasets generated for this study are available in a registered data repository (74).

Competing Interests

The authors declare no conflict of interest was associated with the experimental design, analysis and reporting of the study.

Funding

The author(s) declare no direct financial support was received for the research, authorship, and/or publication of this article. Senior author T.O.C was supported financially by Spanish Ministry of Universities 'Margarita Salas' grants for the training of young doctors. First author K.X was supported by a University of Sydney co-funded scholarship. Author P.K.W was supported by NHMRC Project Grant (APP1125392).

CRediT Author Contribution

K.X.: Investigation, validation, formal analysis, data curation, and writing–original draft. J.H.: Investigation and validation. A.L: Investigation and validation. G.A.: Conceptualization and methodology. P.K.W.: Conceptualization, methodology, project administration, supervision and review and editing of the manuscript. T.O.C.: Investigation, validation, formal analysis, supervision, and writing–original draft and review and editing.

Ethics Approval

All experiments involving animals were in accordance with standards guidelines for the care and use of laboratory animals. All procedures performed in studies were following the approved protocol by the University of Sydney Animal Ethics Committee (Approval #2019/1496).

Acknowledgments

The authors would like to express their sincerest gratitude to Ms. Jessica Tieng, Ms. Nicolette Shiung and Mr. Bruno F. Lemos Wimmer for their assistance in aspects of the animal study, Dr. Belal Chami in colonic NETs imaging and analysis, and acknowledge Dr. Samson Dowland from the Charles Perkins Centre Histology Facility and Dr. Kang-Yu Peng and Dr. Atul Bhatnagar from the Sydney Mass Spectrometry (SydneyMS) of the at The University of Sydney for the resources, scientific and technical expertise provided for the completion of current study.

Abbreviations

ANOVA , Analysis of variance; AZD3241, MPO inhibitor; BSA , Bovine serum albumin; CAT, catalase; CD , Crohn's disease; CP , Calprotectin; CPC, Charles Perkins Centre; CitH3, citrullinated histone H3; Cl^- , Chloride anions; Clb , Blood clearance; DAI , Disease activity index; DAPI, 4′,6-diamidino-2-phenylindole; DPX, Dibutylphthalate plasticiser xylene; DSS, dextran sodium sulphate; ERK, MEK-extracellular-signal-regulated kinase; FCP, faecal calprotectin; GPR, G-protein-coupled receptor GPx; GPx1, glutathione peroxidase 1; GSK484, PAD4 inhibitor; H&E, Haematoxylin & eosin; 5-HIAA , 5-hydroxyindoleacetic acid; 4HNE , 4-hydroxynoneal; HO-1, heme oxygenase-1; H_2O_2, Hydrogen peroxide; IBD, inflammatory bowel disease; IF, Immunofluorescence; IL, Interleukin; IL-18R , Interleukin-18 receptor; MC, mast cells; MIT, Mast cell intracellular trap; MPO, myeloperoxidase; NE, neutrophil elastase; NETs, neutrophil extracellular traps; Nrf2, nuclear factor erythroid factor 2-related factor 2; PAD4, peptidyl-arginine deiminase IV; PB, Peanut butter; ROS, reactive oxygen species; SDS , Sodium dodecyl sulphate; SOD1, superoxide dismutase 1; TBS , Tris-buffered saline; TBST , Tris-buffered saline with Tween 20; TNF-α, Tumour necrosis factor alpha; UC, ulcerative colitis.

References

1 Ng, S.C., Shi, H.Y., Hamidi, N., Underwood, F.E., Tang, W., Benchimol, E.I. et al. (2017) Worldwide incidence and prevalence of inflammatory bowel disease in the 21st century: a systematic review of population-based studies. *Lancet* **390**, 2769–2778 https://doi.org/10.1016/S0140-6736(17)32448-0

2 Roda, G., Chien Ng, S., Kotze, P.G., Argollo, M., Panaccione, R., Spinelli, A. et al. (2020) Crohn's disease. *Nat. Rev. Dis. Primers* **6**, 22 https://doi.org/10.1038/s41572-020-0156-2

3 Kobayashi, T., Siegmund, B., Le Berre, C., Wei, S.C., Ferrante, M., Shen, B. et al. (2020) Ulcerative colitis. *Nat. Rev. Dis. Primers* **6**, 74 https://doi.org/10.1038/s41572-020-0205-x

4 Rozich, J.J., Holmer, A. and Singh, S. (2020) Effect of lifestyle factors on outcomes in patients with inflammatory bowel diseases. *Am. J. Gastroenterol.* **115**, 832–840 https://doi.org/10.14309/ajg.0000000000000608

5 Cai, Z., Wang, S. and Li, J. (2021) Treatment of inflammatory bowel disease: a comprehensive review. *Front. Med. (Lausanne)* **8**, 765474 https://doi.org/10.3389/fmed.2021.765474

6 Pithadia, A.B. and Jain, S. (2011) Treatment of inflammatory bowel disease (IBD). *Pharmacol. Rep.* **63**, 629–642 https://doi.org/10.1016/s1734-1140(11)70575-8

7 Ananthakrishnan, A.N. (2015) Epidemiology and risk factors for IBD. *Nat. Rev. Gastroenterol. Hepatol.* **12**, 205–217 https://doi.org/10.1038/nrgastro.2015.34

8 Hanai, H., Takeuchi, K., Iida, T., Kashiwagi, N., Saniabadi, A.R., Matsushita, I. et al. (2004) Relationship between fecal calprotectin, intestinal inflammation, and peripheral blood neutrophils in patients with active ulcerative colitis. *Dig. Dis. Sci.* **49**, 1438–1443 https://doi.org/10.1023/b:ddas.0000042243.47279.87

9 Bourgonje, A.R., Feelisch, M., Faber, K.N., Pasch, A., Dijkstra, G. and Van Goor, H. (2020) Oxidative stress and redox-modulating therapeutics in inflammatory bowel disease. *Trends Mol. Med.* **26**, 1034–1046 https://doi.org/10.1016/j.molmed.2020.06.006

10 Liu, B., Yang, M.Q., Yu, T.Y., Yin, Y.Y., Liu, Y., Wang, X.D. et al. (2021) Mast cell tryptase promotes inflammatory bowel disease-induced intestinal fibrosis. *Inflamm. Bowel Dis.* **27**, 242–255 https://doi.org/10.1093/ibd/izaa125

11 King, T., Biddle, W., Bhatia, P., Moore, J. and Miner, P.B. (1992) Colonic mucosal mast cell distribution at line of demarcation of active ulcerative colitis. *Dig. Dis. Sci.* **37**, 490–495 https://doi.org/10.1007/BF01307568

12 Sasaki, Y., Tanaka, M. and Kudo, H. (2002) Differentiation between ulcerative colitis and Crohn's disease by a quantitative immunohistochemical evaluation of T lymphocytes, neutrophils, histiocytes and mast cells. *Pathol. Int.* **52**, 277–285 https://doi.org/10.1046/j.1440-1827.2002.01354.x

13 Ortiz-Cerda, T., Argüelles-Arias, F., Macías-García, L., Vázquez-Román, V., Tapia, G., Xie, K. et al. (2023) Effects of polyphenolic maqui (*Aristotelia chilensis*) extract on the inhibition of NLRP3 inflammasome and activation of mast cells in a mouse model of Crohn's disease-like colitis. *Front. Immunol.* **14**, 1229767 https://doi.org/10.3389/fimmu.2023.1229767

14 Cho, E.Y., Choi, S.C., Lee, S.H., Ahn, J.Y., Im, L.R., Kim, J.H. et al. (2011) Nafamostat mesilate attenuates colonic inflammation and mast cell infiltration in the experimental colitis. *Int. Immunopharmacol.* **11**, 412–417 https://doi.org/10.1016/j.intimp.2010.12.008

15 Chen, E., Chuang, L.S., Giri, M., Villaverde, N., Hsu, N.Y., Sabic, K. et al. (2021) Inflamed ulcerative colitis regions associated with MRGPRX2-mediated mast cell degranulation and cell activation modules, defining a new therapeutic target. *Gastroenterology* **160**, 1709–1724 https://doi.org/10.1053/j.gastro.2020.12.076

16 Dudeck, A., Suender, C.A., Kostka, S.L., Von Stebut, E. and Maurer, M. (2011) Mast cells promote Th1 and Th17 responses by modulating dendritic cell maturation and function. *Eur. J. Immunol.* **41**, 1883–1893 https://doi.org/10.1002/eji.201040994

17 Kaieda, S., Kinoshita, T., Chiba, A., Miyake, S. and Hoshino, T. (2024) IL-18 receptor-α signalling pathway contributes to autoantibody-induced arthritis via neutrophil recruitment and mast cell activation. *Mod. Rheumatol.* **34**, 500–508 https://doi.org/10.1093/mr/road043

18 De Giovanni, M., Tam, H., Valet, C., Xu, Y., Looney, M.R. and Cyster, J.G. (2022) GPR35 promotes neutrophil recruitment in response to serotonin metabolite 5-HIAA. *Cell* **185**, 815–830 https://doi.org/10.1016/j.cell.2022.01.010

19 Hawkins, C.L. and Davies, M.J. (2021) Role of myeloperoxidase and oxidant formation in the extracellular environment in inflammation-induced tissue damage. *Free Radic. Biol. Med.* **172**, 633–651 https://doi.org/10.1016/j.freeradbiomed.2021.07.007

20 Pierzchała, K., Pięta, M., Rola, M., Świerczyńska, M., Artelska, A., Dębowska, K. et al. (2022) Fluorescent probes for monitoring myeloperoxidase-derived hypochlorous acid: a comparative study. *Sci. Rep.* **12**, 9314 https://doi.org/10.1038/s41598-022-13317-8

21 Davies, M.J. and Hawkins, C.L. (2020) The role of myeloperoxidase in biomolecule modification, chronic inflammation, and disease. *Antioxid. Redox Signal.* **32**, 957–981 https://doi.org/10.1089/ars.2020.8030

22 Gierlikowska, B., Stachura, A., Gierlikowski, W. and Demkow, U. (2021) Phagocytosis, degranulation and extracellular traps release by neutrophils-the current knowledge, pharmacological modulation and future prospects. *Front. Pharmacol.* **12**, 666732 https://doi.org/10.3389/fphar.2021.666732

23 Papayannopoulos, V. (2018) Neutrophil extracellular traps in immunity and disease. *Nat. Rev. Immunol.* **18**, 134–147 https://doi.org/10.1038/nri.2017.105

24 Papayannopoulos, V., Metzler, K.D., Hakkim, A. and Zychlinsky, A. (2010) Neutrophil elastase and myeloperoxidase regulate the formation of neutrophil extracellular traps. *J. Cell Biol.* **191**, 677–691 https://doi.org/10.1083/jcb.201006052

25 Wang, Y., Wysocka, J., Sayegh, J., Lee, Y.H., Perlin, J.R., Leonelli, L. et al. (2004) Human PAD4 regulates histone arginine methylation levels via demethylimination. *Science* **306**, 279–283 https://doi.org/10.1126/science.1101400

26 Brinkmann, V., Reichard, U., Goosmann, C., Fauler, B., Uhlemann, Y., Weiss, D.S. et al. (2004) Neutrophil extracellular traps kill bacteria. *Science* **303**, 1532–1535 https://doi.org/10.1126/science.1092385

27 Khandpur, R., Carmona-Rivera, C., Vivekanandan-Giri, A., Gizinski, A., Yalavarthi, S., Knight, J.S. et al. (2013) NETs are a source of citrullinated autoantigens and stimulate inflammatory responses in rheumatoid arthritis. *Sci. Transl. Med.* **5**, 178ra40 https://doi.org/10.1126/scitranslmed.3005580

28 Nakazawa, D., Tomaru, U., Yamamoto, C., Jodo, S. and Ishizu, A. (2012) Abundant neutrophil extracellular traps in thrombus of patient with microscopic polyangiitis. *Front. Immunol.* **3**, 333 https://doi.org/10.3389/fimmu.2012.00333

29 Bennike, T.B., Carlsen, T.G., Ellingsen, T., Bonderup, O.K., Glerup, H., Bøgsted, M. et al. (2015) Neutrophil extracellular traps in ulcerative colitis: a proteome analysis of intestinal biopsies. *Inflamm. Bowel Dis.* **21**, 2052–2067 https://doi.org/10.1097/MIB.0000000000000460
30 Gottlieb, Y., Elhasid, R., Berger-Achituv, S., Brazowski, E., Yerushalmy-Feler, A. and Cohen, S. (2018) Neutrophil extracellular traps in pediatric inflammatory bowel disease. *Pathol. Int.* **68**, 517–523 https://doi.org/10.1111/pin.12715
31 Lehmann, T., Schallert, K., Vilchez-Vargas, R., Benndorf, D., Püttker, S., Sydor, S. et al. (2019) Metaproteomics of fecal samples of Crohn's disease and ulcerative colitis. *J. Proteomics* **201**, 93–103 https://doi.org/10.1016/j.jprot.2019.04.009
32 Schroder, A.L., Chami, B., Liu, Y., Doyle, C.M., El Kazzi, M., Ahlenstiel, G. et al. (2022) Neutrophil extracellular trap density increases with increasing histopathological severity of Crohn's disease. *Inflamm. Bowel Dis.* **28**, 586–598 https://doi.org/10.1093/ibd/izab239
33 Ahmad, G., Chami, B., Liu, Y., Schroder, A.L., San Gabriel, P.T., Gao, A. et al. (2020) The synthetic myeloperoxidase inhibitor AZD3241 ameliorates dextran sodium sulfate stimulated experimental colitis. *Front. Pharmacol.* **11**, 556020 https://doi.org/10.3389/fphar.2020.556020
34 Witalison, E.E., Cui, X., Hofseth, A.B., Subramanian, V., Causey, C.P., Thompson, P.R. et al. (2015) Inhibiting protein arginine deiminases has antioxidant consequences. *J. Pharmacol. Exp. Ther.* **353**, 64–70 https://doi.org/10.1124/jpet.115.222745
35 Wang, P., Liu, D., Zhou, Z., Liu, F., Shen, Y., You, Q. et al. (2023) The role of protein arginine deiminase 4-dependent neutrophil extracellular traps formation in ulcerative colitis. *Front. Immunol.* **14**, 1144976 https://doi.org/10.3389/fimmu.2023.1144976
36 Chassaing, B., Aitken, J.D., Malleshappa, M. and Vijay-Kumar, M. (2014) Dextran sulfate sodium (DSS)-induced colitis in mice. *Curr. Protoc. Immunol.* **104**, 15. https://doi.org/10.1002/0471142735.im1525s104
37 Fauny, M., D'Amico, F., Bonovas, S., Netter, P., Danese, S., Loeuille, D. et al. (2020) Faecal calprotectin for the diagnosis of bowel inflammation in patients with rheumatological diseases: a systematic review. *J. Crohns. Colitis* **14**, 688–693 https://doi.org/10.1093/ecco-jcc/jjz205
38 Voganatsi, A., Panyutich, A., Miyasaki, K.T. and Murthy, R.K. (2001) Mechanism of extracellular release of human neutrophil calprotectin complex. *J. Leukoc. Biol.* **70**, 130–134; PMID: 11435495
39 Birchenough, G.M.H., Johansson, M.E.V., Gustafsson, J.K., Bergström, J.H. and Hansson, G.C. (2015) New developments in goblet cell mucus secretion and function. *Mucosal Immunol.* **8**, 712–719 https://doi.org/10.1038/mi.2015.32
40 Nieto, N., Torres, M.I., Fernández, M.I., Girón, M.D., Ríos, A., Suárez, M.D. et al. (2000) Experimental ulcerative colitis impairs antioxidant defense system in rat intestine. *Dig. Dis. Sci.* **45**, 1820–1827 https://doi.org/10.1023/a:1005565708038
41 D'Odorico, A., Bortolan, S., Cardin, R., D'Inca', R., Martines, D., Ferronato, A. et al. (2001) Reduced plasma antioxidant concentrations and increased oxidative DNA damage in inflammatory bowel disease. *Scand. J. Gastroenterol.* **36**, 1289–1294 https://doi.org/10.1080/003655201317097146
42 Lih-Brody, L., Powell, S.R., Collier, K.P., Reddy, G.M., Cerchia, R., Kahn, E. et al. (1996) Increased oxidative stress and decreased antioxidant defenses in mucosa of inflammatory bowel disease. *Dig. Dis. Sci.* **41**, 2078–2086 https://doi.org/10.1007/BF02093613
43 Dong, S., Lu, Y., Peng, G., Li, J., Li, W., Li, M. et al. (2021) Furin inhibits epithelial cell injury and alleviates experimental colitis by activating the Nrf2-Gpx4 signaling pathway. *Dig. Liver Dis.* **53**, 1276–1285 https://doi.org/10.1016/j.dld.2021.02.011
44 Wang, Y.C., Leng, X.X., Zhou, C.B., Lu, S.Y., Tsang, C.K., Xu, J. et al. (2022) Non-enzymatic role of SOD1 in intestinal stem cell growth. *Cell Death Dis.* **13**, 882 https://doi.org/10.1038/s41419-022-05267-w
45 Hwang, J., Jin, J., Jeon, S., Moon, S.H., Park, M.Y., Yum, D.Y. et al. (2020) SOD1 suppresses pro-inflammatory immune responses by protecting against oxidative stress in colitis. *Redox Biol.* **37**, 101760 https://doi.org/10.1016/j.redox.2020.101760
46 Sanchez-Garrido, J., Baghshomali, Y.N., Kaushal, P., Kozik, Z., Perry, R.W., Williams, H.R.T. et al. (2024) Impaired neutrophil migration underpins host susceptibility to infectious colitis. *Mucosal Immunol.* **17**, 939–957 https://doi.org/10.1016/j.mucimm.2024.06.008
47 Tidén, A.K., Sjögren, T., Svensson, M., Bernlind, A., Senthilmohan, R., Auchère, F. et al. (2011) 2-thioxanthines are mechanism-based inactivators of myeloperoxidase that block oxidative stress during inflammation. *J. Biol. Chem.* **286**, 37578–37589 https://doi.org/10.1074/jbc.M111.266981
48 Jucaite, A., Svenningsson, P., Rinne, J.O., Cselényi, Z., Varnäs, K., Johnström, P. et al. (2015) Effect of the myeloperoxidase inhibitor AZD3241 on microglia: a PET study in Parkinson's disease. *Brain* **138**, 2687–2700 https://doi.org/10.1093/brain/awv184
49 Metzler, K.D., Fuchs, T.A., Nauseef, W.M., Reumaux, D., Roesler, J., Schulze, I. et al. (2011) Myeloperoxidase is required for neutrophil extracellular trap formation: implications for innate immunity. *Blood* **117**, 953–959 https://doi.org/10.1182/blood-2010-06-290171
50 Fuchs, T.A., Abed, U., Goosmann, C., Hurwitz, R., Schulze, I., Wahn, V. et al. (2007) Novel cell death program leads to neutrophil extracellular traps. *J. Cell Biol.* **176**, 231–241 https://doi.org/10.1083/jcb.200606027
51 Lewis, H.D., Liddle, J., Coote, J.E., Atkinson, S.J., Barker, M.D., Bax, B.D. et al. (2015) Inhibition of PAD4 activity is sufficient to disrupt mouse and human NET formation. *Nat. Chem. Biol.* **11**, 189–191 https://doi.org/10.1038/nchembio.1735
52 Cedervall, J., Dragomir, A., Saupe, F., Zhang, Y., Ärnlöv, J., Larsson, E. et al. (2017) Pharmacological targeting of peptidylarginine deiminase 4 prevents cancer-associated kidney injury in mice. *Oncoimmunology* **6**, e1320009 https://doi.org/10.1080/2162402X.2017.1320009
53 Yang, K., Gao, R., Chen, H., Hu, J., Zhang, P., Wei, X. et al. (2024) Myocardial reperfusion injury exacerbation due to ALDH2 deficiency is mediated by neutrophil extracellular traps and prevented by leukotriene C4 inhibition. *Eur. Heart J.* **45**, 1662–1680 https://doi.org/10.1093/eurheartj/ehae205
54 SGC. (2024) GSK484 A chemical probe for PAD-4 (Protein-arginine deiminase type-4). https://www.thesgc.org/chemical-probes/gsk484
55 Dragoni, G., Ke, B.J., Picariello, L., Abdurahiman, S., Ceni, E., Biscu, F. et al. (2025) The impact of peptidyl arginine deiminase 4-dependent neutrophil extracellular trap formation on the early development of intestinal fibrosis in Crohn's disease. *J. Crohns. Colitis* **19**, e121 https://doi.org/10.1093/ecco-jcc/jjae121
56 Leppkes, M., Lindemann, A., Gößwein, S., Paulus, S., Roth, D., Hartung, A. et al. (2022) Neutrophils prevent rectal bleeding in ulcerative colitis by peptidyl-arginine deiminase-4-dependent immunothrombosis. *Gut* **71**, 2414–2429 https://doi.org/10.1136/gutjnl-2021-324725
57 Van Remoortel, S., Lambeets, L., De Winter, B., Dong, X., Rodriguez Ruiz, J.P., Kumar-Singh, S. et al. (2024) Mrgprb2-dependent mast cell activation plays a crucial role in acute colitis. *Cell. Mol. Gastroenterol. Hepatol.* **18**, 101391 https://doi.org/10.1016/j.jcmgh.2024.101391
58 Thomas, E.L., Jefferson, M.M., Learn, D.B., King, C.C. and Dabbous, M.K. (2000) Myeloperoxidase-catalyzed chlorination of histamine by stimulated neutrophils. *Redox Rep.* **5**, 191–196 https://doi.org/10.1179/135100000101535744

59 Pattison, D.I. and Davies, M.J. (2006) Evidence for rapid inter- and intramolecular chlorine transfer reactions of histamine and carnosine chloramines: implications for the prevention of hypochlorous-acid-mediated damage. *Biochemistry* **45**, 8152–8162 https://doi.org/10.1021/bi060348s
60 Chichlowski, M., Westwood, G.S., Abraham, S.N. and Hale, L.P. (2010) Role of mast cells in inflammatory bowel disease and inflammation-associated colorectal neoplasia in IL-10-deficient mice. *Plos One* **5**, e12220 https://doi.org/10.1371/journal.pone.0012220
61 Gan, P.Y., O'Sullivan, K.M., Ooi, J.D., Alikhan, M.A., Odobasic, D., Summers, S.A. et al. (2016) Mast cell stabilization ameliorates autoimmune anti-myeloperoxidase glomerulonephritis. *J. Am. Soc. Nephrol.* **27**, 1321–1333 https://doi.org/10.1681/ASN.2014090906
62 Springer, J.M., Raveendran, V.V., Gierer, S.A., Maz, M. and Dileepan, K.N. (2017) Protective role of mast cells in primary systemic vasculitis: a perspective. *Front. Immunol.* **8**, 990 https://doi.org/10.3389/fimmu.2017.00990
63 Mihlan, M., Wissmann, S., Gavrilov, A., Kaltenbach, L., Britz, M., Franke, K. et al. (2024) Neutrophil trapping and nexocytosis, mast cell-mediated processes for inflammatory signal relay. *Cell* **187**, 5316–5335 https://doi.org/10.1016/j.cell.2024.07.014
64 Kurashima, Y., Amiya, T., Nochi, T., Fujisawa, K., Haraguchi, T., Iba, H. et al. (2012) Extracellular ATP mediates mast cell-dependent intestinal inflammation through P2X7 purinoceptors. *Nat. Commun.* **3**, 1034 https://doi.org/10.1038/ncomms2023
65 Okayama, T., Yoshida, N., Uchiyama, K., Takagi, T., Ichikawa, H. and Yoshikawa, T. (2009) Mast cells are involved in the pathogenesis of indomethacin-induced rat enteritis. *J. Gastroenterol.* **44**, 35–39 https://doi.org/10.1007/s00535-008-2267-5
66 Tecchio, C., Micheletti, A. and Cassatella, M.A. (2014) Neutrophil-derived cytokines: facts beyond expression. *Front. Immunol.* **5**, 508 https://doi.org/10.3389/fimmu.2014.00508
67 Sakurai, A., Nishimoto, M., Himeno, S., Imura, N., Tsujimoto, M., Kunimoto, M. et al. (2005) Transcriptional regulation of thioredoxin reductase 1 expression by cadmium in vascular endothelial cells: role of NF-E2-related factor-2. *J. Cell. Physiol.* **203**, 529–537 https://doi.org/10.1002/jcp.20246
68 Kim, Y.C., Masutani, H., Yamaguchi, Y., Itoh, K., Yamamoto, M. and Yodoi, J. (2001) Hemin-induced activation of the thioredoxin gene by Nrf2. A differential regulation of the antioxidant responsive element by a switch of its binding factors. *J. Biol. Chem.* **276**, 18399–18406 https://doi.org/10.1074/jbc.M100103200
69 Kang, Y.P., Mockabee-Macias, A., Jiang, C., Falzone, A., Prieto-Farigua, N., Stone, E. et al. (2021) Non-canonical glutamate-cysteine ligase activity protects against ferroptosis. *Cell Metab.* **33**, 174–189 https://doi.org/10.1016/j.cmet.2020.12.007
70 Ahn, C.B., Je, J.Y., Kim, Y.S., Park, S.J. and Kim, B.I. (2017) Induction of Nrf2-mediated phase II detoxifying/antioxidant enzymes in vitro by chitosan-caffeic acid against hydrogen peroxide-induced hepatotoxicity through JNK/ERK pathway. *Mol. Cell. Biochem.* **424**, 79–86 https://doi.org/10.1007/s11010-016-2845-4
71 Krzystek-Korpacka, M., Neubauer, K., Berdowska, I., Zielinski, B., Paradowski, L. and Gamian, A. (2010) Impaired erythrocyte antioxidant defense in active inflammatory bowel disease: impact of anemia and treatment. *Inflamm. Bowel Dis.* **16**, 1467–1475 https://doi.org/10.1002/ibd.21234
72 Du, M., Yang, W., Schmull, S., Gu, J. and Xue, S. (2020) Inhibition of peptidyl arginine deiminase-4 protects against myocardial infarction induced cardiac dysfunction. *Int. Immunopharmacol.* **78**, 106055 https://doi.org/10.1016/j.intimp.2019.106055
73 Galli, S.J., Gaudenzio, N. and Tsai, M. (2020) Mast cells in inflammation and disease: recent progress and ongoing concerns. *Annu. Rev. Immunol.* **38**, 49–77 https://doi.org/10.1146/annurev-immunol-071719-094903
74 Xie, K. The peptidyl arginine deiminase 4 (PAD4) inhibitor GSK484 diminishes neutrophil extracellular trap (NET) density in colon mucosa but fails to improve clinical and inflammatory biomarkers in experimental ulcerative colitis. Mendeley Data2024

The PAD4 inhibitor GSK484 diminishes neutrophil extracellular trap in the colon mucosa but fails to improve inflammatory biomarkers in experimental colitis

Kangzhe Xie[1,2], Jordan Hunter[1,2,3], Aaron Lee[1,2], Gulfam Ahmad[1,4], Paul K. Witting[1,2#] and Tamara Ortiz-Cerda[1,2,5#*]

[1] Redox Biology Group, School of Medical Sciences, Faculty of Medicine & Health, The University of Sydney, NSW 2006 Australia.

[2] Charles Perkins Centre, School of Medical Sciences, Faculty of Medicine & Health, University of Sydney, Sydney, NSW 2006, Australia

[3] Department of Biological Sciences, Purdue University, West Lafayette, Indiana, United States of America.

[4] Andrology Department, Royal Women's and Children's Pathology, Carlton, VIC 3053, Australia.

[5] Departmento de Citología e Histología Normal y patológica, Facultad de Medicina, Universidad de Sevilla, Spain. Avda. Sánchez-Pizjuán s/n 41009 Sevilla, Spain

[#] P.K.W and T.O.C shares co-senior authorship of this study.

[*] Address correspondence to: Dr Tamara Ortiz-Cerda, Level 4 West, The Charles Perkins Centre, The University of Sydney, Sydney, NSW 2006, Australia (tamara.ortizcerda@sydney.edu.au)

Supplementary Material

Supplementary Tables & Figures

Antigen	Heat Induction Device	Retrieval Settings	Final dilution (v/v)	Cat. number/ Supplier
MPO	Decloaking Chamber (Biocare Medical)	Pre-heat at 80℃ for 30sec and heat induced retrieval at 125℃ for 30sec; followed by cooling fan on at 95℃ and fan off at 90℃.	1:100	PA5-16672/ Invitrogen
NE	Microwave (Midea)	1100W for 2min followed by 220W for 20min.	1:500	PA5-115648/ Invitrogen
CitH3	Microwave (Midea)	1100W for 2min followed by 220W for 20min.	1:200	ab219407/ abcam

Supplementary Table 1. Devices and settings used for heat-induced antigen retrieval for Immunofluorescence analysis. MPO, Myeloperoxidase; NE, Neutrophil Elastase; CitH3, Citrullinated Histone H3.

Antigen	Opal Fluorophore	ZEISS Camera Filter Set	Beam Splitter	Excitation/Emission Wavelength
MPO	Opal 570	Filter set 43	FT570	550/570nm
NE	Opal 520	Filter set 44	FT500	494/525nm
CitH3	Opal 690	Filter set 50	FT660	676/694nm
-	DAPI	Filter set 49	FT395	358/461nm

Supplementary Table 2. Imaging settings for neutrophil extracellular trap markers for immunofluorescence analysis. MPO, Myeloperoxidase; NE, Neutrophil Elastase; CitH3, Citrullinated Histone H3; DAPI, 4',6-diamidino-2-phenylindole.

	Protein analysis	Optimised Dilution (v/v)	Cat. number/ Supplier	Wavelength (nm)
Antigen	Nrf2	1:2000	PA5-88084, Invitrogen	-
	GPx4	1:1000	ab125066, abcam	
	SOD1	1:2000	SAB5200083, Sigma Aldrich	
	4HNE	1:800	BS-6313R, Bioss	
	β actin	1:10000	4967S, Cell Signaling Technology	
	Rabbit HRP	1:2000	A6154, Sigma Aldrich	
	Mouse HRP	1:2000	ab205719, abcam	
Kits	IL-1β ELISA	1:50	BMS6002, Invitrogen	450
	IL-4 ELISA	1:20	BMS613, Invitrogen	450
	IL-10 ELISA	1:100	BMS614, Invitrogen	450
	Calprotectin (Stool) ELISA	1:20	ab263885, Abcam	450
	Calprotectin (Colon) ELISA	1:100	ab263885, Abcam	450
	CAT Activity	1:4	EIACATC, Invitrogen	560
	SOD Activity	No Dilution Performed	ab65354, Abcam	450

Supplementary Table 3. Sample dilution factor used for different Western blot analysis, enzyme linked immunosorbent assay (ELISA) and enzymatic activity assay kits. Nrf2, anti-nuclear factor erythroid 2-related factor 2; GPx4, Glutathione peroxidase 4; SOD1, Superoxide dismutase-1; HRP, Horseradish peroxidase; IL, Interleukin; CAT, Catalase; SOD, Superoxide Dismutase.

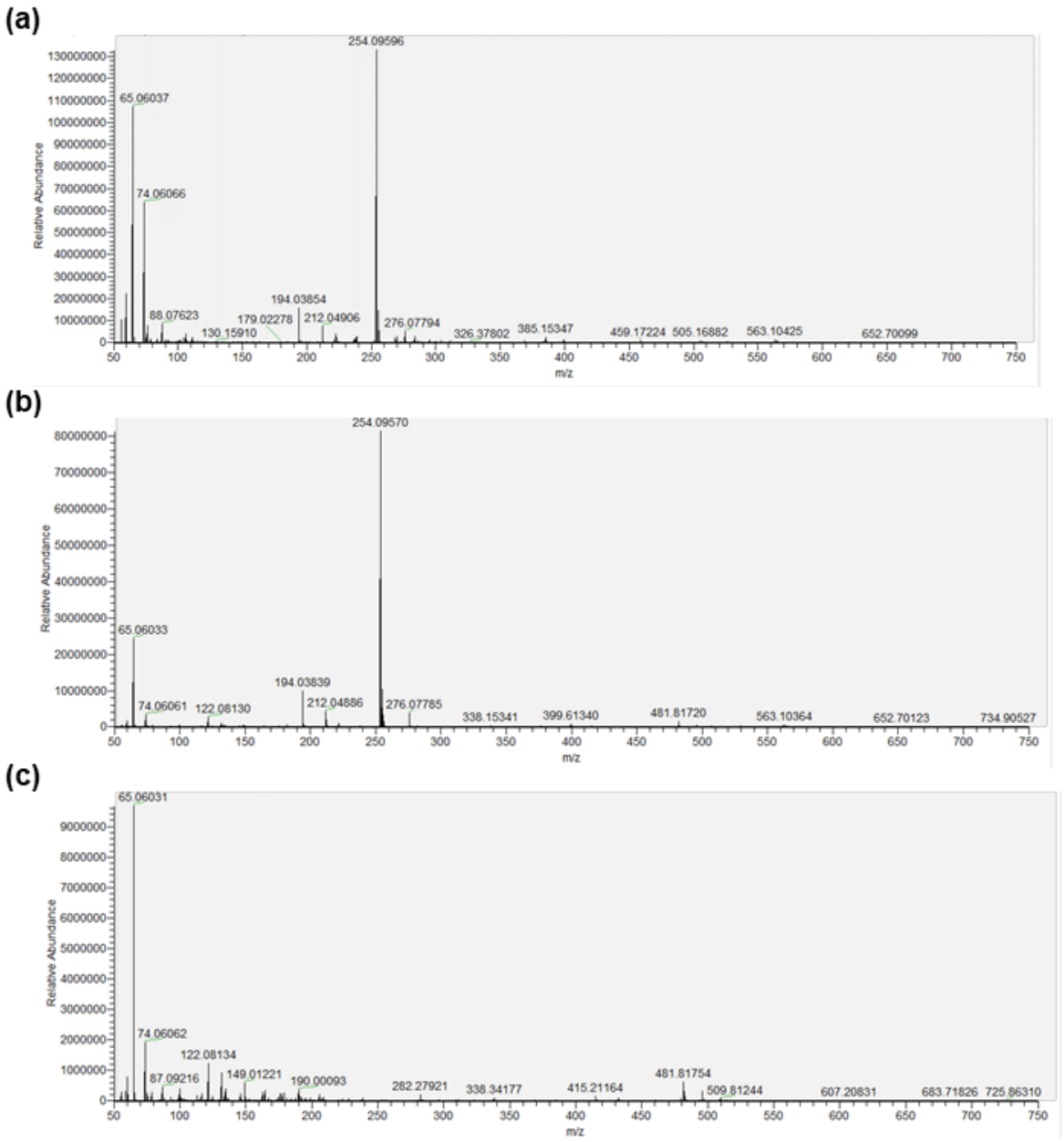

Supplementary Figure 1. Electrospray mass spectrometry of AZD3241 showed impurities in the inhibitor supplied by MedChemExpress. (a) Representative abundance peaks of AZD3241 from MedChemExpress at 5 µg/mL in 50% v/v methanol. (b) Representative abundance peaks of AZD3241 from Pharmaxis at 5 µg/mL in 50% v/v methanol. (c) Representative abundance peaks of 50% v/v methanol as a blank.

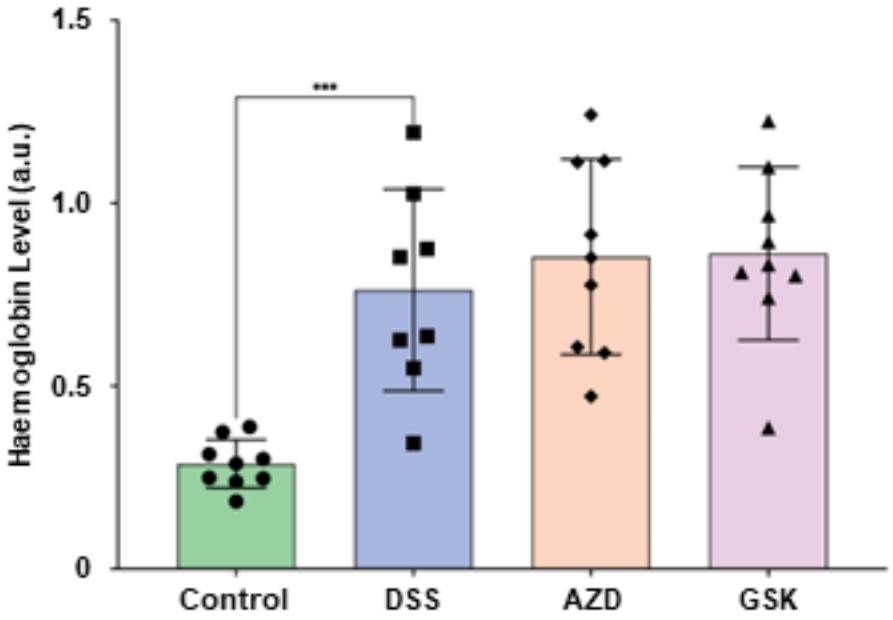

Supplementary Figure 2. The effect of MPO and/or PAD4 inhibition on faecal haemoglobin level. Graphical values represent mean ± SD with n = 9 mice per group. Protocol for faecal haemoglobin assay is described in Appendix 3. Normalcy of the collect data was analysed using Shapiro-Wilk test, group-wise comparison was performed by using one way ANOVA with Tukey's multiple comparison as a post hoc test. * $p \leq 0.05$, ** $p \leq 0.01$, *** $p \leq 0.001$ and **** $p \leq 0.0001$.

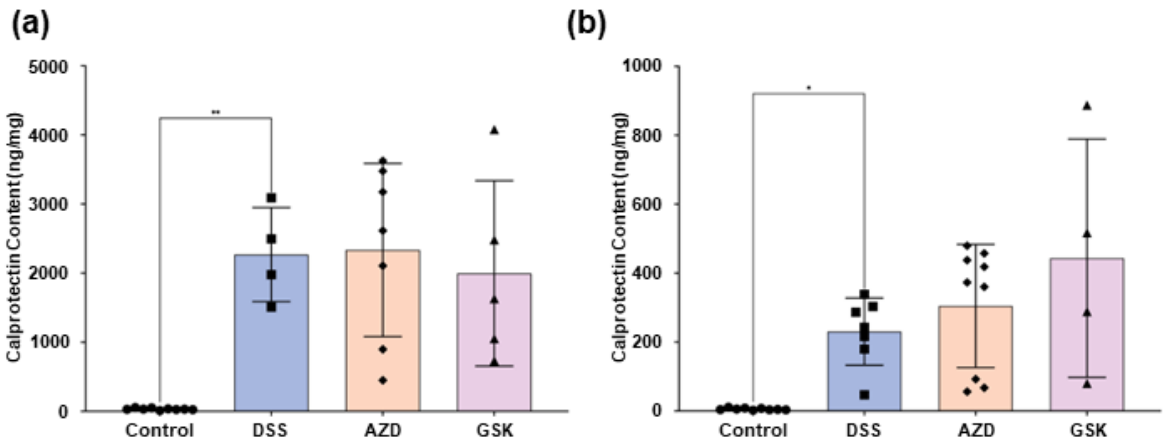

Supplementary Figure 3. The effect of MPO and/or PAD4 inhibition on colon inflammatory markers. (a) Colon calprotectin. (b) FCP, Faecal Calprotectin Stool calprotectin. Graphical values represent mean ± SD with n = 4-9 mice per group after standard curve interpolation. Normalcy of the collect data was analysed using Shapiro-Wilk test, group difference was analysed by one way ANOVA with Tukey's multiple comparison for parametric data and Kruskal-Wallis test with Dunn's multiple comparison test was used for non-parametric data. * $p \leq 0.05$, ** $p \leq 0.01$, *** $p \leq 0.001$ and **** $p \leq 0.0001$.

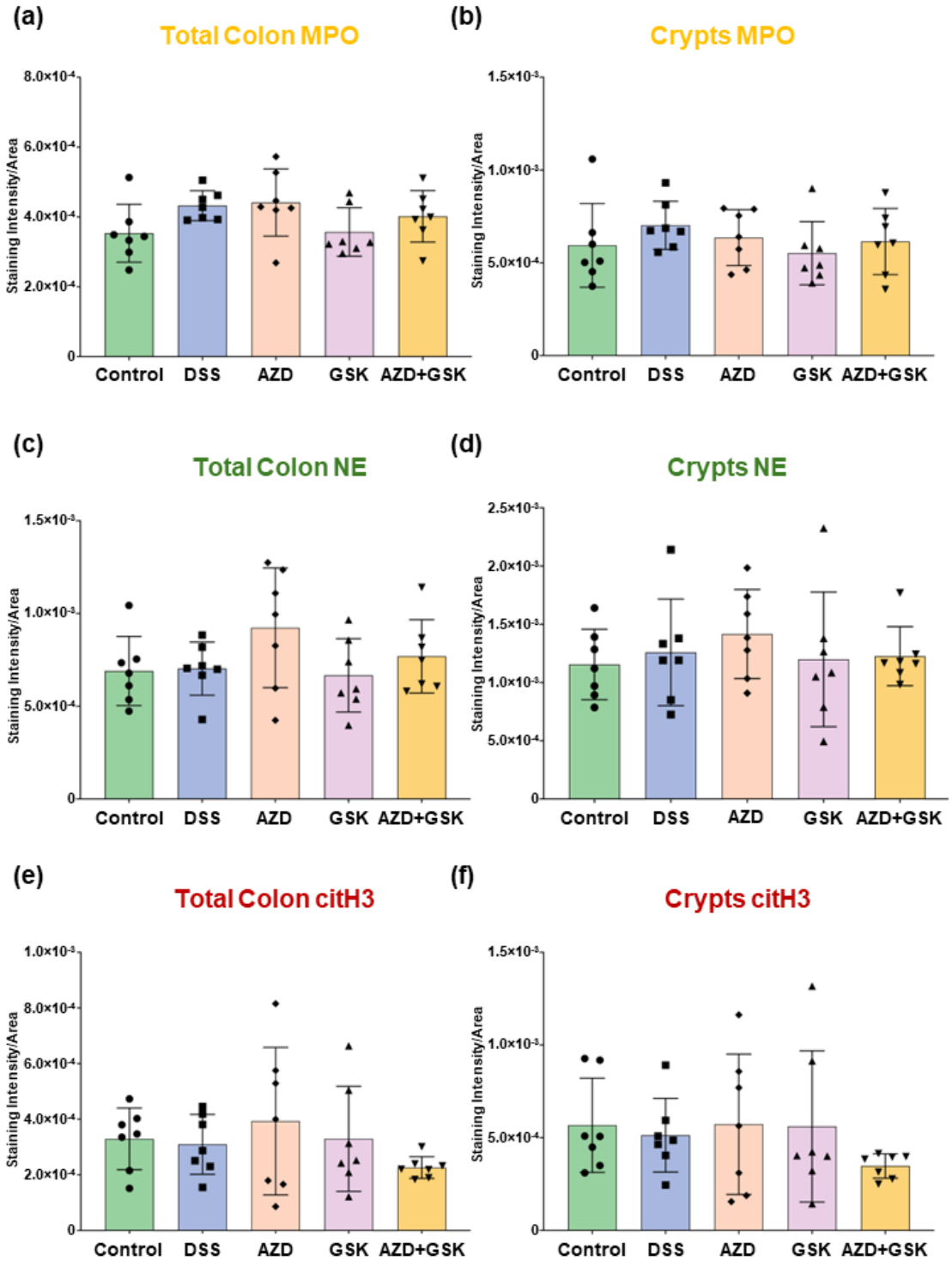

Supplementary Figure 4. Immunofluorescence staining intensity of MPO, NE and citH3 in mouse colons with/without DSS insults. (a) Total MPO staining intensity in the colon. (b) MPO staining intensity in the cryptic region only. (c). Total NE staining intensity in the colon. (d). NE staining intensity in the cryptic region only. (e) Total citH3 staining intensity in the colon. (f) citH3 staining intensity in the cryptic region only. Graphical values represent mean ± SD with n = 7 mice per group. Statistical outliers were identified and removed using the ROUT method (Q = 1%) and data normality was tested using the Shapiro-Wilk test. Group-wise comparison was performed by using one way ANOVA with Tukey's multiple comparison as a post hoc test.

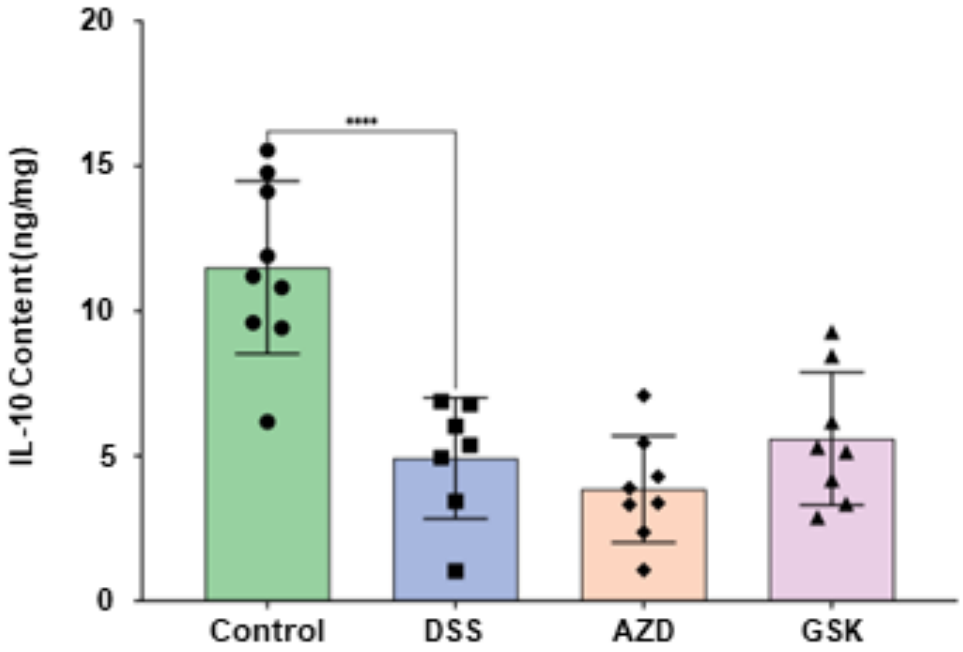

Supplementary Figure 5. The effect of MPO and/or PAD4 inhibition on colon IL-10 levels. Graphical values represent mean ± SD with n = 7-9 mice per group after standard curve interpolation. Normalcy of the collect data was analysed using Shapiro-Wilk test, group difference was analysed by one way ANOVA with Tukey's multiple comparison. * $p \leq 0.05$, ** $p \leq 0.01$, *** $p \leq 0.001$ and **** $p \leq 0.0001$.

Supplementary Information

Appendix 1. Macro code for NETs staining intensity analysis.

```
dir1=getDirectory("");
list=getFileList(dir1);
setBatchMode("show");
for (i=0; i<list.length; i++) {showProgress(i+1, list.length);
open(dir1+list[i]);
fileName = getInfo("image.filename");
selectWindow(fileName + " - C=0");
selectWindow(fileName + " - C=1");
selectWindow(fileName + " - C=2");
selectWindow(fileName + " - C=3");
run("ROI Manager...");
//setTool("freehand");
selectWindow(fileName + " - C=0");
waitForUser("Select Total Colon Area Now");
roiManager("Add");
roiManager("Select", 0);
roiManager("Rename", "Total");
waitForUser("Select Crypts Area Now");
roiManager("Add");
roiManager("Select", 1);
roiManager("Rename", "Crypts");
run("Tile");
selectWindow(fileName + " - C=1");
roiManager("Show All");
selectWindow(fileName + " - C=2");
roiManager("Show All");
selectWindow(fileName + " - C=3");
roiManager("Show All");
roiManager("Deselect");
selectWindow(fileName + " - C=1");
roiManager("multi-measure measure_all one append");
selectWindow(fileName + " - C=2");
roiManager("multi-measure measure_all one append");
selectWindow(fileName + " - C=3");
roiManager("multi-measure measure_all one append");
selectWindow(fileName + " - C=0");
close();
selectWindow(fileName + " - C=1");
close();
selectWindow(fileName + " - C=2");
close();
selectWindow(fileName + " - C=3");
roiManager("Select", 0);
roiManager("Delete");
roiManager("Select", 0);
roiManager("Delete");
close();}
```

Appendix 2. Macro code used for NETs counting analysis.

```
dir1=getDirectory("");
list1=getFileList(dir1);
dir2=getDirectory("");
list2=getFileList(dir2);
setBatchMode("show");
for (i=0; i<list1.length; i++) {showProgress(i+1, list1.length);
for (i=0; i<list2.length; i++) {showProgress(i+1, list2.length);
open(dir1+list1[i]);
fileName1 = getInfo("image.filename");
open(dir2+list2[i]);
fileName2 = getInfo("image.filename");
selectWindow(fileName2);
setAutoThreshold("Default no-reset");
//run("Threshold...");
setThreshold(0, 0, "raw");
//setThreshold(0, 0);
setOption("BlackBackground", true);
run("Convert to Mask");
selectWindow(fileName1);
//setTool("freehand");
run("ROI Manager...");
waitForUser("Select Total Colon Area Now");
roiManager("Add");
roiManager("Select", 0);
roiManager("Rename", "Total");
waitForUser("Select Crypts Area Now");
roiManager("Add");
roiManager("Select", 1);
roiManager("Rename", "Crypts");
selectWindow(fileName2);
roiManager("Select", 0);
run("Analyze Particles...", "summarize");
```

```
wait(3000);
roiManager("Show None");
roiManager("Select", 1);
run("Analyze Particles...", "summarize");
wait(3000);
roiManager("Select", 0);
roiManager("Delete");
roiManager("Select", 0);
roiManager("Delete");
selectWindow(fileName1);
close();
selectWindow(fileName2);
close();}
```

Appendix 3. Protocol for faecal haemoglobin analysis.

The level of haemoglobin in the stool homogenates was analysed using a colorimetric assay that was previously published by our group (See Fecal HB and Calprotectin Analysis in the METHODS section of Ref[1]). Briefly, 200 µL of thawed stool homogenates were loaded onto a 96-well assay plate in duplicates (Greiner Bio-One). The absorbance reading of each sample was measured at 402 nm with a microplate reader (Infinite M200-Pro, Tecan) and quantified against the Soret peak for Hb of 410 nm^2 taking into account the dilution factor for the stool sample.

Appendix 4. Full membrane images of Nrf2 Western blotting.

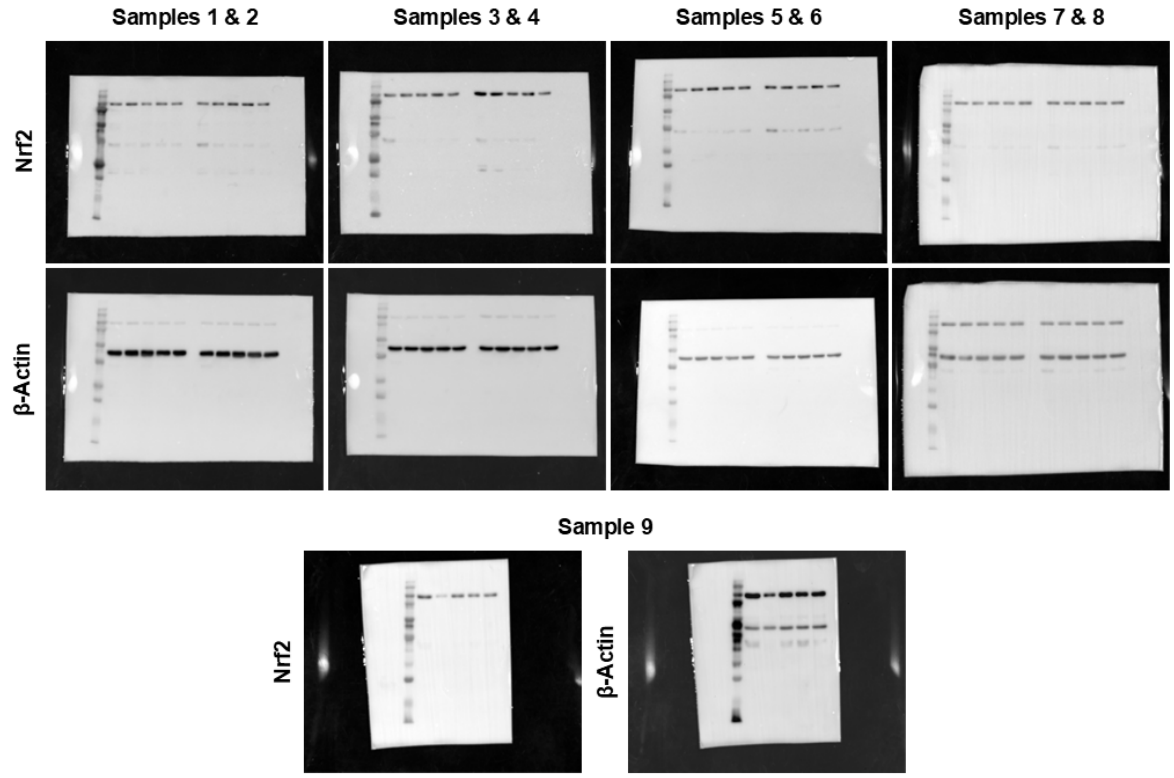

Appendix 5. Full membrane images of GPx4 Western blotting.

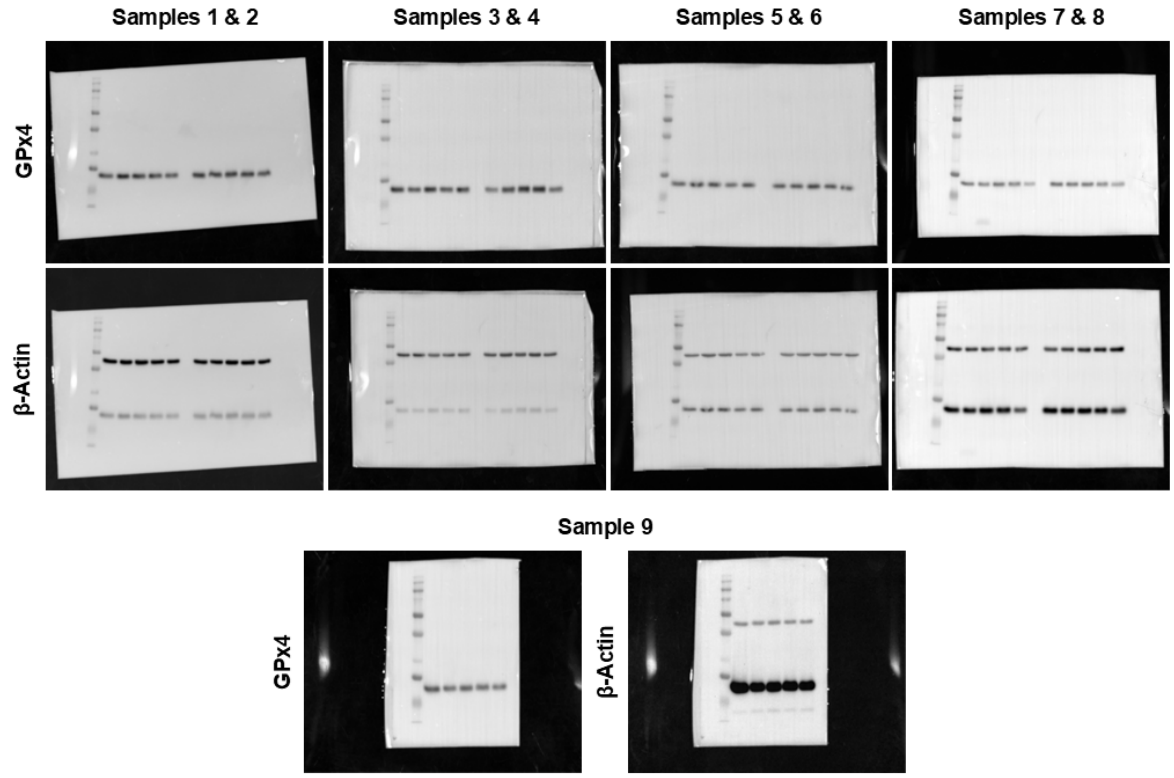

Appendix 6. Full membrane images of SOD1 Western blotting.

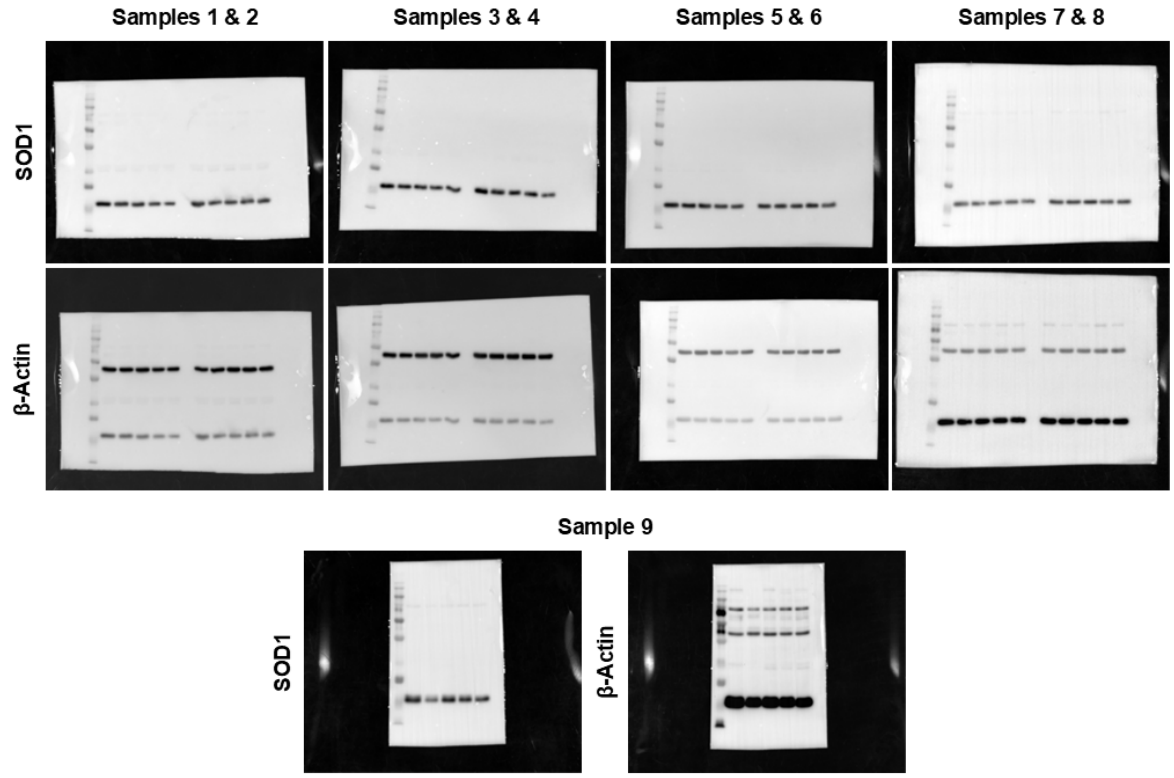

Appendix 7. Full membrane images of 4HNE Western blotting.

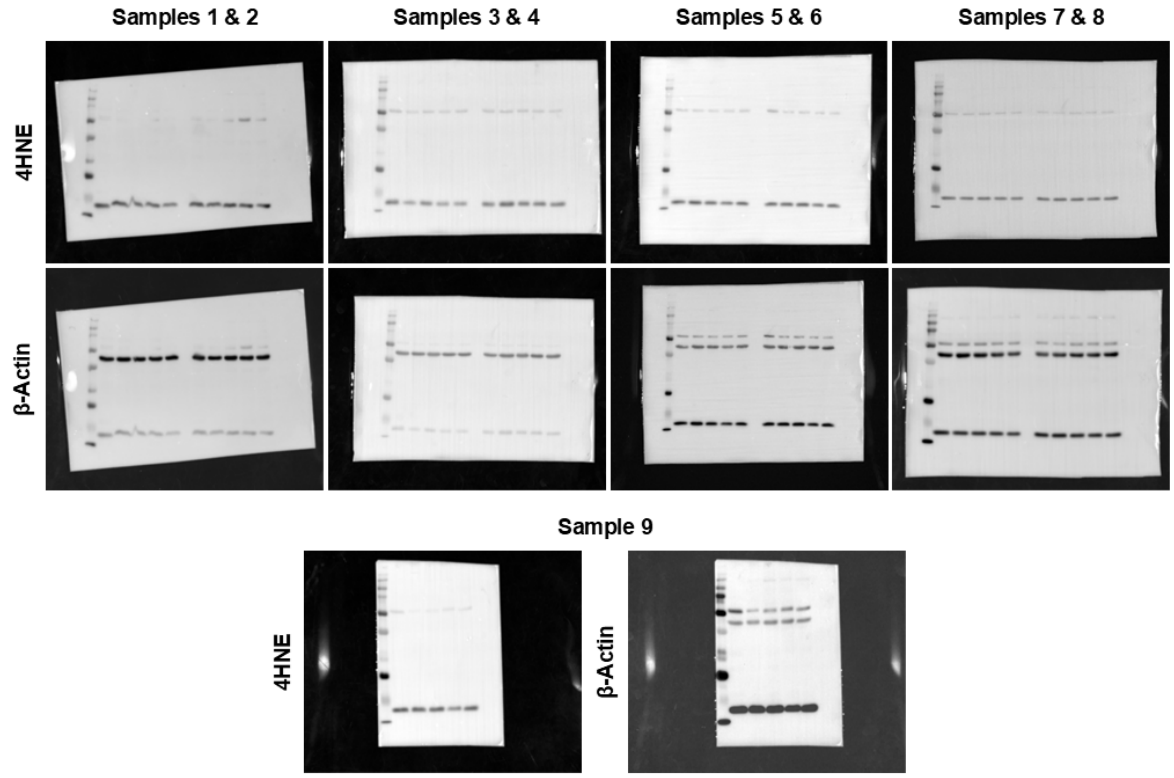

References for Supplementary Information

1. Ahmad G, Chami B, Liu Y, Schroder AL, San Gabriel PT, Gao A, Fong G, Wang X, Witting PK: The Synthetic Myeloperoxidase Inhibitor AZD3241 Ameliorates Dextran Sodium Sulfate Stimulated Experimental Colitis. Front Pharmacol 2020, 11:556020.

2. Hanson EK, Ballantyne, J: A Blue Spectral Shift of the Hemoglobin Soret Band Correlates with the Age (Time Since Deposition) of Dried Bloodstains. PLOS ONE 2010, 5(9):e12830.

Chapter 4: The role SCFA in IBD pathogenesis and disease progression

Below find the validation of submitted work indicating the contribution from the higher degree candidate as verified by the senior author for this manuscript. **The manuscript has been modified to accommodate the format of the current thesis.*

Authorship contribution statement:
Kangzhe Xie (K.X): Investigation, validation, formal analysis, data curation, visualisation and writing – original draft. **Suehad Abou Duhun (S.A.D):** Investigation, validation, formal analysis, data curation, visualisation and writing – original draft. **Tamara Ortiz-Cerda (T.O.C):** Investigation, validation, formal analysis, data curation, visualisation and writing – review & editing. **Hannah Choi (H.C):** Investigation, validation and formal analysis. **Xiao Suo Wang (X.S.W):** Investigation, methodology and software. **John O'Sullivan (J.O.S):** Conceptualisation and methodology. **Ella Verley (E.V):** Investigation, validation and data curation. **Mark Ghali (M.G):** Investigation, data curation and resources. **Viraj Kariyawasam (V.K):** Investigation, data curation and resources. **Nikola Mitrev (N.M):** Investigation, data curation and resources. **Belal Chami (B.C):** Conceptualisation, methodology, project administration, supervision and funding acquisition. **Paul K. Witting (P.K.W):** Conceptualisation, methodology, resources, project administration, supervision, funding acquisition, writing – review & editing.

Confirmation from the senior author:
I confirm that Mr Kangzhe (Steven) Xie was an active contributor and collaborator for this study now submitted to the Redox Report for consideration as a "Research Paper". The authorship statement above accurately describes Steven's contribution and justifies his position as first author for this manuscript submission.

Signed Dated: 28/02/2025

Paul Witting (PhD)
Professor, Redox Biology
School of Medical Sciences
Faculty of Medicine and Health
Charles Perkins Centre
Editor Redox Report

Rm 4212, D17 | The University of Sydney | NSW | 2006
+61 2 91140524
paul.witting@sydney.edu.au

Characterising short chain fatty acid profiles in stool specimens from patients diagnosed with inflammatory bowel disease

Kangzhe Xie[1*], Suehad Abou Duhun[1*], Tamara Ortiz-Cerda[1,2], Hannah Choi[1], XiaoSuo Wang[3], John O'Sullivan[3], Ella Verley[1,4], Mark Ghali[5], Viraj Kariyawasam[5,6], Nikola Mitrev[5,7], Belal Chami[4] & Paul K. Witting[1#]

1. Redox Biology Group, Charles Perkins Centre, School of Medical Sciences, Faculty of Medicine & Health, The University of Sydney, NSW 2006, Australia.
2. Departamento de Citología e Histología Normal y Patológica, Facultad de medicina, Universidad de Sevilla, Avda. Sánchez-Pizjuán s/n 41009, Seville, Spain.
3. Cardiometabolic Medicine Group, Charles Perkin Centre, School of Medical Sciences, Faculty of Medicine & Health, The University of Sydney, NSW 2006, Australia.
4. Redox Inflammation Group, Charles Perkins Centre, School of Medical Sciences, Faculty of Medicine & Health, The University of Sydney, NSW 2006, Australia.
5. Blacktown/Mt. Druitt Clinical School, University of Western Sydney, NSW 2148, Australia.
6. Department of Gastroenterology, Concord Repatriation General hospital, Sydney, NSW 2139 Australia.
7. Department of Gastroenterology, The Sutherland Hospital, NSW 2229, Australia

* Authors K.X and S.A.D contributed equally and share joint first-authorship of the study.

Correspondence address to Professor Paul K. Witting (paul.witting@sydney.edu.au), Level 4 West Room 4212, Charles Perkins Centre, The University of Sydney, NSW 2006, Australia.

Abstract: 250 words

Main text: 6043 words

Abstract

Inflammatory bowel disease (IBD) is characterised by chronic gastrointestinal inflammation. The aetiology of IBD is unknown however, inflammation and altered gut microbiome composition are implicated in IBD pathogenesis. Short-chain-fatty acids (SCFAs) are microbial fermentation products of dietary-fibre, and their involvement in IBD remains unclear. Thus, characterising SCFA profiles in patients with active IBD vs remission remains a knowledge gap in human pathophysiology. Herein, stool and corresponding plasma (where possible) were collected from 42 IBD patients, 12 colonoscopy controls (participants underwent colonoscopy for reasons other than IBD) and 7 healthy controls (relative or household contact of recruited IBD subjects). Characterisation of SCFA profiles in stool samples was performed. Associations between SCFA levels, IBD disease severity and inflammatory biomarkers were also assessed. SCFAs were extracted from stool homogenates (30 mg) with 0.05% v/v orthophosphoric acid/water, analysed using liquid chromatography tandem mass spectrometry and quantified using SciexOS-Analytics software. Validation experiments were performed on stool/plasma samples using enzyme linked immunosorbent assays (ELISA) for several inflammatory markers. The level of SCFAs were markedly decreased in IBD patients. Notably, decreases in acetate, propionate and butyrate concentrations were associated with increasing disease severity as judged by endoscopic score. As anticipated, stool level of pro-inflammatory interleukins (IL) IL-1β/IL-6 significantly increased and IL-10 decreased with increasing disease severity. Similar systemic changes for IL-6 and IL-10 in plasma was also observed. Decreased levels of acetate, propionate and butyrate were inversely associated with increasing IBD severity, suggesting that maintaining physiological levels of these SCFAs may be associated with maintaining disease remission.

Keywords: Inflammatory bowel disease, ulcerative colitis, Crohn's disease, short chain fatty acid, microbiota

Abbreviation used in this paper

5-ASA: 5-aminosalicylate

ANOVA: one-way analysis of variance

CD: Crohn's disease

DSS: Dextran sodium sulfate

EDTA: ethylenediaminetetraacetic acid

ELISA: Enzyme-linked immunosorbent assay

FA: Formic acid

GIT: Gastrointestinal tract

GPR: G-protein coupled receptor

IBD: Inflammatory bowel disease

IL: Interleukin

LC-MS/MS: liquid chromatography tandem mass spectrometry

NF-κB: Nuclear factor kappa B

SCFA: Short chain fatty acid

SES-CD: Simple Endoscopic Score for Crohn's Disease

STAT3: Signal transducer and activator of transcription 3

TNF: Tumour necrosis factor

UC: Ulcerative colitis

UCEIS: Endoscopic Index of Severity for Ulcerative Colitis

WSLHD: Western Sydney Local Health District

4.1 Introduction

Inflammatory bowel disease (IBD) is a group of chronic disorders characterised by excessive inflammation of the gastrointestinal tract (GIT)[1]. The two main forms of IBD are ulcerative colitis (UC) and Crohn's disease (CD). Patients with UC exhibit epithelial ulcerations that impact the rectum and extends proximally to involve contiguous lengths of the colon[2]. In contrast, CD patients exhibit patchy distribution of transmural lesions affecting any part of the GIT[3]. Symptoms of IBD include abdominal pain, diarrhea, rectal bleeding, weight loss[4], and damage to affected bowel accumulates over time[5].

The aetiology of IBD is believed to be multifactorial. An involvement of environmental stimuli, diet[6,7] and altered gut microbiome[8,9] have been long postulated in the pathogenesis of IBD. The healthy gut microbiome consists of a balanced community of archaea, bacteria, bacteriophage, fungi and viruses[10]. These microorganisms work in a symbiotic relationship to maintain the intestinal homeostasis and regulate the immune responses in the gut[5]. The diversity of bacterial species in the healthy gut varies across individuals[11], and it has been shown that dietary choices influence the abundance of several phyla of bacteria. For example, increased abundance of Bacteroides is associated with a typical "Western" high-fat, high-protein diet[12]. On the other hand, enrichment of Prevotella and Faecalibacterium are evident with high-carbohydrate[12] and high-fibre diets[13], respectively.

Reports of gut bacterial dysbiosis in IBD are commonly characterised by reduced abundance of anaerobic microbes such as *Bacteroides*, *Eubacterium* and *Lactobacillus*[14] and elevated abundance of species *Campylobacter*, *Plesiomonas* and *Escherichia coli*[15]. Additionally, this microbiome perturbation has been linked with exacerbated gut inflammation[16,17] and aberrant expression of proinflammatory cytokines such as interleukin (IL)-1β[18-20], IL-6[19,21,22] and tumour necrosis factor (TNF)-α[20,22], and the anti-inflammatory cytokine IL-10[20,21] in various experimental models of IBD. Overall, the altered bacteriome creates a pro-inflammatory environment in the gut which drives the pathogenesis of IBD.

Bacteria consume/ferment undigested dietary fibres to produce short chain fatty acids (SCFAs) mainly acetate, propionate and butyrate[23]. These volatile metabolites predominantly butyrate, serve as an energy source for colon enterocytes[24,25], play a role in maintaining gastrointestinal homeostasis and exert an anti-inflammatory effect on the gut via a myriad of intracellular and extracellular processes[26]. Given the association between SCFAs and gut microbiome, the levels of SCFAs in IBD can potentially influence pathogenesis and disease progression. Accordingly, altered levels of SCFA were documented in IBD patients initially in the 1980s. In 1982, Roediger et al. reported higher level of faecal butyrate in active UC patients[27]. Similarly, van Nuenen et al. found elevated total SCFAs in stool from UC and CD patients[28], suggesting that SCFA utilisation by the colonic mucosa may be impaired in IBD. However, these findings contradicted a more recent study by Machiels et al., which demonstrated reduced levels of acetate, propionate and butyrate in the stool of IBD patients[29]. Additionally, the study by Takaishi et al. also reported significantly diminished faecal propionate and butyrate levels in UC and CD patients[30], highlighting the need for further research to establish a consensus on SCFA levels in IBD patients and determine a correlation between SCFA levels and severity of inflammation. Despite numerous studies examining SCFA levels in IBD patients, there has been no investigation into the temporal changes in SCFA profiles across the spectrum of IBD severities in both UC and CD.

Available treatments such as corticosteroids, 5-aminosalicylates (5-ASA), immunomodulators, biologic agents [e.g., anti-TNF drugs], advanced small molecule therapies and in some severe cases, surgical removal of the affected bowel[31], all aim to induce and maintain remission. None of these therapeutic options offer a definitive cure and commonly have serious adverse reactions. Additionally, ~40% primary non-response rate has been reported in patients prescribed anti-TNF treatments, with an additional 23-26% secondary loss of response observed 1 year post treatment[32]. Thus, alternate treatment options for IBD patients are required. Investigating the correlation between SCFA levels and IBD disease severity may offer crucial insights into novel therapeutic strategies. In the present work, the levels of faecal SCFA acetate, propionate, butyrate and propionate were examined in UC and CD patients with varying disease activity. In addition, common inflammatory cytokines IL-1β, IL-6 and IL-10 from the stool and plasma samples of the same patient cohort were analysed to evaluate the relationship between these biomarkers, levels of faecal SCFA and endoscopic disease activity.

4.2 Materials & Methods

4.2.1 Ethics & Patient Recruitment

All procedures in the current study have strictly adhered to the Declaration of Helsinki ethical principles regarding human experimentation and the study was approved by the Western Sydney Local Health District (WSLHD) ethics committee (approval 2021/PID#03593). Informed consent was obtained from each participant before study enrolment. Between September 2022 and April 2024, healthy individuals (colonoscopy controls) and patients with IBD diagnosis who underwent colonoscopy at metropolitan hospitals including Westmead Hospital, Blacktown Hospital or Norwest Private Hospital in the WSLHD of Sydney, Australia were recruited for the current study. Relatives and/or household contacts of IBD participants were also approached to provide a stool sample (assigned as healthy controls without colonoscopy). Patients that did not consent to sample and/or medical history collection or were diagnosed with tumours at time of colonoscopy were excluded.

4.2.2 Sample Collection

Samples of stool (collected in a commercial specimen collection jar) and blood [in silica blood collection tube] were obtained at the metropolitan hospitals identified here and transferred to the Charles Perkins Centre for laboratory workup within 24 h of collection. Upon arrival to the laboratory, stool samples were transferred into a -80 ℃ freezer until required. Blood samples were centrifuged (1500*x g*, 4 ℃, 15 min) and plasma was isolated and stored at -80 degrees until required. Deidentified electronic patient information such as ethnicity, age, IBD diagnosis, comorbidity, prescription and medical history were stored in accordance with the Australian National Health and Medical Research Council (NHMRC) guidelines.

4.2.3 Disease Severity & Endoscopic Activity Classification

Physical examinations and colonoscopy were conducted at three sites and the attending gastroenterologist (M.G, V. K, or N. M) evaluated the extent of gastrointestinal inflammation and the degree of colon lesion using the Endoscopic Index of Severity for Ulcerative Colitis (UCEIS) and Simple Endoscopic Score for Crohn's Disease (SES-CD) for UC and CD diagnosed patients respectively. In the current study, the UCEIS and SES-CD scores were compiled and categorised according to IBD stage including remission, mild, moderate and severe (see Table 4.1 for detailed classification criteria).

Table 4.1. Summary table of endoscopic classification.[1]

Endoscopic Features	UCEIS Score	SES-CD Score	Classification
No visible bleeding, erosion and/or ulceration	≤ 1	≤ 2	Remission
Presence of erythema, patchy obliteration of vascular pattern, mild friability, mild erosion and/or ulceration	2-4	3-6	Mild
Marked erythema, obliterated vascular pattern, friability and presence of erosion and/or ulceration	5-6	7-5	Moderate
Spontaneous bleeding and marked presence of erosion and/or ulceration	7-8	>15	Severe

[1] The extent of gastrointestinal inflammation and the degree of colon lesion was evaluated during the colonoscopy/endoscopy examination by the attending gastroenterologist. The Endoscopic Index of Severity for Ulcerative Colitis (UCEIS) was used to grade patients with ulcerative colitis whilst Crohn's disease patients were graded using the Simple Endoscopic Score for Crohn's disease (SES-CD) index. Both evaluations employed endoscopic features of presence of vascular patterns, degree of intestinal bleeding, and extent of epithelial erosion and ulceration of the gastrointestinal tract. Next, the UCEIS and SES-CD scores were combined for each individual and subsequently re-classified as remission, mild, moderate and severe IBD for correlation examinations according to the grading ranges indicated in the table.

4.2.4 Faecal Short Chain Fatty Acid Extraction

All chemicals and reagents used in the study were acquired with the highest standards/quality available (see Supplementary Table 1 for listed reagents). When required, frozen stool was placed in a biosafety cabinet then sampled from 3 different locations on the bulk sample using a sharp scalpel to shave thin sections. A combined 25-35 mg of stool from each subject was then transferred into 1.5 mL Eppendorf tubes and faecal SCFAs were extracted by adding 400 µL of 0.5% v/v orthophosphoric acid/water solution containing isotopically labelled standards (comprised of 5 mM acetate d_3, 0.5 mM propionate ^{13}C, 0.5 mM butyrate ^{13}C and 0.5 mM hexanoate d_3). Next, the mixtures were homogenised by vortexing at maximum speed for 1 min, followed by cooling on ice for 30 s and vortexing again (1 min). After homogenisation, samples were centrifuged twice (21300*x g*, 4 ℃, 30 min) to remove any solids or colloidal material from the supernatants. Clarified supernatants were then transferred into chromatographic insert glass vials and stored at -30 ℃ until required for mass analysis as detailed below. All processed samples were analysed within 4 days of the extraction procedure to minimise the potential loss of volatile SCFA.

4.2.5 Liquid Chromatography Tandem Mass Spectrometry (LC-MS/MS)

Prior to performing the liquid chromatography tandem mass spectrometry (LC-MS/MS) analysis, native standards of acetate, propionate, butyrate, valerate and hexanoate were prepared in 0.1% v/v formic acid (FA)/water at final concentrations of 1000, 100, 10, 1, 0.5,

0.25 and 0.1 µM. The SCFAs in each sample were detected using the QTRAP 6500+ high-throughput mass spectrometer (SCIEX) with the following parameters gas 1 at 15psi, gas 2 at 30 psi and curtain gas at 35 psi, at a voltage of 3500 V. Buffer flow rate was 0.2 mL/minute for both aqueous mobile phase A (0.1% v/v FA/water) and organic mobile phase B (0.1% v/v FA/methanol). To ensure data quality and to monitor machine performance, 5 µL of quality control samples (a mixture of all analysing samples) were injected after every 20 sample injections (5 µL) by the autosampler followed by a washout (5 min) cycle between each sample injection to eliminate the risk of cross-over contamination.

4.2.6 LC-MS/MS Data Processing

After LC-MS/MS data acquisition, peak identification and peak areal integration was performed by two independent researchers (K.X and S.A.D) using the available SciexOS Analytic Software (v.3.1.6.44, SCIEX) to determine the relative amount of SCFA within the individual faecal samples. Any discrepancies in peak assignment and areal integration were resolved through discussion and three other researchers (T.O.C, X.S.W and P.K.W) were consulted when consensus was not reached. Integrated areal data was then exported to Microsoft Excel and standard curves of each SCFA were constructed in accordance with the concentration of the authentic native standards. The relative amount of SCFAs within the faecal samples were then interpolated and normalised to isotopically labelled standards and wet stool weight.

4.2.7 Preparation of Stool Homogenates for ELISA

Where required, 25-35 mg of stool were thawed, and 5% w/v stool/homogenising solution (0.01% v/v DNAse in distilled water) was added to each sample. Next, the treated samples were homogenised vigorously by vortex 2x 1 min + intermittent 1 min chill on ice. After homogenisation, samples were then centrifuged at 18,800*x g* at 4 ℃ for 20 min and clarified supernatants were collected and stored at -80 ℃ until required for ELISA (as described below).

4.2.8 Enzyme-Linked Immunosorbent Assay (ELISA)

Enzyme-linked immunosorbent assays (ELISA) of inflammatory cytokine IL-1β, IL-6 and IL-10 were performed to validate the extent of GIT inflammation and confirm the evaluation of the IBD disease severity for each subject. Commercially available ELISA kits for inflammatory cytokine (Human IL-1β ELISA Kit, cat no. BMS224-2 and Human IL-6 ELISA Kit, cat no.EH2IL6) and for anti-inflammatory cytokine (Human IL-10 ELISA kit, cat no. BMS215-2) were purchased from Invitrogen and recommended protocols were followed. Briefly, neat or Mili-Q water diluted clarified stool homogenate and plasma were loaded onto antibody-coated 96-well plates, and colorimetric absorbances were determined at 450 nm using a microplate reader (Infinite M200-Pro, Tecan).

4.2.9 Statistical Analysis

In the current study, Shapiro-Wilk test with alpha (α) error = 0.05 was used to test the parametric distribution of the collected data using the GraphPad® Prism software (v. 10.1.0, La Jolla, USA). For parametric data, differences between data sets were determined with two-tailed unpaired t test or one-way analysis of variance (ANOVA) with Tukey's multiple comparison post-hoc tests. For non-parametrically distributed datasets, Mann-Whitney test or Kruskal-Wallis test with Dunn's multiple comparison was used. Simple linear regression analysis was used to investigate the correlation between SCFA levels and inflammatory

cytokine concentrations. Additionally, the potential effects of IBD pharmacological intervention on SCFA levels at different endoscopic severities was investigated using two-way ANOVA analysis. The statistical significance threshold was set at p-value < 0.05 and graphical values represent mean + standard deviation (SD).

4.3 Results

4.3.1 Patient Characteristics

The study cohort comprised 42 IBD patients, whilst 12 patients that underwent a colonoscopy examination but did not have an IBD diagnosis were assigned as "Colonoscopy Controls". A further 7 healthy individuals were also enrolled, termed "Healthy Controls" comprising random individuals often they were relatives or partners to patients enrolled in this study with no prior diagnosis of IBD. Individuals assigned to "Colonoscopy Control" and "Healthy Control" groups were pooled to form a combined "Control group" for statistical analysis. Of the IBD patients, 22 individuals were diagnosed with UC (UC group) whilst 18 were diagnosed with CD (CD group). In the current study, 2 subjects that underwent colonoscopy (and subsequent IBD diagnosis) were not further categorised as UC or CD. As a result, SCFA and inflammatory cytokine results from these two samples were included in the comparison between gross IBD and controls but were excluded from further sub-group analyses (e.g. UC vs. CD). The median time since IBD diagnosis was 8 and 13 years for UC and CD, respectively. There was no significant difference in mean age between the UC (35.19 ± 15.82 years), CD (33.89 ± 10.73 years), colonoscopy control (39.7 ± 13.6 years) and healthy control (43.58 ± 8.75 years) groups. The gender distribution in the UC group was 54.55% male vs. 36.36% female (9.09% not reported), 50% male vs. 50% female in the CD group and 57.9% male vs. 42.1% females in the control group. Regarding patient ethnicity, 40.91% of the UC patients were Caucasian, 27.27% were identified Asian, and 22.73% were from other ethnicity groups. 9.09% of the patients in the UC group did not disclose their ethnicity. There were 38.89% Caucasian patients in the CD group, 33.33% with Asian background and 22.22% were from other ethnicity groups. 5.56% of CD patients did not report their ethnic background. There was no significant difference in ethnicity distribution between control and the UC and CD groups, overall distributing as 63.2% were Caucasian, 21.1% Asian and 15.8% as other ethnic backgrounds (see Table 4.2 for listed patient characteristics).

In the cohort assigned to the UC group, 40.91% of the patients were symptomatic. In terms of endoscopic disease activity, 9 were in remission, 5 had mild disease activity, 6 had moderate disease activity and 2 had severe disease activity. From the patients assigned to the CD group, a majority were asymptomatic at the time of sample collection (77.78%). Furthermore, endoscopically 9 CD patients were defined as in remission, 5 with mild disease activity, 2 with moderate endoscopic activity and 2 had severe disease activity. With regards to IBD treatments, 7 IBD patients were receiving 5-ASA only at the time of sample collection, 5 were administered immunomodulators only, and 9 others were prescribed biologic agents only. Additionally, 5 patients received both 5-ASA and immunomodulators, 1 patient was prescribed 5-ASA together with a biologic agent, a further 9 patients were prescribed both immunomodulators and biologic agents, and finally, 3 patients did not report any medication use at the time of collection (refer to Table 4.3 for summary of medication usage). Two-way ANOVA was used to evaluate potential drug-interaction as a determinant of faecal SCFA concentrations, however under the experimental design statistical significance was not achieved [$F(6, 75) = 2.129$, $p = 0.06$] suggesting that changes in SCFA determined here were unlikely to be affected by prescribed medications (Supplementary Figure 4.1).

Table 4.2. Demographic information for the study cohort.

	Ulcerative Colitis [n = 22]	**Crohn's Disease [n = 18]**	**Healthy Control [n = 7]**	**Colonoscopy Control [n = 12]**
Mean age, years [SD]	35.19 [15.82]	33.89 [10.73]	39.7 [13.6]	43.58 [8.75]
Male [%]	12 [54.55]	9 [50]	5 [71.43]	6 [50]
Female [%]	8 [36.36]	9 [50]	2 [28.57]	6 [50]
Gender NR [%]	2 [9.09]	-	-	-
Median time since IBD diagnosis [range, years]	8 [0-36]	13 [3-37]	-	-
Caucasian ethnicity [%]	9 [40.91]	7 [38.89]	3 [42.86]	9 [75]
Asian ethnicity [%]	6 [27.27]	6 [33.33]	2 [28.57]	2 [16.67]
Other ethnicity [%]	5 [22.73]	4 [22.22]	2 [28.57]	1 [8.33]
Ethnicity NR [%]	2 [9.09]	1 [5.56]	-	-
Asymptomatic [%]	8 [36.36]	14 [77.78]	-	-
Symptomatic [%]	9 [40.91]	2 [11.11]	-	-
Symptom NR [%]	5 [22.73]	2 [11.11]	-	-
Endoscopic remission [%]	9 [40.91]	9 [50]	-	-
Mild endoscopic activity [%]	5 [22.73]	5 [27.78]	-	-
Moderate endoscopic activity [%]	6 [27.27]	2 [9.09]	-	-
Severe endoscopic activity [%]	2 [9.09]	2 [9.09]	-	-

NR: Not reported.

Table 4.3. Summary table of prescribed medication in the IBD cohort studied.

Medication Type	Ulcerative Colitis [n = 22]	Crohn's Disease [n = 18]
5-ASA [%]	7 [31.81]	0 [0]
Immunomodulators only [%]	1 [4.54]	4 [22.22]
Biologic agents only [%]	3 [13.63]	6 [33.33]
5-ASA + Immunomodulators [%]	5 [22.72]	0 [0]
5-ASA + Biologic agents [%]	1 [4.54]	0 [0]
Immunomodulators + Biologic agents [%]	1 [4.54]	8 [44.44]
5-ASA + Immunomodulators + Biologic agents [%]	1 [4.54]	0 [0]
Not reported [%]	3 [13.63]	0 [0]

5-ASA: 5-aminosalicayde

4.3.2 Lower faecal SCFA levels correlate to increasing IBD disease severity

Quantitative LC-MS/MS was used to determine the amount of SCFA in the cohort of human samples that were designated as Control, Remission, Mild, Moderate and Severe. In the current study, valerate could not be consistently detected by LC-MS/MS and hence emitted from data analysis (Supplementary Figure 4.2a). Quantitative LC-MS/MS analysis showed that the mean total SCFA level in control stools was 557.1 pg/mg, which was substantially lower than IBD patients that are in remission (929 pg/mg), albeit not statistically significant. However, lower concentration of total faecal SCFA level was detected in active patients (430.3 pg/mg) in comparison to the control and remission cohorts, and this reduction was statistically significant when compared to IBD patients in remission (95% CI: 240.6-620.1, p=0.001, Figure 4.1a) although not different to the combined control group (comprising colonoscopy and healthy controls). Further sub-analysis of SCFA levels in accordance with the degree of IBD pathological disease severity demonstrated a similar trend of reduction, where IBD patients with severe endoscopic activity showed greatest decline in total SCFA level (mean value, 281.6 pg/mg). This was followed by the patients with moderate (mean, 387.2 pg/mg) and mild (mean, 557.5 pg/mg) severity (Figure 4.1b). Together, these findings suggest that diminished faecal SCFA levels correlate with increased IBD pathological severities.

Next, we investigated the level of acetate, propionate and butyrate in accordance with classification of IBD disease severities. As shown in Figure 4.1c and Supplementary Figure 4.2b, a slight elevation in mean acetate level was detected in remission, mild and moderate IBD groups when compared to the control. Although not reaching statistical significance, this weak trend to increased levels was followed by a marked decline in mean faecal acetate concentrations as the disease burden progressed to the severe category. On the other hand, faecal propionate levels tended to a gradual decline as IBD progressed from the control group

to severe category (Supplementary Figure 4.2c). Lastly, a notable elevation in faecal butyrate level was found when comparing remission and control groups. However, this was not observed in active IBD patients, where faecal butyrate level diminished sharply in mild, moderate and severe patients (Supplementary Figure 4.2d). While the gross difference between control and IBD groups was significant (Figure 4.1a), evaluation of the changes in individual SCFA did not reach statistical difference. However, the data implies that individual SCFA may play different roles during the pathogenesis and progression of IBD with faecal butyrate likely being a major determinant for the overall change in combined SCFA as disease progressively worsens.

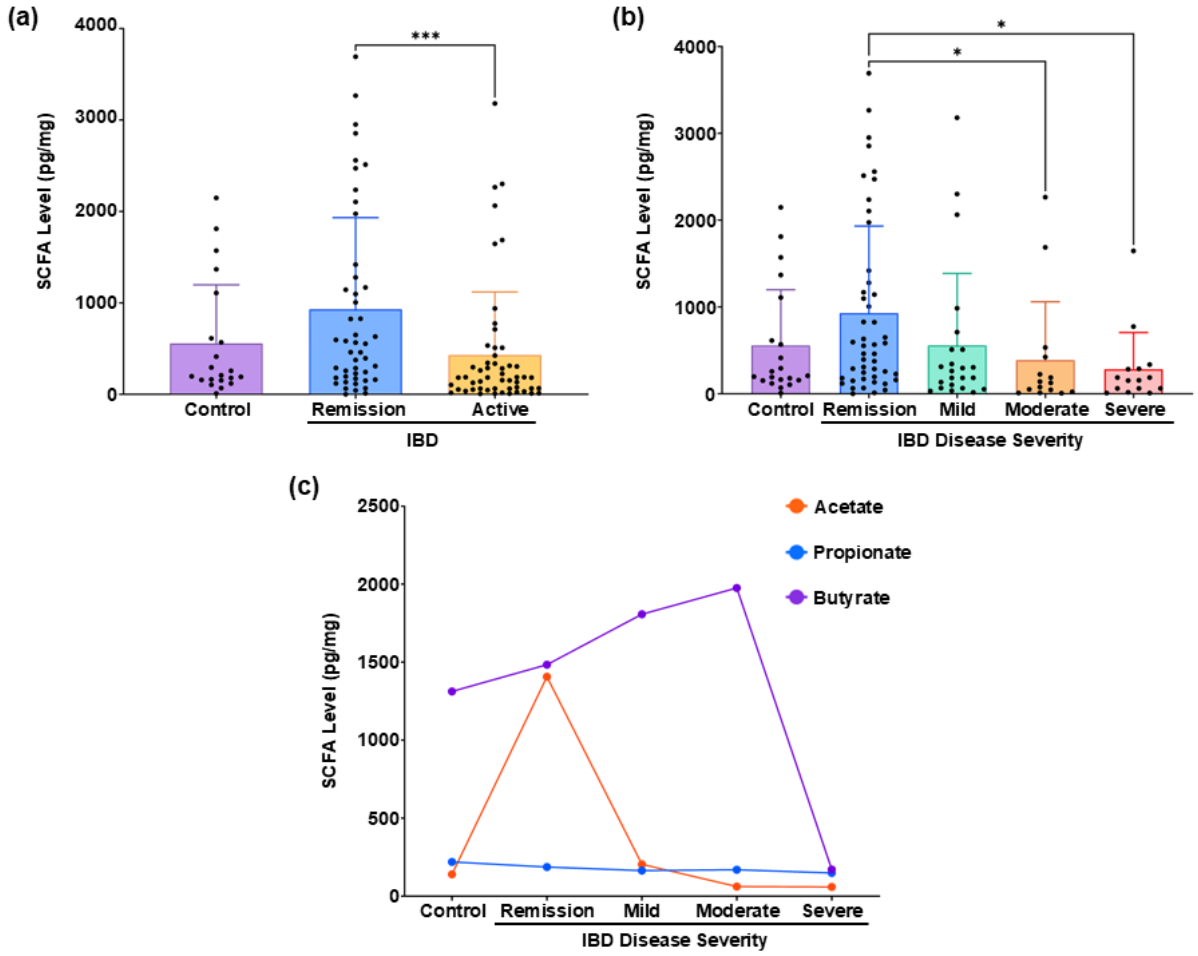

*Figure 4.1. The level of SCFAs in stool of non-IBD individuals and IBD patients. (a) The difference in total SCFA levels between Controls (healthy individuals + individuals who underwent colonoscopy but did not receive an IBD diagnosis) and IBD patients in remission and active phase. (b) The level of SCFAs in relation to IBD disease severity. (c) The amount of acetate, propionate and butyrate in relation to IBD disease severity. Graphical values in (a) and (b) represent mean + SD and values in (c) represent mean with error bars emitted to aid visualisation. n = 19 individuals in the control group and n = 30 IBD patients (n = 18 in remission, n = 10 in mild, n = 8 in moderate and n = 4 in severe). Samples below the detection limit were not included in the analysis. Normalcy of the collected data was analysed using Shapiro-Wilk test and group difference was calculated by Kruskal-Wallis test with Dunn's multiple comparison as a post hoc. *p ≤ 0.05, **p ≤ 0.01, ***p ≤ 0.001 and ****p ≤ 0.0001. Author contributions: K.X – Investigation, validation, formal analysis, data curation and*

visualisation, S.A.D – Investigation, validation, formal analysis, data curation, T.O.C – Investigation, data curation and validation, X.S.W – Investigation, methodology and software, E.V – Investigation, M.G, V.K & N.M – Investigation and data curation.

4.3.3 Higher faecal IL-1β level in patients with moderate and severe IBD

The cytokine IL-1β promotes inflammation by facilitating the migration of immune cells to the affected[33]. In the context of IBD, elevated colonic tissue level of IL-1β, reportedly produced through the activation of NLRP-3 inflammasome has been shown to correlate with greater IBD disease activities[34]. Moreover, elevated level of faecal IL-1β have also been reported in adults and children with IBD[35,36]. In the current study, the level of faecal IL-1β was examined by ELISA to validate the endoscopic evaluation and the extent of gastrointestinal inflammation. As shown in Figure 4.2a, a marked increase in faecal IL-1β level was observed in IBD patients (both in remission and active), albeit not reaching statistical significance ($p = 0.1259$). Notably, active IBD patients had significantly higher levels of IL-1β in their stool (mean value, 204.5 pg/mg) when compared to the controls and IBD patients in remission (means, 11.4 pg/mg and 30.3 pg/mg respectively, $p = 0.004$).

The faecal level of IL-1β was also substantially elevated in subjects in endoscopic remission when compared to the control, however, this difference was not statistically significant ($p > 0.05$, Figure 4.2b). Further sub-analysis of IL-1β showed that patient with moderate IBD severities exhibited greatest increase in stool IL-1β level (mean value 220.2 pg/mg), where it was significantly higher than the remission and control groups (95% CI: 74.71-365.8, $p = 0.0065$ and $p = 0.270$ respectively, Figure 4.2c). Lastly, the current study also compared the difference in IL-1β level between UC and CD patients. As shown in Figure 4.2d, UC patients reported significantly higher level of faecal IL-1β (230.0 pg/mg) in comparison to control and remission groups (95% CI: 99.69-360.4, $p = 0.0023$ and 0.0026 respectively). Similarly, a marked increase in IL-1β in the stool of CD patients was also detected. However, this increase did not reach statistical significance when compared to the corresponding control and remission group (95% CI: -62.11-274.0, $p > 0.05$). The expression of IL-1β in stool was further validated by Western blot analysis that confirmed detection of the anticipated protein band at ~31 kDa in randomly selected samples (see Supplementary Figure 4.3a and b). In summary, these results were consistent with the known response of IL-1β in the inflamed colon, where elevated level of this proinflammatory mediator is noted with increased IBD severity. Circulating IL-1β in plasma samples were below the detection limit of the ELISA kits used in the current study suggesting that systemic levels of IL-1β were low relative to the levels in stool that better reflected the locally inflamed colon tissues.

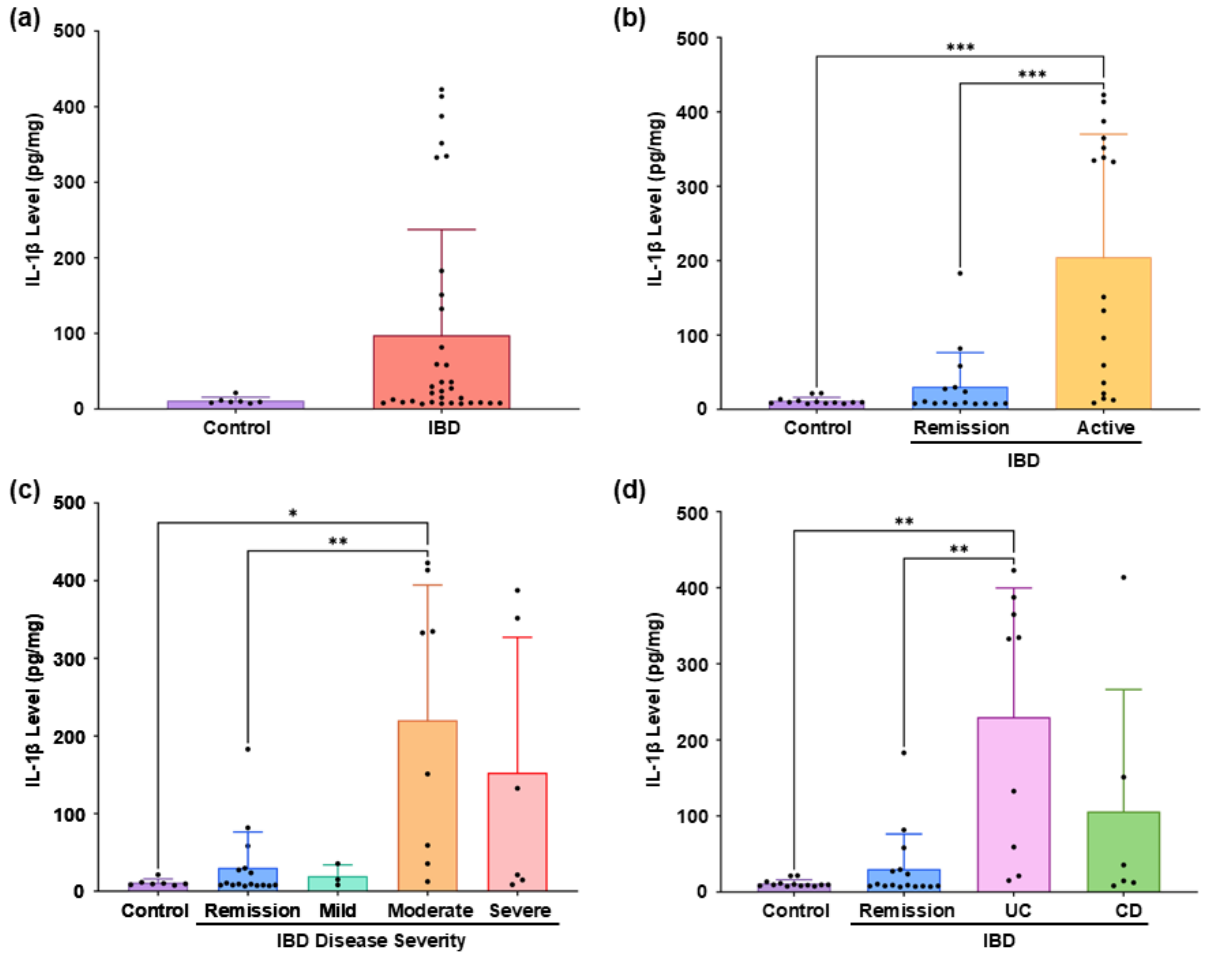

*Figure 4.2. The level of IL-1β in stool. Between panel (a) healthy individuals (n = 7) and IBD patients (n = 33). Panel (b) healthy individuals and IBD patients in remission (n = 16) and active phase (n = 17). Panel (c) The level of IL-1β in relation to IBD disease severity. n = 16 IBD patients in remission, n = 3 in mild, n = 8 in moderate and n = 6 in severe. Panel (d) UC (n = 9) and CD (n = 6) patients. Samples below the detection limit were not included in the analysis. Graphical values represent mean + SD after interpolation from standard curve. Normalcy of the collected data was investigated using Shapiro-Wilk test and group difference was analysed by Mann-Whitney test or Kruskal-Wallis test with Dunn's multiple comparison as a post hoc. *p ≤ 0.05, **p ≤ 0.01, ***p ≤ 0.001 and ****p ≤ 0.0001. Author contributions: K.X – Investigation, validation, formal analysis, data curation and visualisation, S.A.D – Investigation, formal analysis, data curation, T.O.C – Data curation and validation, H.C, M.G, V.K & N.M – Investigation and data curation.*

4.3.4 Propionate and butyrate show weak inverse correlative relationships to faecal IL-1β levels

To investigate the possible inter-dependency between SCFA levels and stool IL-1β concentration, simple linear regression analysis was performed between mean acetate, propionate and butyrate levels and the stool IL-1β concentration in the various group allocations for IBD severities. Figure 4.3a shows the poor correlative relationship between mean acetate concentration and IL-1β level with $R^2 = 0.009$, signified a negligible fit and no meaningful relationship between the two biomarkers. In contrast, the relationship between

average faecal propionate and IL-1β levels demonstrated a stronger inverse correlation (R^2 = 0.12, Figure 4.3b). A weak inverse correlation was also evident between mean butyrate and IL-1β level in the stool (R^2 = 0.32, Figure 4.3c). Correlation evaluation between the total concentrations of SCFA (combined acetate, propionate and butyrate) and the cytokine IL-1β, again identified an improved inverse relationship (R^2 = 0.48, Figure 4.3d). Overall, the results demonstrated the complexity of the interactions among SCFAs and proinflammatory cytokine IL-1β, which also implies that not all SCFAs exert the same influence in IBD pathogenesis or the extent of disease progression in the colon (See Supplementary Figure 4.4 for correlation graphs with inclusion of all analysed samples).

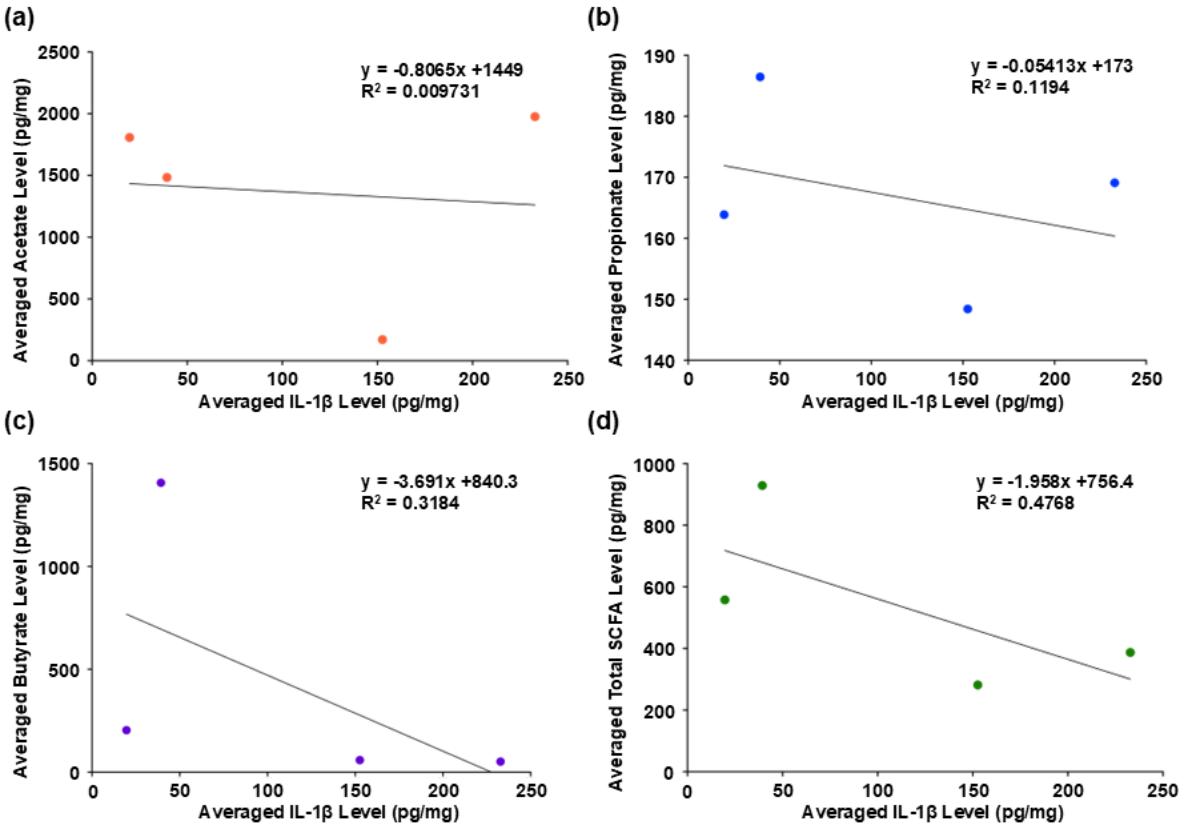

Figure 4.3. Correlation between averaged faecal pro-inflammatory cytokine IL-1β and short chain fatty acid. Panel (a) acetate, panel (b) propionate, panel (c) butyrate and panel (d) total SCFA levels (combined acetate + propionate + butyrate) in the stool from IBD patients. Graphical values represent the mean faecal IL-1β and short chain fatty acid levels at different IBD disease severity. n = 16 IBD patients in remission, n = 3 in mild, n = 8 in moderate and n = 6 in severe. Simple linear regression with 95% confidence was used to evaluate potential correlative relationships. Author contributions: K.X – Investigation, validation, formal analysis, data curation and visualisation, S.A.D – Investigation, formal analysis, data curation, T.O.C – Data curation and validation, H.C, M.G, V.K & N.M – Investigation and data curation.

4.3.5 Elevated faecal IL-6 levels are not reflected in plasma

Quantitative analysis of IL-6 level by ELISA showed a 17.16-fold increase in the stool samples of IBD patients when compared to the control, albeit not reaching statistical significance ($p > 0.05$, Figure 4.4a). Interestingly, such elevation in faecal IL-6 was not observed in plasma

samples, where IBD patients reported similar level of IL-6 when compared to the controls (20.1 vs. 25.6 pg/mL, Figure 4.4b). Furthermore, lower level of circulating IL-6 was detected in plasma of IBD patients with active disease when compared to those in remission although this was not significant (Figure 4.4c and Supplementary Figure 4.5a). Lastly, the difference in circulating IL-6 level between UC and CD patients was not statistically significant (95% CI: -111.5-103.1, $p > 0.05$, Figure 4.4d). Together, these data suggest that IL-6 may promote local colon inflammation as reflected in elevated stool IL-6 levels however, there was no meaningful systemic effect of IL-6 in the same IBD cohort.

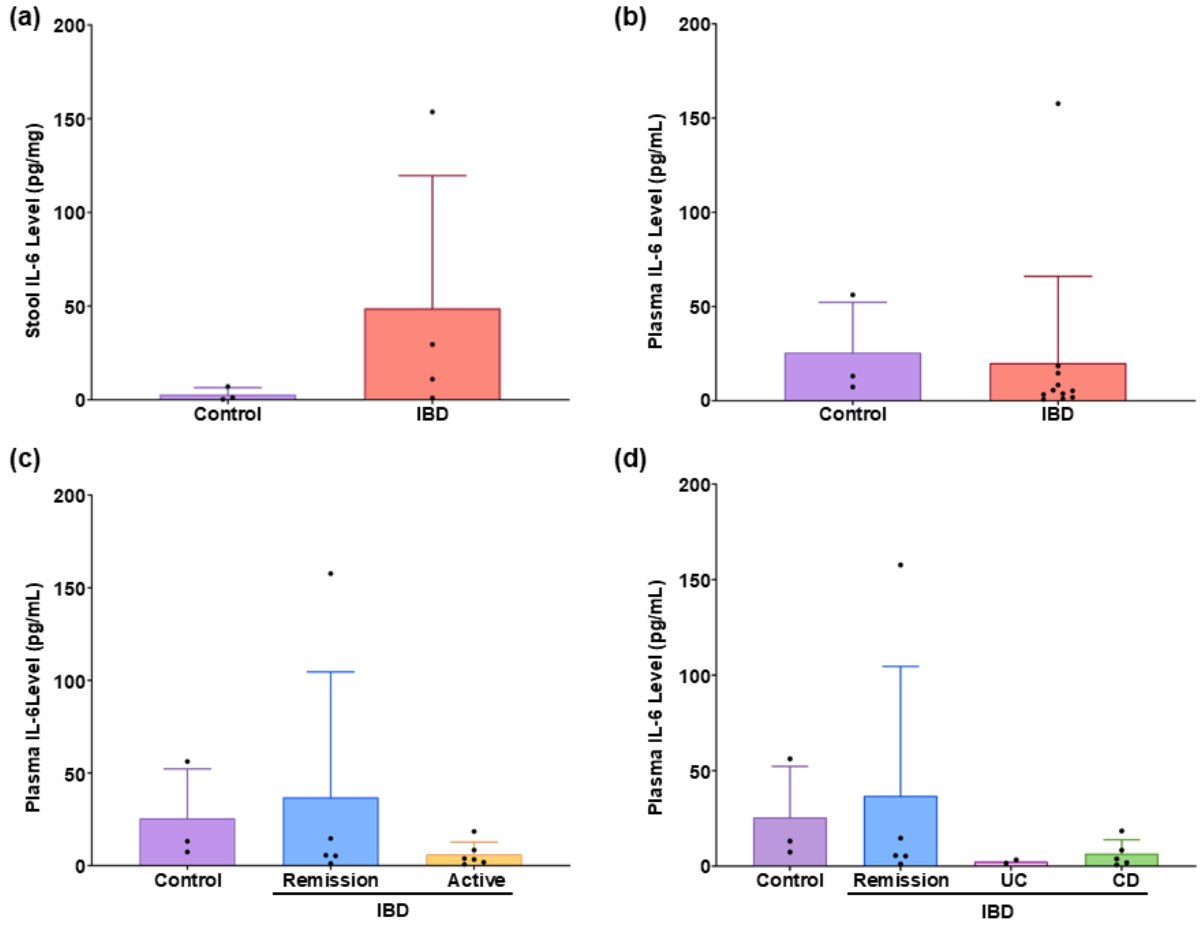

Figure 4.4. The level of IL-6 in healthy individuals and IBD patients. Panel (a) stool samples (n = 3 in control and n = 4 in IBD) and panel (b) plasma (n = 3 in control and n = 11 in IBD). Panel (c) Shows the difference in plasma IL-6 levels between IBD patients in remission (n = 5) and have active IBD flare up (n = 6). Samples below the detection limit were not included in the analysis. Graphical values represent mean + SD after interpolation from standard curve. Normalcy of the collected data was investigated using Shapiro-Wilk test. Group difference was analysed by unpaired t test or one-way ANOVA with Tukey post hoc test for parametric data. Non-parametric data was analysed by Mann-Whitney test or Kruskal-Wallis test with Dunn's multiple comparison as a post hoc. No statistically significant difference between groups was observed. Panel (d) The difference in IL-6 levels in plasma between UC (n =2) and CD (n=5) patients. Graphical values represent mean + SD after interpolation from standard curve and statistical analysis was not performed due to restricted size. Author contributions: K.X – Investigation, validation, formal analysis, data curation

and visualisation, S.A.D – Investigation, formal analysis, data curation, T.O.C – Validation, H.C, M.G, V.K & N.M – Investigation and data curation.

Data here showed that IL-10 concentration in the plasma of IBD patients was markedly decreased relative to the controls (Figure 4.5a). Notably, this reduction was more pronounced in active IBD patients (mean IL-10 level, 7.4 pg/mL) compared to control (mean, 58.4 pg/mL) and IBD patients in remission (14.6 pg/mL, Figure 4.5b). Further sub-analysis across controls groups and various IBD severities showed minimal difference in plasma IL-10 levels (Figure 4.5c). When comparing the control group and remission patients, a substantial reduction in circulating IL-10 levels was observed in patients with active UC. Similarly, a trend of diminished IL-10 was also observed in active CD patients, however, no statistical analyses were performed due to limited sample size (Figure 4.5d). ELISA of IL-10 in faecal samples detected limited results (Supplementary Figure 4.5b). Due to lower datapoints yielded from IL-6 and IL-10 ELISA analyses, simple linear regression of the mean level of these cytokines with SCFA was not performed.

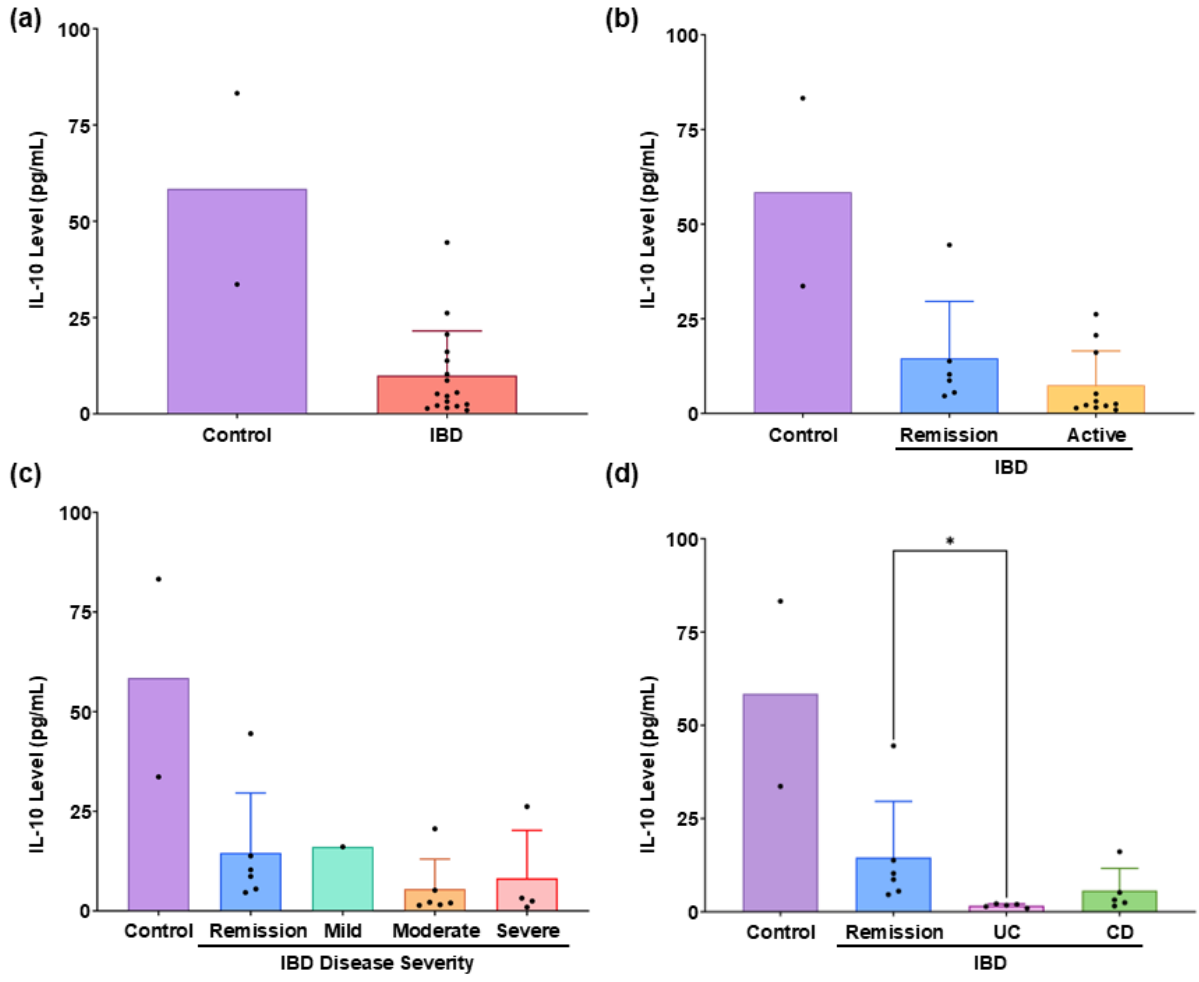

Figure 4.5. The level of IL-10 in patients. Panel (a) healthy (n = 2) and IBD patient (n = 17) plasma samples. Panel (b) The difference in IL-10 levels between healthy individuals and IBD patients in remission (n = 6) and active phase (n = 11). Panel (c) The level of IL-1β in relation to IBD disease severity. n = 6 IBD patients in remission, n = 1 in mild, n = 6 in moderate and n = 4 in severe. Panel (d) The difference in IL-10 levels between UC (n = 5) and CD (n = 5) patients. Samples below the detection limit

*were not included in the analysis. Graphical values represent mean + SD after interpolation from standard curve. Normalcy of the collected data was investigated using Shapiro-Wilk test and group difference was analysed by Mann-Whitney test or Kruskal-Wallis test with Dunn's multiple comparison as a post hoc. *p ≤ 0.05, **p ≤ 0.01, ***p ≤ 0.001 and ****p ≤ 0.0001. Author contributions: K.X – Investigation, validation, formal analysis, data curation and visualisation, S.A.D – Investigation, formal analysis, data curation, T.O.C – Validation, H.C, M.G, V.K & N.M – Investigation and data curation.*

4.4 Discussion

While perturbation of gut bacteriome in UC and CD patients has been widely documented[14,37,38], conflicting findings have been reported for corresponding levels of SCFA metabolites acetate, propionate and butyrate[27-30.] Therefore, relationships between SCFA levels, IBD disease severities and the extent of gut inflammation remain to be identified. The aim of the current study was to examine the levels of acetate, propionate and butyrate in faecal samples of both active and remissive UC and CD patients across a spectrum of disease severities compared with health individuals. A significant reduction in total SCFA level was observed in active IBD patients when compared to patients in remission and in the controls, with each SCFA exhibiting a differential pattern of change as a function of disease severity. Faecal acetate levels increased marginally in IBD patients in remission and with mild or moderate disease severities when compared to the controls. However, acetate declined markedly with increased severe disease activity. Propionate levels were highest in controls and decreased consistently in remission and in those with active IBD. Patients classified in remission showed a distinct peak in faecal butyrate levels, with substantially lower levels of butyrate in controls and active IBD patients. These changes were accompanied by a general trend of elevation in pro-inflammatory cytokines IL-1β and IL-6 in stool, as well as a decrease in serum level of anti-inflammatory IL-10, suggesting that individual SCFA may contribute differently by modulating gut barrier function and colon inflammatory responses, and may potentially play a role in the pathogenesis of IBD.

The pro-inflammatory cytokine IL-1β promotes the release of downstream inflammatory mediators[39] which are markedly increased in patients with severe IBD[34,40]. As anticipated, a significantly higher level of faecal IL-1β was observed in patients with moderate and severe IBD studied here, recapitulating the findings reported by previous studies and thereby indirectly affirming the IBD disease severity classifications made here. Although not reaching statistical significance, outcomes here highlighted a trend towards higher faecal IL-1β level in UC patients when compared to CD patients. This difference may be attributed to inflammation in UC is focal to the colon intestinal mucosa[2]. This is also accompanied with infiltrated immune cells and elevated secretion of pro-inflammatory mediators (e.g., IL-1β in the large intestine)[41], where higher levels of inflammatory mediators can be detected even in areas of the colon without histologically assigned inflammation[42]. Conversely, the patchy transmural lesion of CD may stimulate a greater systemic response[3]. However, larger sample size is required to account for the biological variability observed in the current study and confirm this notion.

Proinflammatory IL-6 is reported to increase in both stool and serum samples of patients with IBD[43,44]. Furthermore, IL-6 exerts proinflammatory action by activating antigen presenting cells and T cells in the intestinal epithelium[43]. Herein, minimal changes on plasma and faecal IL-6 levels were detected owing to small sample size, highlighting the limitation of the current study. On the other hand, IL-10 is an immunomodulatory cytokine that maintains gut immune homeostasis by inhibiting the release of TNF-α[45], limiting antigen presentation[46] and preventing T-cell overactivation[47].

Plasma IL-10 level was markedly higher in healthy control subjects when compared to patients with either active or remissive IBD, albeit not reaching statistical significance. The anti-inflammatory cytokine IL-10 has been reported to provide a protective role to the intestinal epithelium released by anti-inflammatory macrophage as an innate immune response[48],

where loss-of-function mutation of genes encoding IL-10 and IL-10 receptor have shown to associate with very early-onset IBD[49]. Outcomes here highlights the potential dysregulation of immune response in the IBD gut. However, a larger sample size is warranted to confirm this notion. Interestingly, the current study showed similar levels of plasma IL-10 in remission and active IBD patients, which suggests that IL-10 may not serve as a predictor of clinical remission in IBD albeit that this does not rule out that circulating IL-10 may play a role in maintaining IBD patients in the remission phase.

Faecal levels of propionate and butyrate as well as combined total SCFA (total acetate, propionate and butyrate) all showed weak inversely correlative relationships to the level of pro-inflammatory cytokine IL-1β, suggesting a potential immune dampening effect of these SCFAs in the IBD gut. In support of this, the study by Tong et al. demonstrated that supplementation with sodium propionate inhibited the expression of IL-1β and IL-6, and improved dextran sodium sulfate (DSS)-induced colitis symptoms by improving intestinal barrier function in this experimental model[50]. This highlights the potential anti-inflammatory and colon protective properties of this SCFA. Similarly, butyrate supplementation has been shown to reduce the level of serum IL-1β and IL-6[51,52] as well as promote the production of anti-inflammatory cytokine IL-10 levels[53] in IBD experimental animal models. Furthermore, it has been demonstrated that acetate promotes intestinal integrity and reduces colon inflammation by binding to 'metabolite sensing' G-protein coupled receptor (GPR)-43 and GPR109A in a murine model of colitis[54]. However, the anti-inflammatory effect of acetate was not observed in this study, whereby mean acetate level reported no meaningful relationship with averaged IL-1β concentrations in the corresponding stool samples and acetate levels only diminished between moderate and severe disease states. Nevertheless, outcomes here imply that elevated SCFA levels, particularly propionate and butyrate are potentially linked to the extent of inflammation in the gut with decreased levels of these specific SCFA evident in as IBD disease activity increases.

Given the promising anti-inflammatory effects of propionate and butyrate in animal models of IBD, SCFA supplementation poses a great potential as an alternative therapeutic option for IBD patients. Thus, the markedly higher level of butyrate was observed in remissive IBD patients when compared to controls and patients with active IBD, suggests that elevating colon butyrate is likely associated with disease remission. Accordingly, Luhrs et al. showed that 4 and 8 weeks of 100 mM of butyrate supplementation (administered via enema) resulted in the inhibition of macrophage nuclear factor kappa B (NF-κB) activation in the lamina propria of UC patients and significantly improved the disease activity index[55], highlighting the therapeutic potential of SCFA supplementation. Conversely, a double-blind, placebo-controlled pilot study conducted by Facchin et al. showed that oral administration of sodium butyrate capsules in conjunction with conventional therapy increased the abundance of SCFA-producing bacteria in UC and butyrate-producing bacteria in CD patients. Despite improvement to gut bacteriome under these conditions, butyrate supplementation in this cohort only resulted in improved quality-of-life index in UC patients and generally failed to exert any positive effects on clinical activities for either UC or CD patients[56]. A similar finding was reported by Hamer et al., where butyrate enema resulted in minor improvements on gut inflammation in clinically remissive UC patients[57], suggesting that increased butyrate level could promote the shift towards the quiescent state of IBD, consistent with the outcomes identified here, however, this intervention offers limited improvements to IBD pathologies. The treatment dosage of butyrate could potentially be an influencing factor on therapeutic

efficacy. By using a Caco-2 cell monolayer as a model of intestinal barrier, Peng et al. has demonstrated that 2 mM of butyrate increased transepithelial resistance and decreased inulin permeability, however, these beneficial effects were reversed at 8 mM, and butyrate induced dose-dependent apoptosis of the Caco-2 monolayer[58], suggesting that low concentration of butyrate supplementation is more likely to produce favourable therapeutic effects on the intestinal epithelium. Additionally, whether the administration route defines SCFA bioactivity in the colon is unclear since oral dosing is limited by systemic redistribution of SCFA (e.g., acetate and butyrate) following efficient absorption in the stomach[59]. By contrast, supplementing direct to colon via rectal enema may improve delivery of the SCFA in comparison to other routes of butyrate delivery and aid in recovery post-colorectal surgery[60]. The effect of sodium propionate supplementation has been investigated in patients of end-stage renal disease[61,62], with significant decline in inflammatory parameters such as C-reactive proteins, IL-2 and IL-17 reported[62]. However, the therapeutic potential of propionate supplementation in IBD patients remains to be systematically investigated. Furthermore, the outcomes from the current study indicate that further investigation is warranted to fully define the therapeutic potential of SCFAs (butyrate and propionate) in patients with active IBD or testing whether supplementing patients in clinical remission can elongate the period of remission and/or reduce the severity of subsequent phases of active IBD.

In addition to the anti-inflammatory effects of SCFA, the integral role of these volatile lipid metabolites in maintaining colon enterocyte physiology should be considered. The intestinal barrier comprises a layer of epithelial cells that are interconnected by tight junctions[63]. Enhanced tight junction permeability and structural disruption to the gut epithelium exacerbates IBD pathologies in animal models of IBD[64,65], which suggests that efficient epithelial regeneration may underpin the linkage between maintenance of the intestinal epithelial barrier and delaying clinical presentation of IBD. Notably, SCFAs butyrate can elicit signal transducer and activator of transcription 3 (STAT3) activation[66], which subsequently promotes epithelial regeneration via the IL-10[67] and IL-22[68] signalling pathway. In support of this notion, increasing dietary fibre intake to boost SCFA production, suppresses experimental colitis in an IL-10-deficicent murine model[69]. Moreover, administering mixtures of SCFA (containing acetate, propionate and butyrate) reverses the diminished intestinal epithelial cell proliferative activity observed in a germ-free mice[70], highlighting the role for SCFA in supporting epithelial cell proliferation, which further reinforces an involvement in maintaining epithelial barrier structure and function. Thus, elevated SCFA production in the gut may enhance mucosal cell viability to facilitate the shift towards clinical remission in IBD, which is in strong agreement with the higher total SCFA concentration observed in IBD patients assigned to the remission group determined here. However, to confirm this conclusion additional investigations on colon histopathology and tight junction permeability are required to completely validate the barrier maintenance properties of the SCFAs.

As this is a cross-sectional study, it is not completely clear if the observed associations between SCFA levels and disease activity are causative or merely a consequence of active inflammation. Although microbiome products such as SCFA interact with colonic mucosa to influence disease states, it is also possible that active inflammation can influence the gut microbiome composition and SCFA production. To further strengthen the case for causality additional longitudinal studies are required to correlate pre-disease onset or pre-disease flare SCFA and cytokine levels, with documented future disease onset or relapse, respectively.

It is noteworthy that changes in SCFA levels observed here could also be a cause or a consequence of drugs prescribed to the recruited patients. The main pharmacological interventions of IBD include 5-ASA, thiopurines and anti-TNF agents[31], which all target various aspect of the inflammatory cascade. In the current study, over 92% of the recruited patients reported the use of at least one form of these prescription drugs with some taking combinations of these pharmaceuticals. It has been shown that oral administration of 5-ASA increases *Firmicutes* and decreases *Proteobacteria* abundances, in both wildtype mice that have no intestinal inflammation[71] and in patients diagnosed with UC[72], suggesting that 5-ASA may direct the host immune system towards an anti-inflammatory state by altering the intestinal microbiota composition. A similar shift in gut microbiota composition has been reported in IBD patients that received anti-TNF treatments, where Infliximab is known to restore microbiome pattern in children diagnosed with CD children toward a microbial community common in healthy children[73], as well as increasing SCFA-producing bacteria in adult CD patients[74]. Interestingly, the study by Wills et al. demonstrated that thiopurine treatment reduced the bacterial diversity in UC and CD patients[75]. However, this reduction of bacterial diversity could contribute to the growth inhibition of pathogenic bacteria such as *Campylobacter* in the presence of thiopurine treatment[76].

Despite findings highlighting the potential correlative relationship between SCFA levels and IBD disease severity, a limitation here is a lack of gut microbiome analysis. As a result, it is unclear whether the change in SCFA levels is a consequence of reduced SCFA-producing bacteria in the gut or reduced production by these bacteria (or a combination of both factors). Additionally, grouped averaged data was used to investigate the correlative relationship between individual SCFAs and faecal IL-1β level. Thus, the correlation between the individual SCFA and faecal IL-1β level identified in the current study should be interpreted with caution, as relationships observed at the group level may not hold true at the individual level.

In conclusion, the current study was the first to investigate the level of SCFA acetate, propionate and butyrate in both UC and CD patients across a spectrum of disease severities as evaluated clinically by colonoscopy. Active IBD patients are characterised by a substantial reduction of SCFA levels and higher level of proinflammatory cytokine IL-1β in their stool. Overall, decreased levels of acetate, propionate and butyrate were weakly and inversely associated with increasing IBD severity, which suggests that maintaining physiological levels of these SCFAs may be associated with maintaining a state of IBD disease remission; a stronger case may be made for butyrate supplementation and maintenance of remission. Overall, our results would support further interventional studies to determine if butyrate and/or propionate supplementation can help induce or maintain remission among CD or UC patients.

4.5 References

1. Barberio, B., Zamani, M., Black, C.J., Savarino, E.V., and Ford, A.C. (2021). Prevalence of symptoms of anxiety and depression in patients with inflammatory bowel disease: a systematic review and meta-analysis. Lancet Gastroenterol Hepatol *6, 359-370*. 10.1016/S2468-1253(21)00014-5.

2. Kobayashi, T., Siegmund, B., Le Berre, C., Wei, S.C., Ferrante, M., Shen, B., Bernstein, C.N., Danese, S., Peyrin-Biroulet, L., and Hibi, T. (2020). Ulcerative colitis. Nat Rev Dis Primers *6, 74.* 10.1038/s41572-020-0205-x.

3. Roda, G., Chien Ng, S., Kotze, P.G., Argollo, M., Panaccione, R., Spinelli, A., Kaser, A., Peyrin-Biroulet, L., and Danese, S. (2020). Crohn's disease. Nat Rev Dis Primers *6, 22*. 10.1038/s41572-020-0156-2.

4. Blackwell, J., Saxena, S., Jayasooriya, N., Bottle, A., Petersen, I., Hotopf, M., Alexakis, C., Pollok, R.C., and group, P.-I.s. (2020). Prevalence and duration of gastrointestinal symptoms before diagnosis of Inflammatory Bowel Disease and predictors of timely specialist review: a population-based study. J Crohns Colitis. 10.1093/ecco-jcc/jjaa146.

5. Parada Venegas, D., De la Fuente, M.K., Landskron, G., Gonzalez, M.J., Quera, R., Dijkstra, G., Harmsen, H.J.M., Faber, K.N., and Hermoso, M.A. (2019). Short Chain Fatty Acids (SCFAs)-Mediated Gut Epithelial and Immune Regulation and Its Relevance for Inflammatory Bowel Diseases. Front Immunol *10, 277.* 10.3389/fimmu.2019.00277.

6. de Castro, M.M., Pascoal, L.B., Steigleder, K.M., Siqueira, B.P., Corona, L.P., Ayrizono, M.L.S., Milanski, M., and Leal, R.F. (2021). Role of diet and nutrition in inflammatory bowel disease. World J Exp Med *11, 1-16.* 10.5493/wjem.v11.i1.1.

7. Hou, J.K., Abraham, B., and El-Serag, H. (2011). Dietary intake and risk of developing inflammatory bowel disease: a systematic review of the literature. Am J Gastroenterol *106, 563-573.* 10.1038/ajg.2011.44.

8. Nagalingam, N.A., and Lynch, S.V. (2012). Role of the microbiota in inflammatory bowel diseases. Inflamm Bowel Dis *18, 968-984.* 10.1002/ibd.21866.

9. Kostic, A.D., Xavier, R.J., and Gevers, D. (2014). The microbiome in inflammatory bowel disease: current status and the future ahead. Gastroenterology *146, 1489-1499.* 10.1053/j.gastro.2014.02.009.

10. Hou, K., Wu, Z.X., Chen, X.Y., Wang, J.Q., Zhang, D., Xiao, C., Zhu, D., Koya, J.B., Wei, L., Li, J., and Chen, Z.S. (2022). Microbiota in health and diseases. Signal Transduct Target Ther *7, 135.* 10.1038/s41392-022-00974-4.

11. Human Microbiome Project, C. (2012). Structure, function and diversity of the healthy human microbiome. Nature *486, 207-214.* 10.1038/nature11234.

12. Wu, G.D., Chen, J., Hoffmann, C., Bittinger, K., Chen, Y.Y., Keilbaugh, S.A., Bewtra, M., Knights, D., Walters, W.A., Knight, R., et al. (2011). Linking long-term dietary patterns with gut microbial enterotypes. Science *334, 105-108.* 10.1126/science.1208344.

13. Lin, D., Peters, B.A., Friedlander, C., Freiman, H.J., Goedert, J.J., Sinha, R., Miller, G., Bernstein, M.A., Hayes, R.B., and Ahn, J. (2018). Association of dietary fibre intake and gut microbiota in adults. Br J Nutr *120, 1014-1022.* 10.1017/S0007114518002465.

14. Ott, S.J., Musfeldt, M., Wenderoth, D.F., Hampe, J., Brant, O., Folsch, U.R., Timmis, K.N., and Schreiber, S. (2004). Reduction in diversity of the colonic mucosa associated bacterial microflora in patients with active inflammatory bowel disease. Gut *53, 685-693.* 10.1136/gut.2003.025403.

15. Axelrad, J.E., Joelson, A., Green, P.H.R., Lawlor, G., Lichtiger, S., Cadwell, K., and Lebwohl, B. (2018). Enteric Infections Are Common in Patients with Flares of Inflammatory Bowel Disease. Am J Gastroenterol *113, 1530-1539.* 10.1038/s41395-018-0211-8.

16. Kostovcikova, K., Coufal, S., Galanova, N., Fajstova, A., Hudcovic, T., Kostovcik, M., Prochazkova, P., Jiraskova Zakostelska, Z., Cermakova, M., Sediva, B., et al. (2019). Diet Rich in Animal Protein Promotes Pro-inflammatory Macrophage Response and Exacerbates Colitis in Mice. Front Immunol *10, 919.* 10.3389/fimmu.2019.00919.

17. Harrison, C.A., Laubitz, D., Ohland, C.L., Midura-Kiela, M.T., Patil, K., Besselsen, D.G., Jamwal, D.R., Jobin, C., Ghishan, F.K., and Kiela, P.R. (2018). Microbial dysbiosis associated with impaired intestinal Na(+)/H(+) exchange accelerates and exacerbates colitis in ex-germ free mice. Mucosal Immunol *11, 1329-1341.* 10.1038/s41385-018-0035-2.

18. Vesci, L., Tundo, G., Soldi, S., Galletti, S., Stoppoloni, D., Bernardini, R., Modolea, A.B., Luberto, L., Marra, E., Giorgi, F., and Marini, S. (2024). A Novel Lactobacillus brevis Fermented with a Vegetable Substrate (AL0035) Counteracts TNBS-Induced Colitis by Modulating the Gut Microbiota Composition and Intestinal Barrier. Nutrients *16.* 10.3390/nu16070937.

19. Klimesova, K., Kverka, M., Zakostelska, Z., Hudcovic, T., Hrncir, T., Stepankova, R., Rossmann, P., Ridl, J., Kostovcik, M., Mrazek, J., et al. (2013). Altered gut microbiota promotes colitis-associated cancer in IL-1 receptor-associated kinase M-deficient mice. Inflamm Bowel Dis *19, 1266-1277.* 10.1097/MIB.0b013e318281330a.

20. Burrello, C., Garavaglia, F., Cribiu, F.M., Ercoli, G., Lopez, G., Troisi, J., Colucci, A., Guglietta, S., Carloni, S., Guglielmetti, S., et al. (2018). Therapeutic faecal microbiota transplantation controls intestinal inflammation through IL10 secretion by immune cells. Nat Commun *9, 5184.* 10.1038/s41467-018-07359-8.

21. Jang, Y.J., Kim, W.K., Han, D.H., Lee, K., and Ko, G. (2019). Lactobacillus fermentum species ameliorate dextran sulfate sodium-induced colitis by regulating the immune response and altering gut microbiota. Gut Microbes *10, 696-711.* 10.1080/19490976.2019.1589281.

22. Wang, C., Li, W., Wang, H., Ma, Y., Zhao, X., Zhang, X., Yang, H., Qian, J., and Li, J. (2019). Saccharomyces boulardii alleviates ulcerative colitis carcinogenesis in mice by reducing TNF-alpha and IL-6 levels and functions and by rebalancing intestinal microbiota. BMC Microbiol *19, 246.* 10.1186/s12866-019-1610-8.

23. Dalile, B., Van Oudenhove, L., Vervliet, B., and Verbeke, K. (2019). The role of short-chain fatty acids in microbiota-gut-brain communication. Nat Rev Gastroenterol Hepatol *16, 461-478.* 10.1038/s41575-019-0157-3.

24. Donohoe, D.R., Garge, N., Zhang, X., Sun, W., O'Connell, T.M., Bunger, M.K., and Bultman, S.J. (2011). The microbiome and butyrate regulate energy metabolism and autophagy in the mammalian colon. Cell Metab *13, 517-526.* 10.1016/j.cmet.2011.02.018.

25. Zhang, D., Jian, Y.P., Zhang, Y.N., Li, Y., Gu, L.T., Sun, H.H., Liu, M.D., Zhou, H.L., Wang, Y.S., and Xu, Z.X. (2023). Short-chain fatty acids in diseases. Cell Commun Signal *21, 212.* 10.1186/s12964-023-01219-9.

26. Zhang, Z., Zhang, H., Chen, T., Shi, L., Wang, D., and Tang, D. (2022). Regulatory role of short-chain fatty acids in inflammatory bowel disease. Cell Commun Signal *20, 64*. 10.1186/s12964-022-00869-5.

27. Roediger, W.E., Heyworth, M., Willoughby, P., Piris, J., Moore, A., and Truelove, S.C. (1982). Luminal ions and short chain fatty acids as markers of functional activity of the mucosa in ulcerative colitis. J Clin Pathol *35, 323-326.* 10.1136/jcp.35.3.323.

28. van Nuenen, M.H., Venema, K., van der Woude, J.C., and Kuipers, E.J. (2004). The metabolic activity of fecal microbiota from healthy individuals and patients with inflammatory bowel disease. Dig Dis Sci *49, 485-491.* 10.1023/b:ddas.0000020508.64440.73.

29. Machiels, K., Joossens, M., Sabino, J., De Preter, V., Arijs, I., Eeckhaut, V., Ballet, V., Claes, K., Van Immerseel, F., Verbeke, K., et al. (2014). A decrease of the butyrate-producing species Roseburia hominis and Faecalibacterium prausnitzii defines dysbiosis in patients with ulcerative colitis. Gut *63, 1275-1283.* 10.1136/gutjnl-2013-304833.

30. Takaishi, H., Matsuki, T., Nakazawa, A., Takada, T., Kado, S., Asahara, T., Kamada, N., Sakuraba, A., Yajima, T., Higuchi, H., et al. (2008). Imbalance in intestinal microflora constitution could be involved in the pathogenesis of inflammatory bowel disease. Int J Med Microbiol *298, 463-472.* 10.1016/j.ijmm.2007.07.016.

31. Cai, Z., Wang, S., and Li, J. (2021). Treatment of Inflammatory Bowel Disease: A Comprehensive Review. Front Med (Lausanne) *8, 765474.* 10.3389/fmed.2021.765474.

32. Ben-Horin, S., Kopylov, U., and Chowers, Y. (2014). Optimizing anti-TNF treatments in inflammatory bowel disease. Autoimmun Rev *13, 24-30.* 10.1016/j.autrev.2013.06.002.

33. Aggeletopoulou, I., Kalafateli, M., Tsounis, E.P., and Triantos, C. (2024). Exploring the role of IL-1beta in inflammatory bowel disease pathogenesis. Front Med (Lausanne) *11, 1307394.* 10.3389/fmed.2024.1307394.

34. Ranson, N., Veldhuis, M., Mitchell, B., Fanning, S., Cook, A.L., Kunde, D., and Eri, R. (2018). NLRP3-Dependent and -Independent Processing of Interleukin (IL)-1beta in Active Ulcerative Colitis. Int J Mol Sci *20.* 10.3390/ijms20010057.

35. Peterson, C.G., Sangfelt, P., Wagner, M., Hansson, T., Lettesjo, H., and Carlson, M. (2007). Fecal levels of leukocyte markers reflect disease activity in patients with ulcerative colitis. Scand J Clin Lab Invest *67, 810-820.* 10.1080/00365510701452838.

36. Wedrychowicz, A., Tomasik, P., Zajac, A., and Fyderek, K. (2018). Prognostic value of assessment of stool and serum IL-1beta, IL-1ra and IL-6 concentrations in children with active and inactive ulcerative colitis. Arch Med Sci *14, 107-114.* 10.5114/aoms.2017.68696.

37. Takahashi, K., Nishida, A., Fujimoto, T., Fujii, M., Shioya, M., Imaeda, H., Inatomi, O., Bamba, S., Sugimoto, M., and Andoh, A. (2016). Reduced Abundance of Butyrate-Producing Bacteria Species in the Fecal Microbial Community in Crohn's Disease. Digestion *93, 59-65.* 10.1159/000441768.

38. Handa, O., Miura, H., Gu, T., Osawa, M., Matsumoto, H., Umegaki, E., Inoue, R., Naito, Y., and Shiotani, A. (2023). Reduction of butyric acid-producing bacteria in the ileal mucosa-associated microbiota is associated with the history of abdominal surgery in patients with Crohn's disease. Redox Rep *28, 2241615.* 10.1080/13510002.2023.2241615.

39. Mantovani, A., Dinarello, C.A., Molgora, M., and Garlanda, C. (2019). Interleukin-1 and Related Cytokines in the Regulation of Inflammation and Immunity. Immunity *50, 778-795.* 10.1016/j.immuni.2019.03.012.

40. Gao, X., Duan, S., Cao, Y., and Zhang, Y. (2023). Change of monocytes/macrophages in ulcerative colitis patients with symptoms of anxiety and depression. BMC Gastroenterol *23, 67.* 10.1186/s12876-023-02693-8.

41. Kaluzna, A., Olczyk, P., and Komosinska-Vassev, K. (2022). The Role of Innate and Adaptive Immune Cells in the Pathogenesis and Development of the Inflammatory Response in Ulcerative Colitis. J Clin Med *11.* 10.3390/jcm11020400.

42. Reimund, J.M., Wittersheim, C., Dumont, S., Muller, C.D., Kenney, J.S., Baumann, R., Poindron, P., and Duclos, B. (1996). Increased production of tumour necrosis factor-alpha interleukin-1 beta, and interleukin-6 by morphologically normal intestinal biopsies from patients with Crohn's disease. Gut *39, 684-689.* 10.1136/gut.39.5.684.

43. Atreya, R., Mudter, J., Finotto, S., Mullberg, J., Jostock, T., Wirtz, S., Schutz, M., Bartsch, B., Holtmann, M., Becker, C., et al. (2000). Blockade of interleukin 6 trans signaling suppresses T-cell resistance against apoptosis in chronic intestinal inflammation: evidence in crohn disease and experimental colitis in vivo. Nat Med *6, 583-588.* 10.1038/75068.

44. Raab, Y., Hallgren, R., and Gerdin, B. (1994). Enhanced intestinal synthesis of interleukin-6 is related to the disease severity and activity in ulcerative colitis. Digestion *55, 44-49.* 10.1159/000201122.

45. Schreiber, S., Heinig, T., Thiele, H.G., and Raedler, A. (1995). Immunoregulatory role of interleukin 10 in patients with inflammatory bowel disease. Gastroenterology *108, 1434-1444.* 10.1016/0016-5085(95)90692-4.

46. Fiorentino, D.F., Zlotnik, A., Vieira, P., Mosmann, T.R., Howard, M., Moore, K.W., and O'Garra, A. (1991). IL-10 acts on the antigen-presenting cell to inhibit cytokine production by Th1 cells. J Immunol *146, 3444-3451*.

47. Veenbergen, S., Li, P., Raatgeep, H.C., Lindenbergh-Kortleve, D.J., Simons-Oosterhuis, Y., Farrel, A., Costes, L.M.M., Joosse, M.E., van Berkel, L.A., de Ruiter, L.F., et al. (2019). IL-10 signaling in dendritic cells controls IL-1beta-mediated IFNgamma secretion by human CD4(+) T cells: relevance to inflammatory bowel disease. Mucosal Immunol *12, 1201-1211*. 10.1038/s41385-019-0194-9.

48. Murai, M., Turovskaya, O., Kim, G., Madan, R., Karp, C.L., Cheroutre, H., and Kronenberg, M. (2009). Interleukin 10 acts on regulatory T cells to maintain expression of the transcription factor Foxp3 and suppressive function in mice with colitis. Nat Immunol *10, 1178-1184.* 10.1038/ni.1791.

49. Kotlarz, D., Beier, R., Murugan, D., Diestelhorst, J., Jensen, O., Boztug, K., Pfeifer, D., Kreipe, H., Pfister, E.D., Baumann, U., et al. (2012). Loss of interleukin-10 signaling and infantile inflammatory bowel disease: implications for diagnosis and therapy. Gastroenterology *143, 347-355.* 10.1053/j.gastro.2012.04.045.

50. Tong, L.C., Wang, Y., Wang, Z.B., Liu, W.Y., Sun, S., Li, L., Su, D.F., and Zhang, L.C. (2016). Propionate Ameliorates Dextran Sodium Sulfate-Induced Colitis by Improving Intestinal Barrier Function and Reducing Inflammation and Oxidative Stress. Front Pharmacol *7, 253.* 10.3389/fphar.2016.00253.

51. Chen, G., Ran, X., Li, B., Li, Y., He, D., Huang, B., Fu, S., Liu, J., and Wang, W. (2018). Sodium Butyrate Inhibits Inflammation and Maintains Epithelium Barrier Integrity in a TNBS-induced Inflammatory Bowel Disease Mice Model. EBioMedicine *30, 317-325.* 10.1016/j.ebiom.2018.03.030.

52. Zhang, M., Zhou, Q., Dorfman, R.G., Huang, X., Fan, T., Zhang, H., Zhang, J., and Yu, C. (2016). Butyrate inhibits interleukin-17 and generates Tregs to ameliorate colorectal colitis in rats. BMC Gastroenterol *16, 84.* 10.1186/s12876-016-0500-x.

53. Sun, M., Wu, W., Chen, L., Yang, W., Huang, X., Ma, C., Chen, F., Xiao, Y., Zhao, Y., Ma, C., et al. (2018). Microbiota-derived short-chain fatty acids promote Th1 cell IL-10 production to maintain intestinal homeostasis. Nat Commun *9, 3555.* 10.1038/s41467-018-05901-2.

54. Macia, L., Tan, J., Vieira, A.T., Leach, K., Stanley, D., Luong, S., Maruya, M., Ian McKenzie, C., Hijikata, A., Wong, C., et al. (2015). Metabolite-sensing receptors GPR43 and GPR109A facilitate dietary fibre-induced gut homeostasis through regulation of the inflammasome. Nat Commun *6, 6734.* 10.1038/ncomms7734.

55. Luhrs, H., Gerke, T., Muller, J.G., Melcher, R., Schauber, J., Boxberge, F., Scheppach, W., and Menzel, T. (2002). Butyrate inhibits NF-kappaB activation in lamina propria macrophages of patients with ulcerative colitis. Scand J Gastroenterol *37, 458-466.* 10.1080/003655202317316105.

56. Facchin, S., Vitulo, N., Calgaro, M., Buda, A., Romualdi, C., Pohl, D., Perini, B., Lorenzon, G., Marinelli, C., D'Inca, R., et al. (2020). Microbiota changes induced by microencapsulated sodium butyrate in patients with inflammatory bowel disease. Neurogastroenterol Motil *32, e13914.* 10.1111/nmo.13914.

57. Hamer, H.M., Jonkers, D.M., Vanhoutvin, S.A., Troost, F.J., Rijkers, G., de Bruine, A., Bast, A., Venema, K., and Brummer, R.J. (2010). Effect of butyrate enemas on inflammation and antioxidant status in the colonic mucosa of patients with ulcerative colitis in remission. Clin Nutr *29, 738-744.* 10.1016/j.clnu.2010.04.002.

58. Peng, L., He, Z., Chen, W., Holzman, I.R., and Lin, J. (2007). Effects of butyrate on intestinal barrier function in a Caco-2 cell monolayer model of intestinal barrier. Pediatr Res *61, 37-41.* 10.1203/01.pdr.0000250014.92242.f3.

59. Boets, E., Gomand, S.V., Deroover, L., Preston, T., Vermeulen, K., De Preter, V., Hamer, H.M., Van den Mooter, G., De Vuyst, L., Courtin, C.M., et al. (2017). Systemic availability and metabolism of colonic-derived short-chain fatty acids in healthy subjects: a stable isotope study. J Physiol *595, 541-555.* 10.1113/JP272613.

60. Bosmans, J.W., Jongen, A.C., Boonen, B.T., van Rijn, S., Scognamiglio, F., Stucchi, L., Gijbels, M.J., Marsich, E., and Bouvy, N.D. (2017). Comparison of three different application routes of butyrate to improve colonic anastomotic strength in rats. Int J Colorectal Dis *32, 305-313.* 10.1007/s00384-016-2718-z.

61. Meyer, F., Seibert, F.S., Nienen, M., Welzel, M., Beisser, D., Bauer, F., Rohn, B., Westhoff, T.H., Stervbo, U., and Babel, N. (2020). Propionate supplementation promotes the expansion of peripheral regulatory T-Cells in patients with end-stage renal disease. J Nephrol *33, 817-827.* 10.1007/s40620-019-00694-z.

62. Marzocco, S., Fazeli, G., Di Micco, L., Autore, G., Adesso, S., Dal Piaz, F., Heidland, A., and Di Iorio, B. (2018). Supplementation of Short-Chain Fatty Acid, Sodium Propionate, in Patients on Maintenance Hemodialysis: Beneficial Effects on Inflammatory Parameters and Gut-Derived Uremic Toxins, A Pilot Study (PLAN Study). J Clin Med *7*. 10.3390/jcm7100315.

63. Peterson, L.W., and Artis, D. (2014). Intestinal epithelial cells: regulators of barrier function and immune homeostasis. Nat Rev Immunol *14, 141-153.* 10.1038/nri3608.

64. Li, X., Li, Q., Xiong, B., Chen, H., Wang, X., and Zhang, D. (2022). Discoidin domain receptor 1(DDR1) promote intestinal barrier disruption in Ulcerative Colitis through tight junction proteins degradation and epithelium apoptosis. Pharmacol Res *183, 106368.* 10.1016/j.phrs.2022.106368.

65. Nighot, M., Liao, P.L., Morris, N., McCarthy, D., Dharmaprakash, V., Ullah Khan, I., Dalessio, S., Saha, K., Ganapathy, A.S., Wang, A., et al. (2023). Long-Term Use of Proton Pump Inhibitors Disrupts Intestinal Tight Junction Barrier and Exaggerates Experimental Colitis. J Crohns Colitis *17, 565-579.* 10.1093/ecco-jcc/jjac168.

66. Zhao, Y., Chen, F., Wu, W., Sun, M., Bilotta, A.J., Yao, S., Xiao, Y., Huang, X., Eaves-Pyles, T.D., Golovko, G., et al. (2018). GPR43 mediates microbiota metabolite SCFA regulation of antimicrobial peptide expression in intestinal epithelial cells via activation of mTOR and STAT3. Mucosal Immunol *11, 752-762.* 10.1038/mi.2017.118.

67. Fay, N.C., Muthusamy, B.P., Nyugen, L.P., Desai, R.C., Taverner, A., MacKay, J., Seung, M., Hunter, T., Liu, K., Chandalia, A., et al. (2020). A Novel Fusion of IL-10 Engineered to Traffic across Intestinal Epithelium to Treat Colitis. J Immunol *205, 3191-3204.* 10.4049/jimmunol.2000848.

68. Lindemans, C.A., Calafiore, M., Mertelsmann, A.M., O'Connor, M.H., Dudakov, J.A., Jenq, R.R., Velardi, E., Young, L.F., Smith, O.M., Lawrence, G., et al. (2015). Interleukin-22 promotes intestinal-stem-cell-mediated epithelial regeneration. Nature *528, 560-564.* 10.1038/nature16460.

69. Wang, H., Shi, P., Zuo, L., Dong, J., Zhao, J., Liu, Q., and Zhu, W. (2016). Dietary Non-digestible Polysaccharides Ameliorate Intestinal Epithelial Barrier Dysfunction in IL-10 Knockout Mice. J Crohns Colitis *10, 1076-1086.* 10.1093/ecco-jcc/jjw065.

70. Park, J.H., Kotani, T., Konno, T., Setiawan, J., Kitamura, Y., Imada, S., Usui, Y., Hatano, N., Shinohara, M., Saito, Y., et al. (2016). Promotion of Intestinal Epithelial Cell Turnover by Commensal Bacteria: Role of Short-Chain Fatty Acids. PLoS One *11, e0156334.* 10.1371/journal.pone.0156334.

71. Wada, H., Miyoshi, J., Kuronuma, S., Nishinarita, Y., Oguri, N., Hibi, N., Takeuchi, O., Akimoto, Y., Lee, S.T.M., Matsuura, M., et al. (2023). 5-Aminosalicylic acid alters the gut microbiota and altered microbiota transmitted vertically to offspring have protective effects against colitis. Sci Rep *13, 12241.* 10.1038/s41598-023-39491-x.

72. Xu, J., Chen, N., Wu, Z., Song, Y., Zhang, Y., Wu, N., Zhang, F., Ren, X., and Liu, Y. (2018). 5-Aminosalicylic Acid Alters the Gut Bacterial Microbiota in Patients With Ulcerative Colitis. Front Microbiol *9, 1274.* 10.3389/fmicb.2018.01274.

73. Kowalska-Duplaga, K., Kapusta, P., Gosiewski, T., Sroka-Oleksiak, A., Ludwig-Slomczynska, A.H., Wolkow, P.P., and Fyderek, K. (2020). Changes in the Intestinal Microbiota Are Seen Following Treatment with Infliximab in Children with Crohn's Disease. J Clin Med *9.* 10.3390/jcm9030687.

74. Zhuang, X., Tian, Z., Feng, R., Li, M., Li, T., Zhou, G., Qiu, Y., Chen, B., He, Y., Chen, M., et al. (2020). Fecal Microbiota Alterations Associated With Clinical and Endoscopic Response to Infliximab Therapy in Crohn's Disease. Inflamm Bowel Dis *26, 1636-1647.* 10.1093/ibd/izaa253.

75. Wills, E.S., Jonkers, D.M., Savelkoul, P.H., Masclee, A.A., Pierik, M.J., and Penders, J. (2014). Fecal microbial composition of ulcerative colitis and Crohn's disease patients in remission and subsequent exacerbation. PLoS One *9, e90981.* 10.1371/journal.pone.0090981.

76. Liu, F., Ma, R., Riordan, S.M., Grimm, M.C., Liu, L., Wang, Y., and Zhang, L. (2017). Azathioprine, Mercaptopurine, and 5-Aminosalicylic Acid Affect the Growth of IBD-Associated Campylobacter Species and Other Enteric Microbes. Front Microbiol *8, 527.* 10.3389/fmicb.2017.00527.

4.6 Additional Information

4.6.1 Conflict of Interest

The authors declare that they have no conflict of interest associated with the experimental design, analysis and reporting of the current study.

4.6.2 Funding

This study was supported by National Health and Medical Research Council (NHMRC) Project Grant awarded to P.K.W. (Project No. APP1125392) and Crohn's and Colitis Foundation Litwin IBD Pioneers grant (827399) awarded to authors B.C, and P.K.W. This work was also supported by the University of Sydney, Commercial Development and Industry Partnerships (CDIP) program grant (CT31847) awarded to B.C, and P.K.W. First author K.X was supported financially by a University of Sydney Postgraduate Award.

4.6.3 Acknowledgment

The authors would like to acknowledge Blacktown/Mount Druitt Hospital and the Clinical Research Support Unit – Western Sydney Local Health District (WSLHD) for their invaluable assistance and support in facilitating this study. We express sincerest gratitude to Dr. Thomas O'Neil, Ms. Jordan Hunter and Ms. Taylor Davis for their assistance in handling and processing the stool and plasma samples and thank Dr. Kang-Yu Peng and Dr. Atul Bhatnagar from the Sydney Mass Spectrometry (SydneyMS) of the at The University of Sydney for the resources, scientific and technical expertise provided for the completion of current study.

4.6.4 CRediT Authorship Contribution Statement

Kangzhe Xie (K.X): Investigation, validation, formal analysis, data curation, visualisation and writing – original draft. Suehad Abou Duhun (S.A.D): Investigation, validation, formal analysis, data curation, visualisation and writing – original draft. Tamara Ortiz-Cerda (T.O.C): Investigation, validation, formal analysis, data curation, visualisation and writing – review & editing. Hannah Choi (H.C): Investigation, validation and formal analysis. Xiao Suo Wang (X.S.W): Investigation, methodology and software. John O'Sullivan (J.O.S): Conceptualisation and methodology. Ella Verley (E.V): Investigation, validation and data curation. Mark Ghali (M.G): Investigation, data curation and resources. Viraj Kariyawasam (V.K): Investigation, data curation and resources. Nikola Mitrev (N.M): Investigation, data curation and resources. Belal Chami (B.C): Conceptualisation, methodology, project administration, supervision and funding acquisition. Paul K. Witting (P.K.W): Conceptualisation, methodology, resources, project administration, supervision, funding acquisition, writing – review & editing.

Characterising short chain fatty acid profiles in stool specimens from patients diagnosed with inflammatory bowel disease

Kangzhe Xie[1*], Suehad Abou Duhun[1*], Tamara Ortiz-Cerda[1,2], Hannah Choi[1], Xiaosuo Wang[3], John O'Sullivan[3], Ella Verley[1,4], Mark Ghali[5], Viraj Kariyawasam[5,6], Nikola Mitrev[5,7], Belal Chami[4] & Paul K. Witting[1#]

1. Redox Biology Group, Charles Perkins Centre, School of Medical Sciences, Faculty of Medicine & Health, The University of Sydney, NSW 2006, Australia.
2. Departamento de Citología e Histología Normal y Patológica, Facultad de medicina, Universidad de Sevilla, Avda. Sánchez-Pizjuán s/n 41009, Seville, Spain.
3. Cardiometabolic Medicine Group, Charles Perkin Centre, School of Medical Sciences, Faculty of Medicine & Health, The University of Sydney, NSW 2006, Australia.
4. Redox Inflammation Group, Charles Perkins Centre, School of Medical Sciences, Faculty of Medicine & Health, The University of Sydney, NSW 2006, Australia.
5. Blacktown/Mt. Druitt Clinical School, University of Western Sydney, NSW 2148, Australia.
6. Department of Gastroenterology, Concord Repatriation General Hospital, Sydney, NSW 2139 Australia.
7. Department of Gastroenterology, The Sutherland Hospital, NSW 2229, Australia

* Authors K.X and S.A.D contributed equally and share joint first-authorship of the study.

Correspondence address to Professor Paul K. Witting (paul.witting@sydney.edu.au), Level 4 West Room 4212, Charles Perkins Centre, The University of Sydney, NSW 2006, Australia.

Supplementary Material

Supplementary Figures

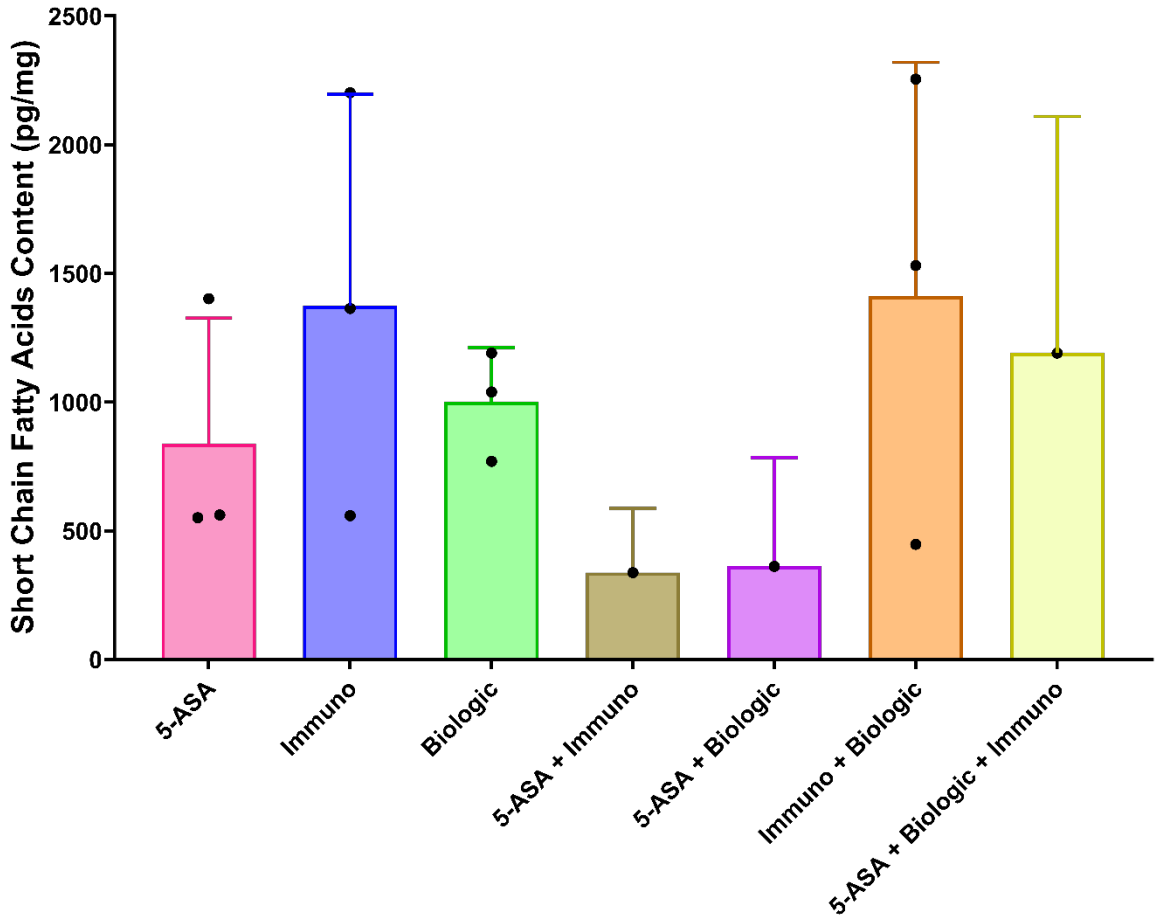

Supplementary Figure 4.1. The level of short chain fatty acids in IBD patients that received different drug treatments. Two-way ANOVA showed no statistical significance on the effect of colonoscopy score and drug use on total short chain fatty acid levels in the stool ($p > 0.05$). However, there was a weak influence of 5-ASA use on short chain fatty acid level ($p = 0.06$) that may become significant for larger sample size. Patient distribution followed n = 7 subjects who received 5-ASA treatment alone (5-ASA), n = 5 others received immunomodulator treatment alone (Immuno), while n = 9 patients received biologic agents treatment alone (Biologic), a further n = 5 patients received 5-ASA and immunomodulator treatments (5-ASA + Immuno), n = 1 subject was treated with 5-ASA and biologic agents (5-ASA + Biologic), n = 9 patients received immunomodulator and biologic agents (Immuno + Biologic), and finally n = 1 patient received a combination of 5-ASA, immunomodulators and biologic agents treatments (5-ASA + Biologic + Immuno). Samples below the detection limit and/or did not report any IBD-related treatments were not included in the analysis. Graphical values represent mean value of SCFA concentration at different IBD severities + SD for each cohort subgroup. Author contributions: K.X – Investigation, validation, formal analysis, data curation and visualisation, S.A.D – Investigation, validation, formal analysis, data curation, T.O.C – Investigation, data curation and validation, X.S.W – Investigation, methodology and software, E.V – Investigation, M.G, V.K & N.M – Investigation and data curation.

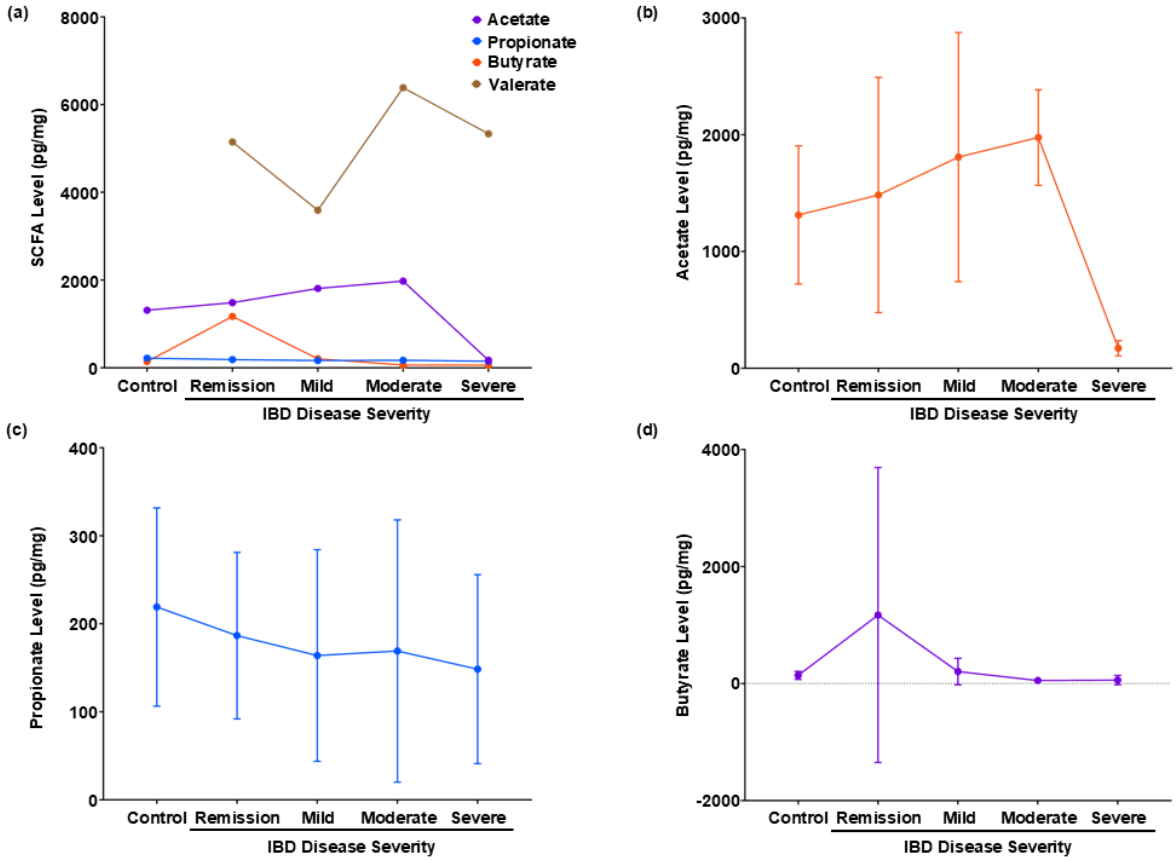

Supplementary Figure 4.2. The level of short chain fatty acids in non-IBD individuals and IBD patients at different disease severities. Panel (a) shows all short chain fatty acids examined in the study. Graphical values represent mean with error bars that were omitted in the accompanying paper to aid visualisation. Valerate was excluded from further analysis due to inconsistent detection of this short chain fatty acids LC/MS-MS from the stool samples. The disease stage-dependent change of Panel (b) acetate (n= 31 patient samples), Panel (c) propionate (n= 43 samples), and Panel (d) butyrate (n= 42 samples), levels in the stool of IBD patients assigned to the various disease severity groups. Samples below the detection limit were not included in the analysis. Graphical values represent mean ± SD. Author contributions: K.X – Investigation, validation, formal analysis, data curation and visualisation, S.A.D – Investigation, validation, formal analysis, data curation, T.O.C – Investigation, data curation and validation, X.S.W – Investigation, methodology and software, E.V – Investigation, M.G, V.K & N.M – Investigation and data curation.

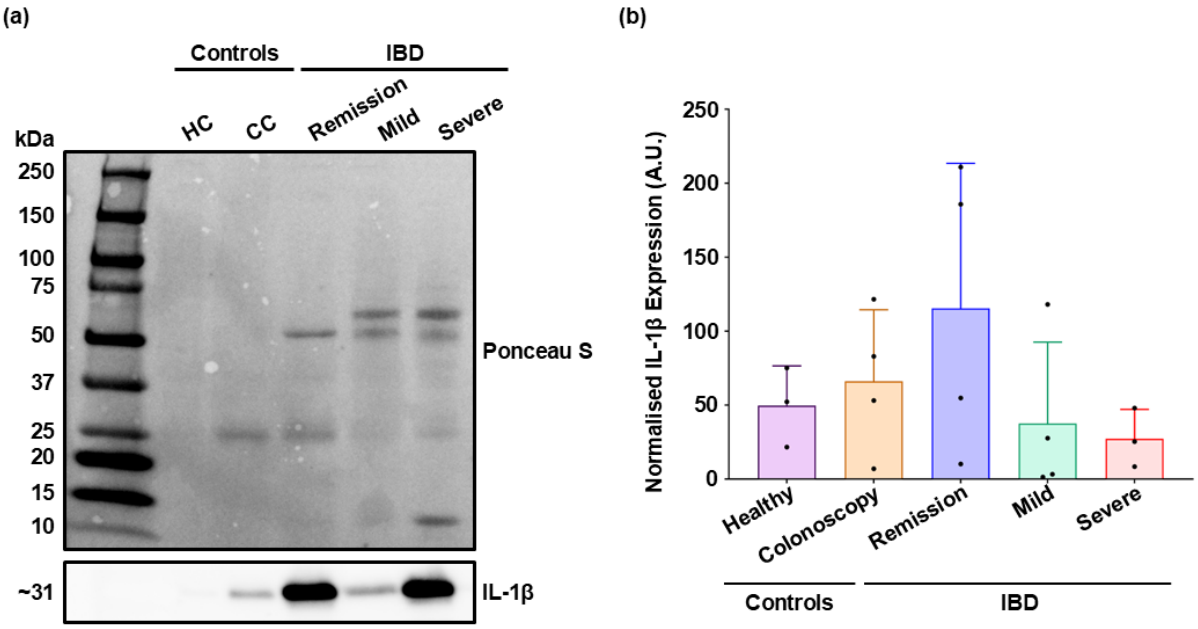

Supplementary Figure 4.3. The presence of pro-inflammatory cytokine IL-1β in stool samples obtained from healthy and IBD patients of different disease severities. Panel (a) Representative images of Ponceau S staining of total proteins loaded and corresponding Western blot image of IL-1β in stool from randomly selected patients. Panel (b) Densiometric analysis of IL-1β levels detected from Western blotting. n = 4 samples per group in Colonoscopy Control, Remission and Mild IBD and n=3 samples per group in Healthy Control and Severe IBD. Author contributions: K.X – Investigation, validation, formal analysis, data curation and visualisation, S.A.D – Investigation, validation, formal analysis, data curation, T.O.C – Investigation, data curation and validation, X.S.W – Investigation, methodology and software, E.V – Investigation, M.G, V.K & N.M – Investigation and data curation.

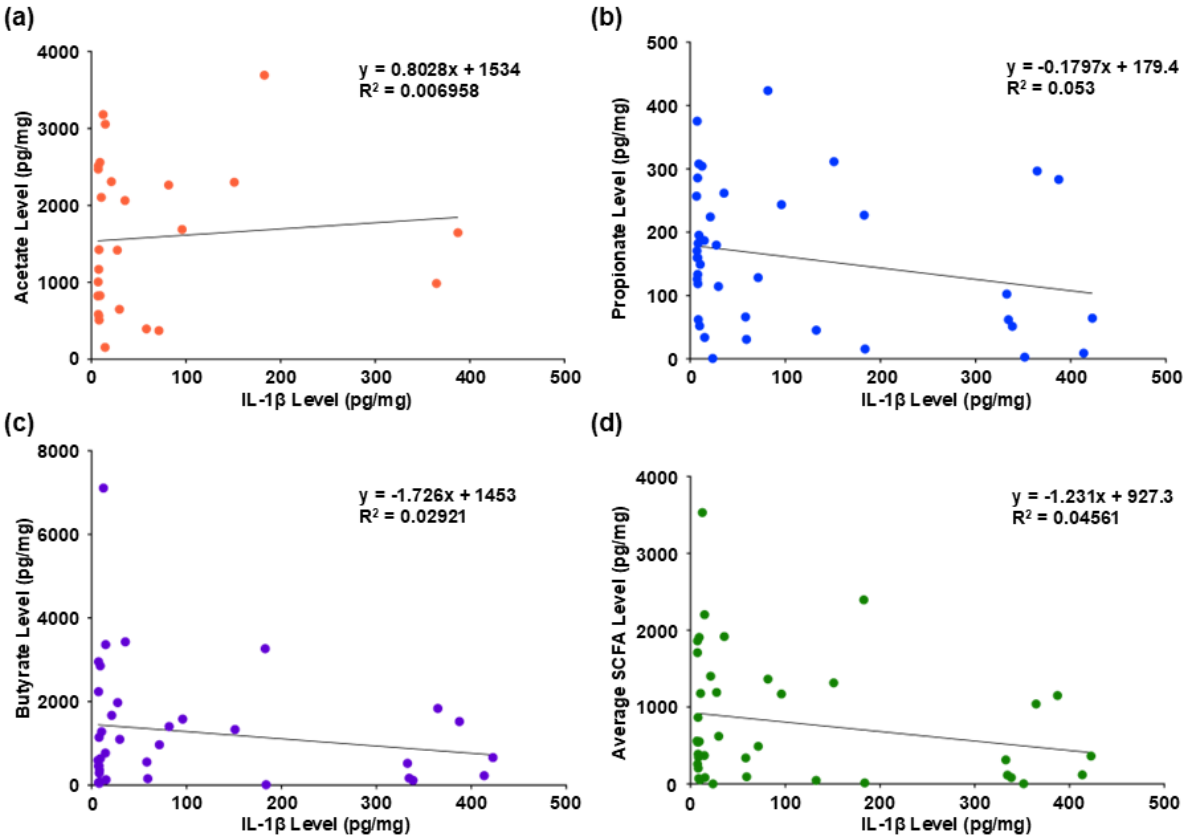

Supplementary Figure 4.4. The Correlation between faecal pro-inflammatory cytokine IL-1β and short chain fatty acid. Panel (a) acetate, panel (b) propionate, panel (c) butyrate and panel (d) average acetate + propionate + butyrate levels in the stool from IBD patients. Graphical values represent the mean faecal IL-1β and short chain fatty acid levels at different IBD disease severity. n = 16 IBD patients in remission, n = 3 in mild, n = 8 in moderate and n = 6 in severe. Simple linear regression with 95% confidence was used to evaluate potential correlative relationships. Author contributions: K.X – Investigation, validation, formal analysis, data curation and visualisation, S.A.D – Investigation, formal analysis, data curation, T.O.C – Data curation and validation, H.C, M.G, V.K & N.M – Investigation and data curation.

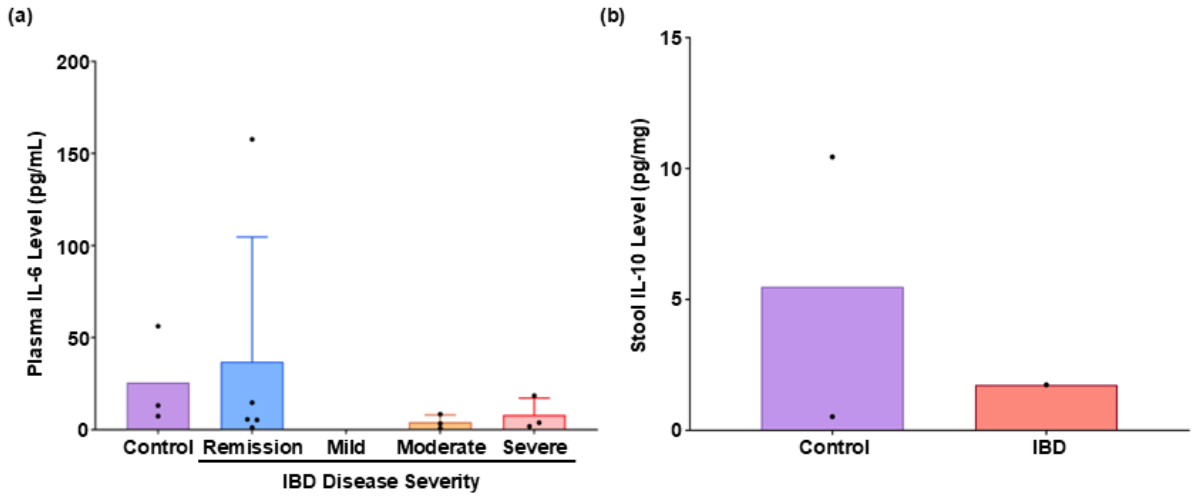

Supplementary Figure 4.5. The level of IL-6 & IL-10 inflammatory cytokines in patients. Panel (a) IL-6 in plasma samples of healthy individuals and IBD patients of different disease severities. Panel (b) IL-10 in stool samples of both healthy and IBD patients. Samples below the detection limit were not included in the analysis. Graphical values represent mean + SD. Statistical analysis was not performed due to the limited number of samples detected by ELISA. Author contributions: K.X – Investigation, validation, formal analysis, data curation and visualisation, S.A.D – Investigation, validation, formal analysis, data curation, T.O.C – Investigation, data curation and validation, X.S.W – Investigation, methodology and software, E.V – Investigation, M.G, V.K & N.M – Investigation and data curation.

Supplementary Table

Supplementary Table 4.1. Table of chemicals and reagents used in the current study (in alphabetical order).

Chemical/Reagent	Manufacture	Catalogue Number
Acetic acid	Sigma Aldrich	695092
Acetic acid-d_4	Sigma Aldrich	151785
Butyric acid-1,2-$^{13}C_2$	Sigma Aldrich	491993
DNase	Sigma Aldrich	DN25
Formic acid	Supelco	5.33002
Hexanoic acid	Sigma Aldrich	153745
Hexanoic acid-6,6,6-d_3	Sigma Aldrich	489727
Human IL-10 ELISA kit	Invitrogen	BMS215-2
Human IL-1β ELISA kit	Invitrogen	BMS224-2
Human IL-6 ELISA kit	Invitrogen	EH2IL6
Methanol	Supelco	1.06035
Orthophosphoric acid	Supelco	5.43828
Propionic acid-1-^{13}C	Sigma Aldrich	282448
Sodium butyrate	Sigma Aldrich	B5887
Sodium propionate	Sigma Aldrich	P1880
Valeric acid	Sigma Aldrich	240376
Water (LC-MS Grade)	Supelco	1.15333

Supplementary Methods

Method for IL-1β Western Blot Analysis

A Bicinchoninic Acid assay was conducted on two sets of faecal samples, each comprising one healthy control, one colonoscopy control, and one sample with a colonoscopy score representing remission, mild, and severe IBD. 20 µg of each sample was mixed with sodium dodecyl sulfate (SDS) loading buffer (50 mM Tris-HCl (pH 6.8), 2% w/v SDS, 6% v/v glycerol, and 0.004% w/v bromophenol blue). Samples were heated (95°C, 5 min), followed by brief vortex and centrifugation. Samples were then loaded onto a Mini-PROTEAN electrophoresis

system (BioRad) and separated in SDS-Tris-Glycine buffer (25 mM Tris, pH 8.3, 192 mM glycine, and 0.1% w/v SDS) at 35 mA per gel for ~40 min. Precision Plus Protein Kaleidoscope ladder (Cat. #1610375, BioRad) was loaded as a molecular weight marker. Upon completion of electrophoresis, separated proteins were transferred onto a 0.2 μm polyvinylidene fluoride or polyvinylidene difluoride membrane using the Trans-Blot Turbo Transfer System (BioRad). Next, the membrane was washed with 1x Tris-Buffered Saline (TBS) followed by 1x TBS containing Tween 20 (TBST; 5 min). The PVDF membrane was then incubated in blocking buffer (5% (w/v) skim milk/TBST; 22 °C, 1 h).

After blocking, the membrane was incubated overnight with primary anti-IL-1β antibody (Cell Signaling, cat. # 12307T, diluted 1:2000 v/v in 5% w/v BSA and 0.05% w/v sodium azide mixed in TBS) at 4°C on a roller. After ~12 h, the membrane was washed again then stained with Ponceau S solution (5 min, 22 °C) with gentle agitation to visualise total protein loaded in each well. The stained membrane was imaged using the ChemiDoc™ Touch Gel/Membrane Imaging System (BioRad) to assist in normalising target protein signals in subsequent analyses. Next, the membrane was washed thoroughly to remove traces of Ponceau S solution. The cleared PVDF membranes were then incubated with HRP-conjugated secondary antibody (Sigma Aldrich, Cat. #A6154, anti-mouse HRP/5% w/v skim milk/TBST) for 2 h in a cold room. Next, the membrane was washed with TBST then PBS and subsequently treated with Clarity™ Western ECL Substrate (Cat. #1705060, BioRad; 5 min in the dark with gentle agitation) prior to imaging using Image Lab software (v6.1, BioRad). Finally, densiometric intensity of the separated protein bands were analysed and normalised for between group comparisons.

Chapter 5: Herbal remedies as potential IBD treatments

Below find the validation of submitted work indicating the contribution from the higher degree candidate as verified by the senior author for this manuscript. **The manuscript has been modified to accommodate the format of the current thesis.*

Authorship contribution statement:
Kangzhe Xie (K.X); Investigation (IHC, Western blot, LC-MS/MS), validation, methodology, formal analysis, data curation, and writing – original draft. **Tamara Ortiz-Cerda (T.O.C.);** Investigation (IHC, LC-MS/MS), validation, formal analysis, data curation, supervision, and writing – original draft. **Nicolette Shiung (N.S);** Investigation (lipolysis assay), validation, methodology and formal analysis. **Siqi Chen (S.C);** Investigation (animal works, colon histoarchitecture, IF, ELISA), validation and formal analysis. **Laylaa Hoosen (L.H);** Investigation (LC-MS/MS), validation and formal analysis. **Gulfam Ahmad (G.A);** Conceptualization, methodology and formal analysis. **Bruno Lemos Wimmer (B.L.W);** Investigation (IHC, Western blot) and formal analysis. **Ash David (A.D);** Investigation (colon histoarchitecture), validation and formal analysis. **Belal Chami (B.C);** Conceptualization, methodology and resources. **Xiaosuo Wang (X.W);** Methodology, validation and software. **Collin Tran (C.T);** Methodology, validation and software. **John O'Sullivan (J.O.S);** Resources. **Anthony S. Don (A.S.D);** Resources**.** and **Paul K. Witting (P.K.W.):** Conceptualization, methodology, project administration, supervision and review & editing of the manuscript.

Confirmation from the senior author:
I confirm that Mr Kangzhe (Steven) Xie was an active contributor and collaborator for this study. The authorship statement above accurately describes Steven's contribution and justifies his position as first author for this manuscript submission.

Signed Dated: 28/02/2025

Paul Witting (PhD)
Professor, Redox Biology
School of Medical Sciences
Faculty of Medicine and Health
Charles Perkins Centre
Editor Redox Report

Rm 4212, D17 | The University of Sydney | NSW | 2006
+61 2 91140524
paul.witting@sydney.edu.au

Herbal remedies curcumin, *Hedyotis Diffusa* and *Amomum Villosum* reduced colon inflammation by altering colon lipidome and restoring dysregulated redox balance in an animal model of ulcerative colitis

Kangzhe Xie[1*], Tamara Ortiz-Cerda[1,2*], Nicolette Shiung[1], Siqi Chen[1], Laylaa Hoosen[1], Gulfam Ahmad[3], Bruno Lemos Wimmer[1,4], Ash David[1], Belal Chami[5], Xiaosuo Wang[6], Collin Tran[7], John O'Sullivan[6], Anthony S. Don[7] & Paul K. Witting[1#].

1. Redox Biology Group, Charles Perkins Centre, School of Medical Sciences, Faculty of Medicine & Health, The University of Sydney, NSW 2006, Australia.

2. Departmento de Citología e Histología Normal y Patológica, Facultad de Medicina, Universidad de Sevilla, Avda. Sanchez-Pizjuan s/n 41009, Seville, Spain.

3. Andrology Department, Royal Women's and Children's Pathology, Carlton, VIC 3053, Australia.

4. Department of Life Sciences, Faculty of Chemistry, The University of Konstanz, BW, 78464 Konstanz, Germany.

5. Redox Inflammation Group, Charles Perkins Centre, School of Medical Sciences, Faculty of Medicine & Health, The University of Sydney, NSW 2006, Australia.

6. Cardiometabolic Medicine Group, Charles Perkins Centre, School of Medical Sciences, Faculty of Medicine & Health, The University of Sydney, NSW 2006, Australia.

7. Brain Lipidomic and Metabolism Group, Charles Perkins Centre, School of Medical Sciences, Faculty of Medicine & Health, The University of Sydney, NSW 2006, Australia.

* Kangzhe Xie and Tamara Ortiz-Cerda contributed equally to all aspects of the study and shares joint first-authorship of this manuscript.

Address correspondence to: Professor Paul K. Witting (paul.witting@sydney.edu.au), Level 4 West Room 4212, Charles Perkins Centre, The University of Sydney, NSW 2006, Australia.

Abstract

Ulcerative colitis (UC) is a clinical subtype of inflammatory bowel disease (IBD) that is characterized by relapsing and remitting abdominal pain and diarrhea. There is no definitive cure for IBD, and most available therapies have poor response rate and variable tolerance due to adverse side effects. As a result, herbal medicine has emerged as a promising complementary and alternative treatment option for IBD patients due to their well-established anti-inflammatory and antioxidant properties and relatively safe pharmacological profiles. Damage to the colon mucosa during the pathogenesis of IBD is accompanied by dysregulation of redox signaling molecule expressions and inflammatory protein activities and alterations to lipid distribution.

Aim: The goal for this study is to investigate the therapeutic effect of curcumin, *Hedyotis Diffusa* and *Amomum Villosum* in an experimental animal model of colitis and to evaluate their influence on colon damage, redox biomarker expression and the lipidome.

Methods and Results: Experimental colitis was induced in C57BL/6 mice with 2% w/v dextran sodium sulfate (DSS) in drinking water ± herbal medicines *ad libitum*. All three herbal remedies improved clinical score, DSS-induced colon histoarchitectural damage, mucin production and decreased colon IFN-γ levels, while antioxidant protein HO-1 expression increased. The colonic lipid composition was examined using untargeted liquid chromatography tandem mass spectrometry and significant changes in lipid species were analyzed using MetaboAnalyst software. DSS stimulation significantly reduced diacylglycerol abundances and increased triacylglycerol species in the colon, whilst herbal treatments ameliorated these changes in glycerolipid composition. Metabolic pathway analysis using the same software discovered that glycerophospholipid metabolism, glycophosphatidylinositol anchor biosynthesis and α-linolenic acid metabolism were significantly impacted in the DSS insulted colons. Validation of altered glycerolipid composition was obtained by monitoring DG and TG levels in the same colon tissues.

Conclusion: Overall, this study highlighted the potential therapeutic effects of the natural products in order *Amomum Villosum* > *Hedyotis Diffusa* ≈ curcumin in ameliorating UC-like experimental colitis and modulating colonic lipid compositions, which may reinforce their use as complementary and alternative treatment options for IBD patients.

Glossary

UC	Ulcerative colitis
IBD	Inflammatory bowel disease
ROS	Reactive oxygen species
$O_2 \cdot^-$	Superoxide anion radical
H_2O_2	Hydrogen peroxide
DNA	Deoxyribonucleic acid
8-OHdG	8-hydroxyguanosine
MDA	Malondialdehyde
4-HNE	4-hydroxynoneal
Nrf2	Nuclear factor erythroid 2-related factor 2
SOD	Superoxide dismutase
GPx	Glutathione peroxidase
HO-1	Heme oxygenase-1
PC	Phosphatidylcholine
PE	Phosphatidylethanolamine
TG	Triacylglycerol
NF-κB	Nuclear factor kappa B
TNF-α	Tumor necrosis factor alpha
IL	Interleukin
DSS	Dextran sodium sulfate
PB	Peanut butter
$ONOO^-$	Peroxynitrite
PBS	Phosphate buffered saline
IF	Immunofluorescence
IHC	Immunohistochemical
DPX	Dibutyl phthalate plasticizer xylene
HPLC	High performance liquid chromatography
MeOH	Methanol
LC-MS/MS	Liquid chromatography tandem mass spectrometry
FA	Formic acid
AUC	Area-under-the-curve
DG	Diacylglycerol
HIAR	Heat-induced antigen retrieval
TBS	Tris-buffered saline
TBST	TBS with Tween® 20
DAB	3,3'-daminobenzidine
ELSIA	Enzyme-linked immunosorbent assay
PVDF	Polyvinylidene fluoride
ANOVA	Analysis of variance
SD	Standard deviation

PCA	Principal component analysis
FDR	False discovery rate
OPLS-DA	Orthogonal partial least square discriminant analysis
VIP	Variable importance point
SEC-MALS	Size exclusion chromatography with multi-angle light scattering analysis
H&E	Hematoxylin and eosin
PS	Phosphatidylserine
LPC	Lysophosphatidylcholine
LPE	Lysophosphatidylethanolamine
HSL	Hormone-sensitive lipase
MPO	Myeloperoxidase
HOCl	Hypochlorous acid
COX	Cyclooxygenase
iNOS	Inducible nitric oxide synthase
TNBS	Trinitrobenzene sulfonic acid
NLRP3	NOD-like receptor protein 3
STAT6	Signal transducer and activation of transcription 6
SCFA	Short chain fatty acid

5.1 Introduction

Ulcerative colitis (UC) is a clinical subtype of inflammatory bowel disease (IBD) characterized by chronic inflammation of the large intestine[1]. Symptoms of UC are largely shared with other IBD subtypes, which includes abdominal pain, weight loss, fatigue, chronic diarrhea, rectal bleeding and bloody stool[2], leading to the manifestation of hallmark histological features such as extensive loss of intestinal crypts, severe mucosal ulceration and prominent immune infiltration[3]. These symptoms compromise national productivity, introducing health care and economic burden to the society and substantially impair patients' quality of life[4,5]. According to the latest statistics, UC affects approximately 5 million people worldwide[6], with its incidence rate rapidly increasing, particularly in the developing nations[7], owing to the introduction and adaptation to Western diets and lifestyles. Chronically unregulated UC is associated with the severe complications such as toxic megacolon and colorectal cancer[8,9]. It has been shown that UC is the third highest risk factor for colorectal cancer development and accounting for ~15% of deaths in UC patients[10,11].

Despite extensive research, the etiology of UC is currently unknown. However, it is increasingly appreciated that the pathogenesis of UC is a product of complex interactions between factors of genetic predisposition (such as familial history and risk gene loci) and environmental stimulus (such as smoking, antibiotics and diets)[12]. Collectively, these complex interactions promote immune dysregulation, which leads to increased production of reactive oxygen species (ROS) such as hydrogen peroxide (H_2O_2) and superoxide anion radical ($O_2\cdot^-$)[13]. Whilst physiological ROS production in the gut facilitates pathogen clearance and maintains intestinal homeostatic balance, excessive ROS levels can cause non-specific tissue damage and perpetuate inflammation[14]. Accordingly, elevated number of ROS-producing cells have been reported in the inflamed mucosa of UC patients[15]. This is associated with increased oxidative damage evident in significantly higher deoxyribonucleic acid (DNA) damage marker 8-hydroxyguanosine (8-OHdG) and lipid peroxidation marker malondialdehyde (MDA) and 4-hydroxynoneal (4HNE) in both colon tissue and serum samples of patients with UC[16-19], highlighting the altered oxidation-reduction (redox) state in the gut.

In mammalian cells, the level of ROS is intricately regulated by the master antioxidant response transcription factor nuclear factor erythroid 2-related factor 2 (Nrf2)[20]. For example, cellular $O_2\cdot^-$ are converted to H_2O_2 by the antioxidant response element superoxide dismutase (SOD)[21], whilst catalase and glutathione peroxidases (GPx1-4) convert the reactive peroxide to water[22]. Concurrently, heme oxygenase-1 (HO-1) expression regulated by Nrf2 signaling, degrades free heme to form anti-inflammatory carbon monoxide, bilirubin and iron[23]. However, in addition to elevated oxidative stress, diminished antioxidant capacity and antioxidant enzyme expression have also been documented in patients with UC. For example, the study by Rana et al. reported significantly lower level of glutathione and decreased SOD expression in the blood of UC patients[24], whilst reduced serum expression of total GPx was observed by Akman et al.[25]. Collectively, the imbalance of ROS production and antioxidant capacity serve as constant stimulus to trigger immune response in the gut, which leads to perpetuation of inflammation and exacerbation of tissue damage in the UC gut.

Lipids are fatty compounds that serve various functions in the body, including energy storage, cell signaling, transduction regulation and formation of cellular membranes[26]. The primary lipid families present in the colon consist of short chain fatty acids, glycerolipids, glycerophospholipids and sphingolipids[27]. Glycerophospholipids phosphatidylcholine (PC)

and phosphatidylethanolamine (PE) are the two most abundant lipid classes in the intestinal epithelium, each contributing to cell membrane structural integrity[28]. These lipids form membrane bilayers that act as a barrier, preventing the passage of harmful substances from entering the colonic mucosa[29,30]. On the other hand, sphingolipids have been found to maintain gastrointestinal immune balance by mediating crosstalk between the gut microbiota and intestinal immune cells[31]. Given their role in maintaining gut homeostasis and barrier function, changes in colonic lipid composition have been emerging as an integral component during IBD pathogenesis. Accordingly, significant variations in PC, ceramide and sphingomyelin compositions have been detected in treatment-naïve UC and UC patients in deep remission[32], whilst lowered total cholesterol and elevated triglyceride (TG) levels were also reported in IBD patients when compared to healthy controls[33]. Additionally, perturbed glycerophospholipid metabolism has been shown to associate with elevated oxidative stress and redox imbalance in various inflammatory conditions in the brain[34,35], which suggests that similar mechanism of redox imbalance induction may be implicated in other pathologies such as IBD. However, the links between redox imbalance and changes in colonic lipid profiles during IBD pathogenesis are yet to be fully established.

Presently, there is no available cure for IBD. Available treatment options dampen the extent of inflammation in the gut and are often associated with adverse side-effects such as nephrotoxicity and neutropenia[36,37]. Therefore, the use of natural products and nutraceuticals offer promising alternative or adjunct treatment options for IBD patients owing to their robust anti-inflammatory and antioxidant properties. Curcumin, the active ingredient in turmeric, has been shown to inhibit nuclear factor kappa B (NF-κB) and suppress the production of proinflammatory cytokines tumor necrosis factor alpha (TNF-α) and interleukin (IL)-1β[38], highlighting the anti-inflammatory property of this herbal product. Clinical studies have demonstrated its efficacy in inducing and maintaining remission in patients with UC[39-41], whilst *Hedyotis Diffusa*, a traditional Chinese herbal medicine with anti-inflammatory and antioxidant actions have shown to improve clinical outcomes and reduce IL-1β and IL-6 release in animal model of experimental colitis[42]. Furthermore, *Amomum Villosum*, another Chinese herb that originates from the ginger family has been found to enhance the intestinal mucosal barrier and alleviate colon inflammation by activating the Nrf2 signaling pathway[43]. In the current study, the therapeutic potential of three herbal remedies: curcumin, *Hedyotis Diffusa* and *Amomum Villosum* in restoring altered redox balance and tissue homeostasis and their impact on the colon lipidome have been examined in a murine model of dextran sodium sulfate (DSS)-induced experimental colitis.

5.2 Materials and Methods

5.2.1 Chemicals & Reagents

All chemicals and reagents used in the current study were sourced with the highest quality possible, see Supplementary Table 1 for full list of chemicals and reagents.

5.2.2 Animals

Six-week-old male C57BL/6 mice were purchased from Animal Resources Centre (Perth, Australia) and acclimated for 7 days in The University of Sydney Laboratory Animal Service facility at the Charles Perkins Centre before the start of experimentation. The mice were housed in environmentally enriched husbandry cages and fed on standard chow diet with heat-sterilized tap water available *ad libitum* under 12:12 h light-dark cycle at 22°C. Each mouse was individually identified by tail marking with permanent markers. All animal experiments and associated analyses were conducted using an approved protocol obtained from The University of Sydney Animal Ethics Committee (Approval #1496/2019).

5.2.3 Induction of experimental colitis & Treatment administration

Acute experimental colitis was induced by the administration of DSS (CAS# 9011-18-1; molecular range: 36-50 kDa) in accordance with previous studies from our group[44]. Briefly, DSS was purchased from MP Biomedicals (cat no. 160110) and administered at 2% w/v in drinking water to mimic the acute phase of human ulcerative colitis-like disease in mice by inducing epithelial toxicity, which compromises gut barrier integrity and causes subsequent infection by commensal microbiota[45]. Water consumption was monitored daily and fresh mixture of DSS was replenished every 3 days.

Powdered-curcumin was acquired from Beijing Tongrentang (Sydney, Australia), whilst raw *Hedyotis Diffusa* and *Amomum Villosum* were also purchased from the same supplier. The dosage and administration methods for the herbs were selected based on published literatures[46-48]. During the acclimation phase, mice were trained to accept 100 mg of peanut butter (PB) via oral intake to avoid an invasive oral gavage pathway for curcumin. Thus, curcumin was administered to mice by dispersing into PB at 200 mg/kg of body weight daily.

Different to curcumin treatment, *Diffusa* and *Villosum* were administered in the form of herbal tonics ad libitum, mimicking the consumption of herbal tea in humans. Briefly, raw *Diffusa* and *Villosum* (10 g) were crushed and blended using a pestle and mortar before soaking in 100 mL Milli-Q® water at 22 °C for 10 min and boiling vigorously in a clay-pot for 5 min. After boiling, concentrated tonics were cooled on ice to avoid evaporation of volatile plant oils. Next, the tonics were filtered to remove any solid particles and additional Milli-Q® water was added to top the volume up to 100 mL to achieve a final dosage of 100 mg raw material/mL. The tonic teas were prepared daily and administered to the mice concomitantly with 2% w/v DSS immediately after preparation. The physical properties of DSS dispersed in the herbal tonic preparations were examined to ensure minimal interference to experimental colitis induction (refer to the results section and Appendix 1 for details).

5.2.4 Experimental design

After the period of acclimation, each individually tail-marked mouse was randomly divided into 5 treatment groups (n = 6 mice per group) summarized in Figure 5.1a and described as below:

I. Control Group: Mice received standard chow diet and drinking water *ad libitum* and 100 mg PB administered daily (as a diet control in the absence of both the natural product and DSS insult).
II. DSS Group: Mice received standard chow diet and 2% w/v DSS in drinking water *ad libitum* and 100 mg PB with no added drug administered daily.
III. Curcumin Group: Mice received standard chow diet and 2% w/v DSS in drinking water *ad libitum* and 100 mg PB with curcumin at 200 mg/kg of body weight administered daily.
IV. *Villosum* Group: Mice received standard chow diet and 2% w/v DSS dispersed in *Villosum* tonic *ad libitum* and 100 mg PB administered daily.
V. *Diffusa* Group: Mice received standard chow diet and 2% w/v DSS dispersed in *Diffusa* tonic *ad libitum* and 100 mg PB administered daily.

In accordance with the local animal ethics protocol approval, the study was terminated after mice were determined to have lost 15% of their original body weight or after 9 days of DSS administration in drinking water.

5.2.5 Clinical markers & colon macroscopic evaluation

Disease progression and severity were monitored and assessed daily following the initiation of DSS induction using previously established criteria[49,50]. The monitoring process involved assessing four gross observational parameters including body weight change, stool consistency, presence of rectal prolapse and grooming (See Supplementary Table 2 for detailed parameter scoring criteria). This observational data was then combined to generate a corresponding clinical score value used for between group comparisons. Body weight loss was recorded daily and compared to the original body weight of each respective mice from the beginning of the experiment. Additionally, colon lengths of all mice were recorded on the day of sacrifice to account for macroscopic changes to the gut.

5.2.6 *In vivo* monitoring of intestinal inflammation

Prior to sacrifice mice were anesthetized under 2% v/v isoflurane and the extents of colon inflammation were examined in unconscious mice by *in vivo* imaging using in situ oxidation of 5-amino-2,3-dihydro-1,4-phthalazine-dione (luminol) as a biomarker. Systemically administrated, redox-sensitive luminol can be oxidized by peroxidase activity or ROS such as H_2O_2, $O_2^{\cdot -}$ and peroxynitrite ($ONOO^-$) to yield a chemiluminescent signal with emission at λ_{max} = 425 nm[51]. Briefly, mice were administered freshly prepared luminol [100µL of 475 nM of luminol in sterile phosphate buffered saline (PBS), pH 7.4] via subcutaneous injection. Next, in situ oxidation of luminol was imaged using an IVIS® Spectrum CT *In Vivo* Imaging System Chamber (PerkinElmer) and in vivo bioluminescence signal was quantified using Living Image® (PerkinElmer) standard analysis software. Oxidized luminol was detected in the abdomen of mice using a 3 min exposure time and 2D planar bioluminescence images were presented as total radiance expressed in units of photon/sec/cm^2/sr. Mice were euthanized after imaging and colon and fecal tissues were harvested and snap frozen in liquid nitrogen and stored in cryotubes at -80℃ until required.

5.2.7 Tissue fixation & Slide preparation

Isolated colon tissues were fixed in 10% v/v neutral buffered formalin overnight followed by embedding with paraffin wax. Next, embedded colon tissues were section at 5 µm thickness

using a rotary microtome (SHANDON FINESSE 325, Thermo) and sections were collected onto Superfrost™ Plus Microscope Slides (Thermo Scientific). Mounted slides were initially air-dried then dried at a 37°C oven overnight. Where required, slides were blinded with randomly generated codes and subsequently dewaxed then rehydrated before tissues were sectioned (@ 10 µm) for histopathological, immunofluorescence (IF) and immunohistochemical (IHC) staining analyses.

5.2.8 Histopathological analyses

5.2.8.1 Hematoxylin and eosin (H&E) staining

Dewaxed and rehydrated colon sections were stained with filtered Harris Hematoxylin for 2 min prior to rinsing thoroughly in tap water. This was followed by immersion in Scott's blue solution for 30 s, then differentiation in acidified alcohol for 10 s. Next, slides were stained with eosin (1 min), prior to dehydration in 95% v/v ethanol (10 s) followed by 100% ethanol (2x 1 min). Subsequently, the stained slides were cleared in histolene and mounted with dibutyl phthalate plasticizer xylene (DPX) medium. Stained colon sections were imaged under light microscopy using an Axio Lab.A1 light microscope (ZEISS) equipped with an Axiocam 105 Color Camera (ZEISS). Five imaging fields per slide were captured at 20x magnification with Zen Blue Software (v.3.8, ZEISS).

5.2.8.2 Histoarchitectural and dysplasia analysis

Histopathological assessment was scored by three independent researchers (S.C., A.D. & G.A.) in accordance with the pathological criteria adapted from our published study[44] (See Supplementary Table 3 for detailed scoring summary). The pathological criteria accounted for the loss of crypts, loss of surface epithelium and the extent of cellular (neutrophils) infiltration, with each parameter scored from 0 (no damage) to 4 (severe damage). A summation of scores from each parameter yielded the total histological score (out of 12) for each mouse/group.

The current study also investigated the effect of DSS ± intervention on colon dysplasia, an early marker of ulcerative colitis progression to colorectal cancer. Histological criteria used in this study was adapted from previously published literature[3], as summarized in Supplementary Table 4. The histoarchitecture of the mucosa and crypts, hyperchromaticity and stratification of the nucleus, dystrophicity of goblet cells and presence of immune infiltration were evaluated to get the final dysplasia score of 0 = no dysplasia; 1 = indefinite but probably negative; 2 = indefinite but probably positive and 3 = positive dysplasia (Refer to Supplementary Table 5 for detailed evaluation criteria). The extent of dysplasia was scored by two independent researchers (N.S. & T.O.C) and presented as a mean score.

5.2.8.3 Alcian blue staining & Mucin production analysis

Where required, dewaxed and rehydrated colon sections were stained with Alcian Blue Staining Solution (containing: 0.1% w/v Alcian blue in 3% v/v acetic acid, pH 2.5) for 30 min at 22°C prior to a thorough rinse with distilled water (5 min). Next, the slides were counterstained in acetic Safranin-O solution (0.1% w/v, 10 min). Following this process, the slides were washed again in distilled water, dehydrated through graded ethanol before being cleared in xylene and finally cover-slipped with DPX.

Cover-slipped slides were imaged under light microscopy at 20x objective over 5 fields of view per sample using the same imaging system described above. Positive mucin staining was quantified with ImageJ software (v.1.54d, National Institute of Health, USA).

5.2.9 Tissue Homogenization

Isolated colon and faecal tissues were homogenized prior to lipidomic, molecular or biochemical analyses. Briefly, snap frozen colon or fecal samples were grounded into a fine powder with a pestle and mortar and then suspended in complete lysis buffer [containing: 50 mM PBS pH 7.4, 1 mM ethylenediamine-tetra-acetic acid, 10 µM butylated hydroxytoluene, 0.05 mM sodium azide, 1 tablet each of protease and phosphatase inhibitor cocktails] before transferring to a 5mL Teflon-coated tube. Next a rotating Teflon-coated piston was employed to homogenize the suspension (500 r.p.m., 5 min, 4℃). After homogenization, colon and fecal samples were centrifuged (5000*x g*, 15 min,4℃) and the clarified supernatants containing isolated proteins were collected and stored at -80℃ until required. The Teflon-coated tube and piston were thoroughly washed with 80% v/v ethanol and distilled water (30 s each) between samples to minimize sample cross-contamination. Total protein concentration of the colon and fecal homogenates were obtained by utilizing a commercial bicinchoninic acid assay kit (cat no. 23225, Thermo Scientific) and individual protein data was used as a normalization factor in subsequent molecular and biochemical analyses.

5.2.10 Colon Lipidomic Analysis

5.2.10.1 Colon lipid extraction

The colon lipid extraction was performed in a glass test tube and the protocol was adapted from previously described methods[52,53]. Briefly, colon homogenates containing 0.5 mg protein were mixed with high performance liquid chromatography (HPLC) grade methyl tert-butyl ether, methanol (MeOH) and water (final ratio 10:3:2.5 v/v/v). An aliquot (2 µL) of commercially acquired lipid standards (cat no. 330707-1EA, Avanti) was also added to the samples to serve as internal standards. Next, the samples were vortexed vigorously (1 min) with the tubes were capped with parafilm to prevent spillage, before incubating (22℃, 10 min) to facilitate phase separation. Subsequently, samples were centrifuged (1000*x g*, 22℃, 5 min) and the upper layer, containing non-polar lipids was collected then dried using a vacuum concentrator overnight (SPD140DDA, Thermo Scientific). Dried pellets were stored at -30℃ until required. On the day of analysis, frozen pellets were reconstituted with 100 µL of 1:1 v/v isopropyl alcohol/MeOH solution and centrifuged (25644*x g*, 4℃, 10 min) before the clarified supernatants were transferred into HPLC inserts for analysis. All samples were then immediately loaded onto the autosampler and analyzed by liquid chromatography tandem mass spectrometry (LC-MS/MS) within 24 h of reconstitution.

5.2.10.2 Lipidomic LC-MS/MS analysis

Targeted lipidomic LC-MS/MS analysis was performed using a hydrophilic interaction liquid chromatography column (Waters) coupled to a Q Exactive HF-X hybrid Quadrupole-Orbitrap™ mass spectrometer (Thermo Scientific) under both positive and negative electrospray ionisation (ESI) detection mode. The flow rate of the machine was set to 0.25 mL/min and sample injection volume was 5 µL and 10 µL for positive and negative ESI detection mode respectively. The spray voltage was 3.49 kV and compound fragments between 100-1250 m/z were scanned. Mobile phase A contains 10 mM of ammonium formate in 0.1% v/v formic acid

(FA), whilst mobile phase B contains 0.1% FA v/v in acetonitrile. The top 10 most abundant analytes at each time point were isolated.

5.2.10.3 Lipid identification & data processing

After LC-MS/MS analysis, the process of peak identification, alignment, rejection, extraction and quantification was performed using the LipidSearch™ software (v5.0, Thermo Scientific). Lipid species were identified by comparing m/z ratios and retention times across samples, with the acquired data expressed as area-under-the-curve (AUC) values. The AUC value of each analyte was normalized to internal standards before converting to concentration in Microsoft Excel using the formula below:

$$Lipid\ concentration = \frac{AUC\ of\ identified\ lipid}{AUC\ of\ internal\ standard} \times Concentration\ of\ internal\ standard$$

5.2.10.4 Lipolysis assay

Lipolysis activity in colon tissues was determined by monitoring diacylglycerol (DG) and TG levels in colon homogenates using a commercially sourced colorimetric assay kit (MAK211, Sigma Aldrich) following the manufacture's recommended protocol. In summary, colon homogenates (each sample diluted to 5 mg of total protein) were incubated with isoproterenol for 3 h at 22℃ before loading onto a 384-well microplate with the reaction mix provided. The samples were then incubated for further 3 h at 22℃ in the dark. After incubation, the sample absorbance was read at 570 nm using a microplate reader (SPARK®, Tecan) and data was exported in Microsoft Excel to construct kinetic curves to compare lipolysis activity.

5.2.11 Immunofluorescence & Immunohistochemical analyses

5.2.11.1 Heat-induced antigen retrieval & Peroxidase and non-specific protein blocking

All immuno-labelling steps were performed at 22℃ in an opaque staining humidity chamber unless specified otherwise. Following the dewaxing and rehydration processes, colon samples underwent heat-induced antigen retrieval (HIAR) for 40 min by using a Decloaking Chamber (Biocare Medical) and peroxidase and non-specific protein blocking before incubation with primary antibodies. The HIAR process was performed inside an opaque Coplin jar containing pH 6.0 sodium citrate-based (S2369, DAKO) or 9.0 EDTA-based (S2367, DAKO) antigen retrieval buffer (See Supplementary Table 6 for HIAR retrieval settings).

After the HIAR process, slides were cooled using a cold-water bath and rinsed thoroughly with tris-buffer saline (TBS) and 0.1% v/v Tween® 20 (TBST) and distilled water to remove residual retrieval solution. Next, the slides were blocked with 6% v/v H_2O_2 for 15 min and serum free protein block for 30 min to remove endogenous peroxidase activities and minimize non-specific protein binding respectively.

5.2.11.2 Immunofluorescence (IF) analysis

The expression of antioxidant response proteins Nrf-2 and HO-1 were visualized via immune-fluorescence staining with the Opal 7-Color IHC kit (NEL811001KT, Akoya Biosciences). After peroxidase and protein blocking, colon sections were incubated with anti-Nrf-2 and anti-HO-1 primary antibodies for 1h (See Supplementary Table 6 for antibody details and optimized dilution). This step was followed by thorough washing (3x 2min of TBST then 1x 2min of PBS) before incubation with Opal Polymer HRP Ms+Rb secondary antibodies obtained from the IHC detection kit for 30 min. Subsequently, colon slides were incubated with diluted Opal 570

fluorophore (1:50 v/v) and stained with DAPI (1:800 v/v, 10 min) in the dark to avoid photo-bleaching. All fluorophores and the nuclear probe DAPI were obtained from the IHC detection kit. Next, the slides were then cover-slipped with fluorescence mounting media (S3023, DAKO) and stored at 4℃ until imaging. Fluorescence images were captured by an upright microscope (Axio Scope.A1, ZEISS) equipped with an AxioCam-ICm1 camera (ZEISS) at 20x magnifications. The intensities of Nrf2+ and HO-1+ fluorescence were analyzed in the ImageJ software (v.1.54d, National Institute of Health) by using the "Freehand Selections" tool embedded in the software. Regions of interest such as colon crypts were highlighted, and the mean grey pixel value was obtained using the "Measure" function as biomarker for staining intensities.

5.2.11.3 Immunohistochemical (IHC) analysis

5.2.11.3.1 IHC labelling

Redox signaling proteins SOD-1, GPx4 and lipid peroxidation marker 4HNE were assessed using IHC labelling. Peroxidase and protein blocked slides were incubated with anti-SOD-1, anti-GPx4 and anti-4HNE primary antibodies at 4℃ overnight. The following day, primary antibodies were removed, and slides were thoroughly rinsed with TBST and PBS before incubating with anti-rabbit HRP conjugated secondary antibody for 45 min. After secondary antibody incubation, the slides were washed with TBST and PBS prior to visualization with 3,3'-diaminobenzidine (DAB, 10 min) and counterstained with hematoxylin (5 s). Slides were then washed in tap water, immersed in acid alcohol for 10 s and Scott's blue solution for 30 s and rehydrated in ascending series of alcohol before clearing with xylene and cover slipped with DPX (See Supplementary Table 6 for optimized antibody dilutions). The DAB+-stained images were captured with 10 imaging fields at 40x magnification using an Axio Lab.A1 light microscope (ZEISS) equipped with an Axiocam 105 Color Camera (ZEISS).

5.2.11.3.2 IHC immunoreactivity score

The immunoreactivity of the IHC images were quantified using the immunoreactivity scoring criteria, which accounts for the percentage of positive staining in the samples and the intensity of the staining. The quantification of immune-positive cells was performed with ImageJ software (v.1.54d, National Institute of Health), before converting to the percentage of positive staining and intensity of the IHC staining were determined in the samples using previously published protocols[54,55], where a negative expression was scored as 0, whilst weak, moderate and strong staining intensity were scored as 1,2 and 3, respectively. The total immunoreactivity score, ranges from 0-12, was obtained by multiplying the percentage of positive staining score (ranges from 0-4) by the intensity score (ranges from 0-3). The scoring criteria for both parameters were summarized in Supplementary Table 7.

5.2.12 Molecular and biochemical analyses

5.2.12.1 Fecal calprotectin analysis

Fecal calprotectin was measured by using a commercially purchased enzyme-linked immunosorbent assay (ELISA) kit (ab263885, abcam). The test was conducted by following the manufacture's recommended protocol. Briefly, fecal homogenates were thawed at 22℃ then diluted with PBS 1:20 v/v to enable accurate interpolation from the standard curve. The samples were run in duplicates and absorbance reading was measured using a microplate reader (Infinite M200-Pro, Tecan) at 450 nm.

5.2.12.2 Western blotting analyses

Where required, proteins within 20 µg of heat-reduced colon homogenates were resolved on a 4-15% Mini-PROTEAN® gel (BioRad) using a Mini-PROTEAN® electrophoresis chamber (BioRad). Proteins were separated with constant amperage of 35 mA per gel for 45 min in running buffer (containing: 25 mM Tris pH 8.3, 192 mM glycine and 0.1% w/v sodium dodecyl sulphate) and Precision Plus Protein™ Kaleidoscope™ (1610375, Bio-Rad) was used as a molecular weight marker. After separation, resolved gel was transferred onto a 0.2 µm polyvinylidene fluoride (PVDF) membrane in the Trans-Blot Turbo transferring system (BioRad).

Next the PVDF membrane was blocked with 5% w/v skim milk before incubating with primary antibodies: anti-Nrf2, anti-SOD-1, anti-GPx4, anti-4HNE or anti-β-actin at 4℃ overnight. The following day, membranes were washed with TBST and TBS before incubation with anti-rabbit (polyclonal) or anti-mouse (mono-clonal) HRP-conjugated secondary antibodies for 2 h at room temperature (optimized antibody dilutions are summarized in Supplementary Table 8). Following incubation with secondary antibodies, protein bands were visualise using Clarity™ Western ECL Substrate. Chemiluminescent signals were captured using the ChemiDoc™ Touch Gel/Membrane Imaging System (BioRad) and densiometric intensity of the protein bands was analyzed and normalized to β-actin to express as a relative ratio (relative expression) using the Image Lab software (v6.1, BioRad).

5.2.12.3 Colon inflammatory cytokine analyses

Commercially available GM-CSF (0010, ELISAkit.com) and IFN-γ (EK00002, ELISAkit.com) ELISA kits were acquired and the level of these two inflammatory markers were examined according to manufacturer's recommended protocols. Briefly, colon homogenates were diluted 1:10 v/v for GM-CSF and 1:200 v/v for IFN-γ analysis and absorbance reading was obtained at 450 nm by using a microplate reader (Infinite M200-Pro, Tecan). The samples were tested in duplicates, interpolated onto a standard curve and normalised to total protein concentration obtained from the BCA results.

5.2.13 Statistical analysis

All data collected in the current study, apart from lipidomic analysis data were subjected to heterogeneity and parametric testing with Shapiro-Wilk test (α error = 0.05) before conducting statistical analysis for group-wise comparisons using GraphPad® Prism (v. 10.1.0, GraphPad). For data sets that were identified to be parametrically distributed, one-way analysis of variance (ANOVA) with Tukey's post hoc multiple comparison was performed to examine between group differences. On the other hand, Kruskal-Wallis test with Dunn's post hoc test was used to investigate the differences between treatment groups for non-parametrically distributed datasets. All graphical values were expressed as mean ± standard deviation (SD) with statistical significance threshold was set to $p < 0.05$.

The difference in lipid concentration and composition between treatment groups were analyzed using MetaboAnalyst (v6.0, Xia Lab). Firstly, lipid data sets were normalized to median, log-transformed and scaled by Pareto method before outliers were identified using Grubb's test. To account for false positive discoveries, principal component analysis (PCA) outcomes were tested for false discovery rate (FDR) between 0.05 and 0.1 and compared with raw p-value ($p < 0.05$) obtained from GraphPad Prism embedded-multiple unpaired T-tests. This identified that the number of statistically significant lipid species showed a strong

dependency on FDR. Thus, one-way ANOVA with FDR of 0.05 was used to determine statistically significant lipid species whilst PCA and orthogonal partial least squares discriminant analysis (OPLS-DA) were used to investigate the intragroup similarities and intergroups differences, respectively.

The screening range for differential lipids were adopted from previously published literature[56-58]. Differential lipids were identified by screening and filtering statistically significant lipid species with two criteria derived from univariate and multivariate analyses using the following criteria: unpaired T-test with $p < 0.05$ and PCA with variable importance point (VIP) > 1.5. Metabolite-enzyme interaction network analysis was performed on identified differential lipids using MetScape, a plugin within the Cytoscape software (v3.10.3, Cytoscape Consortium).

5.3 Results

5.3.1 Diffusa and Villosum tonics did not alter the physical property of DSS

To ensure that Diffusa and Villosum have minimal interaction with the DSS polymer and do not compromise its ability to induce colon inflammation and experimental colitis, the physical properties of DSS in the presence of these two herbal tonics were analyzed using polarimetry and size exclusion chromatography with multi-angle light scattering analysis (SEC-MALS). Polarimetry analysis showed no significant difference in optical rotation at 546 nm when DSS were mixed with Diffusa or Villosum tonics when compared with DSS was dissolved in water alone ($p > 0.005$, Supplementary Figure 5.1a). Whilst there was no significant difference in angle of rotation at 578 nm between DSS in Diffusa tonics and DSS in water ($p > 0.05$), a significantly different optical rotation was observed when DSS was mixed with Villosum tonics at the same wavelength ($p = 0.157$, Supplementary Figure 5.1a). However, the dark color of the herbal tonic may have affected the optical measurements.

To ascertain changes observed above, SEC-MALS was performed to examine the molecular distribution of polymeric DSS ± the presence of herbal tonics. As shown in Supplementary Figure 5.1b, DSS in Diffusa and Villosum tonics displayed identical elution peak profiles and distribution when compared to DSS in water alone, indicating that the molecular weight of DSS remained comparable in both water and herbal tonics. Furthermore, the continuous availability of DSS in the drinking water of mice suggests that altered physical properties of DSS are unlikely to account for the protective effects of these herbal treatments.

5.3.2 Herbal remedies alleviated DSS-induced experimental colitis symptoms.

The use of oral DSS supplementation in drinking water has been shown to elicit colon epithelial toxicity, which compromises intestinal barrier integrity, resulting in the formation of acute inflammation and colitis in mice[59]. As anticipated, mice stimulated with DSS/drinking water exhibited a marked reduction in body weight starting from day 5, whilst body weight for mice not insulted with DSS (control) continued to increase over the 9-day monitoring period (yielding an average 101.9% ± 3.6% of their original body weight). In contrast, a significantly lower body weight was recorded in mice that were insulted with DSS alone compared to the control ($p = 0.007$) (Figure 5.1b). Conversely, mice treated with *Diffusa* tonic exhibited the least weight loss, averaging 97.2% of their original body weight, whilst curcumin powder and *Villosum* tonic treatments showed moderate improvement to body weight, averaging 92.39% and 94.61% of the body weight prior to DSS induction, respectively. This difference in body weight obtained for mice co-treated with DSS and natural products was not significantly different to either the DSS or control groups ($p > 0.05$, Figure 5.1c).

The clinical score of DSS-stimulated mice increased from Day 3, reaching an average of value 3.3 by the end of the monitoring period. On the contrary, the clinical score in the absence of DSS, or in mice treated with herbal interventions remained negligible over the same period (Figure 5.1d). At the day of sacrifice, a significantly higher clinical score was observed in mice challenged with DSS when compared to the control group ($p < 0.0001$). The administration of *Diffusa* and *Villosum* tonics resulted in significant decreases in clinical scores when compared to the DSS group, with mice averaging clinical scores of 1.75 ($p = 0.0004$) and 0.25 ($p < 0.0001$), respectively. In mice that received curcumin treatment, a marginally lower clinical score (mean 2.4) was observed by Day 9 however, this difference was not statistically significant when compared to the DSS group (Figure 5.1e).

Oxidation of luminol in the gut was used as an indirect marker to measure the extent of colon inflammation *in vivo*. As shown in Supplementary Figure 5.2a, a visibly stronger luminescence signal was observed in the DSS treated mice, whilst markedly weaker luminescence signals were detected in mice treated with curcumin, *Diffusa* and *Villosum*. Minimal luminescence signal was observed in the control mice, consistent with the maintenance of physiological homeostasis in this group. Quantification of luminescence signals identified changs in some of treated animals and did not reach statistical significance ($p > 0.05$). Notably, there was a 2-fold increase in luminescence signal in the DSS group. The administration of curcumin powder or *Diffusa* or *Villosum* tonics resulted in a ~50% reduction in luminescence signals, with the *Villosum*-treated mice showing the most noticeable decrease (Supplementary Figure 5.2b), suggesting a reduction in inflammatory burden in the colon.

Macroscopic examination showed severe and visible inflammation of colons isolated from DSS-treated mice, characterized by the presence of hemorrhage and inflammatory oedema of the colon tissue (indicated by green and red arrow respectively, Figure 5.1f). Treatment with curcumin, *Diffusa* and *Villosum* alleviated macroscopic damage, where isolated colon tissues exhibited largely intact morphology with an absence of obvious hemorrhage. Colon length was used as a secondary marker for macroscopic colon damage. As shown in Figure 5.1g, DSS insult resulted in lower mean colon length when compared to the control group, albeit this was not statistically significance ($p > 0.05$).

Next, fecal calprotectin, a colon inflammatory marker, was investigated. DSS stimulation resulted in significantly higher calprotectin levels in stool that that detected in stool from the control group ($p = 0.002$). Treatment with herbal tonics mitigated such elevation, albeit this was not statistically significant ($p > 0.05$, Figure 5.1h). Collectively, these outcomes demonstrated that DSS supplementation in water caused extensive colon inflammation in parallel with declining body weight and greater clinical score, whilst treatments with herbal medicine curcumin, *Diffusa* and *Villosum* improved the clinical scores.

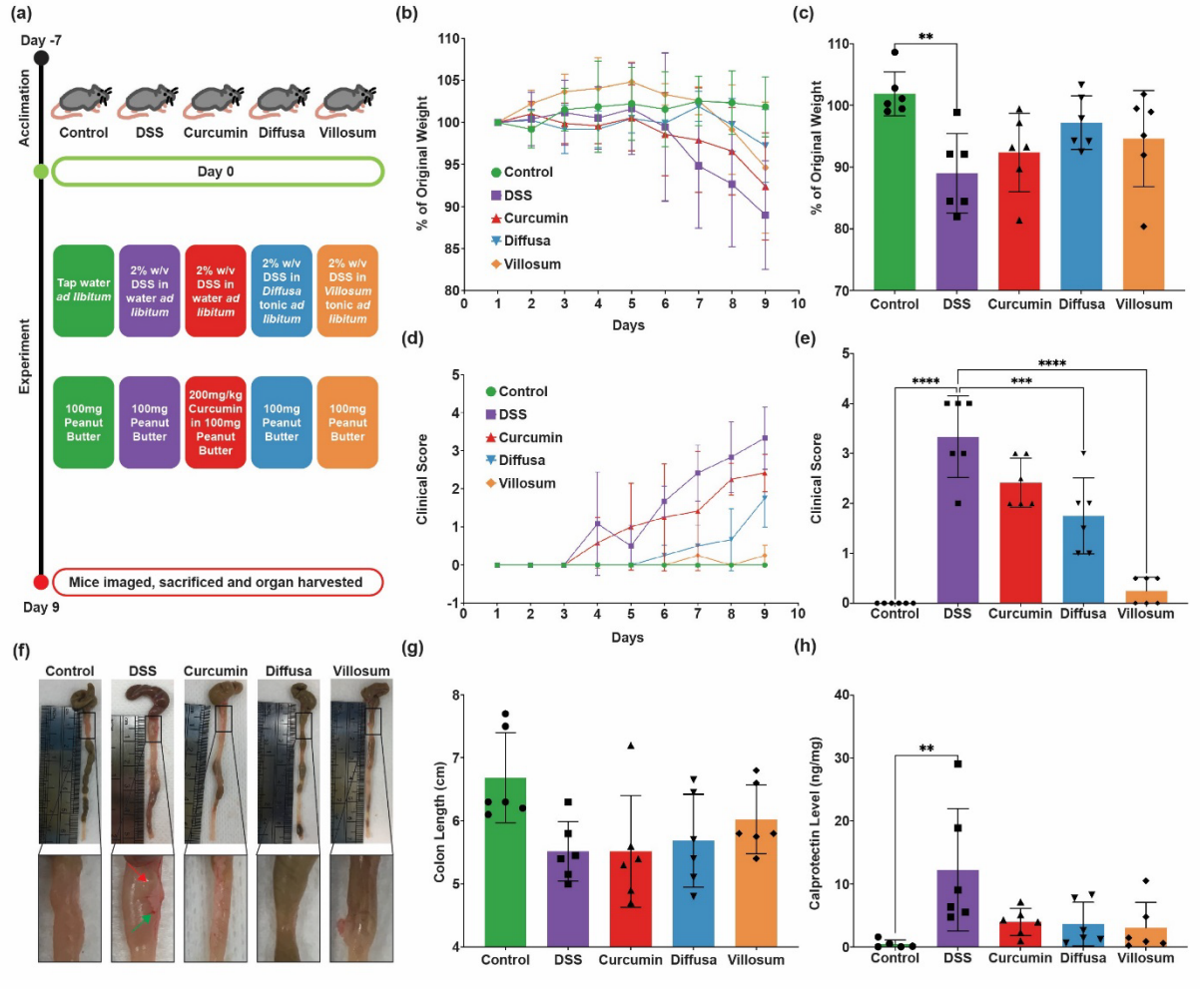

*Figure 5.1. The efficacy of herbal remedies treatment on DSS-induced UC-like experimental colitis. (a). male C57BL/6 mice at 6 weeks of age were randomly into: i). Control group; ii) DSS group, dextran sodium sulfate (DSS) at 2% w/v was supplemented in drinking water; iii). Curcumin Group, 200 mg/kg of curcumin powder in 100 mg of peanut butter (PB) daily; iv). Diffusa Group, 2% w/v DSS was supplemented in Diffusa tonic; v). Villosum Group, 2% w/v DSS was supplemented in Villosum tonic. (b). Percentage of original body weight throughout the experiment. (c). Percentage of original body weight at the day of sacrifice. (d). Clinical score throughout the experiment. (e). Clinical score at the day of sacrifice. (f). Representative images of isolated colons from different experimental groups. Red arrow shows the presence of inflammatory oedema and green arrow indicates hemorrhage. (g). Isolated colon length recorded at the day of sacrifice. (h). Calprotectin level in the stool samples. Graphical values represent mean ± SD or mean + SD when error bars were below 0 with n = 6 mice per group. Normalcy of the collected data was analysed using Shapiro-Wilk test and group differences were analysed using one way ANOVA with Tukey's multiple comparison and Kruskal-Wallis test with Dunn's multiple comparison for parametric and non-parametric data sets respectively. * $p \leq 0.05$, ** $p \leq 0.01$, *** $p \leq 0.001$ and **** $p \leq 0.0001$. Author contributions: K.X – Validation, methodology, formal analysis, data curation, T.O.C – Formal analysis, S.C – Investigation, data curation.*

5.3.3 Herbal remedies restored DSS-induced colon histoarchitectural damage and maintained mucin production

Hematoxylin and eosin (H&E) staining was used to identify colon histoarchitectural damage induced by DSS insult. As shown in representative images from Figure 5.2a, tissues isolated from the control mice present with intact surface epithelium and cryptic structure, accompanied with an absence of cellular infiltration in the mucosal and submucosal regions of the colon. On the contrary, colon tissues from mice insulted with DSS exhibited extensive epithelial erosion, inflammatory cell infiltration and complete loss of the cryptic structure. Herbal treatment of curcumin, *Diffusa* and *Villosum* resulted in improved colon histoarchitecture, where more preserved surface epithelium and cryptic structures and reduced immune infiltration were detected in colon tissues isolated from these groups (see black arrow indicate the presence of inflammatory cell infiltration on the representative images).

The H&E-stained images were also evaluated semi-quantitatively, with a focus on crypt and surface epithelium loss and the extent of cellular (neutrophil) infiltration. When compared to the control group, mice insulted with DSS exhibited a significantly greater extent of crypt ($p < 0.0001$, Figure 5.2c) and surface epithelium loss ($p < 0.0001$, Figure 5.2d). These histoarchitectural changes were accompanied by significantly enhanced neutrophil infiltration in the colon ($p < 0.0001$, Figure 5.2e). Mice treated with curcumin and *Diffusa* demonstrated significantly lower extents of crypt loss ($p = 0.001$ and $p < 0.0001$ respectively, Figure 5.2c), whilst mice that received *Villosum* tonic exhibited a significantly lower neutrophil infiltration ($p = 0.02$, Figure 5.2e) in addition to diminished crypt loss ($p < 0.0001$, Figure 5.2c).

Mice from the control group showed no evidence of dysplasia-associated morphological change whereas, mice insulted with DSS presented with hyperchromatic and enlarged nuclei, both considered as features of dysplastic colon tissue. Improved dysplasia-associated histoarchitectural changes were observed in mice treat with curcumin, *Diffusa* and *Villosum*, with varying degree of normal goblet cell morphologies and epithelial cell stratification in these corresponding colon tissues (Figure 5.2a). These changes were reflected in the quantification of the dysplasia score, where DSS-treated mice exhibited significantly (6-fold) higher dysplasia score than mice from the control group (1.3 vs. 0.22, $p = 0.01$, Figure 5.2f). Conversely, the dysplasia scores in the mice from the curcumin, *Diffusa* and *Villosum* treated groups were somewhat decreased, albeit that these differences did not reach statistical significance ($p > 0.05$ vs DSS group).

Next, the extent of Alcian blue and Safranin-O staining was investigated to evaluate the impact of different herbal treatments on mucus producing goblet cells. Concomitant with extensive colon histoarchitectural damage observed in mice insulted with DSS alone, a visibly weak Alcian blue$^+$-staining was consistently observed in the same colon tissues (Figure 5.2b). This outcome was confirmed by quantitative analysis of Alcian blue$^+$-staining, where Alcian blue$^+$ intensity was significantly lower than in colon tissues taken from the corresponding control mice ($p = 0.0042$, Figure 5.2g). In mice treated with herbal interventions curcumin, *Diffusa* and *Villosum*, higher mean mucin production was observed when compared to the DSS group. However, the percentage (%) of Alcian blue$^+$-staining from all three treatment groups was not significantly different when compared to the DSS group ($p > 0.005$, Figure 5.2g).

Together, these findings suggest that DSS insult resulted in extensive colon histoarchitectural disruption, immune infiltration and impaired goblet cell-mucin production, while supplemented curcumin, *Diffusa* and *Villosum* inhibited crypt loss induced by DSS.

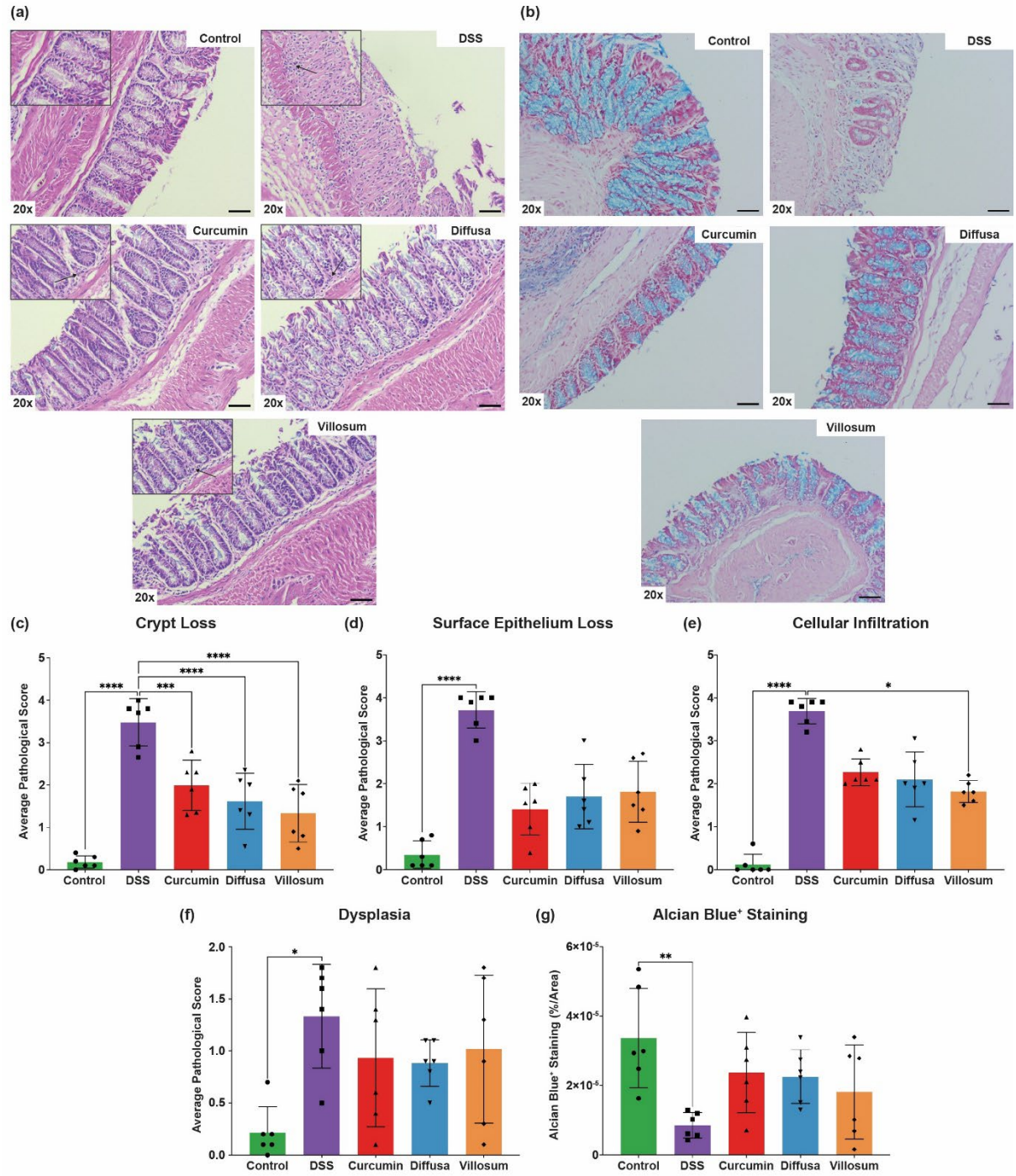

Figure 5.2. Histoarchitectural analysis of colon. (a). Representative images of hematoxylin and eosin (H&E) staining isolated mouse colons. Black arrows highlight the presence of immune infiltration. (b). Representative images of Alcian blue and Safranin O staining for goblet cells and mucin in mouse colons. Images were captured using Axiocam 105 Color camera at 20x magnification. Scale bar = 50 µm. Average histoarchitectural pathological score of (c). Crypt loss. (d). Surface epithelium loss. (e). Cellular infiltration and (f). Dysplasia. (g). Quantification of positive staining for Alcian

*blue is expressed as % of positive stain vs. colon area. Graphical values represent mean ± SD or mean + SD when error bars were below 0 with n = 6 mice per group. The normalcy of the collected data was analysed using Shapiro-Wilk test and group differences were analysed using one way ANOVA with Tukey's multiple comparison and Kruskal-Wallis test with Dunn's multiple comparison for parametric and non-parametric data sets respectively. * p ≤ 0.05, ** p ≤ 0.01, *** p ≤ 0.001 and **** p ≤ 0.0001. Author contributions: K.X – Investigation, validation, methodology, formal analysis, data curation, T.O.C – Validation, formal analysis, data curation, N.S, S.C & A.D – Investigation, formal analysis.*

5.3.4 Identification of lipid species in the colon

Targeted lipidomic LC-MS/MS analysis was used to identify lipid species extracted from isolated colon samples, where a total of 786 lipids, spanning 12 lipid classes were identified (Figure 5.3a). In the current study, lipid species belonging to the cholesterol (unesterified and esterified) and monoacylglycerol classes could not be reliably detected and were therefore excluded from analysis. The remaining lipid classes were detected and validated using the corresponding internal standards. Of the 12 identified lipid classes, further categorization afforded collation of lipid identities into 4 distinct lipid families. It was determined that glycerophospholipids comprise most of colonic lipids (~60.3%). Glycerolipids were the second most abundant lipid class in the colon, making up to ~29.6% of the total lipid species routinely detected, followed by sphingolipids and steroids, comprising ~9.3% and ~0.8% of the total species analyzed, respectively (Figure 5.3b).

Initially, to evaluate differences in lipid composition among treatment groups, a PCA approach was employed to reduce the complexity of analyses by minimizing the number of variables whilst retaining as much information as possible. As shown in Figure 5.3c and d, samples within each treatment group were clustered together, with distinct trends observed between groups, indicating differences in lipid profiles between control and different treatments. Notably, the control group showed a tight cluster of data, whereas DSS-treated mice exhibited a broader distribution, suggesting a potential shift in lipid profiles in colons from mice with experimental colitis. Treatment with curcumin, *Diffusa* and *Villosum* resulted in varying degrees of change for the same lipid profiles. Thus, although the profiles in mice treated with natural products were in general markedly different to that in mice insulted with DSS alone, they remained somewhat different to the corresponding control group.

To further investigate group differences, an OPLS-DA model was constructed, where the generated T score measures the extent of variation between the different treatment groups. Despite a small overlap in the 95% confidence regions, DSS-insulted mice displayed a distinct separation when compared to the control mice (Figure 5.3e), confirming the changes in lipid composition determined from the PCA study. In mice that received herbal medicine treatments, curcumin and Villosum exhibited the clearest distinction from mice treated with DSS alone (Figure 5.3f and h), whilst a small overlap in 95% confidence regions in the Diffusa group was observed when compared to the DSS group alone (Figure 5.3g).

The lipid species with significant alteration across groups were identified using one way ANOVA with an FDR setting at 0.05. From a total of 786 identified lipid species, 165 distinct lipids showed statistically significant differences (Figure 5.3i).

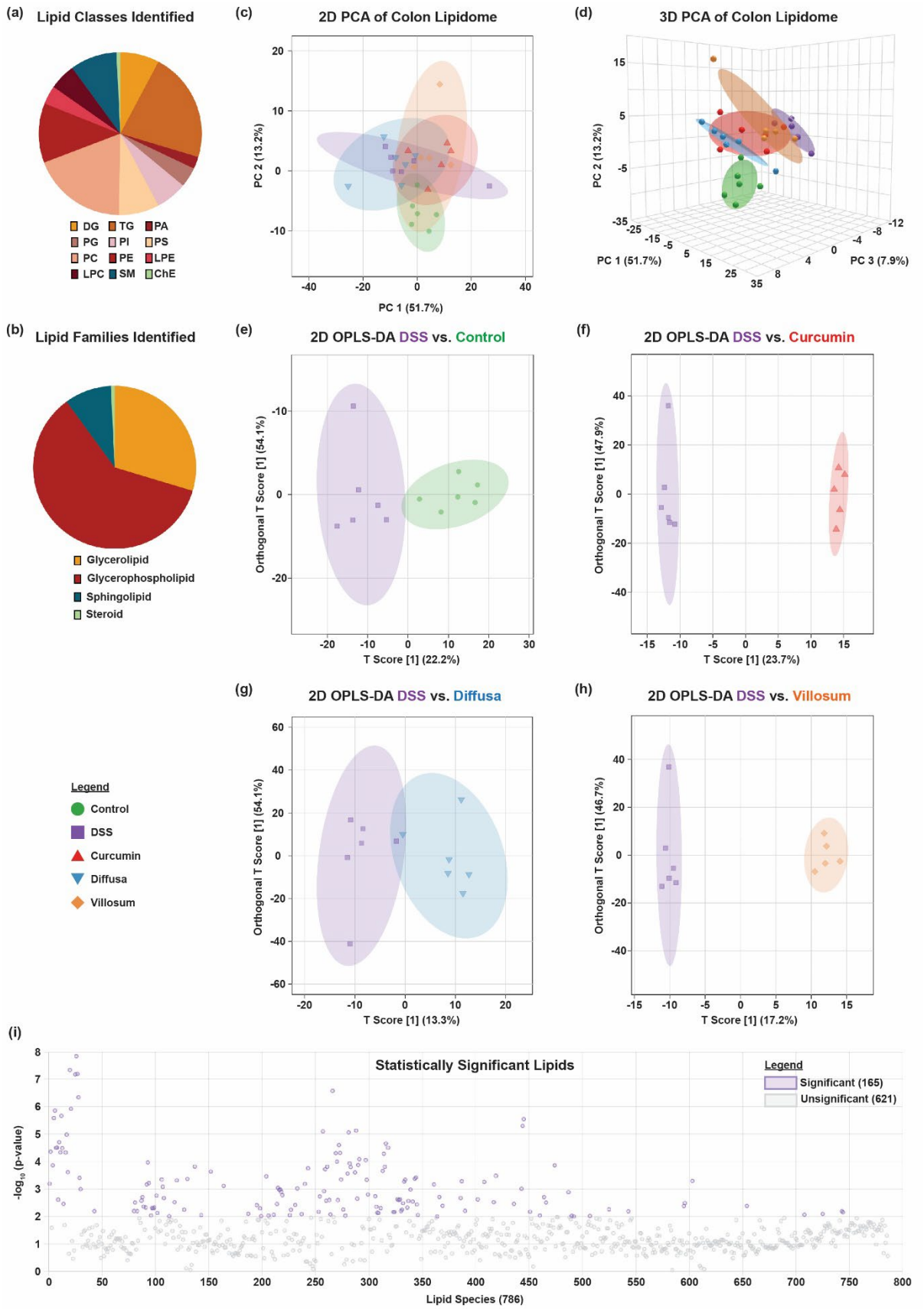

Figure 5.3. Lipid species identification via LC-MS/MS analysis. Targeted lipidomic LC-MS/MS was performed using a hydrophilic interaction LC column coupled to a Q Exactive HF-X Quadrupole-Orbitrap™ mass spectrometer and lipid species were

identified using the LipidSearch™ software v5.0. (a). The proportion of lipid classes of diacylglycerol (DG), phosphatidylglycerol (PG), phosphatidylcholine (PC), lysophosphatidylcholine (LPC), triacylglycerol (TG), phosphatidylinositol (PI), phosphatidylethanolamine (PE), sphingomyelin (SM), phosphatidic acid (PA), phosphatidylserine (PS) and lysophosphatidylethanolamine (LPE) and choline esterase (ChE) identified from mass spectrometry. (b). The proportion of lipid families of glycerolipid, glycerophospholipid, sphingolipid and steroid identified from the analysis. (c). 2D PCA scatter plot and (d). 3D PCA scatter plot of colon lipidome from different experimental groups. 2D OPLS-DA scatter plot between DSS Group and (e). Control group. (f). Curcumin Group. (g). Diffusa Group. (h). Villosum Group. (i). Statistically significant lipids in colon samples of all experimental groups identified by one way ANOVA with FDR set to 0.05. n = 6 mice per group apart from the Curcumin Group and Villosum Group of n = 5 mice per group due to 1 sample was identified as outlier from each of these two groups. Graphs were generated from MetaboAnalyst v6.0 and colours with figures consistently correspond to the Control, DSS, Curcumin, Diffusa and Villosum groups. Authors contributions: K.X – Investigation, validation, methodology, formal analysis, data curation, T.O.C – Investigation, validation, data curation, N.S – Validation, formal analysis, L.H & X.W – Investigation, C.T – Methodology, software.

5.3.5 Distinct changes in lipid composition in colons from DSS-treated mice

We next investigated statistically significant differential lipids between DSS and control groups to account for changes in lipid profiles that may be implicated in DSS pathophysiology. The screening of statistically significant lipids using T test-derived p-values and PCA-derived VIP scores identified 77 differential lipids from the initial screen of 165 species. The number of differential lipids determined by each screening criteria are shown in Supplementary Table 9 and listed extensively in Supplementary Table 5.10. A sub-analysis of the 77 identified differential lipids identified 11 distinct lipid classes (Figure 5.4a), with a majority being glycerophospholipids (~81.8%, Figure 5.4b). The remaining lipid species were from glycerolipid (~13%) and sphingolipid (~5.2%) families as shown using a heat map (Figure 5.4c), that highlights the substantial alterations in lipid species in colons from mice from treated with DSS alone. Specifically, an increase in PE and phosphatidylserine (PS) species is evident, whilst a decrease in PC, lysophosphatidylcholine (LPC) and lysophosphatidylethanolamine (LPE) species was also determined. Taken together these outcomes indicate a potential role of glycerophospholipids in the pathogenesis of DSS-induced experimental colitis. Notably, alteration to the glycerolipid lipid family were also identified, with lower abundance of some DG and TG species identified in DSS-insulted mice.

Next, key metabolic pathways involving these differentially expressed lipids were determined by MetPa, an analysis plugin embedded within the most recent version of MetaboAnalyst software available. Overall, the data implicated the involvement of 3 primary metabolic pathways (Figure 5.4d). Among the pathways identified, glycerophospholipid metabolism was found to be extensively impacted, as indicated by its high statistical significance ($p = 0.0025433$) and pathway impact score (0.21708) (Supplementary Figure 5.3a and Supplementary Table 5.11). The metabolic pathways of glycosylphosphatidylinositol anchor biosynthesis and α-linolenic acid metabolism was also found to be significantly altered (Supplementary Figure 5.3b & c and Supplementary Table 5.11).

Metabolic interaction network analysis was then performed to highlight the interconnections between altered lipid species, enzymes and their associated genes. As highlighted by Figure 5.4e, 4 lipid species (DG, PE, LPC and PC) were central to the disrupted enzymatic processes observed in the mice insulted with DSS, which reinforces the involvement of glycerophospholipids and glycerolipids metabolism during experimental colitis. Together, these outcomes demonstrate that DSS insult induced profound lipidomic alteration in the colon, particularly in glycerophospholipid metabolism.

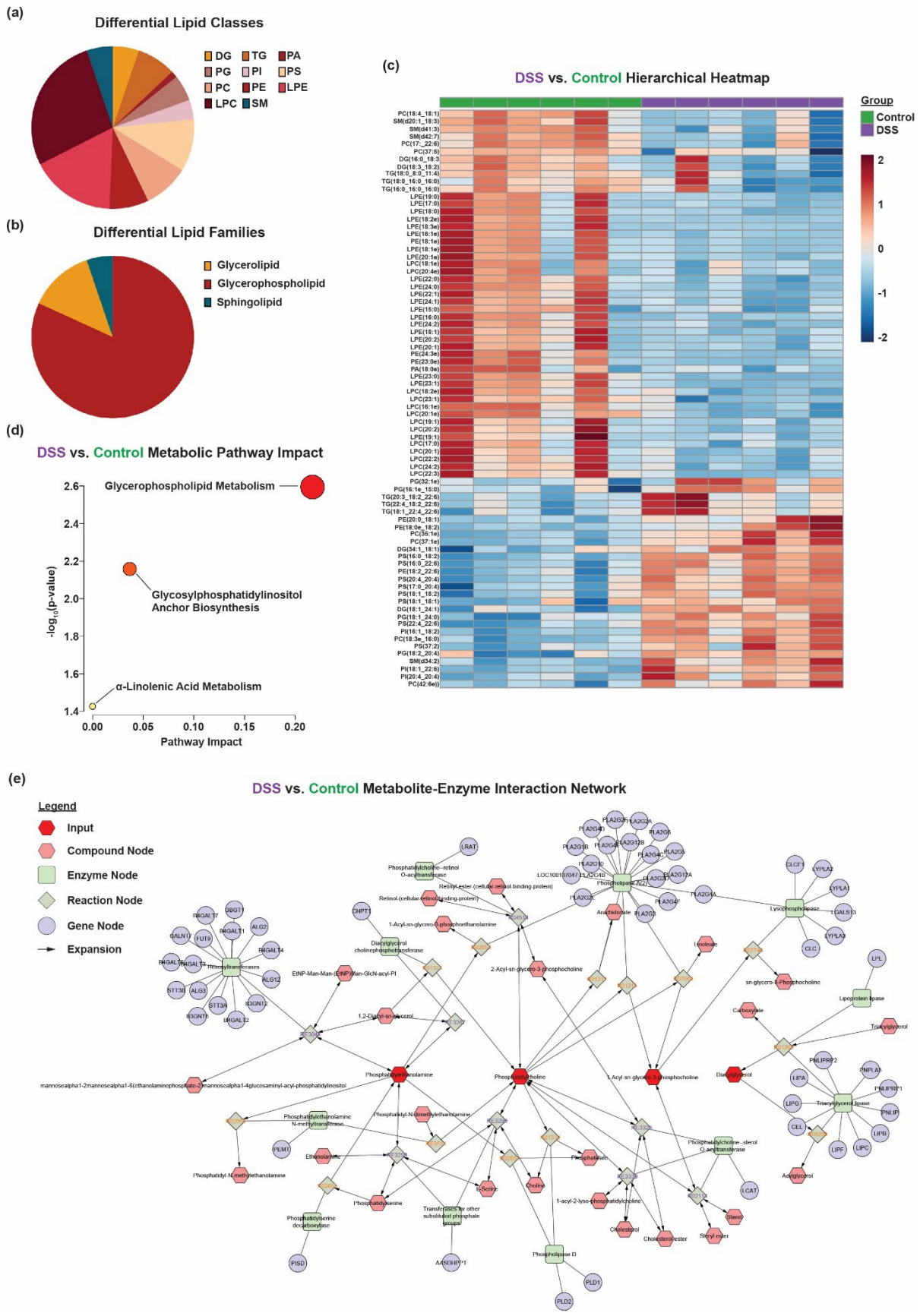

Figure 5.4. Differential lipids between Control and DSS Groups. Targeted lipidomic LC-MS/MS on colon homogenates was performed using a hydrophilic interaction LC

column coupled to a Q Exactive HF-X Quadrupole-Orbitrap™ mass spectrometer and lipid species were identified using the LipidSearch™ software v5.0. (a). The proportion of differential lipid classes and (b). The proportion of lipid families identified by lipidomic analysis. (c). Hierarchical heatmap of identified differential lipid species. (d). Metabolic pathway impact scatter plot. (e). Metabolite-enzyme interaction network of identified differential lipids between Control and DSS Groups. n = 6 mice per group apart from the Curcumin Group and Villosum Group of n = 5 mice per group due to 1 sample was identified as outlier from each of these two groups. Heatmap and scatter plots were generated from MetaboAnalyst v6.0 and network interaction analyses were performed in MetScape. Authors contributions: K.X – Investigation, validation, methodology, formal analysis, data curation, T.O.C – Investigation, validation, data curation, N.S – Validation, formal analysis, L.H & X.W – Investigation, C.T – Methodology, software.

5.3.6 Modulation of colonic lipid composition by herbal treatments

Differential lipid analysis demonstrated changes in the colon lipidomes in mice that received curcumin, *Diffusa* and *Villosum* herbal treatments. The number of differential lipids determined by each screening criteria are shown in Supplementary Table 5.9 and listed in Supplementary Table 5.12-14. In curcumin-treated mice, 60 lipid species spanning 10 lipid families were determined to be differential accumulated (Figure 5.5a). Of these 60 lipids, ~63.3% were allocated to the glycerophospholipid family, ~35% glycerolipids and ~1.7% were from the sphingolipid family (Figure 5.5b). Identical analyses of colon lipid extract from the *Diffusa* and *Villosum*-treated mice identified 36 and 53 lipid species, respectively that differed in concentration when compared to DSS-insulted mice (Figure 5.5c & e). The pattern of differential lipid accumulation between DSS-insulted mice and mice that received DSS+*Diffusa* tonic were further categorized into 4 lipid families (glycerolipid, glycerophospholipid, sphingolipid and steroid) at varying proportions (~19.4%, ~75%. ~2.8% and ~2.8%, respectively), whilst only lipids from the glycerolipid and glycerophospholipid families (~20.8% and ~79.2% respectively) were detected in differential lipid analysis that compared mice treated with DSS alone or DSS+ *Villosum* (Figure 5.5d &f).

The difference in lipid expression profiles between DSS and curcumin groups was highlighted by the hierarchical heatmap shown in Figure 5.5g. Under these conditions, decreased TG, LPE and LPC lipid species were again observed in the curcumin treated mice. Notably, an increased abundance of PE lipids was also observed in these mice, a group of lipids that was found to have significantly lower concentration in the DSS-treated mice when compared to the controls. This outcome for PE suggested a potential restoration of PE lipid compositions in mice that received curcumin powder. Subsequent MetPa analysis determined that metabolic pathways associated with glycerophospholipid metabolism, glycosylphosphatidylinositol anchor biosynthesis and α-linolenic acid metabolism were significantly affected (Figure 5.5i, Supplementary Figure 5.4a-c and Supplementary Table 5.15), whilst complementary interaction network analysis demonstrated that the lipid species of PE, PC LPC and TG-associated enzymatic processes were disrupted (Supplementary Figure 5.5). In mice that received DSS+*Diffusa* tonic, no prominent trend in differential lipids was observed and metabolic pathway and interaction network analyses could not be performed as less than 3 metabolites were matched with the identified differentially expressed lipids and hence further analyses would not provide meaningful outcomes (Supplementary Figure 5.6).

With regards to mice that received DSS+*Villosum* tonic, a marked increase in DG concentrations, along with moderate decrease in LPC, LPE and phosphatidylinositol levels was observed (Figure 5.5h). The changes of lipid concentration were shown to associate with significantly altered glycerophospholipid metabolism, glycophosphatidylinositol anchor biosynthesis and glycerolipid metabolism pathways (Figure 5.5j, Supplementary Figure 5.7a-c and Supplementary Table 5.15). Furthermore, interaction network analysis demonstrated that enzymatic processes associated with lipid species of phosphatidate, PE, LPC and DG were significantly impacted (Supplementary Figure 5.8). Overall, these outcomes indicated that herbal treatments, particularly curcumin and Villosum co-administered with DSS significantly modulated lipidomic alterations induced by DSS alone, with the glycerophospholipid metabolic pathway consistently identified to be impacted across all treatment groups.

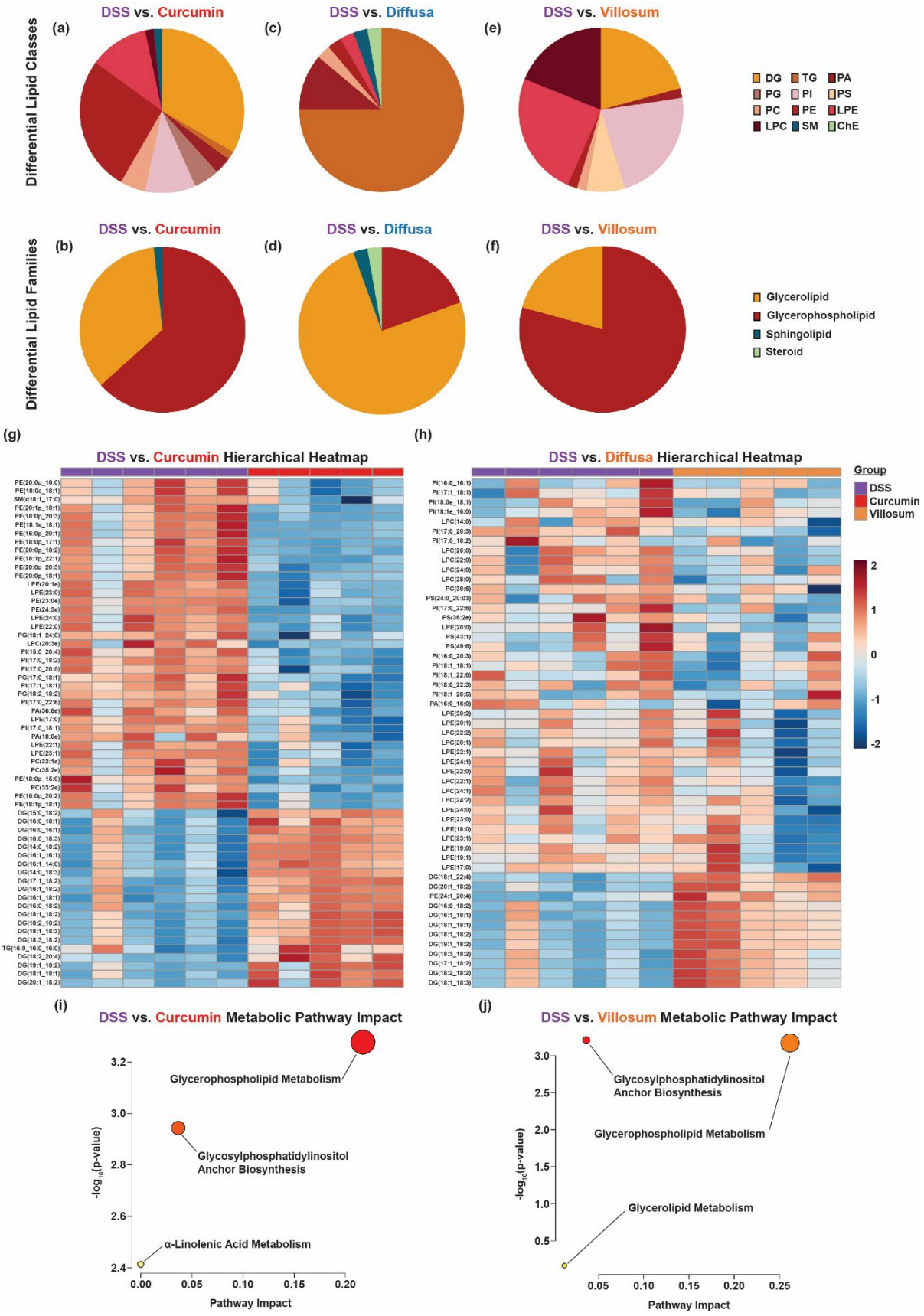

Figure 5.5. Differential lipids between DSS and herbal remedies treated groups. Targeted lipidomic LC-MS/MS on colon homogenates was performed using a hydrophilic interaction LC column coupled to a Q Exactive HF-X Quadrupole-

Orbitrap™ mass spectrometer and lipid species were identified using the LipidSearch™ software v5.0. (a). The proportion of differential lipid classes and (b). The proportion of differential lipid families identified between DSS and Curcumin Group. (c). The proportion of differential lipid classes and (d). The proportion of differential lipid families identified between DSS and Diffusa Group. (e). The proportion of differential lipid classes and (f). The proportion of differential lipid families identified between DSS and Villosum Group. (g). Hierarchical heatmap of identified differential lipid species between DSS and Curcumin Group and (h). Between DSS and Villosum Group. (i). Metabolic pathway impact scatter plot of identified differential lipids between DSS and Curcumin Group and (j). DSS and Villosum Group. n = 6 mice per group apart from the Curcumin Group and Villosum Group of n = 5 mice per group due to 1 sample was identified as an outlier from each of these two groups as judged using the outlier test in GraphPad prism. Graphs were generated from MetaboAnalyst. Authors contributions: K.X – Investigation, validation, methodology, formal analysis, data curation, T.O.C – Investigation, validation, data curation, N.S – Validation, formal analysis, L.H & X.W – Investigation, C.T – Methodology, software.

5.3.7 Validation of DG and TG lipolysis activity in the colon homogenates

In addition to altered glycerophospholipid metabolism identified above, substantial changes to glycerolipid species were also consistently observed in mice allocated to the herbal treatment groups. To validate the involvement of glycerolipids in DSS-induced experimental colitis, determination of hormone-sensitive lipase (HSL) was performed. As indicated from Figure 5.6a, DSS supplementation in drinking water significantly lowered colon HSL activity ($p < 0.0001$), whilst treatments with curcumin, *Diffusa* and *Villosum* significantly increased HSL activity in the colon tissue, returning to levels like the control group ($p < 0.0001$ for all three treatment groups vs DSS).

These outcomes were paralleled to the lipidomic findings, where significantly higher abundance of DG lipids was observed in mice that received curcumin, *Diffusa* and *Villosum* treatments ($p < 0.0001$ for all three treatment groups compared to DSS group, Figure 5.6b & d). The abundance of TG lipid species was found to be significantly increased in the DSS-challenged mice when compared to the healthy controls ($p < 0.0001$), whilst a marginal shift towards normal TG level was observed in the DSS+curcumin and DSS+*Villosum* groups, coinciding with the outcomes of the lipolysis assay. Notably, the lipidomic analysis outcome on TG species in the DSS+*Diffusa* group did not match the findings of the lipolysis assay, where a significant lower abundance of TG lipids was observed in the colon tissues ($p < 0.0001$, Figure 5.6c & e). Nevertheless, results from the lipolysis assay generally validated the findings from differential lipidomic analyses, which reinforces the influence of herbal medicine in the colon lipidome of mice with experimental colitis.

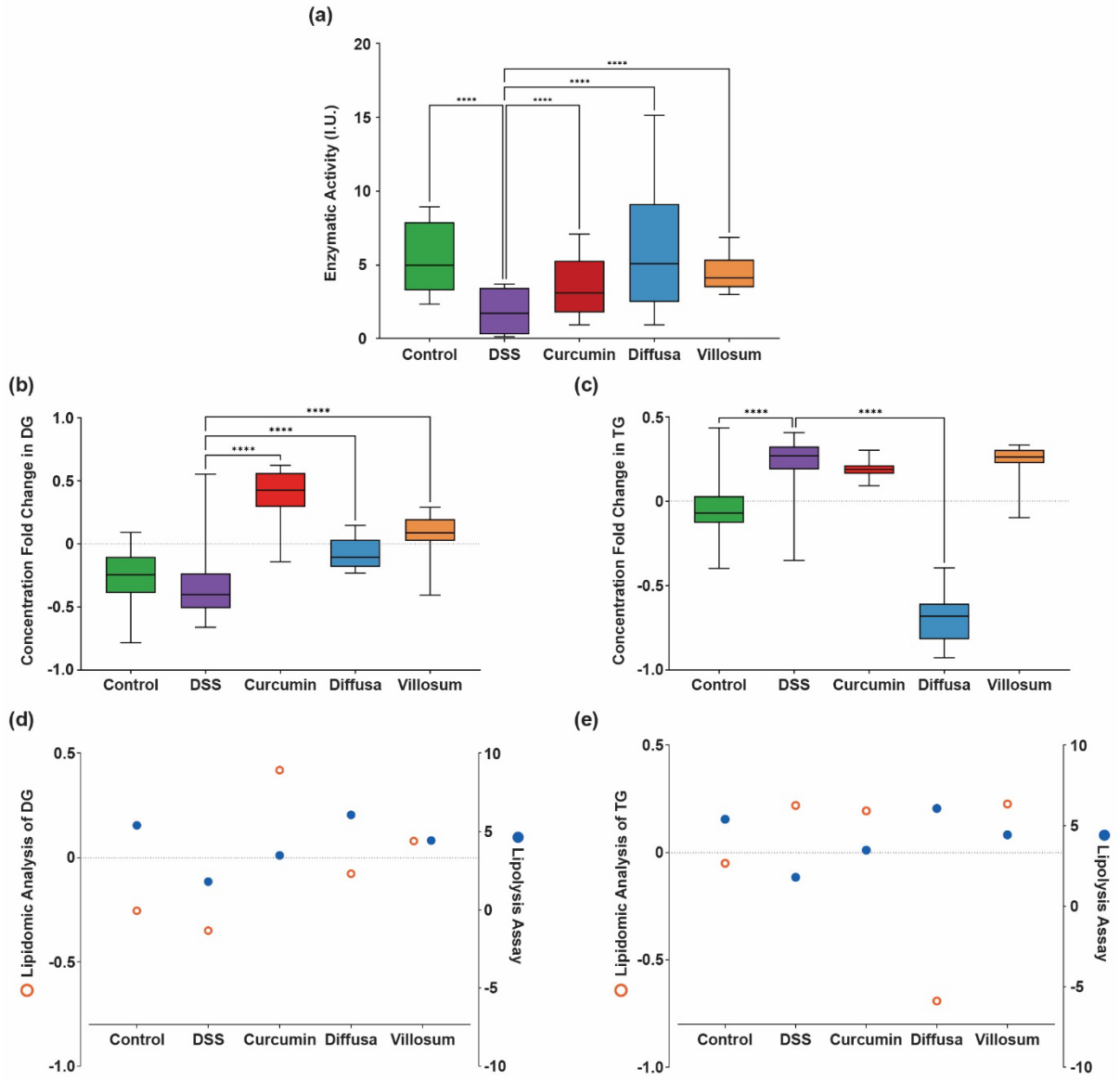

*Figure 5.6. Validation of glycerolipid levels in the colon homogenates using a commercially available lipolysis assay kit. (a). Hormone-sensitive lipase activity examined by lipolysis assay. (b). Box and whisker plot of differential DG and (c). TG changes identified from lipidomic analysis. (d). Correlation graphs showing relationship between DG and (e). TG changes and HSL activities from different experimental groups. Graphical values represent mean ± SD n = 6 mice per group apart from the Curcumin Group and Villosum Group of n = 5 mice per group due to 1 sample was identified as outlier from each of these two groups. The normalcy of the collected data was analysed using Shapiro-Wilk test and group differences were analysed using one way ANOVA with Tukey's multiple comparison and Kruskal-Wallis test with Dunn's multiple comparison for parametric and non-parametric data sets respectively. * $p \leq 0.05$, ** $p \leq 0.01$, *** $p \leq 0.001$ and **** $p \leq 0.0001$. Authors contributions: K.X – Investigation, validation, methodology, formal analysis, data curation, T.O.C – Investigation, validation, data curation, N.S – Investigation, validation, formal analysis, L.H – Investigation.*

5.3.8 Herbal treatments upregulate HO-1 expressions in the DSS-insulted colons

The expressions of antioxidant response master regulator Nrf2 and its downstream antioxidant enzyme HO-1 were examined with IF analysis. As shown in Figure 5.7a, $Nrf2^{+}$-staining was observed in the cytoplasm and nuclei across all experimental groups. The merged images highlighted that DSS insult did not result in any visible changes in colonic Nrf2 expressions when compared to the controls, whilst minimal difference in localization and expression of Nrf2 was also observed in mice that received DSS + one of curcumin, *Diffusa* or *Villosum* treatments. Quantification of Nrf2 staining intensity was performed using ImageJ software, where no statistical difference in Nrf2 expression was reported across all groups ($p > 0.05$, Figure 5.7b). This outcome was reinforced by Western blot analysis, in which it confirms the presence of Nrf2 proteins in colon homogenates, with no statistical difference in expression levels across all treatment groups (Figure 5.7c and d).

The expression of antioxidant enzyme HO-1 was found to primarily localized to the cytoplasm, with small population of cells also exhibited nuclear expression. When compared to the colons of control mice, colon tissues from DSS-insulted mice exhibited a slightly weaker staining of HO-1. Conversely, co-treatment with curcumin, *Diffusa* or *Villosum* in the presence of DSS resulted in stronger staining with more prominent nuclear localization of HO-1 (Figure 5.7e). Staining intensity quantification analysis showed a significantly higher intensity of HO-1 in the colons of mice that received curcumin and *Diffusa* treatments, suggesting a potential upregulation of this enzyme in response to DSS-induced colitis ($p = 0.008$ and $p = 0.04$ respectively). Whilst mice treated with DDD+*Villosum* also exhibited higher staining intensity of HO-1 in the colons, this difference was not statistically significant when compared to the DSS group ($p > 0.05$, Figure 5.7f). Collectively, these findings suggests that curcumin and *Diffusa* may dampen DSS-induced experimental colitis symptoms by exerting antioxidant effects through HO-1 pathway activation.

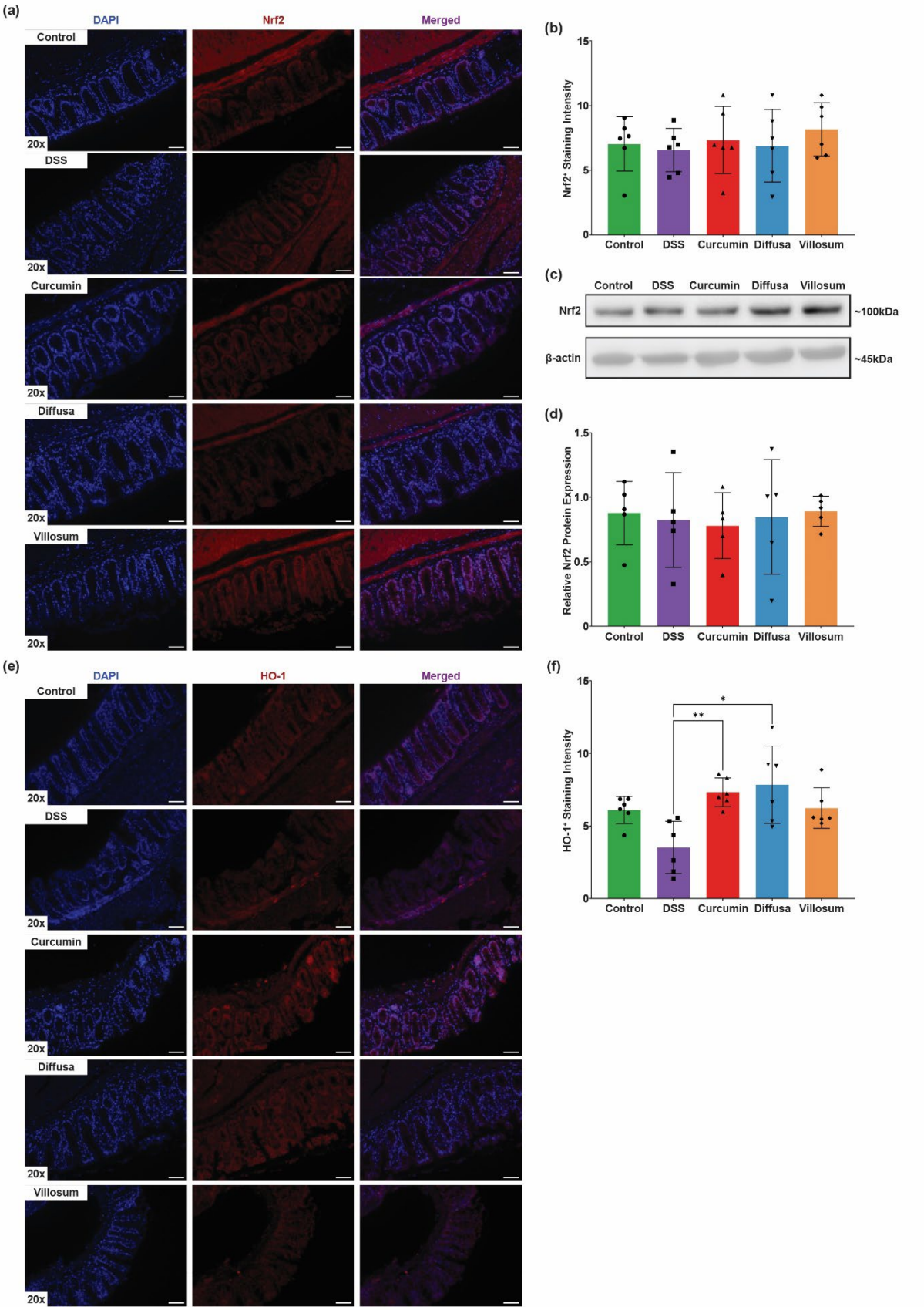

Figure 5.7. The effect of herbal medicines on Nrf2/HO-1 signaling pathway. (a). Representative images of immunofluorescence (IF) labelling of Nrf2. (b). Quantification of Nrf2⁺ staining intensity. (c). Western blot analysis Nrf2 protein in

*colon homogenates from different experimental groups. (d). Semi-quantitative analysis of Nrf2 expression from Western blot analysis (e). Representative images of IF labelling of HO-1. IF images were captured at 20x magnifications using Axio Scope.A1 fluorescence microscope with AxioCam-ICm1 camera. Scale bar = 50 µm. Graphical values represent mean ± SD with n = 6 mice per group. The normalcy of the collected data was analysed using Shapiro-Wilk test and group differences were analysed using one way ANOVA with Tukey's multiple comparison and Kruskal-Wallis test with Dunn's multiple comparison for parametric and non-parametric data sets respectively. * p ≤ 0.05, ** p ≤ 0.01, *** p ≤ 0.001 and **** p ≤ 0.0001. Author contributions: K.X – Investigation, validation, methodology, formal analysis, data curation, S.C – Investigation, formal analysis, B.L.W – Investigation.*

5.3.9 Herbal remedies modulate redox balance and alter pro-inflammatory cytokine profiles in DSS-stimulated colons.

The antioxidant properties of curcumin, *Diffusa* and *Villosum* in DSS-insulted colons were further explored using IHC staining. SOD1 is an antioxidant enzyme that catalyzes the conversion of $O_2\cdot^-$ into H_2O_2 and genetic polymorphism of SOD1 has been shown to decrease the risk of UC development[60]. As shown in Figure 5.8a, distinct cytoplasmic staining of SOD1 was observed in cells in the crypts, with no visible difference in SOD1 expression between all groups. Albeit not reaching statistical significance, a mild increase in SOD1 staining score was reported when compared to the control group, whilst DSS+*Villosum* treatment resulted in a significant decrease in $SOD1^+$ staining score, suggesting the potential modulation of this antioxidant response enzyme in the presence of the herbal tonics ($p = 0.0356$, Figure 5.8b). A trend towards reduced $SOD1^+$ staining score was observed in the DSS+*Difussa* group. However, this change in staining score was not significant when compared to the DSS group ($p > 0.05$, Figure 5.8b). Western blot analysis on colon homogenates confirmed the expression of SOD1 in the tissue (Figure 5.8e). As indicated in Figure 5.8f, DSS supplementation in water reduced relative colonic SOD1 expression whilst treatments with curcumin, *Diffusa* and *Villosum* did not affect this trend ($p > 0.05$).

The colonic staining scores for another Nrf2 regulated antioxidant enzyme, GPx4 were decreased in mice that were treated with curcumin, *Diffusa* and *Villosum*, although these changes were not significantly different to all groups ($p > 0.05$, Figure 5.8a & c). Western blot analysis confirms the expression of this enzyme at ~23 kDa and displayed similar trends of expression to the outcomes observed in IHC staining (Figure 5.8g & h). Overall, findings on antioxidant proteins and lipid peroxidation markers suggest that herbal products curcumin, *Diffusa* and *Villosum* exert antioxidant effects in the DSS stimulated colon to varying degrees. The discrepancy in expressions between IHC and western blot analysis may be due to the use of homogenized total colon tissue for immunoblotting, which includes both inflamed and non-inflamed areas whilst IHC analysis focused on colon tissue at the site of damage.

The lipid oxidation biomarker 4HNE displayed diffuse staining congregated near the surface epithelium of the colon tissues (Figure 5.8a). In the DSS-insulted group, the staining of 4HNE was stronger and extended deeper towards the submucosa regions of the colon. In support of this outcome, quantification analysis of 4HNE demonstrated a significantly increased $4HNE^+$ staining score in the DSS group when compared to the controls ($p = 0.0432$, Figure 5.8d). Conversely, the extension of $4HNE^+$ staining toward the submucosal regions were less pronounced in mice that received curcumin, *Diffusa* and *Villosum* treatments (Figure 5.8a),

with trends of reduction in 4HNE^{+} staining scores to the level similar to the control group ($p > 0.05$, Figure 5.8d). Western blot analysis on colon homogenates led to the visualization of 5 prominent 4HNE+ protein bands at ~12, ~15, ~25, ~50 and ~125 kDa (Figure 5.8i). Despite not being statistically significant, lower relative 4HNE expressions were observed in both the DSS and herbal medicine treated groups ($p > 0.05$, Figure 5.8j).

Lastly, the effect of herbal treatments on the extent of colon inflammation was examined by ELISA of GM-CSF and IFN-γ. A higher mean GM-CSF level was observed in mice that were challenged with DSS. However, this change was not statistically significant when compared to the controls ($p > 0.05$). When DSS-insulted mice were treated with curcumin, *Diffusa* and *Villosum*, the level GM-CSF was comparable to the DSS-challenged mice with no treatment (Figure 5.8k), suggesting that herbal medicines have no effect on GM-CSF level in the mouse colon. On the other hand, a marginal increase in IFN-γ level was observed in mice that were stimulated with DSS, albeit not reaching statistical significance when compared with the control group ($p > 0.05$). Contrastingly, co-treatments with curcumin, *Diffusa* and *Villosum* in the presence of DSS appeared to diminish any increase in IFN-γ in the colon. Notably, this difference was statistically significant in the curcumin- and *Villosum*-treated groups ($p = 0.006$ and $p = 0.012$ respectively), but not in the *Diffusa*-treated group when compared to mice treated with DSS alone ($p > 0.05$, Figure 5.8l), which highlights that selected herbal medicines can alter pro-inflammatory cytokine profiles in isolated mouse colons after experimental colitis.

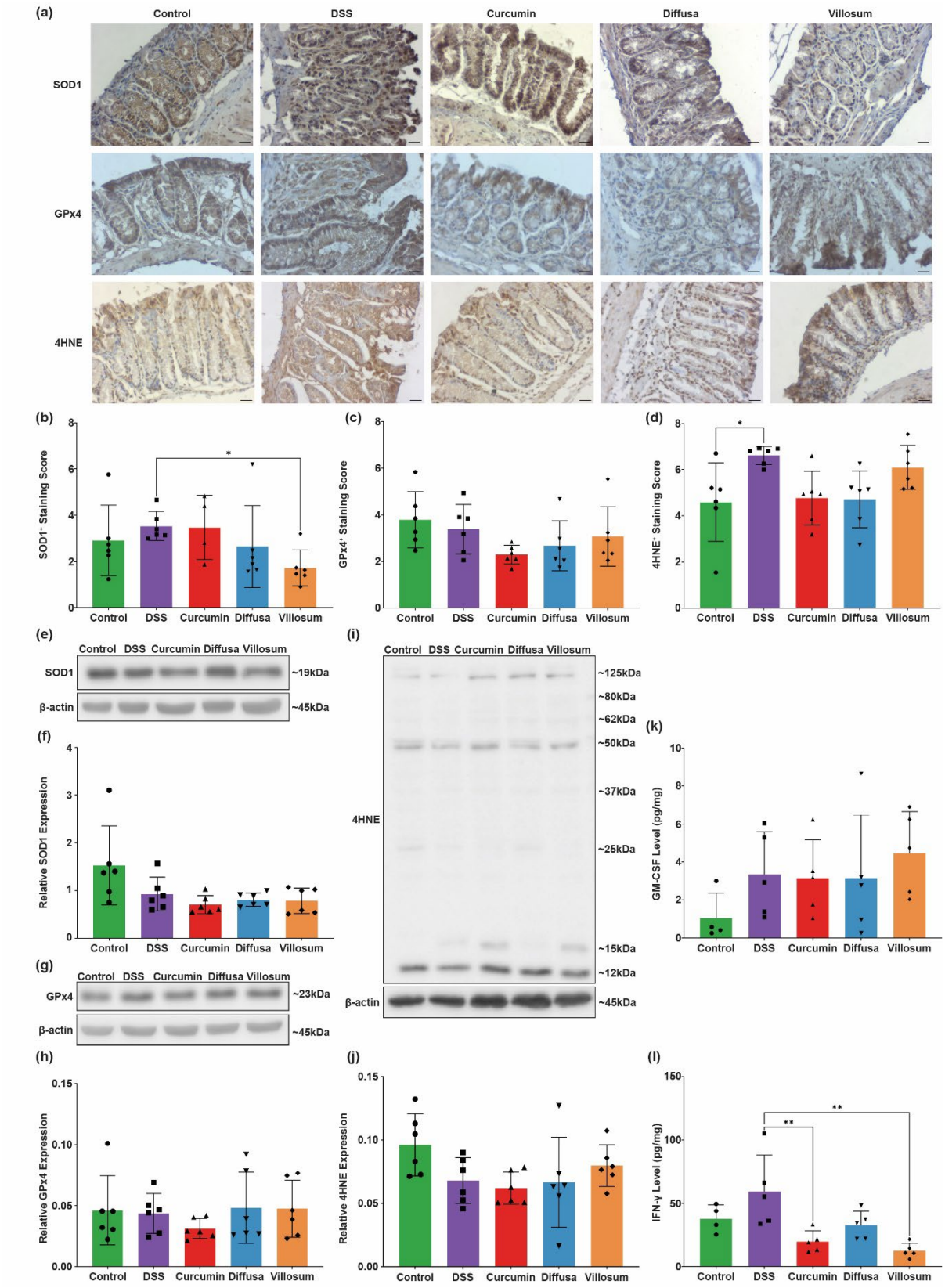

Figure 5.8. The effect of herbal treatments on antioxidant response protein expressions, lipid peroxidation and inflammatory cytokines in colon tissues. (a). Representative images of immunohistochemistry labelling of SOD1, GPx4 and 4HNE. IHC images were captured using Axiocam 105 Color camera at 20x magnification. Scale bar = 50 µm. Quantification of IHC staining scores of (b). SOD1, (c). GPx4 and

*(d). 4HNE. Representative Western blot bands of (e). SOD1 and (f). densitometric analysis of the same protein. Representative Western blot bands of (g). GPx4 and (h). densitometric analysis of the same protein. Representative Western blot bands of (i). 4HNE and (j). densitometric analysis of the same protein. (k). expression of GM-CSF and (l). IFN-γ in mouse colon homogenates. Graphical values represent mean ± SD with n = 6 mice per group, apart from cytokine profile analyses, where n = 4 mice from the Control Group and n = 5 mice for all other treatment groups were analysed after interpolation from standard curves. The normalcy of the collected data was analysed using Shapiro-Wilk test and group differences were analysed using one way ANOVA with Tukey's multiple comparison and Kruskal-Wallis test with Dunn's multiple comparison for parametric and non-parametric data sets respectively. * $p \leq 0.05$, ** $p \leq 0.01$, *** $p \leq 0.001$ and **** $p \leq 0.0001$. Author contributions: K.X – Investigation, validation, methodology, formal analysis, data curation, T.O.C – Investigation, formal analysis, data curation, S.C – Investigation, B.L.W – formal analysis.*

5.4 Discussions

Despite the wide range of available treatments, no current therapy has proven to be a definitive cure for IBD[61]. Conventional interventions often have high non-response rates and undesirable adverse effects[61-63], leading to many patients with IBD to perceive these contemporary therapies as ineffective with low tolerability[64]. As a result, there is a growing interest in complementary and alternative medicines for the disease, particularly in the field of natural products[65]. Accordingly, several plant-based compounds such as berry extracts and aloe vera have demonstrated therapeutic efficacy in alleviating gastric inflammation and restore redox balance[66-69]. In this study, we investigate the therapeutic potential of three herbal remedies – curcumin, *Hedyotis Diffusa* and *Amomum Villosum* in a murine model of DSS-induced experimental colitis and highlight for the first time the potential interplay between lipid composition and redox imbalances in colonic inflammation. Outcomes here demonstrated that herbal treatments effectively alleviated colitis symptoms, as evidenced by reductions in clinical score, macroscopic colon damage and oxidative stress, accompanied by improvements in histoarchitecture and mucin production. Additionally, the administration of powdered-curcumin, as well as *Diffusa* and *Villosum*-based herbal tonics led to significant upregulation of HO-1 expression and downregulation of IFN-γ together with notable modulation of key antioxidant signaling proteins such as SOD1 and GPx4 in the DSS challenged colon tissue. Given the critical roles of glycerophospholipids and glycerolipids in maintaining gut barrier integrity and cellular signaling, the current study concurrently investigated changes in the colonic lipidome in response to DSS insult ± the presence of herbal treatments. As anticipated, DSS exposure resulted in decreased glycerolipid abundance and caused disruptions to glycerophospholipid and α-linolenic acid metabolism, indicating their likely involvement in IBD pathogenesis. Notably, treatment with the three herbal remedies restored glycerolipid levels and modulated other lipid metabolic pathways, further supporting the notion that these natural products have potential as therapeutic agents in IBD.

The antioxidant effects of curcumin, *Diffusa* and *Villosum* observed in the current study are likely mediated through multiple mechanisms. One potential pathway involves the regulation of neutrophil activity and their endogenous enzyme myeloperoxidase (MPO). Under normal physiological conditions, activated neutrophils utilize H_2O_2 to generate hypochlorous acid (HOCl)[70], a potent oxidant that exerts bactericidal effects by inducing non-specific DNA damage in infected cells in an intricately regulated manner[71]. However, excessive and dysregulated neutrophil recruitment in the inflamed colon can lead to amplified oxidative stress which drives the production of pro-inflammatory cytokines, perpetuating a cycle of inflammation and further oxidative damage[72]. In the current study, mice that received herbal medicine treatments exhibited significantly lower immune cell infiltration (refer to Figure 2a), which given the acute nature of the model, is likely attributed to reduced neutrophil migration. This was accompanied by attenuated luminal oxidation, as indicated by diminished bioluminescence signals in the mouse abdomens, suggesting that the herbs mitigate oxidative stress by limiting neutrophil recruitment and its associated oxidative burst. Interestingly, whilst GPx typically converts H_2O_2 into water as a protective mechanism[22], no significant differences in GPx4 levels were observed between groups. This suggests that curcumin, *Diffusa* and *Villosum* may alleviate oxidative stress through pathways that are independent of GPx4-mediated H_2O_2 detoxification. Nonetheless, further research is warranted to confirm the precise relationships between neutrophil recruitment, MPO activity and oxidative stress reduction in this context.

Another key mechanism by which these herbal remedies may exert their antioxidant action is through the direct activation of Nrf2/HO-1 signaling pathway. Nrf2 is a master regulator of antioxidant responses[20], and elevated expression of this transcription factor has been reported in the inflamed colons of patients with UC[73]. Enhanced expression of downstream HO-1 has been shown to protect against DSS-induced colon inflammation by mitigating oxidative damage and restoring cellular homeostasis[74,75]. Although the current study did not observe a significant change in colonic Nrf2 expressions, herbal treatments, particularly curcumin and *Diffusa* significantly upregulated HO-1 levels, which indicates that these herbal medicines may enhance antioxidant capacity by directly stimulating the Nrf2/HO-1 signaling pathway. The ability of these herbs to reduce neutrophil-mediated oxidative stress and concurrent modulation of Nrf2/HO-1 pathway suggests a potential synergistic effect that re-balances the oxidative environment in the inflamed colon. However, further investigations are needed to determine whether the herbal treatments can modulate additional downstream targets of Nrf2 transcriptional activation or whether other antioxidant signaling pathways to confer their broader cytoprotective effects.

The third potential mechanism involves the inhibition of IFN-γ-driven inflammatory cascade. IFN-γ is known to activate macrophages, leading to the production of pro-inflammatory cytokines TNF-α, IL-1β and IL-6[76]. This inflammatory response has been implicated in exacerbating oxidative stress and promoting disease progression of UC-like experimental colitis[77,78]. Under these conditions, the ferulic acid decreases oxidative stress by suppressing IFN-γ-mediated inflammation whilst enhancing the expression of antioxidant enzymes such as cyclooxygenase (COX)-2 and inducible nitric oxide synthase (iNOS)[79]. Consistent with these findings, the present study showed supplemented natural products significantly lowered IFN-γ levels in the colon of mice, suggesting that their biological activities may in part be attributed to the suppression of this inflammatory cascade. Further studies elucidating the role of curcumin, *Diffusa* and *Villosum* in modulating IFN-γ-mediated inflammation and oxidative stress are required to investigate downstream signaling pathways.

Different to curcumin, which was administered as a dispersion in PB, *Diffusa* and *Villosum* were provided as herbal tonics to better replicate their traditional modes of consumption in humans. Most studies investigating the therapeutic potential of herbal medicines have focused on nutraceutical formations[80], where extensive research has demonstrated that these highly concentrated derivatives containing bioactive compounds can attenuate IBD symptoms. For instance, *Cordyceps militaris* mushroom extract has been shown to alleviate epithelial damage while suppressing iNOS and TNF-α expressions[81]. Similarly, polyphenol extract from the native Chilean berry *Maqui* exert potent antioxidant and anti-inflammatory effects, reducing trinitrobenzene sulfonic acid (TNBS)-induced colitis by inhibiting the NF-κB and NOD-like receptor protein 3 (NLRP3) inflammasome pathways[66]. Pomegranate-derived ellagitannins and ellagic acid have also demonstrated anti-inflammatory activity by down-regulating TNF-α, COX-2, IL-4 and signal transducer and activation of transcription 6 (STAT6)[82]. Additionally, zingerone, a bioactive compound found in ginger that is also a botanical relative of *Villosum* has been reported to reduce mucosal injury[83], which further supports the potential gastrointestinal protective effects of this plant family and highlights the therapeutic potential of nutraceuticals in the context as viable alternatives for the treatment of IBD.

Efforts to isolate and characterize the bioactive components of Diffusa have revealed over 50 distinct compounds such as anthraquinones, iridoids and flavonoids[84]. Some of these have been isolated and extensively studied for their anti-tumor properties, particularly in colorectal

cancer[85], a severe complication of chronic, unregulated UC[9]. However, despite growing evidence of their therapeutic potential, the anti-inflammatory and antioxidant effects of Diffusa extracts remain largely untested in humans and in animal models of IBD. Similarly, *Villosum* has been found to contain bioactive polysaccharides and volatile oils with significant pharmacological properties. A study by Liu et al. identified two acidic polysaccharide extracts of Villosum (AVPG-1 and AVPG-2) that inhibited immune cell infiltration and protected the colon from ethanol-induced gastric mucosal injuries and exhibited potent anti-inflammatory and antioxidant effects by reducing MPO, TNF-α and MDA expressions and upregulating SOD expressions[86]. Another study demonstrated that water-based polysaccharide extracts and volatile oil from *Villosum* significantly attenuated TNBS-induced colitis, reducing IFN-γ levels whilst increasing IL-10 and TGF-β expressions[46], highlighting its potential for modulating inflammatory responses. Additionally, it should be noted that current study did not study the physiological role of these herbs on the gut epithelium in the absence of DSS administration. As a result, studies evaluating pharmacological safety and toxicity profiles of these herbs are also essential before their clinical application can be fully considered. Nevertheless, the findings from the present study align with previous literature, further substantiating the antioxidant and anti-inflammatory properties of these herbs in a form that closely resembles their traditional human consumption. While these results are promising, further research is necessary to elucidate the pharmacokinetics and pharmacodynamics differences between *Diffusa* and *Villosum* raw herbs and their corresponding bioactive compounds to determine whether more efficacious treatment outcomes can be achieved.

Glycerophospholipids play a crucial role in maintaining the integrity of the intestinal epithelial cell membrane whilst also serving as significant energy reserves and bioactive molecules during signal transduction[28]. Disruption in glycerophospholipid metabolism has been reported in IBD, where patients with CD exhibited decreased plasma levels of lysophosphatidylinositol, PC and PE[87], whilst UC patients displayed significant disturbances in PC, ceramide and sphingomyelin levels[32]. These findings suggest that lipid imbalance may be implicated in the pathogenesis of IBD through impaired membrane stability and cellular signaling pathways.

By mass, PC is the most abundant glycerophospholipid found in mammalian cell membranes[88], and alone this lipid class can exert anti-inflammatory effects by inhibiting M1 macrophage polarization and reducing expression of pro-inflammatory cytokines including TNF-α, IL-1β and IL-6[89,90]. Furthermore, both *in vitro* and *in vivo* studies have demonstrated that PC supplementation can enhance intestinal barrier function, modulate gut microbiota composition and mitigate inflammatory responses[91-93], highlighting its potential therapeutic value in IBD. In the current study, significantly reduced levels of PC, LPC and LPE were observed in DSS-challenged mice, indicating substantial alterations in glycerophospholipid composition in the colon, consistent with decreased colon PC levels being critical to promoting pathology. Subsequent metabolic pathway analysis highlighted that glycerophospholipid metabolism being one of the main affected pathways in these tissues, which further confirms these disruptions, suggesting that inflammation-associated metabolic shifts may compromise intestinal membrane integrity and cellular homeostasis during the pathogenesis of experimental colitis.

In addition to PC, PE represents the second most abundant phospholipid in the mammalian cells and is essential for providing mechanical protection to intestinal epithelial cells[94,95]. Notably, PE depletion has been linked to mitochondrial dysfunction as it negatively impacts

energy metabolism, impairs intestinal epithelial cell survival and disrupts gut homeostasis[96]. Additionally, PE also serves as a key precursor molecule for the endocannabinoid system, which regulates motility, barrier function and enteric nerve activity whilst promoting anti-inflammatory responses in the intestinal epithelium[97]. Interestingly, DSS insult resulted in a marked reduction of colonic PE species, whilst curcumin treatments significantly reduced PE abundance, which are in contrary to the outcomes described above. On the other hand, herbal treatments with *Diffusa* and *Villosum* tonics resulted in minimal changes to colon PE abundances.

Given the acute nature of the DSS-induced colitis model used in the current study, it is possible that the observed alterations in PE levels in the curcumin-treated mice reflect a temporary compensatory response by the intestinal epithelium to inflammation. In support of this notion, it has been demonstrated that mitochondrial respiration in colonic crypts is significantly upregulated during the inflammatory phase of colitis, likely due to the increased energy expenditure associated with intestinal repair and barrier restoration[98]. This heightened metabolic activity may contribute to the shift in PE metabolism observed in the current study. Furthermore, outcomes from the current study also highlighted a potential link between altered lipid metabolism and redox imbalance. However, the physiological consequences of dysregulated glycerophospholipid metabolism in DSS-induced experimental colitis remain to be elucidated. Future investigations probing the mechanistic implication of altered lipid metabolism in IBD could offer novel therapeutic strategies for managing intestinal inflammation.

Glycerolipid metabolism plays a fundamental role in maintaining cellular energy balance and gut homeostasis, primarily through the synthesis and hydrolysis of glycerolipids[99]. This process involves the esterification of free fatty acids to a glycerol backbone, forming neutral glycerolipids such as monoacylglycerols, DG and TG[100]. Among these lipids, DG serves as both an intermediate molecule in phospholipid biosynthesis and a signaling molecule capable of activating protein kinase C and NF-κB[101,102], thereby promoting downstream inflammatory cytokine production thereby, eliciting a heightened immune response. On the other hand, TG functions as crucial energy reserve in mammalian cells[103]. Alterations in glycerolipid metabolism have been implicated in IBD pathogenesis, with clinical studies reporting significantly lower TG levels in patients with mild UC compared to those who are in remission[104]. Interestingly, the present study showed that DSS-induced experimental colitis resulted in a marked reduction in DG abundance, coupled with a substantial increase in TG lipid species. This was also accompanied by decreased HSL activity in the lipolysis assay. Whilst these outcomes were contradictory to published literature in IBD patients, it is suggestive that DSS stimulation resulted in impaired lipid turnover and a significant disruption in glycerolipid metabolism within the inflamed colon. Additionally, the discrepancy observed here could possibly attributed to the acute nature of the DSS model employed in the current study, whereas IBD represents a pathological condition with a chronic time course. However, further study is warranted to address this difference. The treatment with powdered-curcumin and *Villosum* tonic reversed the changes of glycerolipid compositions, restoring DG and TG levels toward those observed in control mice. Thus, it is conceivable that the colon protective effects of curcumin and *Villosum* were mediated through reduced pro-inflammatory signaling (e.g., via protein kinase C and/or NF-κB activation).

In addition to glycerolipid metabolism, the present study also identified significant alterations in α-linolenic acid metabolism, a pathway known to be crucial in inflammatory regulation.

Alpha (α)-linolenic acid is an essential polyunsaturated fatty acid that serves as a precursor for the biosynthesis of bioactive omega-3 polyunsaturated fatty acids, including eicosapentaenoic acid and docosahexaenoic acid[105], both of which possess well-documented anti-inflammatory properties[106]. Given the essential role of these metabolites in modulating immune responses and maintaining gut homeostasis, disruption in α-linolenic acid metabolism pathway may contribute to disease progression in colitis. However, further investigations are warranted to elucidate the functional implication of these lipidomic changes.

A major limitation identified in the current study was the lack of short chain fatty acid (SCFA) analysis due to the volatility nature of this group of lipids. SCFA includes acetate, propionate, butyrate and valerate are products of the bacterial fermentation of undigested dietary fiber in the gut[107], in which they serve as energy source for colon enterocytes and also maintain gastrointestinal homeostatic balance by exerting anti-inflammatory effects to the colon mucosa[108,109]. Altered levels of SCFA have been documented in IBD patients, where significantly reduced levels of acetate, propionate and butyrate were reported in the stools of patients with UC[110,111], suggesting their potential role in implicating pathogenesis. Accordingly, the supplementation of butyrate or propionate has been shown to reduce colon inflammation and disease activity in both IBD patients and animals of experimental colitis[112-114]. As a result, analysis into the profiles of SCFA in the herbal remedies treated mice could provide a more comprehensive view of how these natural products influence the colon lipidome in the context of DSS-induced experimental colitis, which may pave the way to identify novel therapeutic targets and approach for UC treatments.

In summary, the current study investigated the therapeutic effects of curcumin, *Hedyotis Diffusa* and *Amomum Villosum* in a murine model of DSS-induced experimental colitis. It was demonstrated that treatment with these herbal remedies alleviated colitis-like symptoms and significantly increased expression of the antioxidant enzymes HO-1 and downregulated pro-inflammatory cytokine IFN-γ levels in the DSS-insulted colons. The current study also showed that DSS supplementation resulted in marked alteration to colon lipidome whilst treatments with curcumin, *Diffusa* and *Villosum* further adjusted the lipidome albeit, without returning the lipid composition to the control. These outcomes highlight a potential link between colon lipid compositions and redox imbalance during the pathogenesis of UC-like experimental colitis and through in silico pathway analysis provided 4 key pathways namely: (i) glycerophospholipid metabolism, (ii) glycophosphatidylinositol anchor biosynthesis, (iii) α-linolenic acid metabolism and (iv) glycerolipid metabolism that are also linked to several enzymic nodes that should be validated and explored further for potential therapeutic intervention.

5.5 References

1. Kobayashi, T., Siegmund, B., Le Berre, C., Wei, S.C., Ferrante, M., Shen, B., Bernstein, C.N., Danese, S., Peyrin-Biroulet, L., and Hibi, T. (2020). Ulcerative colitis. Nat Rev Dis Primers 6, 74. 10.1038/s41572-020-0205-x.

2. Yu, Y.R., and Rodriguez, J.R. (2017). Clinical presentation of Crohn's, ulcerative colitis, and indeterminate colitis: Symptoms, extraintestinal manifestations, and disease phenotypes. Semin Pediatr Surg 26, 349-355. 10.1053/j.sempedsurg.2017.10.003.

3. Riddell, R.H., Goldman, H., Ransohoff, D.F., Appelman, H.D., Fenoglio, C.M., Haggitt, R.C., Ahren, C., Correa, P., Hamilton, S.R., Morson, B.C., and et al. (1983). Dysplasia in inflammatory bowel disease: standardized classification with provisional clinical applications. Hum Pathol 14, 931-968. 10.1016/s0046-8177(83)80175-0.

4. Kuenzig, M.E., Lee, L., El-Matary, W., Weizman, A.V., Benchimol, E.I., Kaplan, G.G., Nguyen, G.C., Bernstein, C.N., Bitton, A., Lee, K., et al. (2019). The Impact of Inflammatory Bowel Disease in Canada 2018: Indirect Costs of IBD Care. J Can Assoc Gastroenterol 2, S34-S41. 10.1093/jcag/gwy050.

5. Rozich, J.J., Holmer, A., and Singh, S. (2020). Effect of Lifestyle Factors on Outcomes in Patients With Inflammatory Bowel Diseases. Am J Gastroenterol 115, 832-840. 10.14309/ajg.0000000000000608.

6. Le Berre, C., Honap, S., and Peyrin-Biroulet, L. (2023). Ulcerative colitis. Lancet 402, 571-584. 10.1016/S0140-6736(23)00966-2.

7. Ng, S.C., Kaplan, G.G., Tang, W., Banerjee, R., Adigopula, B., Underwood, F.E., Tanyingoh, D., Wei, S.C., Lin, W.C., Lin, H.H., et al. (2019). Population Density and Risk of Inflammatory Bowel Disease: A Prospective Population-Based Study in 13 Countries or Regions in Asia-Pacific. Am J Gastroenterol 114, 107-115. 10.1038/s41395-018-0233-2.

8. Greenstein, A.J., Sachar, D.B., Gibas, A., Schrag, D., Heimann, T., Janowitz, H.D., and Aufses, A.H., Jr. (1985). Outcome of toxic dilatation in ulcerative and Crohn's colitis. J Clin Gastroenterol 7, 137-143. 10.1097/00004836-198504000-00007.

9. Keller, D.S., Windsor, A., Cohen, R., and Chand, M. (2019). Colorectal cancer in inflammatory bowel disease: review of the evidence. Tech Coloproctol 23, 3-13. 10.1007/s10151-019-1926-2.

10. Kim, E.R., and Chang, D.K. (2014). Colorectal cancer in inflammatory bowel disease: the risk, pathogenesis, prevention and diagnosis. World J Gastroenterol 20, 9872-9881. 10.3748/wjg.v20.i29.9872.

11. Sato, Y., Tsujinaka, S., Miura, T., Kitamura, Y., Suzuki, H., and Shibata, C. (2023). Inflammatory Bowel Disease and Colorectal Cancer: Epidemiology, Etiology, Surveillance, and Management. Cancers (Basel) 15. 10.3390/cancers15164154.

12. Ananthakrishnan, A.N. (2015). Epidemiology and risk factors for IBD. Nat Rev Gastroenterol Hepatol 12, 205-217. 10.1038/nrgastro.2015.34.

13. Checa, J., and Aran, J.M. (2020). Reactive Oxygen Species: Drivers of Physiological and Pathological Processes. J Inflamm Res 13, 1057-1073. 10.2147/JIR.S275595.

14. Campbell, E.L., and Colgan, S.P. (2019). Control and dysregulation of redox signalling in the gastrointestinal tract. Nat Rev Gastroenterol Hepatol 16, 106-120. 10.1038/s41575-018-0079-5.

15. Dijkstra, G., Moshage, H., van Dullemen, H.M., de Jager-Krikken, A., Tiebosch, A.T., Kleibeuker, J.H., Jansen, P.L., and van Goor, H. (1998). Expression of nitric oxide synthases and formation of nitrotyrosine and reactive oxygen species in inflammatory bowel disease. J Pathol 186, 416-421. 10.1002/(SICI)1096-9896(199812)186:4<416::AID-PATH201>3.0.CO;2-U.

16. Wang, Y., Wang, W., Yang, H., Shao, D., Zhao, X., and Zhang, G. (2019). Intraperitoneal injection of 4-hydroxynonenal (4-HNE), a lipid peroxidation product, exacerbates colonic inflammation through activation of Toll-like receptor 4 signaling. Free Radic Biol Med 131, 237-242. 10.1016/j.freeradbiomed.2018.11.037.

17. D'Inca, R., Cardin, R., Benazzato, L., Angriman, I., Martines, D., and Sturniolo, G.C. (2004). Oxidative DNA damage in the mucosa of ulcerative colitis increases with disease duration and dysplasia. Inflamm Bowel Dis 10, 23-27. 10.1097/00054725-200401000-00003.

18. Lih-Brody, L., Powell, S.R., Collier, K.P., Reddy, G.M., Cerchia, R., Kahn, E., Weissman, G.S., Katz, S., Floyd, R.A., McKinley, M.J., et al. (1996). Increased oxidative stress and decreased antioxidant defenses in mucosa of inflammatory bowel disease. Dig Dis Sci 41, 2078-2086. 10.1007/BF02093613.

19. Kruidenier, L., Kuiper, I., Lamers, C.B., and Verspaget, H.W. (2003). Intestinal oxidative damage in inflammatory bowel disease: semi-quantification, localization, and association with mucosal antioxidants. J Pathol 201, 28-36. 10.1002/path.1409.

20. Ma, Q. (2013). Role of nrf2 in oxidative stress and toxicity. Annu Rev Pharmacol Toxicol 53, 401-426. 10.1146/annurev-pharmtox-011112-140320.

21. Genova, M.L., Ventura, B., Giuliano, G., Bovina, C., Formiggini, G., Parenti Castelli, G., and Lenaz, G. (2001). The site of production of superoxide radical in mitochondrial Complex I is not a bound ubisemiquinone but presumably iron-sulfur cluster N2. FEBS Lett 505, 364-368. 10.1016/s0014-5793(01)02850-2.

22. Pei, J., Pan, X., Wei, G., and Hua, Y. (2023). Research progress of glutathione peroxidase family (GPX) in redoxidation. Front Pharmacol 14, 1147414. 10.3389/fphar.2023.1147414.

23. Chen, Y.H., Yet, S.F., and Perrella, M.A. (2003). Role of heme oxygenase-1 in the regulation of blood pressure and cardiac function. Exp Biol Med (Maywood) 228, 447-453. 10.1177/15353702-0322805-03.

24. Rana, S.V., Sharma, S., Prasad, K.K., Sinha, S.K., and Singh, K. (2014). Role of oxidative stress & antioxidant defence in ulcerative colitis patients from north India. Indian J Med Res 139, 568-571.

25. Akman, T., Akarsu, M., Akpinar, H., Resmi, H., and Taylan, E. (2012). Erythrocyte deformability and oxidative stress in inflammatory bowel disease. Dig Dis Sci 57, 458-464. 10.1007/s10620-011-1882-9.

26. Harayama, T., and Riezman, H. (2018). Understanding the diversity of membrane lipid composition. Nat Rev Mol Cell Biol 19, 281-296. 10.1038/nrm.2017.138.

27. Morozumi, S., Ueda, M., Okahashi, N., and Arita, M. (2022). Structures and functions of the gut microbial lipidome. Biochim Biophys Acta Mol Cell Biol Lipids 1867, 159110. 10.1016/j.bbalip.2021.159110.

28. Boldyreva, L.V., Morozova, M.V., Saydakova, S.S., and Kozhevnikova, E.N. (2021). Fat of the Gut: Epithelial Phospholipids in Inflammatory Bowel Diseases. Int J Mol Sci 22. 10.3390/ijms222111682.

29. Vance, J.E. (2008). Phosphatidylserine and phosphatidylethanolamine in mammalian cells: two metabolically related aminophospholipids. J Lipid Res 49, 1377-1387. 10.1194/jlr.R700020-JLR200.

30. van der Veen, J.N., Kennelly, J.P., Wan, S., Vance, J.E., Vance, D.E., and Jacobs, R.L. (2017). The critical role of phosphatidylcholine and phosphatidylethanolamine metabolism in health and disease. Biochim Biophys Acta Biomembr 1859, 1558-1572. 10.1016/j.bbamem.2017.04.006.

31. Rohrhofer, J., Zwirzitz, B., Selberherr, E., and Untersmayr, E. (2021). The Impact of Dietary Sphingolipids on Intestinal Microbiota and Gastrointestinal Immune Homeostasis. Front Immunol 12, 635704. 10.3389/fimmu.2021.635704.

32. Diab, J., Hansen, T., Goll, R., Stenlund, H., Ahnlund, M., Jensen, E., Moritz, T., Florholmen, J., and Forsdahl, G. (2019). Lipidomics in Ulcerative Colitis Reveal Alteration in Mucosal Lipid Composition Associated With the Disease State. Inflamm Bowel Dis 25, 1780-1787. 10.1093/ibd/izz098.

33. Koutroumpakis, E., Ramos-Rivers, C., Regueiro, M., Hashash, J.G., Barrie, A., Swoger, J., Baidoo, L., Schwartz, M., Dunn, M.A., Koutroubakis, I.E., and Binion, D.G. (2016). Association Between Long-Term Lipid Profiles and Disease Severity in a Large Cohort of Patients with Inflammatory Bowel Disease. Dig Dis Sci 61, 865-871. 10.1007/s10620-015-3932-1.

34. Frisardi, V., Panza, F., Seripa, D., Farooqui, T., and Farooqui, A.A. (2011). Glycerophospholipids and glycerophospholipid-derived lipid mediators: a complex meshwork in Alzheimer's disease pathology. Prog Lipid Res 50, 313-330. 10.1016/j.plipres.2011.06.001.

35. Ruiz, M., Jove, M., Schluter, A., Casasnovas, C., Villarroya, F., Guilera, C., Ortega, F.J., Naudi, A., Pamplona, R., Gimeno, R., et al. (2015). Altered glycolipid and glycerophospholipid signaling drive inflammatory cascades in adrenomyeloneuropathy. Hum Mol Genet 24, 6861-6876. 10.1093/hmg/ddv375.

36. Hastings, R., Ding, T., Butt, S., Gadsby, K., Zhang, W., Moots, R.J., and Deighton, C. (2010). Neutropenia in patients receiving anti-tumor necrosis factor therapy. Arthritis Care Res (Hoboken) 62, 764-769. 10.1002/acr.20037.

37. Gisbert, J.P., Gonzalez-Lama, Y., and Mate, J. (2007). 5-Aminosalicylates and renal function in inflammatory bowel disease: a systematic review. Inflamm Bowel Dis 13, 629-638. 10.1002/ibd.20099.

38. Vecchi Brumatti, L., Marcuzzi, A., Tricarico, P.M., Zanin, V., Girardelli, M., and Bianco, A.M. (2014). Curcumin and inflammatory bowel disease: potential and limits of innovative treatments. Molecules 19, 21127-21153. 10.3390/molecules191221127.

39. Hanai, H., Iida, T., Takeuchi, K., Watanabe, F., Maruyama, Y., Andoh, A., Tsujikawa, T., Fujiyama, Y., Mitsuyama, K., Sata, M., et al. (2006). Curcumin maintenance therapy for ulcerative colitis: randomized, multicenter, double-blind, placebo-controlled trial. Clin Gastroenterol Hepatol 4, 1502-1506. 10.1016/j.cgh.2006.08.008.

40. Singla, V., Pratap Mouli, V., Garg, S.K., Rai, T., Choudhury, B.N., Verma, P., Deb, R., Tiwari, V., Rohatgi, S., Dhingra, R., et al. (2014). Induction with NCB-02 (curcumin) enema for mild-to-moderate distal ulcerative colitis - a randomized, placebo-controlled, pilot study. J Crohns Colitis 8, 208-214. 10.1016/j.crohns.2013.08.006.

41. Lang, A., Salomon, N., Wu, J.C., Kopylov, U., Lahat, A., Har-Noy, O., Ching, J.Y., Cheong, P.K., Avidan, B., Gamus, D., et al. (2015). Curcumin in Combination With Mesalamine Induces Remission in Patients With Mild-to-Moderate Ulcerative Colitis in a Randomized Controlled Trial. Clin Gastroenterol Hepatol 13, 1444-1449 e1441. 10.1016/j.cgh.2015.02.019.

42. Kim, S.J., Kim, Y.G., Kim, D.S., Jeon, Y.D., Kim, M.C., Kim, H.L., Kim, S.Y., Jang, H.J., Lee, B.C., Hong, S.H., and Um, J.Y. (2011). Oldenlandia diffusa Ameliorates Dextran Sulphate Sodium-Induced Colitis Through Inhibition of NF-kappaB Activation. Am J Chin Med 39, 957-969. 10.1142/S0192415X11009330.

43. Lim, D.W., Choi, H.J., Park, S.D., Kim, H., Yu, G.R., Kim, J.E., and Park, W.H. (2020). Activation of the Nrf2/HO-1 Pathway by Amomum villosum Extract Suppresses LPS-Induced Oxidative Stress In Vitro and Ex Vivo. Evid Based Complement Alternat Med 2020, 2837853. 10.1155/2020/2837853.

44. Ahmad, G., Chami, B., Liu, Y., Schroder, A.L., San Gabriel, P.T., Gao, A., Fong, G., Wang, X., and Witting, P.K. (2020). The Synthetic Myeloperoxidase Inhibitor AZD3241 Ameliorates Dextran Sodium Sulfate Stimulated Experimental Colitis. Front Pharmacol 11, 556020. 10.3389/fphar.2020.556020.

45. Chassaing, B., Aitken, J.D., Malleshappa, M., and Vijay-Kumar, M. (2014). Dextran sulfate sodium (DSS)-induced colitis in mice. Curr Protoc Immunol 104, 15 25 11-15 25 14. 10.1002/0471142735.im1525s104.

46. Chen, Z., Ni, W., Yang, C., Zhang, T., Lu, S., Zhao, R., Mao, X., and Yu, J. (2018). Therapeutic Effect of Amomum villosum on Inflammatory Bowel Disease in Rats. Front Pharmacol 9, 639. 10.3389/fphar.2018.00639.

47. Ye, J.H., Liu, M.H., Zhang, X.L., and He, J.Y. (2015). Chemical Profiles and Protective Effect of Hedyotis diffusa Willd in Lipopolysaccharide-Induced Renal Inflammation Mice. Int J Mol Sci 16, 27252-27269. 10.3390/ijms161126021.

48. Farombi, E.O., and Ekor, M. (2006). Curcumin attenuates gentamicin-induced renal oxidative damage in rats. Food Chem Toxicol 44, 1443-1448. 10.1016/j.fct.2006.05.005.

49. Zhou, J., Li, M., Chen, Q., Li, X., Chen, L., Dong, Z., Zhu, W., Yang, Y., Liu, Z., and Chen, Q. (2022). Programmable probiotics modulate inflammation and gut microbiota for inflammatory bowel disease treatment after effective oral delivery. Nat Commun 13, 3432. 10.1038/s41467-022-31171-0.

50. Praveschotinunt, P., Duraj-Thatte, A.M., Gelfat, I., Bahl, F., Chou, D.B., and Joshi, N.S. (2019). Engineered E. coli Nissle 1917 for the delivery of matrix-tethered therapeutic domains to the gut. Nat Commun 10, 5580. 10.1038/s41467-019-13336-6.

51. Gross, S., Gammon, S.T., Moss, B.L., Rauch, D., Harding, J., Heinecke, J.W., Ratner, L., and Piwnica-Worms, D. (2009). Bioluminescence imaging of myeloperoxidase activity in vivo. Nat Med 15, 455-461. 10.1038/nm.1886.

52. Matyash, V., Liebisch, G., Kurzchalia, T.V., Shevchenko, A., and Schwudke, D. (2008). Lipid extraction by methyl-tert-butyl ether for high-throughput lipidomics. J Lipid Res 49, 1137-1146. 10.1194/jlr.D700041-JLR200.

53. Breitkopf, S.B., Ricoult, S.J.H., Yuan, M., Xu, Y., Peake, D.A., Manning, B.D., and Asara, J.M. (2017). A relative quantitative positive/negative ion switching method for untargeted lipidomics via high resolution LC-MS/MS from any biological source. Metabolomics 13. 10.1007/s11306-016-1157-8.

54. Remmele, W., and Stegner, H.E. (1987). [Recommendation for uniform definition of an immunoreactive score (IRS) for immunohistochemical estrogen receptor detection (ER-ICA) in breast cancer tissue]. Pathologe 8, 138-140.

55. Rios Garcia, M., Steinbauer, B., Srivastava, K., Singhal, M., Mattijssen, F., Maida, A., Christian, S., Hess-Stumpp, H., Augustin, H.G., Muller-Decker, K., et al. (2017). Acetyl-CoA Carboxylase 1-Dependent Protein Acetylation Controls Breast Cancer Metastasis and Recurrence. Cell Metab 26, 842-855 e845. 10.1016/j.cmet.2017.09.018.

56. Deng, Y., Pan, M., Nie, H., Zheng, C., Tang, K., Zhang, Y., and Yang, Q. (2019). Lipidomic Analysis of the Protective Effects of Shenling Baizhu San on Non-Alcoholic Fatty Liver Disease in Rats. Molecules 24. 10.3390/molecules24213943.

57. Yu, L., Sun, R., Xu, K., Pu, Y., Huang, J., Liu, M., Chen, M., Zhang, J., Yin, L., and Pu, Y. (2021). Lipidomic analysis reveals disturbances in glycerophospholipid and sphingolipid metabolic pathways in benzene-exposed mice. Toxicol Res (Camb) 10, 706-718. 10.1093/toxres/tfab053.

58. Ge, N., Kong, L., Zhang, A.H., Sun, Y., Zhao, M.Q., Zhang, B., Xu, L., Ke, X., Sun, H., and Wang, X.J. (2021). Identification of key lipid metabolites during metabolic dysregulation in the diabetic retinopathy disease mouse model and efficacy of Keluoxin capsule using an UHPLC-MS-based non-targeted lipidomics approach. RSC Adv 11, 5491-5505. 10.1039/d0ra00343c.

59. Luther, J., Owyang, S.Y., Takeuchi, T., Cole, T.S., Zhang, M., Liu, M., Erb-Downward, J., Rubenstein, J.H., Chen, C.C., Pierzchala, A.V., et al. (2011). Helicobacter pylori DNA

decreases pro-inflammatory cytokine production by dendritic cells and attenuates dextran sodium sulphate-induced colitis. Gut 60, 1479-1486. 10.1136/gut.2010.220087.

60. El-Kheshen, G., Moeini, M., and Saadat, M. (2016). Susceptibility to Ulcerative Colitis and Genetic Polymorphisms of A251G SOD1 and C-262T CAT. J Med Biochem 35, 333-336. 10.1515/jomb-2016-0002.

61. Cai, Z., Wang, S., and Li, J. (2021). Treatment of Inflammatory Bowel Disease: A Comprehensive Review. Front Med (Lausanne) 8, 765474. 10.3389/fmed.2021.765474.

62. Ben-Horin, S., Kopylov, U., and Chowers, Y. (2014). Optimizing anti-TNF treatments in inflammatory bowel disease. Autoimmun Rev 13, 24-30. 10.1016/j.autrev.2013.06.002.

63. Taffet, S.L., and Das, K.M. (1983). Sulfasalazine. Adverse effects and desensitization. Dig Dis Sci 28, 833-842. 10.1007/BF01296907.

64. Chen, Y., Zhang, G., Yang, Y., Zhang, S., Jiang, H., Tian, K., Arenbaoligao, and Chen, D. (2023). The treatment of inflammatory bowel disease with monoclonal antibodies in Asia. Biomed Pharmacother 157, 114081. 10.1016/j.biopha.2022.114081.

65. Triantafyllidi, A., Xanthos, T., Papalois, A., and Triantafillidis, J.K. (2015). Herbal and plant therapy in patients with inflammatory bowel disease. Ann Gastroenterol 28, 210-220.

66. Ortiz-Cerda, T., Arguelles-Arias, F., Macias-Garcia, L., Vazquez-Roman, V., Tapia, G., Xie, K., Garcia-Garcia, M.D., Merinero, M., Garcia-Montes, J.M., Alcudia, A., et al. (2023). Effects of polyphenolic maqui (Aristotelia chilensis) extract on the inhibition of NLRP3 inflammasome and activation of mast cells in a mouse model of Crohn's disease-like colitis. Front Immunol 14, 1229767. 10.3389/fimmu.2023.1229767.

67. Langmead, L., Feakins, R.M., Goldthorpe, S., Holt, H., Tsironi, E., De Silva, A., Jewell, D.P., and Rampton, D.S. (2004). Randomized, double-blind, placebo-controlled trial of oral aloe vera gel for active ulcerative colitis. Aliment Pharmacol Ther 19, 739-747. 10.1111/j.1365-2036.2004.01902.x.

68. Pervin, M., Hasnat, M.A., Lim, J.H., Lee, Y.M., Kim, E.O., Um, B.H., and Lim, B.O. (2016). Preventive and therapeutic effects of blueberry (Vaccinium corymbosum) extract against DSS-induced ulcerative colitis by regulation of antioxidant and inflammatory mediators. J Nutr Biochem 28, 103-113. 10.1016/j.jnutbio.2015.10.006.

69. Suluvoy, J.K., Sakthivel, K.M., Guruvayoorappan, C., and Berlin Grace, V.M. (2017). Protective effect of Averrhoa bilimbi L. fruit extract on ulcerative colitis in wistar rats via regulation of inflammatory mediators and cytokines. Biomed Pharmacother 91, 1113-1121. 10.1016/j.biopha.2017.05.057.

70. Pierzchala, K., Pieta, M., Rola, M., Swierczynska, M., Artelska, A., Debowska, K., Podsiadly, R., Pieta, J., Zielonka, J., Sikora, A., et al. (2022). Fluorescent probes for monitoring myeloperoxidase-derived hypochlorous acid: a comparative study. Sci Rep 12, 9314. 10.1038/s41598-022-13317-8.

71. Davies, M.J., and Hawkins, C.L. (2020). The Role of Myeloperoxidase in Biomolecule Modification, Chronic Inflammation, and Disease. Antioxid Redox Signal 32, 957-981. 10.1089/ars.2020.8030.

72. Chami, B., Martin, N.J.J., Dennis, J.M., and Witting, P.K. (2018). Myeloperoxidase in the inflamed colon: A novel target for treating inflammatory bowel disease. Arch Biochem Biophys 645, 61-71. 10.1016/j.abb.2018.03.012.

73. Sabzevary-Ghahfarokhi, M., Shohan, M., Shirzad, H., Rahimian, G., Soltani, A., Ghatreh-Samani, M., Deris, F., Bagheri, N., Shafigh, M., and Tahmasbi, K. (2018). The regulatory role of Nrf2 in antioxidants phase2 enzymes and IL-17A expression in patients with ulcerative colitis. Pathol Res Pract 214, 1149-1155. 10.1016/j.prp.2018.06.001.

74. Li, J., Wang, H., Zheng, Z., Luo, L., Wang, P., Liu, K., Namani, A., Jiang, Z., Wang, X.J., and Tang, X. (2018). Mkp-1 cross-talks with Nrf2/Ho-1 pathway protecting against intestinal inflammation. Free Radic Biol Med 124, 541-549. 10.1016/j.freeradbiomed.2018.07.002.

75. Sangaraju, R., Nalban, N., Alavala, S., Rajendran, V., Jerald, M.K., and Sistla, R. (2019). Protective effect of galangin against dextran sulfate sodium (DSS)-induced ulcerative colitis in Balb/c mice. Inflamm Res 68, 691-704. 10.1007/s00011-019-01252-w.

76. Hu, X., Chakravarty, S.D., and Ivashkiv, L.B. (2008). Regulation of interferon and Toll-like receptor signaling during macrophage activation by opposing feedforward and feedback inhibition mechanisms. Immunol Rev 226, 41-56. 10.1111/j.1600-065X.2008.00707.x.

77. Ito, R., Shin-Ya, M., Kishida, T., Urano, A., Takada, R., Sakagami, J., Imanishi, J., Kita, M., Ueda, Y., Iwakura, Y., et al. (2006). Interferon-gamma is causatively involved in experimental inflammatory bowel disease in mice. Clin Exp Immunol 146, 330-338. 10.1111/j.1365-2249.2006.03214.x.

78. Obermeier, F., Kojouharoff, G., Hans, W., Scholmerich, J., Gross, V., and Falk, W. (1999). Interferon-gamma (IFN-gamma)- and tumour necrosis factor (TNF)-induced nitric oxide as toxic effector molecule in chronic dextran sulphate sodium (DSS)-induced colitis in mice. Clin Exp Immunol 116, 238-245. 10.1046/j.1365-2249.1999.00878.x.

79. Sadar, S.S., Vyawahare, N.S., and Bodhankar, S.L. (2016). Ferulic acid ameliorates TNBS-induced ulcerative colitis through modulation of cytokines, oxidative stress, iNOs, COX-2, and apoptosis in laboratory rats. EXCLI J 15, 482-499. 10.17179/excli2016-393.

80. Mijan, M.A., and Lim, B.O. (2018). Diets, functional foods, and nutraceuticals as alternative therapies for inflammatory bowel disease: Present status and future trends. World J Gastroenterol 24, 2673-2685. 10.3748/wjg.v24.i25.2673.

81. Han, E.S., Oh, J.Y., and Park, H.J. (2011). Cordyceps militaris extract suppresses dextran sodium sulfate-induced acute colitis in mice and production of inflammatory mediators from macrophages and mast cells. J Ethnopharmacol 134, 703-710. 10.1016/j.jep.2011.01.022.

82. Kamali, M., Tavakoli, H., Khodadoost, M., Daghaghzadeh, H., Kamalinejad, M., Gachkar, L., Mansourian, M., and Adibi, P. (2015). Efficacy of the Punica granatum peels aqueous extract for symptom management in ulcerative colitis patients. A randomized, placebo-controlled, clinical trial. Complement Ther Clin Pract 21, 141-146. 10.1016/j.ctcp.2015.03.001.

83. Hsiang, C.Y., Lo, H.Y., Huang, H.C., Li, C.C., Wu, S.L., and Ho, T.Y. (2013). Ginger extract and zingerone ameliorated trinitrobenzene sulphonic acid-induced colitis in mice via modulation of nuclear factor-kappaB activity and interleukin-1beta signalling pathway. Food Chem 136, 170-177. 10.1016/j.foodchem.2012.07.124.

84. Han, X., Zhang, X., Wang, Q., Wang, L., and Yu, S. (2020). Antitumor potential of Hedyotis diffusa Willd: A systematic review of bioactive constituents and underlying molecular mechanisms. Biomed Pharmacother 130, 110735. 10.1016/j.biopha.2020.110735.

85. Wu, Z., Yin, B., and You, F. (2022). Molecular Mechanism of Anti-Colorectal Cancer Effect of Hedyotis diffusa Willd and Its Extracts. Front Pharmacol 13, 820474. 10.3389/fphar.2022.820474.

86. Liu, H., Zhuang, S., Liang, C., He, J., Brennan, C.S., Brennan, M.A., Ma, L., Xiao, G., Chen, H., and Wan, S. (2022). Effects of a polysaccharide extract from Amomum villosum Lour. on gastric mucosal injury and its potential underlying mechanism. Carbohydr Polym 294, 119822. 10.1016/j.carbpol.2022.119822.

87. Iwatani, S., Iijima, H., Otake, Y., Amano, T., Tani, M., Yoshihara, T., Tashiro, T., Tsujii, Y., Inoue, T., Hayashi, Y., et al. (2020). Novel mass spectrometry-based comprehensive lipidomic analysis of plasma from patients with inflammatory bowel disease. J Gastroenterol Hepatol 35, 1355-1364. 10.1111/jgh.15067.

88. Farooqui, A.A., Horrocks, L.A., and Farooqui, T. (2000). Glycerophospholipids in brain: their metabolism, incorporation into membranes, functions, and involvement in neurological disorders. Chem Phys Lipids 106, 1-29. 10.1016/s0009-3084(00)00128-6.

89. Ai, R., Xu, J., Ji, G., and Cui, B. (2022). Exploring the Phosphatidylcholine in Inflammatory Bowel Disease: Potential Mechanisms and Therapeutic Interventions. Curr Pharm Des 28, 3486-3491. 10.2174/1381612829666221124112803.

90. Chen, C., Quan, J., Chen, X., Yang, T., Yu, C., Ye, S., Yang, Y., Wu, X., Jiang, D., and Weng, Y. (2024). Explore key genes of Crohn's disease based on glycerophospholipid metabolism: A comprehensive analysis Utilizing Mendelian Randomization, Multi-Omics integration, Machine Learning, and SHAP methodology. Int Immunopharmacol 141, 112905. 10.1016/j.intimp.2024.112905.

91. Li, Q., Chen, G., Zhu, D., Zhang, W., Qi, S., Xue, X., Wang, K., and Wu, L. (2022). Effects of dietary phosphatidylcholine and sphingomyelin on DSS-induced colitis by regulating metabolism and gut microbiota in mice. J Nutr Biochem 105, 109004. 10.1016/j.jnutbio.2022.109004.

92. Kovacs, T., Varga, G., Erces, D., Tokes, T., Tiszlavicz, L., Ghyczy, M., Boros, M., and Kaszaki, J. (2012). Dietary phosphatidylcholine supplementation attenuates inflammatory mucosal damage in a rat model of experimental colitis. Shock 38, 177-185. 10.1097/SHK.0b013e31825d1ed0.

93. Leucht, K., Fischbeck, A., Caj, M., Liebisch, G., Hartlieb, E., Benes, P., Fried, M., Humpf, H.U., Rogler, G., and Hausmann, M. (2014). Sphingomyelin and phosphatidylcholine contrarily affect the induction of apoptosis in intestinal epithelial cells. Mol Nutr Food Res 58, 782-798. 10.1002/mnfr.201300369.

94. Calzada, E., Onguka, O., and Claypool, S.M. (2016). Phosphatidylethanolamine Metabolism in Health and Disease. Int Rev Cell Mol Biol 321, 29-88. 10.1016/bs.ircmb.2015.10.001.

95. Vance, J.E. (2015). Phospholipid synthesis and transport in mammalian cells. Traffic 16, 1-18. 10.1111/tra.12230.

96. Kennelly, J.P., Carlin, S., Ju, T., van der Veen, J.N., Nelson, R.C., Buteau, J., Thiesen, A., Richard, C., Willing, B.P., and Jacobs, R.L. (2021). Intestinal Phospholipid Disequilibrium Initiates an ER Stress Response That Drives Goblet Cell Necroptosis and Spontaneous Colitis in Mice. Cell Mol Gastroenterol Hepatol 11, 999-1021. 10.1016/j.jcmgh.2020.11.006.

97. Lu, H.C., and Mackie, K. (2016). An Introduction to the Endogenous Cannabinoid System. Biol Psychiatry 79, 516-525. 10.1016/j.biopsych.2015.07.028.

98. Lan, A., Guerbette, T., Andriamihaja, M., Magnin, B., Bordet, M., Ferron, P.J., Burel, A., Viel, R., Fromenty, B., Corlu, A., et al. (2023). Mitochondrial remodeling and energy metabolism adaptations in colonic crypts during spontaneous epithelial repair after colitis induction in mice. Free Radic Biol Med 205, 224-233. 10.1016/j.freeradbiomed.2023.06.007.

99. Prentki, M., and Madiraju, S.R. (2008). Glycerolipid metabolism and signaling in health and disease. Endocr Rev 29, 647-676. 10.1210/er.2008-0007.

100. Prentki, M., Corkey, B.E., and Madiraju, S.R.M. (2020). Lipid-associated metabolic signalling networks in pancreatic beta cell function. Diabetologia 63, 10-20. 10.1007/s00125-019-04976-w.

101. Jornayvaz, F.R., and Shulman, G.I. (2012). Diacylglycerol activation of protein kinase Cepsilon and hepatic insulin resistance. Cell Metab 15, 574-584. 10.1016/j.cmet.2012.03.005.

102. Yang, C., and Kazanietz, M.G. (2007). Chimaerins: GAPs that bridge diacylglycerol signalling and the small G-protein Rac. Biochem J 403, 1-12. 10.1042/BJ20061750.

103. Alves-Bezerra, M., and Cohen, D.E. (2017). Triglyceride Metabolism in the Liver. Compr Physiol 8, 1-8. 10.1002/cphy.c170012.

104. Bazarganipour, S., Hausmann, J., Oertel, S., El-Hindi, K., Brachtendorf, S., Blumenstein, I., Kubesch, A., Sprinzl, K., Birod, K., Hahnefeld, L., et al. (2019). The Lipid Status in Patients with Ulcerative Colitis: Sphingolipids are Disease-Dependent Regulated. J Clin Med 8. 10.3390/jcm8070971.

105. Burdge, G.C. (2006). Metabolism of alpha-linolenic acid in humans. Prostaglandins Leukot Essent Fatty Acids 75, 161-168. 10.1016/j.plefa.2006.05.013.

106. Reifen, R., Karlinsky, A., Stark, A.H., Berkovich, Z., and Nyska, A. (2015). alpha-Linolenic acid (ALA) is an anti-inflammatory agent in inflammatory bowel disease. J Nutr Biochem 26, 1632-1640. 10.1016/j.jnutbio.2015.08.006.

107. Dalile, B., Van Oudenhove, L., Vervliet, B., and Verbeke, K. (2019). The role of short-chain fatty acids in microbiota-gut-brain communication. Nat Rev Gastroenterol Hepatol 16, 461-478. 10.1038/s41575-019-0157-3.

108. Donohoe, D.R., Garge, N., Zhang, X., Sun, W., O'Connell, T.M., Bunger, M.K., and Bultman, S.J. (2011). The microbiome and butyrate regulate energy metabolism and autophagy in the mammalian colon. Cell Metab 13, 517-526. 10.1016/j.cmet.2011.02.018.

109. Zhang, Z., Zhang, H., Chen, T., Shi, L., Wang, D., and Tang, D. (2022). Regulatory role of short-chain fatty acids in inflammatory bowel disease. Cell Commun Signal 20, 64. 10.1186/s12964-022-00869-5.

110. Machiels, K., Joossens, M., Sabino, J., De Preter, V., Arijs, I., Eeckhaut, V., Ballet, V., Claes, K., Van Immerseel, F., Verbeke, K., et al. (2014). A decrease of the butyrate-producing species Roseburia hominis and Faecalibacterium prausnitzii defines dysbiosis in patients with ulcerative colitis. Gut 63, 1275-1283. 10.1136/gutjnl-2013-304833.

111. Takaishi, H., Matsuki, T., Nakazawa, A., Takada, T., Kado, S., Asahara, T., Kamada, N., Sakuraba, A., Yajima, T., Higuchi, H., et al. (2008). Imbalance in intestinal microflora constitution could be involved in the pathogenesis of inflammatory bowel disease. Int J Med Microbiol 298, 463-472. 10.1016/j.ijmm.2007.07.016.

112. Luhrs, H., Gerke, T., Muller, J.G., Melcher, R., Schauber, J., Boxberge, F., Scheppach, W., and Menzel, T. (2002). Butyrate inhibits NF-kappaB activation in lamina propria macrophages of patients with ulcerative colitis. Scand J Gastroenterol 37, 458-466. 10.1080/003655202317316105.

113. Hamer, H.M., Jonkers, D.M., Vanhoutvin, S.A., Troost, F.J., Rijkers, G., de Bruine, A., Bast, A., Venema, K., and Brummer, R.J. (2010). Effect of butyrate enemas on inflammation and antioxidant status in the colonic mucosa of patients with ulcerative colitis in remission. Clin Nutr 29, 738-744. 10.1016/j.clnu.2010.04.002.

114. Park, J.H., Kotani, T., Konno, T., Setiawan, J., Kitamura, Y., Imada, S., Usui, Y., Hatano, N., Shinohara, M., Saito, Y., et al. (2016). Promotion of Intestinal Epithelial Cell Turnover by Commensal Bacteria: Role of Short-Chain Fatty Acids. PLoS One 11, e0156334. 10.1371/journal.pone.0156334.

5.6 Additional Information

5.6.1 Conflict of Interests

The authors declare no conflict of interest was associated with the experimental design, analysis and reporting of the study.

5.6.2 Funding

The current study was supported by NHMRC Project Grant (APP1125392) awarded to senior author P.K.W and the Crohn's and Colitis Foundation Litwin IBD Pioneers grant (827399) and the University of Sydney Commercial Development and Industry Partnerships program grant (CT31847) awarded to B.C and P.K.W. First author K.X was supported by the University of Sydney funded postgraduate scholarship whist second-first author T.O.C was supported by the Spanish Ministry of Universities 'Magarita Salas' grant for the training of young doctors. Author N.S was financially supported by the University of Sydney Honours scholarship.

5.6.3 Ethics approval

All experiments involving animals were in accordance with standards guidelines for the care and use of laboratory animals. All procedures performed in studies were following the approved protocol by the University of Sydney Animal Ethics Committee (Approval #2019/1496).

5.6.4 CRediT authorship contribution statement:

Kangzhe Xie (K.X); Investigation, validation, methodology, formal analysis, data curation, and writing – original draft. Tamara Ortiz-Cerda (T.O.C.); Investigation, validation, formal analysis, data curation, supervision, and writing – original draft. Nicolette Shiung (N.S); Investigation, validation, methodology and formal analysis. Siqi Chen (S.C); Investigation, validation and formal analysis. Laylaa Hoosen (L.H); Investigation, validation and formal analysis. Gulfam Ahmad (G.A); Conceptualization, methodology and formal analysis. Bruno Lemos Wimmer (B.L.W); Investigation and formal analysis. Ash David (A.D); Investigation, validation and formal analysis. Belal Chami (B.C); Conceptualization, methodology and resources. Xiaosuo Wang (X.W); Methodology, validation and software. Collin Tran (C.T); Methodology, validation and software. John O'Sullivan (J.O.S); Resources. Anthony S. Don (A.S.D); Resources. Paul K. Witting (P.K.W.): Conceptualization, methodology, project administration, supervision and review & editing of the manuscript.

5.6.5 Acknowledgements

The authors would like to acknowledge Dr. Samson Dowland from the Charles Perkins Centre Histology Facility and Dr. Kang-Yu Peng and Dr. Atul Bhatnagar from the Sydney Mass Spectrometry (SydneyMS) of the at The University of Sydney for the resources, scientific and technical expertise provided for the completion of the current study.

Herbal remedies curcumin, *Hedyotis diffusa* and *Amomum villosum* reduced colon inflammation by altering colon lipidome and restoring dysregulated redox balance in an animal model of ulcerative colitis

Kangzhe Xie[1*], Tamara Ortiz-Cerda[1,2*], Nicolette Shiung[1], Siqi Chen[1], Laylaa Hoosen[1], Gulfam Ahmad[3], Bruno Lemos Wimmer[1,4], Ash David[1], Belal Chami[5], Xiaosuo Wang[6], Collin Tran[7], John O'Sullivan[6], Anthony S. Don[7] & Paul K. Witting[1#].

1. Redox Biology Group, Charles Perkins Centre, School of Medical Sciences, Faculty of Medicine & Health, The University of Sydney, NSW 2006, Australia.

2. Departmento de Citología e Histología Normal y Patológica, Facultad de Medicina, Universidad de Sevilla, Avda. Sanchez-Pizjuan s/n 41009, Seville, Spain.

3. Andrology Department, Royal Women's and Children's Pathology, Carlton, VIC 3053, Australia.

4. Department of Life Sciences, Faculty of Chemistry, The University of Konstanz, BW, 78464 Konstanz, Germany.

5. Redox Inflammation Group, Charles Perkins Centre, School of Medical Sciences, Faculty of Medicine & Health, The University of Sydney, NSW 2006, Australia.

6. Cardiometabolic Medicine Group, Charles Perkins Centre, School of Medical Sciences, Faculty of Medicine & Health, The University of Sydney, NSW 2006, Australia.

7. Brain Lipidomic and Metabolism Group, Charles Perkins Centre, School of Medical Sciences, Faculty of Medicine & Health, The University of Sydney, NSW 2006, Australia.

* Kangzhe Xie and Tamara Ortiz-Cerda contributed equally in all aspect of the study and shares joint first-authorship of this manuscript.

Address correspondence to: Professor Paul K. Witting (paul.witting@sydney.edu.au), Level 4 West Room 4212, Charles Perkins Centre, The University of Sydney, NSW 2006, Australia.

Supplementary Material

Supplementary Tables

Supplementary Table 5.1. List of reagents used for animal experiment.

Reagents	Catalogue Number	Supplier
0.5% alcoholic eosin Y-solution	1.02439	Sigma Aldrich
2,6-Di-tert-butyl-4-methylphenol	112990010	ACROS
30% hydrogen peroxide	H3410	Sigma Aldrich
4-15% Mini-PROTEAN TGX precast protein gels – 15-well	4561086	Bio-Rad
Acetic acid	695092	Sigma Aldrich
Acetonitrile	FSBA955-4	Thermo Fisher
Alcian blue 8GX powder	A5268	Sigma Aldrich
Ammonium formate	714690	Supelco
Amomum villosum	110001-1	Beijing Tongrentang Sydney
Bovine serum albumin	A7906	Sigma Aldrich
Clarity Western ECL substrate	1705060	Bio-Rad
cOmplete protease inhibitor cocktail	CO-RO	Roche
Curcumin	110001-2	Beijing Tongrentang Sydney
DAB substrate kit	K3468	DAKO
Disodium 5-amino-2,3-dihydro-1,4-phthalazinedion	A4685	Sigma Aldrich
DPX medium	06522	Sigma Aldrich
Ethylenediamine-tetra-acetic acid	E6758	Sigma Aldrich
Formalin solution, neutral buffered, 105	HT501640	Sigma Aldrich
Formic acid	5.33002	Supelco
Glycine	AJA1083	Ajax Finechem
Harris hematoxylin solution	HHS32	Sigma Aldrich
Hedyotis diffusa	110001-3	Beijing Tongrentang Sydney
Histolene	H2779	Sigma Aldrich
Isopropyl alcohol	34863	Sigma Aldrich
LCMS grade water	1.15333	Supelco
Lipolysis (3T3-L1) colorimetric assay kit	MAK211	Sigma Aldrich
Methanol	1.06035	Supelco
Methyl tert-butyl ether	34875	Sigma Aldrich
Peanut butter	-	Bega
PhosSTOP	PHOSS-RO	Roche
Safranin O	S2255	Sigma Aldrich
Scott's Tap Water Substitute Concentrate	S5134	Sigma Aldrich
Serum-free protein block	X0909	DAKO
Skim milk powder	-	Coles
Sodium azide	S2002	Sigma Aldrich
Sodium dodecyl sulfate	428023	Calbiochem
Trans-Blot Turbo Midi 0.2 μm PVDF transfer packs	1704157	Bio-Rad
Triton X-100	270733	Sigma Aldrich

Reagents were listed in alphabetical order. Antibodies used for immunohistochemical, immunofluorescence and western blot analyses were summarized in other tables below.

Supplementary Table 5.2. Scoring criteria applied to yield a universal clinical parameter.

Clinical Markers	Score	Description
Body Weight	0	No weight loss
	1	1-10% weight loss
	2	>10% weight loss
Stool and/or bleeding	0	Normal consistency of stool
	1	Soft stool
	2	Watery/bloody stool
Grooming	0	No hunched posture, bristle fur, or skin lesions
	1	Presence of hunched posture, bristle fur or skin lesions
Presence of rectal prolapse	0	Not present
	1	Prolapse present

Supplementary Table 5.3. Clinical assessment scoring criteria applied to observational histological data.

Pathological Parameter	Score	Description
Loss of crypts	0	Intact crypts
	1	Disoriented crypts
	2	Crypts with variable diameters
	3	Presence of crypts atrophy
	4	Mucosa devoid of crypts
Loss of surface epithelium	0	Intact surface epithelium
	1	Sloughing off of surface epithelium
	2	Patchy loss of surface epithelium
	3	Moderate loss of surface epithelium
	4	Severe loss/erosion of surface epithelium
Cellular Infiltration	0	No immune infiltration presence
	1	Infiltration to the lamina propria/mucosa
	2	Infiltration to mucosa and submucosa
	3	Infiltration to crypts and moderate cryptitis
	4	Infiltration to crypts and severe cryptitis

Supplementary Table 5.4. Criteria for dysplasia scoring applied to histological images.

Histological criterion	Description
Enlarged crypts	Increased crypt width or length
Enlarged and hyperchromatic nucleus	Increased nuclear to cytoplasmic ratio accompanied with intense staining of nucleus
Stratification of epithelial cells	No all crypts are attached to the basement membrane
Dystrophic goblet cells	Lack of goblet cells and crypt lumen stains pink in H&E stain

Supplementary Table 5.5. Clinical assessment scoring criteria applied to observational histological data.

Grade	Score	Description
No dysplasia	0	No histological criterion for dysplasia is present
Indefinite but probably negative	1	1 histological criterion is present and accompanied with inflammation or surface maturation
Indefinite but probably positive	2	More than 1 histological criterion for dysplasia is present and accompanied with inflammation or surface maturation
Positive dysplasia	3	All 4 histological criteria for dysplasia are present

Supplementary Table 5.6 Heat induced antigen retrieval reagents and decloaking chamber settings for immunofluorescence and immunohistochemical staining.

Antigen	Retrieval Buffer	Antibodies Catalogue No. (Dilution)	Supplier	Decloaking Chamber Settings
Nrf2	pH 9.0 EDTA-based	ab137550 (1:2000)	abcam	Pre-heat at 80℃ for 30 s, heat-induced retrieval at 125℃ for 30 s, cooling fan-on at 95℃ and cooling fan-off at 90℃.
HO-1	pH 9.0 EDTA-based	SAB5700731 (1:500)	Sigma Aldrich	
SOD1	pH 9.0 EDTA-based	SAB5200083 (1:800)	Sigma Aldrich	
4HNE	pH 6.0 sodium citrate based	BS-6313R (1:500)	Bioss	
GPx4	pH 9.0 EDTA-based	ab125066 (1:300)	abcam	
Rabbit IgG	-	A6154 (1:200)	Sigma Aldrich	-

Supplementary Table 5.7. Immunoreactivity scoring criteria applied to IHC imagery.

Scoring Parameter	Quantitative Score	Intensity Description	Score
Percentage of Positive Staining	0% of immune-positive cells	-	0
	1-20% of immune-positive cells	-	1
	21-50% of immune-positive cells	-	2
	51-80% of immune positive cells	-	3
	81-100% of immune positive cells	-	4
Staining Intensity	-	Negative	0
	-	Weak	1
	-	Moderate	2
	-	Intense	3

Supplementary Table 5.8. Antibodies used for Western blot analysis of homogenized colon.

Protein analysis	Optimised Dilution (v/v)	Cat. number/Supplier
Nrf2	1:2000	PA5-88084, Invitrogen
GPx4	1:1000	ab125066, abcam
SOD1	1:2000	SAB5200083, Sigma Aldrich
4HNE	1:800	BS-6313R, Bioss
β actin	1:10000	4967S, Cell Signaling Technology
Rabbit HRP	1:2000	A6154, Sigma Aldrich
Mouse HRP	1:2000	ab205719, abcam

Supplementary Table 5.9. The number of differential lipids between control mice and DSS alone or groups co-treated with DSS and natural products.

Treatment Group	p < 0.05	VIP > 1.5	Number of Differential Lipids
Control vs. DSS	155	86	77
DSS vs. Curcumin	214	67	60
DSS vs. Diffusa	45	100	36
DSS vs. Villosum	112	73	53

Supplementary Table 5.10. List of identified differential lipids in mouse colon obtained from mice in the absence and presence of DSS insult.

Lipid Species	p < 0.05	VIP Score > 1.5
PG(16:1e_15:0)	0.014294	3.417
DG(34:1_18:1)	0.01421	3.145
PC(37:5)	0.027049	2.3962
PA(18:0e)	0.032389	2.3422
LPC(20:1e)	5.29E-05	2.3017
LPE(23:1)	0.0004013	2.2643
PS(16:0_22:6)	0.00010721	2.257
PS(20:4_20:4)	0.0019934	2.2483
PS(16:0_18:2)	0.00012825	2.2447
LPE(23:0)	0.00038475	2.2057
LPE(18:3e)	0.0070161	2.1848
PE(23:0e)	0.0012423	2.1405
PG(32:1e)	0.047948	2.1267
LPE(24:0)	0.0010161	2.1064
LPE(16:1e)	0.0071163	2.1046
LPC(16:1e)	0.00037451	2.0634
LPE(18:2e)	0.0066272	2.0541
SM(d20:1_18:3)	0.0018046	2.036
LPE(17:0)	0.0028929	2.0303
LPC(18:2e)	0.0010228	2.0279
TG(16:0_16:0_16:0)	0.0024054	2.0228
DG(18:3_18:2)	0.0084919	2.0053
LPE(24:2)	0.001349	2.0052
LPE(18:0)	0.0024534	2.0014
TG(22:4_18:2_22:6)	0.012971	1.9831
LPE(18:1e)	0.0072683	1.9349
PE(24:3e)	0.0028129	1.9307
LPE(16:0)	0.0042586	1.9269
LPE(24:1)	0.0033145	1.9155
LPE(19:0)	0.005039	1.9035
TG(20:3_18:2_22:6)	0.02357	1.9031
PE(18:0e_18:2)	0.027292	1.8959
LPC(22:3)	0.0030391	1.8889
TG(18:1_22:4_22:6)	0.012679	1.8652
LPE(22:0)	0.0023774	1.8552
PS(18:1_18:2)	0.0068292	1.8504
LPE(15:0)	0.01229	1.8438
LPE(20:2)	0.0061127	1.8387
LPC(23:1)	0.0031169	1.8175
LPC(22:2)	0.0086811	1.7961
PC(37:1e)	0.0091368	1.7877
LPE(22:1)	0.0043809	1.781
LPC(20:2)	0.0047819	1.7609
PC(18:3e_16:0)	0.0021381	1.7381
LPE(20:1e)	0.008973	1.7329
LPE(18:1)	0.0063362	1.7133
LPE(19:1)	0.019451	1.7125
PC(18:4_18:1)	0.0029083	1.7068
PS(18:1_18:1)	0.031815	1.705
PC(35:1e)	0.010649	1.7044
PI(16:1_18:2)	0.00096466	1.7038
LPC(19:1)	0.012272	1.6958
LPC(20:4e)	0.043358	1.6929
PI(18:1_22:6)	0.0016516	1.6785
PE(18:2_22:6)	0.0051328	1.6687
DG(16:0_18:3)	0.017434	1.6562
LPC(18:1e)	0.046284	1.6547
PI(20:4_20:4)	0.0024815	1.6442
LPE(20:1)	0.011299	1.6396
PE(20:0_18:1)	0.04309	1.6362
SM(d41:3)	0.009105	1.635
PS(22:4_22:6)	0.004114	1.6189
TG(18:0_16:0_16:0)	0.024399	1.6071
PG(18:1_24:0)	0.010041	1.6055
PC(42:6e)	0.015819	1.6028
LPC(17:0)	0.0096535	1.6
LPC(20:1)	0.014346	1.5971
DG(18:1_24:1)	0.0054036	1.5833
LPC(24:2)	0.012874	1.574
SM(d34:2)	0.011934	1.5737
PS(17:0_20:4)	0.014946	1.5543
PE(18:1e)	0.017477	1.5536
PC(17:1_22:6)	0.005956	1.5365
SM(d42:7)	0.0067237	1.5195
PG(18:2_20:4)	0.024492	1.5112
PS(37:2)	0.026494	1.5065
TG(18:0_8:0_11:4)	0.0054169	1.5

Supplementary Table 5.11. Metabolic pathways involved in DSS-induced experimental colitis using in silico pathway analysis.

Pathways	Number of Metabolites in the Pathway	Number of Metabolites Matched	Pathway Impact Score	-Log_{10}(p-value)	FDR
Glycerophospholipid Metabolism	36	3	0.21708	2.5946	0.012717
Glycosylphosphatidylinositol Anchor Biosynthesis	32	1	0.03665	2.158	0.017377
α-Linolenic Acid Metabolism	13	1	0.001	1.4264	0.037464

Supplementary Table 5.12. List of identified differential lipids in mouse colon obtained from mice insulted with DSS in the absence and presence of curcumin.

Lipid Species	p < 0.05	VIP Score > 1.5
DG(14:0_18:3)	0.0020257	2.5121
DG(16:1_18:1)	0.0011371	2.5071
DG(18:3_18:2)	0.00074223	2.4953
DG(16:1_14:0)	0.0016947	2.3431
DG(16:1_18:2)	0.0015962	2.3115
DG(18:1_18:3)	0.00052955	2.2606
DG(18:2_18:2)	0.00053104	2.2585
DG(16:1_16:1)	0.00071533	2.2199
DG(14:0_18:2)	0.00072191	2.219
DG(17:1_18:2)	0.0014801	2.1523
DG(16:0_18:3)	0.00095864	2.1466
DG(18:1_18:2)	0.001018	2.1248
DG(16:0_16:1)	0.0014375	2.1121
PA(36:6e)	0.0022839	2.0547
PG(18:1_24:0)	0.0072631	1.9449
LPC(20:3e)	0.0074416	1.9266
DG(18:1_18:1)	0.0032979	1.895
PE(23:0e)	0.0027721	1.8465
DG(16:0_18:2)	0.0033117	1.8387
PE(24:3e)	0.00055292	1.8254
DG(18:2_20:4)	3.76E-06	1.8073
LPE(22:0)	0.0016593	1.7487
LPE(23:0)	0.0035431	1.7419
SM(d18:1_17:0)	0.023272	1.7237
DG(16:0_18:1)	0.0056425	1.7167
PE(18:0p_20:3)	0.0010184	1.7028
PI(17:0_18:2)	0.0010641	1.6893
PE(18:1p_22:1)	0.0039012	1.6461
PE(20:0p_18:1)	0.0059406	1.6411
LPE(23:1)	0.00058929	1.6296
DG(20:1_18:2)	0.0085225	1.6293
PI(17:0_18:1)	0.00079737	1.622
LPE(24:0)	0.0025649	1.6159
DG(15:0_18:2)	0.0090355	1.6126
DG(19:1_18:2)	0.0068516	1.603
PA(18:0e)	0.021258	1.575
PE(20:0p_18:2)	0.004019	1.574
PG(18:2_18:2)	0.0037296	1.5665
PI(17:0_20:5)	0.011521	1.5635
PI(17:0_22:6)	0.0013174	1.5609
PC(33:2e)	0.0030676	1.5582
PE(18:0e_18:1)	0.026117	1.5511
PE(20:0p_20:3)	0.0084772	1.5491
PE(18:0p_15:0)	0.00023214	1.5484
LPE(20:1e)	0.0071011	1.5458
PE(20:0p_16:0)	0.026494	1.5441
PI(17:1_18:1)	0.0010765	1.5417
PE(18:0p_17:1)	0.0026209	1.537
TG(16:0_16:0_16:0)	0.011572	1.5315
LPE(22:1)	0.0013753	1.5288
PE(16:0p_20:1)	0.0055885	1.5274
PC(35:2e)	0.0034405	1.5272
PE(18:1e_18:1)	0.005554	1.5272
PG(17:0_18:1)	0.0029652	1.5192
LPE(17:0)	0.0013495	1.5158
PE(20:1p_18:1)	0.0041521	1.5144
PE(18:1p_18:1)	0.0025155	1.5119
PE(16:0p_20:2)	0.0025871	1.5078
PC(33:1e)	0.0016467	1.5047
PI(15:0_20:4)	0.0039695	1.5004

Supplementary Table 5.13. List of identified differential lipids in mouse colon obtained from mice insulted with DSS in the absence and presence of Diffusa tonic.

Lipid Species	p < 0.05	VIP Score > 1.5
TG(25:0_16:0_18:1)	0.025151	2.8591
TG(26:0_18:1_18:1)	0.023993	2.8408
TG(26:1_18:1_18:1)	0.026366	2.7932
TG(18:0_18:1_24:0)	0.023974	2.705
TG(18:1_18:1_24:0)	0.032258	2.6561
TG(25:0_18:1_18:2)	0.041392	2.5827
PA(18:0_18:2)	0.03918	2.5406
PA(38:4)	0.032734	2.4869
TG(18:1_18:1_23:0)	0.04815	2.4557
TG(16:0_18:1_24:0)	0.045705	2.4478
TG(18:1_18:2_24:1)	0.046967	2.4477
PA(20:0_18:2)	0.04858	2.447
TG(26:1_18:1_18:2)	0.049003	2.4417
TG(16:0e_18:1_18:1)	0.027178	2.4185
TG(16:0_20:4_22:6)	0.033871	2.3767
TG(20:3_18:2_22:6)	0.026944	2.3631
TG(20:1_18:1_22:4)	0.025169	2.3586
TG(20:1_18:2_22:4)	0.019727	2.3526
TG(16:0e_18:1_18:2)	0.015681	2.2985
TG(18:1_18:2_22:1)	0.039673	2.2727
TG(20:1_18:2_22:6)	0.026874	2.2549
TG(18:1_20:3_22:4)	0.031641	2.2383
TG(18:1_18:2_22:5)	0.035902	2.2381
TG(16:0_22:6_22:6)	0.039608	2.2367
TG(18:1_18:1_22:4)	0.032783	2.2009
TG(18:1e_16:0_16:0)	0.047565	2.1939
PA(40:4)	0.0073616	2.1878
PE(20:1e_20:4)	0.0033104	2.181
ChE(22:4)	0.014672	2.1179
TG(18:0_20:4_22:6)	0.041772	2.0922
TG(16:0_16:0_24:0)	0.017841	1.9987
TG(18:2_18:2_21:1)	0.045226	1.9877
LPE(20:0)	0.040182	1.8618
TG(18:0_18:0_18:0)	0.020923	1.7653
SM(t33:1)	0.021633	1.5764
PC(33:5)	0.022185	1.5715

Supplementary Table 5.14. List of identified differential lipids in mouse colon obtained from mice insulted with DSS in the absence and presence of Villosum tonic.

Lipid Species	p <0.05	VIP Score > 1.5
LPE(20:0)	0.0096192	2.4528
DG(16:1_18:1)	0.014329	2.3487
DG(18:1_18:2)	0.0063086	2.0454
PS(36:2e)	0.0044729	2.0349
PE(24:1_20:4)	0.011301	1.9765
DG(17:1_18:2)	0.030636	1.9728
DG(18:3_18:2)	0.044567	1.9593
DG(18:1_18:3)	0.021553	1.9327
DG(18:2_18:2)	0.021867	1.9275
LPC(24:1)	0.0094576	1.806
PI(17:0_20:3)	0.0014358	1.7984
LPE(22:0)	0.0047779	1.7959
DG(18:1_18:1)	0.010975	1.7896
LPE(24:1)	0.0064269	1.7784
LPE(24:0)	0.010938	1.7734
LPC(28:0)	0.016446	1.7542
DG(20:1_18:2)	0.0024073	1.7505
PI(18:1_22:6)	0.0099281	1.7082
LPE(20:1)	0.0061872	1.7026
LPC(22:1)	0.011255	1.683
PI(18:0_22:3)	0.016788	1.6809
PI(17:0_22:6)	0.0058657	1.6802
DG(19:1_18:2)	0.0065567	1.6781
LPE(19:1)	0.019456	1.6642
LPC(22:0)	0.021794	1.6579
LPE(22:1)	0.0077977	1.6551
PI(18:1_18:1)	0.0071929	1.6501
LPC(20:1)	0.013167	1.6498
LPE(18:0)	0.010051	1.6389
PS(49:6)	0.033671	1.6048
DG(16:0_18:2)	0.041539	1.5962
LPC(20:0)	0.021093	1.5953
PI(17:0_18:2)	0.001899	1.5828
LPE(17:0)	0.026296	1.5783
LPE(23:1)	0.013121	1.5779
LPC(14:0)	0.020892	1.5754
LPC(22:2)	0.025714	1.571
LPC(24:2)	0.02232	1.5646
LPE(19:0)	0.017833	1.5622
PS(24:0_20:3)	0.023674	1.5548
PC(39:6)	0.028617	1.5542
LPC(24:0)	0.031949	1.5497
DG(18:1_22:4)	0.0022089	1.5441
PA(16:0_16:0)	0.035663	1.5415
PI(16:0_20:3)	0.0073529	1.5405
LPE(23:0)	0.019187	1.5348
PS(43:1)	0.048106	1.5262
PI(18:1e_16:0)	0.014951	1.5245
PI(17:1_18:1)	0.0064895	1.5211
PI(18:1_20:5)	0.0041868	1.5121
PI(18:0e_18:1)	0.026803	1.5085
LPE(20:2)	0.015134	1.5081
PI(16:0_16:1)	0.0088489	1.5062

Supplementary Table 5.15. Metabolic pathways involved in mouse colon obtained from mice treated with curcumin or Villosum.

Treatment Groups	Pathways	Number of Metabolites in the Pathway	Number of Metabolites Matched	Pathway Impact Score	-Log_{10}(p-value)	FDR
DSS vs. Curcumin	Glycerophospholipid Metabolism	36	3	0.21708	3.2783	0.0026345
	Glycosylphosphatidylinositol Anchor Biosynthesis	32	1	0.03665	2.9441	0.0028435
	α-Linolenic Acid Metabolism	13	1	0.001	2.4137	0.0038577
DSS vs. Villosum	Glycerophospholipid Metabolism	36	3	0.26141	3.1718	0.0010099
	Glycosylphosphatidylinositol Anchor Biosynthesis	32	1	0.03665	3.208	0.0010099
	α-Linolenic Acid Metabolism	13	1	0.01246	0.16431	0.685

Supplementary Figures

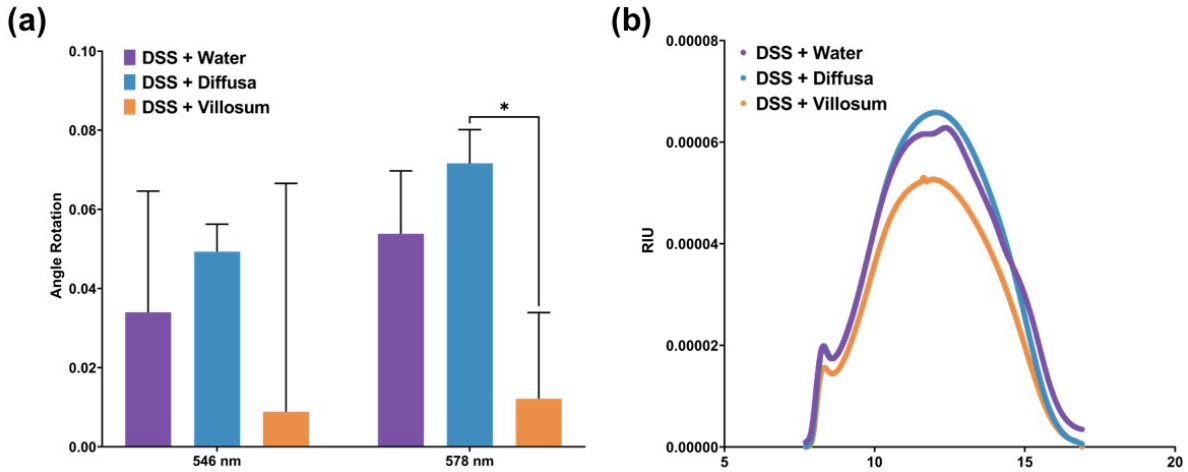

*Supplementary Figure 5.1. Physical property analysis of DSS in herbal tonics. (a). Optical angle rotation of DSS in water and DSS in Diffusa and Villosum herbal tonics obtained from polarimetry analysis. (b). Molecular weight analysis of DSS in water and DSS in Diffusa and Villosum herbal tonics. n = 3 independent trials per samples and graphical values were expressed as mean + standard deviation (SD). * $p < 0.05$. Authors contributions: K.X – Validation, methodology, formal analysis, data curation, T.O.C – Investigation, validation, data curation, L.H– Investigation.*

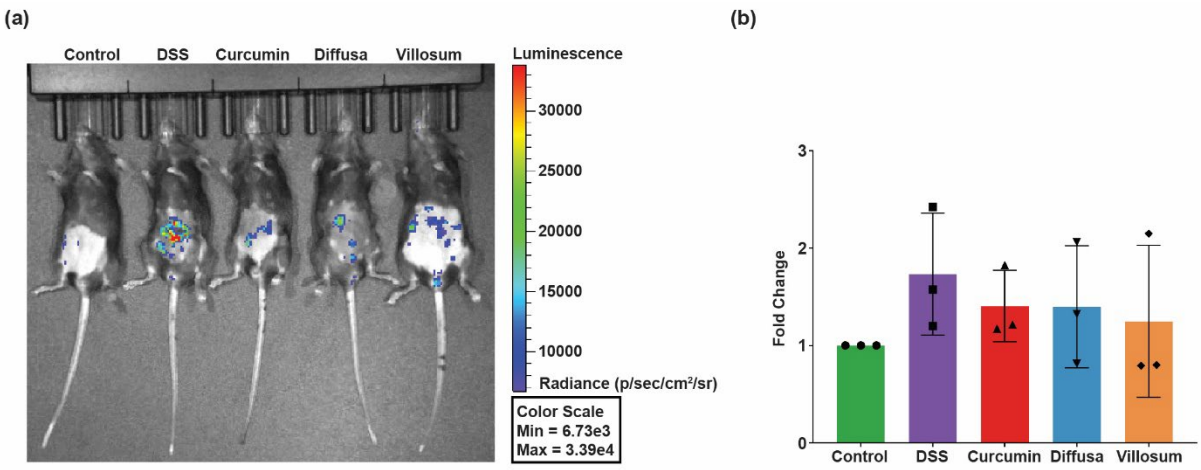

Supplementary Figure 5.2. The efficacy of herbal remedies treatment on DSS-induced UC-like experimental colitis. (a). Representative image of in vivo bioluminescence imaging. (b). Quantification of luminescence signal. Graphical values represent mean ± SD or mean + SD when error bars were below 0 with n = 3 mice per group. Normalcy of the collected data was analysed using Shapiro-Wilk test and group differences were analysed using Kruskal-Wallis test with Dunn's multiple comparison. Authors contribution: K.X - Validation, methodology, formal analysis, data curation, S.C – Investigation, data curation, G.A – Methodology.

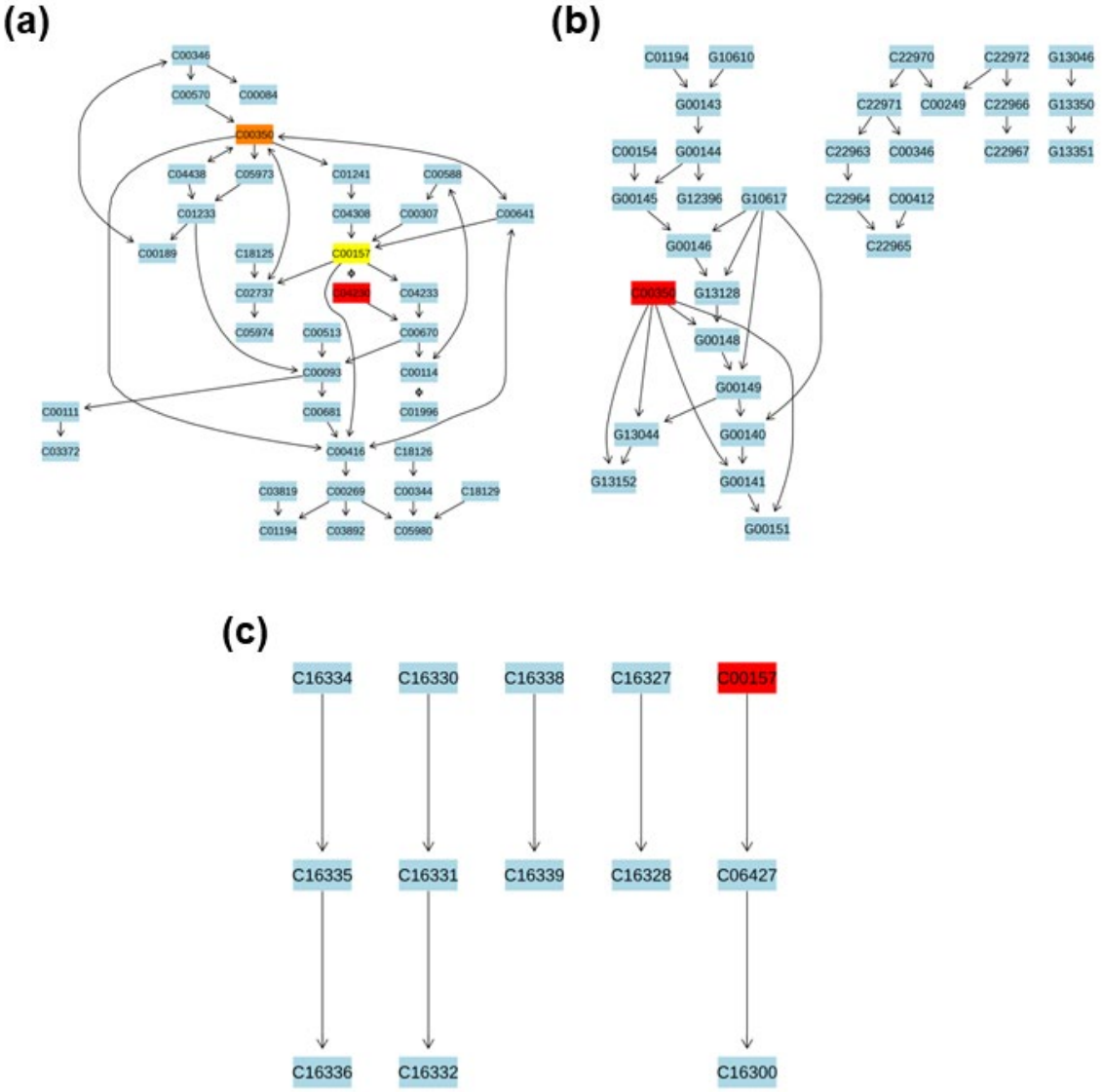

Supplementary Figure 5.3. Metabolic pathways implicated in mouse colon obtained from mice after DSS-insult to induce experimental colitis. (a). Glycerophospholipid metabolism. (b). Glycophosphatidylinositol anchor biosynthesis and (c). α-linolenic acid metabolism. Red, orange and yellow colors indicate metabolites matched with the identified differential lipids. Authors contributions: K.X – Validation, methodology, formal analysis, data curation, T.O.C – Investigation, validation, data curation, N.S – Formal analysis, L.H– Investigation.

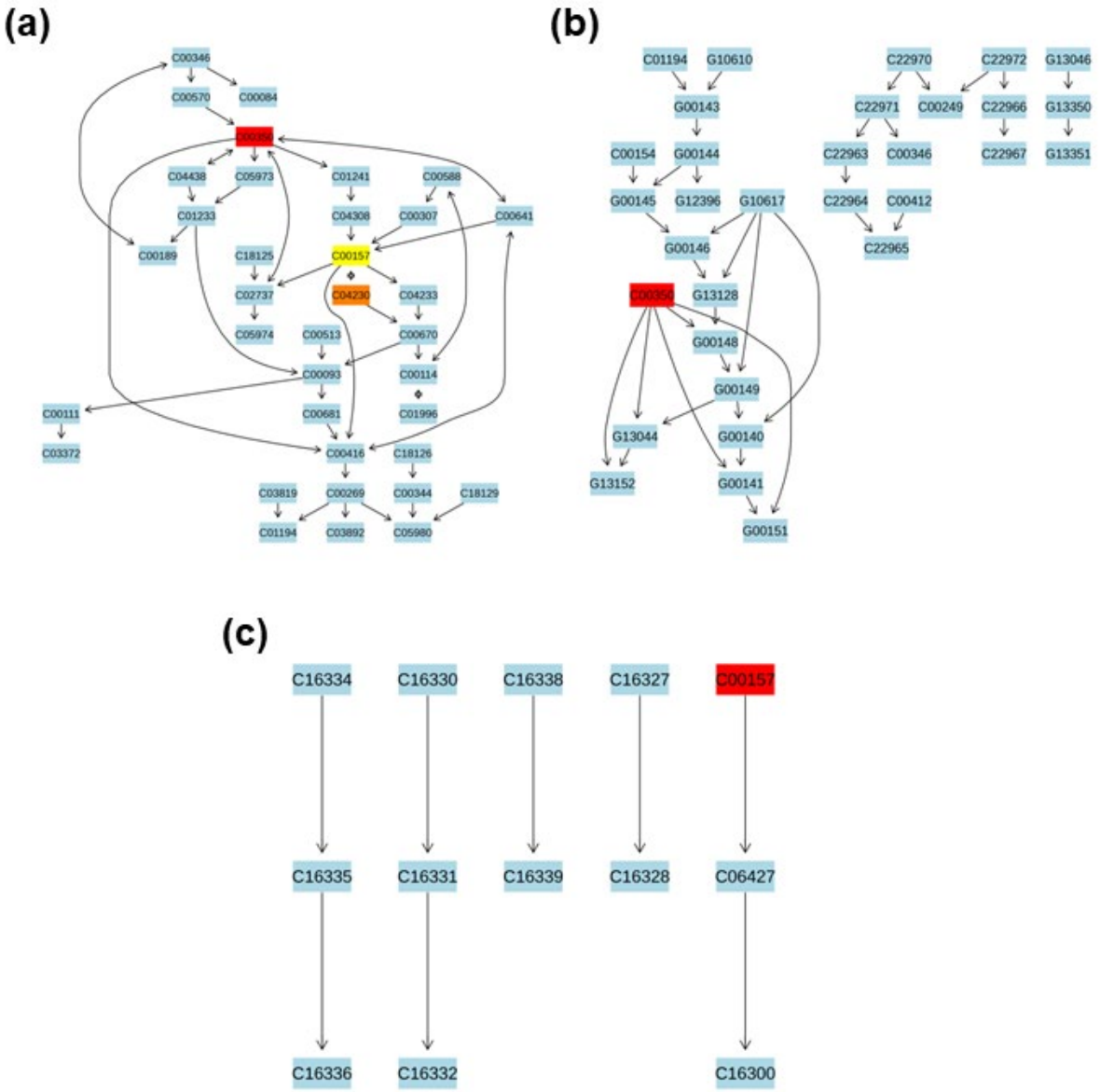

Supplementary Figure 5.4. Metabolic pathways implicated in mouse colon obtained from mice supplemented curcumin dispersed in peanut butter. (a). Glycerophospholipid metabolism. (b). Glycophosphatidylinositol anchor biosynthesis and (c). α-linolenic acid metabolism. Red, orange and yellow colors indicate metabolites matched with the identified differential lipids. Authors contributions: K.X – Validation, methodology, formal analysis, data curation, T.O.C – Investigation, validation, data curation, N.S – Formal analysis, L.H– Investigation.

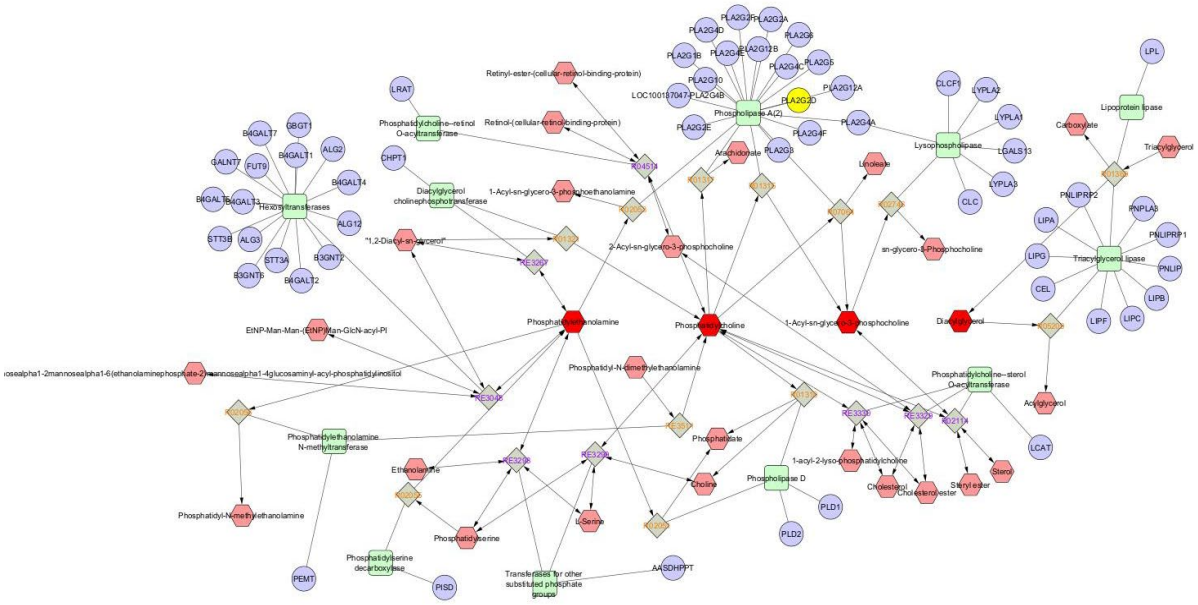

Supplementary Figure 5.5. Interaction network analysis of differential lipids identified between mice insulted with DSS in the absence and presence of curcumin supplementation. Authors contributions: K.X – Validation, methodology, formal analysis, data curation, T.O.C – Investigation, validation, data curation, N.S – Formal analysis, L.H– Investigation.

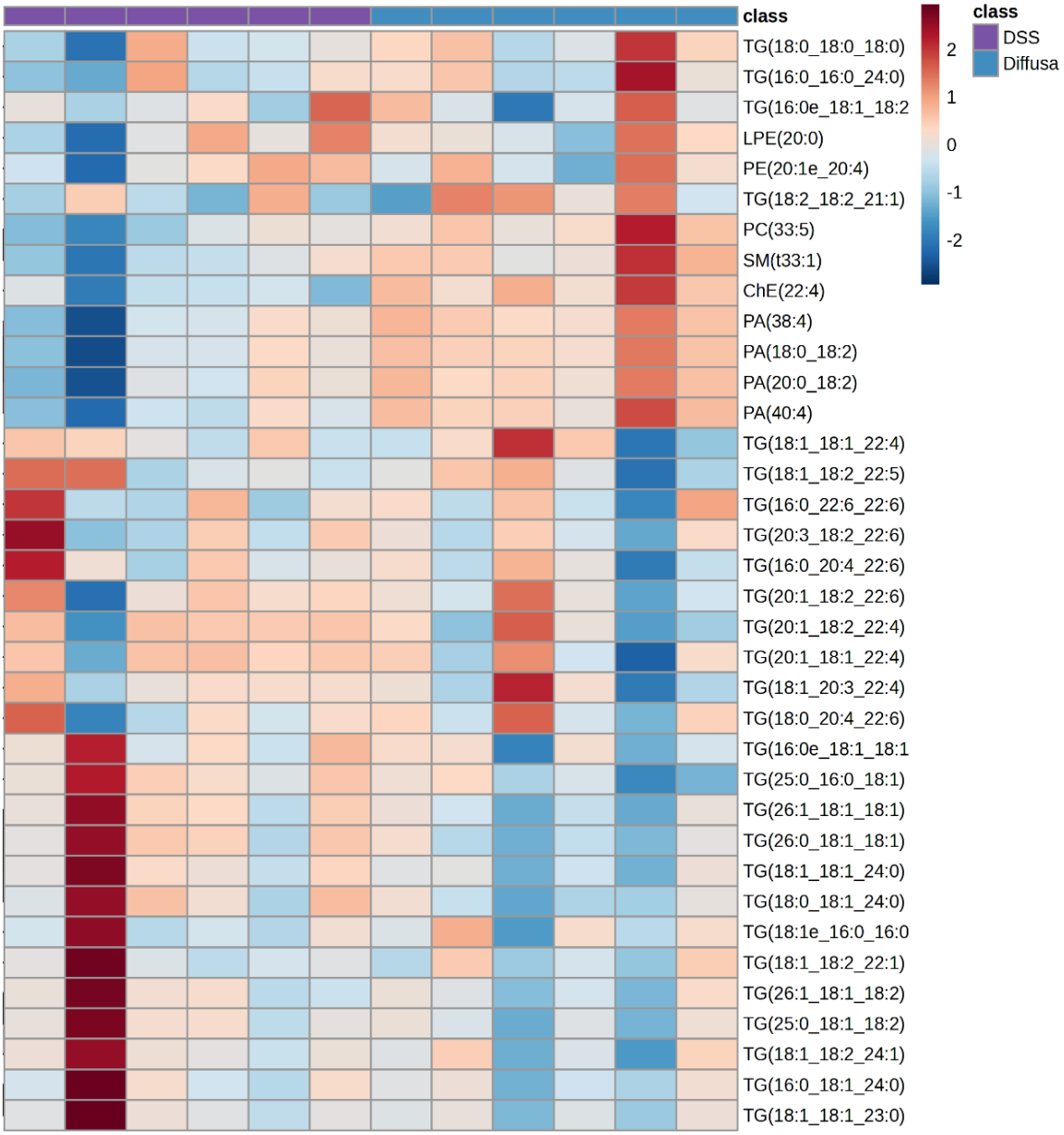

Supplementary Figure 5.6. Heatmap evaluation showing differential lipid species in mouse colon obtained from mice insulted with DSS and mice that were supplemented Diffusa tonic in drinking water. Data derived from n = 6 mice per treatment group. Authors contributions: K.X – Validation, methodology, formal analysis, data curation, T.O.C – Investigation, validation, data curation, N.S – Formal analysis, L.H– Investigation.

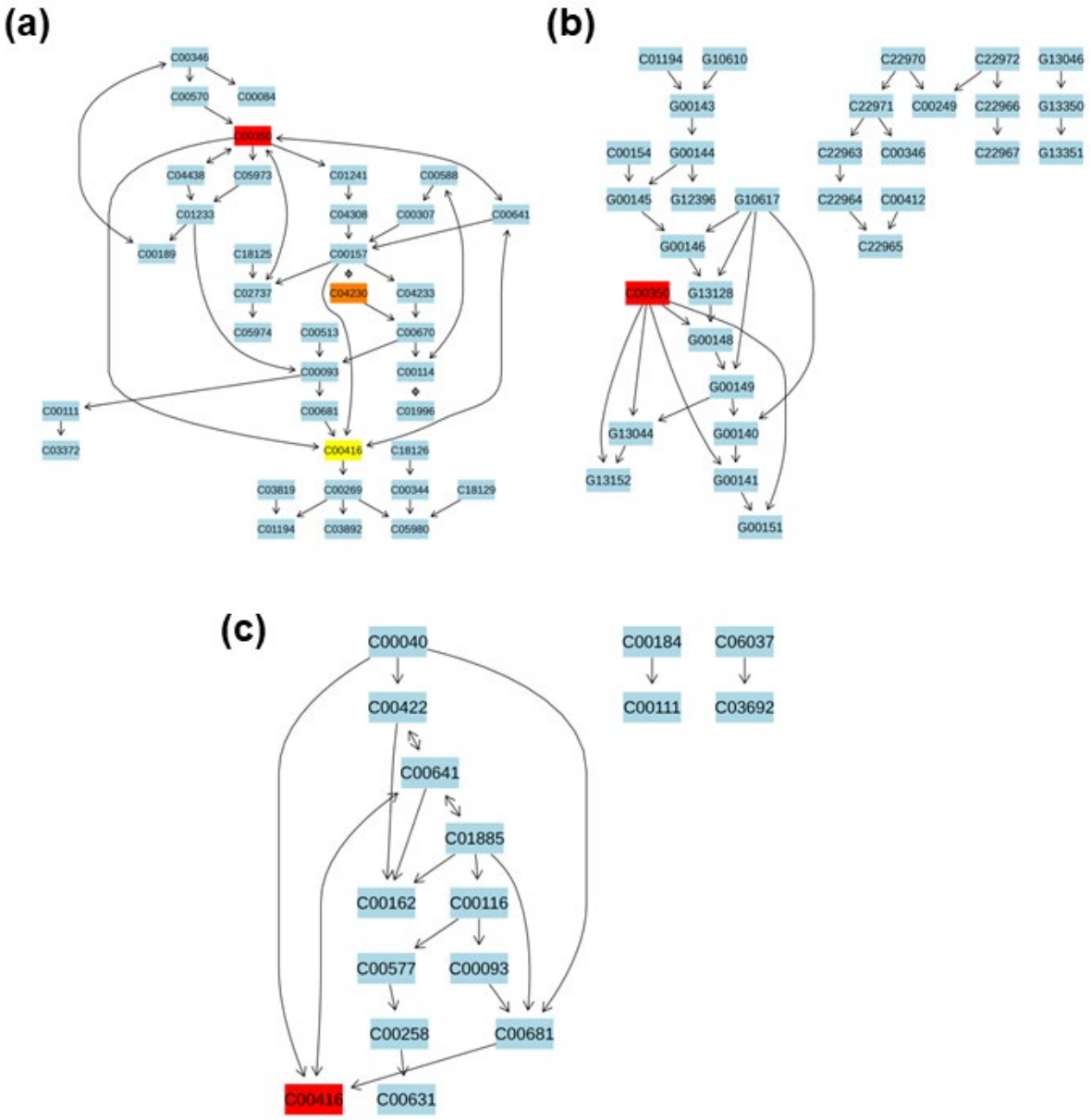

Supplementary Figure 5.7. Metabolic pathways implicated in mouse colon obtained from mice that were supplemented with Villosum tonic. (a). Glycerophospholipid metabolism. (b). Glycophosphatidylinositol anchor biosynthesis and (c). glycerolipid metabolism. Red, orange and yellow colors indicate metabolites matched with the identified differential lipids. Authors contributions: K.X – Validation, methodology, formal analysis, data curation, T.O.C – Investigation, validation, data curation, N.S – Formal analysis, L.H– Investigation.

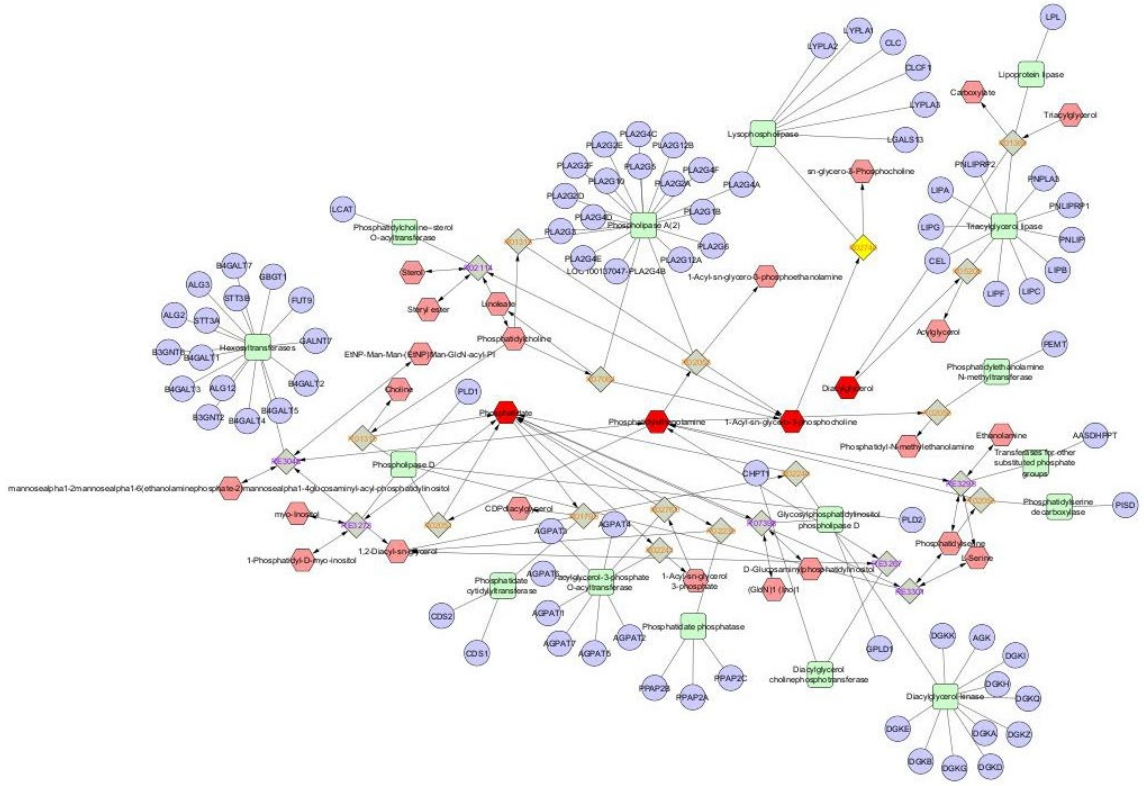

Supplementary Figure 5.8. Interaction network analysis of differential lipids in mouse colon obtained from mice insulted with DSS in the absence and presence of Villosum groups. Authors contributions: K.X – Validation, methodology, formal analysis, data curation, T.O.C – Investigation, validation, data curation, N.S – Formal analysis, L.H– Investigation.

Appendix

Appendix 1. Protocol for assessing the physical properties of DSS

To evaluate whether herbal tonics interfered with the DSS polymer and rendered the mixture unable to promote colon inflammation, physical properties of DSS were investigated with polarimetry and size exclusion chromatography with multi-angle light scattering (SEC-MALS) analyses.

Appendix 1.1 Polarimetry analysis

A Perkin Elmer 341 polarimeter was used to illuminate herbal tonics ± DSS with polarized light to measure changes in optical angle rotation. Briefly, prepared herbal tonics were further diluted to 40% v/v with Milli-Q® water. A blank sample with only Milli-Q® water was used to calibrate the system at 546 and 578 nm. Next, the angle of rotations of neat solutions of diluted *Diffusa* and *Villosum* tonics were measured and re-calibrated as tonic blanks. After re-calibration, the angle of rotation of *Diffusa* and *Villosum* and their corresponding DSS-containing tonics were measured. All measurements were performed in duplicates at 20°C and the Na/Hal and Hg light sources were activated with normal aperture.

Appendix 1.2 Size exclusion chromatography with multi-angle light scattering analysis

SEC-MALS was employed to quantify the polymer distribution and gross size range of prepared Diffusa and Villosum tonics ± DSS solutions. Phosphate buffered saline (10 mM Na_2HPO_4, 1.8 mM KH_2PO_4, 137 mM NaCl, 2.7 mM KCl, pH 7.4; PBS) was used instead of water to optimize the substrate-stationary phase interactions in an AKTA FPLC instrument (Amersham Biosciences). Liquid chromatography was performed at 20°C with flow rate of 0.5 mL/min and samples (300µL) were injected into a PBS equilibrated Superose 12 10/300 GL size exclusion column (GE Life Sciences). Subsequent simultaneous real-time conductance and absorbance readings at 215, 254 and 280 nm were determined for the eluting volume. Light scattering, refractive index units (RIU) and absolute refractive index (aRI) were recorded using a miniDAWN TREOS multi-angle light scattering detector (Wyatt Technology) coupled to an Optilab T-rEX refractive index detector (Wyatt Technology).

Chapter 6: General Discussion

Clinical presentation of IBD is described by three main presentations: UC, CD and IC and the disease is considered a chronic, relapsing autoimmune disorder of the GIT [246]. Patients with IBD experience symptoms such as abdominal pain, rectal bleeding, diarrhea as well as EIMs such as anaemia, arthritis, osteoporosis, musculoskeletal conditions and hepatobiliary conditions [254, 571]. Despite extensive research, the precise aetiology of the disease remains unclear. However, it is increasingly accepted that IBD arises from a complex interplay of genetic predisposition, immune dysregulation, altered gut microbiota, along with a series of environmental triggers [572]. The unpredictable nature of IBD, with alternating periods of remission and active flares poses significant challenges in symptom management that impact the quality of life of affected individuals [573]. According to the newly released findings from the State of the Nation in Inflammatory Bowel Disease in Australia reports by Crohn's and Colitis Australia, Australia is amongst the highest incidence of IBD in the world, with 179,420 Australians living with IBD in 2025 and over 90,000 experiencing active disease. This translates into health, economic and social burdens of $7.8 billion Australian dollar (AUD) and it is projected to be over $77.9 billion AUD in the next decade [574].

Current therapeutic strategies of IBD primarily focus on symptom control, suppression of inflammatory responses and induction of the quiescent (remission) disease state. However, these treatments are often associated with high failure rates, severe adverse effects and diminishing clinical responses over time [426]. Additionally, none of contemporary drugs offer a definitive cure for the disease, leaving patients with limited long-term options. Given these limitations, there is an urgent need to investigate the pathogenic mechanism of IBD and discover pathways and novel therapeutic target that can positively impact patients with the disease in the context of management and cure.

As outlined in the Introduction Chapter, approaches such as the use of synthetic inhibitors, modulation of the gut microbiome and administration of nutraceuticals have demonstrated beneficial clinical outcomes in both human IBD patients and experimental colitis animal models. Thus, I hypothesised that a multifaceted investigation strategy into novel synthetic inhibitors, determinants of gut microbiome composition, systemic lipidomic alterations and the mechanisms of actions of various nutraceuticals may yield important insights into IBD pathogenesis and uncover novel therapeutic targets for the development of innovative treatments.

To address these challenges in IBD, I evaluated the therapeutic efficacy of synthetic enzyme inhibitors and complementary and alternative medicines in restoring redox and immune imbalances characteristics of the disease with specific focus on three key loci:

1. Dysregulated neutrophil response and NET formations in the colon mucosa;
2. Altered SCFA and inflammatory marker profiles in the stool;
3. Redox imbalance and lipid composition alteration in the intestinal epithelium.

6.1 MPO and PAD4 inhibition in DSS-induced experimental colitis

Chapter 3 of this thesis described the effect of MPO and PAD4 inhibition in a murine model of DSS-induced experimental colitis. The study demonstrated that NETs formation was

significantly inhibited by commercially available PAD4 inhibitor GSK484 in the colon mucosa Whilst the inhibition of colonic NET formation did not translate into clinical improvement to experimental colitis, this study was the first to unambiguously characterise the formation of NETs in mouse colons through the using of multi-plex immunofluorescence labelling of three essential markers involved in the formation of NETs: NE, MPO and citH3. Notably, the pathology of IBD is keenly linked to changes in the mucosa and epithelial regions of the colon [315]. The outcomes from this study partially divorce the involvement of NETs from the pathogenesis of IBD. Accordingly, the study by Leppkes et al. demonstrated that NETs prevented bleeding in a murine model of UC through immuno-thrombosis and PAD4-dependent remodelling of blood clot was essential efficient mucosal wound healing [575], suggesting a potential colon protective effect of NET structures in IBD. In support of this notion, flow cytometry analysis led to the identification of the colon protective $CD177^+$ subset of neutrophils from the blood of IBD patients [85]. These neutrophils were found to have a different cytokine-release profile, evident in reduced production of pro-inflammatory cytokines IL-6, IL-17A and IFN-γ and elevated production of tissue-healing mediators IL-22 and TGF-β [85, 86], highlighting the potential immune dampening and tissue repair promoting effects of this subset of leukocytes, which further reinforces their colon protective function in IBD. However, the proportion of $CD177^+$ neutrophils in the infiltrated cells observed in the Chapter 3 remains to be elucidated. Thus, further investigation examining the heterogeneity profile of neutrophils in the colon homogenates may yield valuable insights into the involvement and contribution of NETs during the pathogenesis of IBD.

Alternately, the outcomes from Chapter 3 could also support the pathogenic role of NETs in IBD, implying that a beneficial clinical outcome can be achieved when a certain threshold of NET inhibition is achieved in the colon mucosa. The logical extension here is that this study failed to reach this threshold and provide therapeutic benefit. This notion is supported by the study by Tang et al., where intraperitoneal administration of GSK484 at 4 mg/kg daily (compared to GSK484 administered every second day in Chapter 3) resulted in a near-complete abolishment of NETs in the colonic mucosa (compared to ~50% inhibition in Chapter 3) and markedly improved DSS-induced experimental colitis symptoms [541]. Similarly, the administration of PAD4 inhibitors at a higher concentration (10 mg/kg) has been shown to have a profound inhibition on NET formation in murine myocardial infarction model with minimal adverse side effects [576], which further reinforces that extensive PAD4 (and downstream NET) inhibition is required to achieve a suitable threshold that underpins a therapeutic effect.

The involvement of mast cells in autoimmune conditions such as multiple sclerosis, rheumatoid arthritis and bullous pemphigoid has been extensively documented. However, the specific mechanisms in which mast cells contribute to the development of these autoimmune conditions are not completely understood and published literature investigating the immunomodulatory role of mast cells in IBD remains scarce. It has been reported that mast cells can interact with other immune cell types such as T-lymphocytes and dendritic cells to enhance self-activation and migration. Specifically, it has been demonstrated that Tregs suppress mast cell activation via the OX40-OX40L axis [577] and inhibit FcεRI-dependent mast cell degranulation [578], whilst mast cells regulate the activation, migration and function of dendritic cells via pattern recognition receptor signalling and the release of TNF and prostaglandin E_2 [579, 580].

Given that dendritic cells closely interact with T-lymphocytes to maintain gut homeostatic balance and dysregulation in Treg-mediated function is implicated in the pathogenesis of IBD (See Introduction Chapter Sections 1.1.1.3.2 and 1.3.4), it is not unreasonable to suggest mast cells may potentiate IBD pathologies through the documented cell-cell interactions. Outcomes from Chapter 3 revealed a novel potential immune crosstalk between mast cells and apoptotic neutrophils (NETs), where the parallel activation of mast cells in the presence of NETs could provide colon protective effects by preventing non-discriminatory HOCl damage via histamine modifications (although this was not proven here).

6.2 SCFA and inflammatory profile alteration in stool of IBD patients

Chapter 4 of this body of work utilised human faecal samples and investigated the level of SCFA and inflammatory stool biomarkers in healthy and IBD subjects. To the best of my knowledge, this study was the first attempt to compare faecal SCFA levels between healthy subjects and IBD patients stratified by disease severities (remission, mild, moderate and severe) as judged by standard colonoscopy activity index, the Ulcerative Colitis Endoscopic Index of Severity (UCEIS) and Simple Endoscopic Score for Crohn's Disease (SES-CD) for patients diagnosed with UC and CD, respectively. The main finding here is the link between maintaining elevated levels of SCFA and maintenance of disease remission, with butyrate identified as providing the greatest level of bioactivity. Additionally, reduced SCFA levels in the stool weakly correlate with increased faecal pro-inflammatory cytokine concentrations, particularly IL-1β, which validates the assignments of severity in the IBD cohort.

The outcomes of this study pose significant clinical relevance as there are multiple commercial sodium butyrate supplements available. However, mixed effect of butyrate supplementation in IBD patients have been reported by numerous clinical studies. For instances, 100 mM of sodium butyrate supplementation in the form of colon enema for 4 and 8 weeks has been demonstrated to reduce inflammation and improve colitis symptoms in patients with UC [554]. On the contrary, adjunct oral administration of the sodium butyrate capsule (1800mg/day) with conventional treatments did not improve the clinical activity of UC patients [555]. The results from published literature suggest that that the therapeutic effects of butyrate supplementation are likely to be dosage and administration route dependent. Additionally, the metabolism of these supplemented butyrate should also be considered. Under physiological condition, microbiota-derived butyrate is rapidly sequestered by colon enterocytes via the solute carrier family of transporter(s) pathway [581, 582]. However, altered butyrate metabolism occurs in patients with IBD, where UC patients commonly exhibit deficiency in butyrate transport [583]. As a result, together with the findings identified from Chapter 4, large scale multi-centre studies are urgently needed to determine the optimal dosage and administration for butyrate (as well as other SCFAs) supplementation to determine whether butyrate is a viable therapeutic for IBD.

6.3 Herbal medicines & Redox imbalances and altered colon lipid composition

Chapter 5 of the current thesis investigated the effects of three herbal remedies: curcumin, *Hedyotis Diffusa* and *Amomum Villosum* in restoring redox imbalance and modulating colonic lipid composition in an acute murine model of DSS-induced experimental colitis. This study was the first to examine the potential relationships between redox imbalance and altered colon lipid composition in the context of IBD. The outcomes obtained reinforced the anti-

inflammatory and antioxidative properties of these natural products, in which they all alleviated experimental colitis symptoms and increased antioxidant capacity in the gut to varying extents. Additionally, treatment with these herbs were also found to modulate colonic lipid composition, shunting DSS-induced alteration of glycerolipid metabolism towards that in the control mice; albeit not reaching the control levels. Given these promising data, and overwhelming anecdotal evidence of the relatively safe pharmacological profiles of the natural products tested here, the outcomes strongly support the need for future clinical trials to assess their potential as an alternative or complementary medicine for IBD patients.

One major limitation identified in this study was the lack of SCFA analysis on the colon homogenates obtained from mice in the various groups. As demonstrated by Chapter 3, SCFA particularly butyrate correlates with disease severities in patients with IBD. Given that therapeutic outcome has been described by butyrate supplementation studies, it is interesting to see the effects of these herbal remedies on acetate, propionate, butyrate and valerate level in the colitis gut. In the GIT, SCFA are largely produced by gut bacteria from the phyla of *Firmicutes* and *Bacteroidetes*. Over the recent years, a plethora of animal studies have reported the SCFA modulatory effects of herbal medicines. For example, the study by Chang et al. has shown that the water extract of *Ganoderma lucidum* mycelium reduced inflammation and decreased *Firmicutes*-to-*Bacteroidetes* ratios in mice fed on a high-fat diet [584], whilst Shao et al. demonstrated that the polysaccharide extract isolated from *Hericium erinaceus* mycelium modulated intestinal flora structure and increased SCFA levels in a rat model of acetic acid induced experimental UC [585], suggesting that the herb remedies tested in Chapter 5 could also result in positive modulatory effects on SCFA levels. In support of this notion, Sun et al. showed that curcumin increased the level of faecal butyrate and butyrate-producing bacteria in a mouse model of myasthenia gravis [586], highlighting the SCFA modulatory effect of the herb in animal models of autoimmune condition. However, to the best of my knowledge, the effects of curcumin, *Diffusa* and *Villosum* on faecal SCFA has not been investigated in the context of IBD, presenting an exciting area of future research.

6.4 Model of experimental colitis in the current thesis

The animal model selected here remains a gold-standard for evaluating the potential in vivo efficacy of drugs against IBD. Commercially sourced DSS is comprised of water-soluble polysaccharides that, when administered orally, disrupts the gut epithelial monolayer, leading to marked body weight loss and intestinal inflammation in rodents, which closely resembles the pathologies observed in acute human UC [587]. However, IBD is an autoimmune disease of chronic nature. As a result, the outcomes presented in the current thesis will ultimately lead to an obvious question: How would these synthetic inhibitors and herbal remedies perform in animal models of prolonged experimental colitis? Additionally, the long-term toxicity and adverse side effects of the drugs tested in this thesis, as well as their tolerability should also be considered. Accordingly, chemically induced chronic experimental colitis as well as transgenic animal models of IBD have been described by published literature [588, 589] (also refer to Introduction Chapter Section 1.6). Thus, future studies could be directed to address the chronic therapeutic effects of MPO and PAD4 inhibitors, as well as curcumin, *Diffusa* and *Villosum* in these alternate animal models of IBD.

6.5 Synergistic effects with conventional IBD therapies

The outcomes presented in Chapter 3 and 5 uncovered a possible future direction of testing these synthetic inhibitors and the herbal nutraceuticals as adjunct treatments. Accordingly, positive synergistic effects of co-administering compounds with anti-inflammatory and antioxidant properties with conventional IBD therapies such as 5-ASA has been reported by numerous studies using animal models of IBD. For example, poly adenosine diphosphate-ribose polymerases (PARP) play a critical role in mediating inflammation and synthetic PARP inhibitor has been shown to suppress intestinal inflammation by inhibiting NF-κB and STAT3 activations [590]. In the study by Kang et al., co-administration of synthetic PARP inhibitor with mesalamine resulted in enhanced treatment efficacy when compared to administering the inhibitor or 5-ASA alone, which highlights its potential as an adjunct treatment option [591]. Similar findings were reported by Mostafapour et al., where significantly better clinical outcomes were observed in DSS-insulted mice that received combination therapy of ACE inhibitor Enalapril with SASP compared the mice that received Enalapril or SASP alone [592]. Future investigations studying the potential synergistic effects of the synthetic inhibitors and herbal remedies describe in this thesis hold great excitements and could offer short-immediate solutions for IBD patients that have poor response rates with currently available therapies.

6.6. Limitation to IBD statistics & Concluding remarks

Lastly, it should be noted that most of the IBD-related statistics presented in the current thesis were collected in or before the year of 2019, the period before the Coronavirus disease 2019 (COVID-19) pandemic. Soon after the declaration of the outbreak by World Health Organisation, quarantine measures have been introduced by numerous countries in the world to stop the spread of this contagious disease. As a result of these measures, significant psychological disturbances such as emotional disturbance, depression and anxiety disorders have emerged in the quarantined societies [593]. Concurrently, the society have adapted to these policies by the introduction of working from home [594], increasing the prominence of sedative lifestyles [595]. As physical inactivity and poor mental health are major risk factors of IBD and other GIT disorders (See Introduction Chapter Sections 1.1.2 and 1.2.5.3), the estimated incidence rate cited here could potentially be understated, further reinforcing the need to identify novel complementary and/or alternate treatment options for IBD.

To conclude, novel therapeutic target research continues to be a topic of immense interest and great importance, with the current thesis contributed to the field by describing the therapeutic effects of synthetic MPO and PAD4 inhibitors and herbal remedies curcumin, *Hedyotis Diffusa* and *Amomum Villosum* in animal models of IBD and defining the changes in faecal SCFA levels in IBD patients on a spectrum disease severity.

References

Note: references from Chapter 3, 4 and 5 are not included here.

1. Cheng, L.K., et al., *Gastrointestinal system.* Wiley Interdiscip Rev Syst Biol Med, 2010. **2**(1): p. 65-79.
2. Van de Graaff, K.M., *Anatomy and physiology of the gastrointestinal tract.* Pediatr Infect Dis, 1986. **5**(1 Suppl): p. S11-6.
3. Schneeman, B.O., *Gastrointestinal physiology and functions.* Br J Nutr, 2002. **88 Suppl 2**: p. S159-63.
4. Santucci, N.R. and A. Velez, *Physiology of lower gastrointestinal tract.* Aliment Pharmacol Ther, 2024. **60 Suppl 1**: p. S1-S19.
5. Reed, K.K. and R. Wickham, *Review of the gastrointestinal tract: from macro to micro.* Semin Oncol Nurs, 2009. **25**(1): p. 3-14.
6. Sanchez de Medina, F., et al., *Intestinal inflammation and mucosal barrier function.* Inflamm Bowel Dis, 2014. **20**(12): p. 2394-404.
7. Greenwood-Van Meerveld, B., A.C. Johnson, and D. Grundy, *Gastrointestinal Physiology and Function.* Handb Exp Pharmacol, 2017. **239**: p. 1-16.
8. Huizinga, J.D. and W.J. Lammers, *Gut peristalsis is governed by a multitude of cooperating mechanisms.* Am J Physiol Gastrointest Liver Physiol, 2009. **296**(1): p. G1-8.
9. Karasov, W.H. and A.E. Douglas, *Comparative digestive physiology.* Compr Physiol, 2013. **3**(2): p. 741-83.
10. O'Connor, A. and C. O'Morain, *Digestive function of the stomach.* Dig Dis, 2014. **32**(3): p. 186-91.
11. Engevik, A.C., I. Kaji, and J.R. Goldenring, *The Physiology of the Gastric Parietal Cell.* Physiol Rev, 2020. **100**(2): p. 573-602.
12. Muller, M.J., J. Defize, and R.H. Hunt, *Control of pepsinogen synthesis and secretion.* Gastroenterol Clin North Am, 1990. **19**(1): p. 27-40.
13. Gribble, F.M. and F. Reimann, *Function and mechanisms of enteroendocrine cells and gut hormones in metabolism.* Nat Rev Endocrinol, 2019. **15**(4): p. 226-237.
14. Wang, F. and S. Roy, *Gut Homeostasis, Microbial Dysbiosis, and Opioids.* Toxicol Pathol, 2017. **45**(1): p. 150-156.
15. Groschwitz, K.R. and S.P. Hogan, *Intestinal barrier function: molecular regulation and disease pathogenesis.* J Allergy Clin Immunol, 2009. **124**(1): p. 3-20; quiz 21-2.
16. Helander, H.F. and L. Fandriks, *Surface area of the digestive tract - revisited.* Scand J Gastroenterol, 2014. **49**(6): p. 681-9.
17. Carlier, F.M., C. de Fays, and C. Pilette, *Epithelial Barrier Dysfunction in Chronic Respiratory Diseases.* Front Physiol, 2021. **12**: p. 691227.
18. Wells, J.M., et al., *Homeostasis of the gut barrier and potential biomarkers.* Am J Physiol Gastrointest Liver Physiol, 2017. **312**(3): p. G171-G193.
19. Ulluwishewa, D., et al., *Regulation of tight junction permeability by intestinal bacteria and dietary components.* J Nutr, 2011. **141**(5): p. 769-76.
20. Allam-Ndoul, B., S. Castonguay-Paradis, and A. Veilleux, *Gut Microbiota and Intestinal Trans-Epithelial Permeability.* Int J Mol Sci, 2020. **21**(17).
21. Bischoff, S.C., et al., *Intestinal permeability--a new target for disease prevention and therapy.* BMC Gastroenterol, 2014. **14**: p. 189.

22. Farquhar, M.G. and G.E. Palade, *Junctional complexes in various epithelia.* J Cell Biol, 1963. **17**(2): p. 375-412.
23. Garrod, D. and M. Chidgey, *Desmosome structure, composition and function.* Biochim Biophys Acta, 2008. **1778**(3): p. 572-87.
24. Sosinsky, G.E. and B.J. Nicholson, *Structural organization of gap junction channels.* Biochim Biophys Acta, 2005. **1711**(2): p. 99-125.
25. Tuma, P. and A.L. Hubbard, *Transcytosis: crossing cellular barriers.* Physiol Rev, 2003. **83**(3): p. 871-932.
26. van der Flier, L.G. and H. Clevers, *Stem cells, self-renewal, and differentiation in the intestinal epithelium.* Annu Rev Physiol, 2009. **71**: p. 241-60.
27. Oncel, S. and M.D. Basson, *Gut homeostasis, injury, and healing: New therapeutic targets.* World J Gastroenterol, 2022. **28**(17): p. 1725-1750.
28. Umar, S., *Intestinal stem cells.* Curr Gastroenterol Rep, 2010. **12**(5): p. 340-8.
29. Kai, Y., *Intestinal villus structure contributes to even shedding of epithelial cells.* Biophys J, 2021. **120**(4): p. 699-710.
30. Noah, T.K., B. Donahue, and N.F. Shroyer, *Intestinal development and differentiation.* Exp Cell Res, 2011. **317**(19): p. 2702-10.
31. Yang, H., et al., *Energy metabolism in intestinal epithelial cells during maturation along the crypt-villus axis.* Sci Rep, 2016. **6**: p. 31917.
32. Arandjelovic, S. and K.S. Ravichandran, *Phagocytosis of apoptotic cells in homeostasis.* Nat Immunol, 2015. **16**(9): p. 907-17.
33. von Herbay, A. and J. Rudi, *Role of apoptosis in gastric epithelial turnover.* Microsc Res Tech, 2000. **48**(5): p. 303-11.
34. Negroni, A., S. Cucchiara, and L. Stronati, *Apoptosis, Necrosis, and Necroptosis in the Gut and Intestinal Homeostasis.* Mediators Inflamm, 2015. **2015**: p. 250762.
35. Chelakkot, C., J. Ghim, and S.H. Ryu, *Mechanisms regulating intestinal barrier integrity and its pathological implications.* Exp Mol Med, 2018. **50**(8): p. 1-9.
36. Rivera, C.A. and A.M. Lennon-Dumenil, *Gut immune cells and intestinal niche imprinting.* Semin Cell Dev Biol, 2023. **150-151**: p. 50-57.
37. Bujko, A., et al., *Transcriptional and functional profiling defines human small intestinal macrophage subsets.* J Exp Med, 2018. **215**(2): p. 441-458.
38. De Calisto, J., E.J. Villablanca, and J.R. Mora, *FcgammaRI (CD64): an identity card for intestinal macrophages.* Eur J Immunol, 2012. **42**(12): p. 3136-40.
39. Domanska, D., et al., *Single-cell transcriptomic analysis of human colonic macrophages reveals niche-specific subsets.* J Exp Med, 2022. **219**(3).
40. Sayed, I.M., et al., *Host engulfment pathway controls inflammation in inflammatory bowel disease.* FEBS J, 2020. **287**(18): p. 3967-3988.
41. Meriwether, D., et al., *Macrophage COX2 Mediates Efferocytosis, Resolution Reprogramming, and Intestinal Epithelial Repair.* Cell Mol Gastroenterol Hepatol, 2022. **13**(4): p. 1095-1120.
42. D'Angelo, F., et al., *Macrophages promote epithelial repair through hepatocyte growth factor secretion.* Clin Exp Immunol, 2013. **174**(1): p. 60-72.
43. Cosin-Roger, J., et al., *The activation of Wnt signaling by a STAT6-dependent macrophage phenotype promotes mucosal repair in murine IBD.* Mucosal Immunol, 2016. **9**(4): p. 986-98.

44. Murai, M., et al., *Interleukin 10 acts on regulatory T cells to maintain expression of the transcription factor Foxp3 and suppressive function in mice with colitis.* Nat Immunol, 2009. **10**(11): p. 1178-84.
45. Kayama, H., et al., *Intestinal CX3C chemokine receptor 1(high) (CX3CR1(high)) myeloid cells prevent T-cell-dependent colitis.* Proc Natl Acad Sci U S A, 2012. **109**(13): p. 5010-5.
46. Panea, C., et al., *Intestinal Monocyte-Derived Macrophages Control Commensal-Specific Th17 Responses.* Cell Rep, 2015. **12**(8): p. 1314-24.
47. Ruder, B., R. Atreya, and C. Becker, *Tumour Necrosis Factor Alpha in Intestinal Homeostasis and Gut Related Diseases.* Int J Mol Sci, 2019. **20**(8).
48. Coombes, J.L. and F. Powrie, *Dendritic cells in intestinal immune regulation.* Nat Rev Immunol, 2008. **8**(6): p. 435-46.
49. Tezuka, H. and T. Ohteki, *Regulation of intestinal homeostasis by dendritic cells.* Immunol Rev, 2010. **234**(1): p. 247-58.
50. Sun, C.M., et al., *Small intestine lamina propria dendritic cells promote de novo generation of Foxp3 T reg cells via retinoic acid.* J Exp Med, 2007. **204**(8): p. 1775-85.
51. Coombes, J.L., et al., *A functionally specialized population of mucosal CD103+ DCs induces Foxp3+ regulatory T cells via a TGF-beta and retinoic acid-dependent mechanism.* J Exp Med, 2007. **204**(8): p. 1757-64.
52. Atarashi, K., et al., *ATP drives lamina propria T(H)17 cell differentiation.* Nature, 2008. **455**(7214): p. 808-12.
53. Niess, J.H., et al., *CX3CR1-mediated dendritic cell access to the intestinal lumen and bacterial clearance.* Science, 2005. **307**(5707): p. 254-8.
54. Chieppa, M., et al., *Dynamic imaging of dendritic cell extension into the small bowel lumen in response to epithelial cell TLR engagement.* J Exp Med, 2006. **203**(13): p. 2841-52.
55. Jang, M.H., et al., *CCR7 is critically important for migration of dendritic cells in intestinal lamina propria to mesenteric lymph nodes.* J Immunol, 2006. **176**(2): p. 803-10.
56. Iwasaki, A. and B.L. Kelsall, *Unique functions of CD11b+, CD8 alpha+, and double-negative Peyer's patch dendritic cells.* J Immunol, 2001. **166**(8): p. 4884-90.
57. Gronlund, M.M., et al., *Importance of intestinal colonisation in the maturation of humoral immunity in early infancy: a prospective follow up study of healthy infants aged 0-6 months.* Arch Dis Child Fetal Neonatal Ed, 2000. **83**(3): p. F186-92.
58. Shikina, T., et al., *IgA class switch occurs in the organized nasopharynx- and gut-associated lymphoid tissue, but not in the diffuse lamina propria of airways and gut.* J Immunol, 2004. **172**(10): p. 6259-64.
59. Cerutti, A., *Location, location, location: B-cell differentiation in the gut lamina propria.* Mucosal Immunol, 2008. **1**(1): p. 8-10.
60. Tezuka, H. and T. Ohteki, *Regulation of IgA Production by Intestinal Dendritic Cells and Related Cells.* Front Immunol, 2019. **10**: p. 1891.
61. Mantis, N.J., et al., *Immunoglobulin A antibodies against ricin A and B subunits protect epithelial cells from ricin intoxication.* Infect Immun, 2006. **74**(6): p. 3455-62.
62. Helander, A., et al., *Protective immunoglobulin A and G antibodies bind to overlapping intersubunit epitopes in the head domain of type 1 reovirus adhesin sigma1.* J Virol, 2004. **78**(19): p. 10695-705.
63. Mantis, N.J. and S.J. Forbes, *Secretory IgA: arresting microbial pathogens at epithelial borders.* Immunol Invest, 2010. **39**(4-5): p. 383-406.

64. Bollinger, R.R., et al., *Human secretory immunoglobulin A may contribute to biofilm formation in the gut.* Immunology, 2003. **109**(4): p. 580-7.
65. van der Waaij, L.A., et al., *In vivo IgA coating of anaerobic bacteria in human faeces.* Gut, 1996. **38**(3): p. 348-54.
66. Bollinger, R.R., et al., *Secretory IgA and mucin-mediated biofilm formation by environmental strains of Escherichia coli: role of type 1 pili.* Mol Immunol, 2006. **43**(4): p. 378-87.
67. Huus, K.E., et al., *Commensal Bacteria Modulate Immunoglobulin A Binding in Response to Host Nutrition.* Cell Host Microbe, 2020. **27**(6): p. 909-921 e5.
68. Fagarasan, S., et al., *Critical roles of activation-induced cytidine deaminase in the homeostasis of gut flora.* Science, 2002. **298**(5597): p. 1424-7.
69. Peterson, D.A., et al., *IgA response to symbiotic bacteria as a mediator of gut homeostasis.* Cell Host Microbe, 2007. **2**(5): p. 328-39.
70. Mantovani, A., et al., *Neutrophils in the activation and regulation of innate and adaptive immunity.* Nat Rev Immunol, 2011. **11**(8): p. 519-31.
71. Mortaz, E., et al., *Update on Neutrophil Function in Severe Inflammation.* Front Immunol, 2018. **9**: p. 2171.
72. Kuhl, A.A., et al., *Aggravation of different types of experimental colitis by depletion or adhesion blockade of neutrophils.* Gastroenterology, 2007. **133**(6): p. 1882-92.
73. Kim, N.D. and A.D. Luster, *The role of tissue resident cells in neutrophil recruitment.* Trends Immunol, 2015. **36**(9): p. 547-55.
74. Amara, N., et al., *Selective activation of PFKL suppresses the phagocytic oxidative burst.* Cell, 2021. **184**(17): p. 4480-4494 e15.
75. Pierzchala, K., et al., *Fluorescent probes for monitoring myeloperoxidase-derived hypochlorous acid: a comparative study.* Sci Rep, 2022. **12**(1): p. 9314.
76. Davies, M.J. and C.L. Hawkins, *The Role of Myeloperoxidase in Biomolecule Modification, Chronic Inflammation, and Disease.* Antioxid Redox Signal, 2020. **32**(13): p. 957-981.
77. Rees, M.D. and M.J. Davies, *Heparan sulfate degradation via reductive homolysis of its N-chloro derivatives.* J Am Chem Soc, 2006. **128**(9): p. 3085-97.
78. Brinkmann, V., et al., *Neutrophil extracellular traps kill bacteria.* Science, 2004. **303**(5663): p. 1532-5.
79. Papayannopoulos, V., et al., *Neutrophil elastase and myeloperoxidase regulate the formation of neutrophil extracellular traps.* J Cell Biol, 2010. **191**(3): p. 677-91.
80. Wang, Y., et al., *Human PAD4 regulates histone arginine methylation levels via demethylimination.* Science, 2004. **306**(5694): p. 279-83.
81. Papayannopoulos, V., *Neutrophil extracellular traps in immunity and disease.* Nat Rev Immunol, 2018. **18**(2): p. 134-147.
82. Wang, H., et al., *Neutrophil extracellular traps in homeostasis and disease.* Signal Transduct Target Ther, 2024. **9**(1): p. 235.
83. Ng, L.G., R. Ostuni, and A. Hidalgo, *Heterogeneity of neutrophils.* Nat Rev Immunol, 2019. **19**(4): p. 255-265.
84. Silvestre-Roig, C., A. Hidalgo, and O. Soehnlein, *Neutrophil heterogeneity: implications for homeostasis and pathogenesis.* Blood, 2016. **127**(18): p. 2173-81.
85. Zhou, G., et al., *CD177(+) neutrophils as functionally activated neutrophils negatively regulate IBD.* Gut, 2018. **67**(6): p. 1052-1063.

86. Seo, D.H., et al., *Triggering Receptor Expressed on Myeloid Cells-1 Agonist Regulates Intestinal Inflammation via Cd177(+) Neutrophils.* Front Immunol, 2021. **12**: p. 650864.
87. Gaudry, M., et al., *Intracellular pool of vascular endothelial growth factor in human neutrophils.* Blood, 1997. **90**(10): p. 4153-61.
88. Schwab, J.M., et al., *Resolvin E1 and protectin D1 activate inflammation-resolution programmes.* Nature, 2007. **447**(7146): p. 869-74.
89. El Kebir, D., P. Gjorstrup, and J.G. Filep, *Resolvin E1 promotes phagocytosis-induced neutrophil apoptosis and accelerates resolution of pulmonary inflammation.* Proc Natl Acad Sci U S A, 2012. **109**(37): p. 14983-8.
90. Freire, M.O., et al., *Neutrophil Resolvin E1 Receptor Expression and Function in Type 2 Diabetes.* J Immunol, 2017. **198**(2): p. 718-728.
91. Fredman, G., et al., *Impaired phagocytosis in localized aggressive periodontitis: rescue by Resolvin E1.* PLoS One, 2011. **6**(9): p. e24422.
92. Wang, G.L. and G.L. Semenza, *General involvement of hypoxia-inducible factor 1 in transcriptional response to hypoxia.* Proc Natl Acad Sci U S A, 1993. **90**(9): p. 4304-8.
93. Kelly, C.J., et al., *Fundamental role for HIF-1alpha in constitutive expression of human beta defensin-1.* Mucosal Immunol, 2013. **6**(6): p. 1110-8.
94. Kelly, C.J., et al., *Crosstalk between Microbiota-Derived Short-Chain Fatty Acids and Intestinal Epithelial HIF Augments Tissue Barrier Function.* Cell Host Microbe, 2015. **17**(5): p. 662-71.
95. Boeckxstaens, G., *Mast cells and inflammatory bowel disease.* Curr Opin Pharmacol, 2015. **25**: p. 45-9.
96. Bischoff, S.C. and S. Kramer, *Human mast cells, bacteria, and intestinal immunity.* Immunol Rev, 2007. **217**: p. 329-37.
97. Terakawa, M., et al., *Eosinophil migration induced by mast cell chymase is mediated by extracellular signal-regulated kinase pathway.* Biochem Biophys Res Commun, 2005. **332**(4): p. 969-75.
98. Malaviya, R., et al., *Mast cell modulation of neutrophil influx and bacterial clearance at sites of infection through TNF-alpha.* Nature, 1996. **381**(6577): p. 77-80.
99. Valeri, V., et al., *Mast cells crosstalk with B cells in the gut and sustain IgA response in the inflamed intestine.* Eur J Immunol, 2021. **51**(2): p. 445-458.
100. Merluzzi, S., et al., *Mast cells enhance proliferation of B lymphocytes and drive their differentiation toward IgA-secreting plasma cells.* Blood, 2010. **115**(14): p. 2810-7.
101. Groschwitz, K.R., et al., *Chymase-mediated intestinal epithelial permeability is regulated by a protease-activating receptor/matrix metalloproteinase-2-dependent mechanism.* Am J Physiol Gastrointest Liver Physiol, 2013. **304**(5): p. G479-89.
102. Tomasello, E. and S. Bedoui, *Intestinal innate immune cells in gut homeostasis and immunosurveillance.* Immunol Cell Biol, 2013. **91**(3): p. 201-3.
103. Walker, J.A., J.L. Barlow, and A.N. McKenzie, *Innate lymphoid cells--how did we miss them?* Nat Rev Immunol, 2013. **13**(2): p. 75-87.
104. Aujla, S.J. and J.K. Kolls, *IL-22: a critical mediator in mucosal host defense.* J Mol Med (Berl), 2009. **87**(5): p. 451-4.
105. Zheng, Y., et al., *Interleukin-22 mediates early host defense against attaching and effacing bacterial pathogens.* Nat Med, 2008. **14**(3): p. 282-9.
106. Hanash, A.M., et al., *Interleukin-22 protects intestinal stem cells from immune-mediated tissue damage and regulates sensitivity to graft versus host disease.* Immunity, 2012. **37**(2): p. 339-50.

107. Marchesi, J.R. and J. Ravel, *The vocabulary of microbiome research: a proposal.* Microbiome, 2015. **3**: p. 31.
108. Hou, K., et al., *Microbiota in health and diseases.* Signal Transduct Target Ther, 2022. **7**(1): p. 135.
109. Das, B., et al., *Analysis of the Gut Microbiome of Rural and Urban Healthy Indians Living in Sea Level and High Altitude Areas.* Sci Rep, 2018. **8**(1): p. 10104.
110. Das, B. and G.B. Nair, *Homeostasis and dysbiosis of the gut microbiome in health and disease.* J Biosci, 2019. **44**(5).
111. Caporaso, J.G., et al., *Moving pictures of the human microbiome.* Genome Biol, 2011. **12**(5): p. R50.
112. van Duynhoven, J., et al., *Metabolic fate of polyphenols in the human superorganism.* Proc Natl Acad Sci U S A, 2011. **108 Suppl 1**(Suppl 1): p. 4531-8.
113. Lee, J.Y., R.M. Tsolis, and A.J. Baumler, *The microbiome and gut homeostasis.* Science, 2022. **377**(6601): p. eabp9960.
114. Bures, J., et al., *Small intestinal bacterial overgrowth syndrome.* World J Gastroenterol, 2010. **16**(24): p. 2978-90.
115. Sender, R., S. Fuchs, and R. Milo, *Revised Estimates for the Number of Human and Bacteria Cells in the Body.* PLoS Biol, 2016. **14**(8): p. e1002533.
116. Morrison, D.J. and T. Preston, *Formation of short chain fatty acids by the gut microbiota and their impact on human metabolism.* Gut Microbes, 2016. **7**(3): p. 189-200.
117. Fukuda, S., et al., *Bifidobacteria can protect from enteropathogenic infection through production of acetate.* Nature, 2011. **469**(7331): p. 543-7.
118. Maslowski, K.M., et al., *Regulation of inflammatory responses by gut microbiota and chemoattractant receptor GPR43.* Nature, 2009. **461**(7268): p. 1282-6.
119. Peng, L., et al., *Effects of butyrate on intestinal barrier function in a Caco-2 cell monolayer model of intestinal barrier.* Pediatr Res, 2007. **61**(1): p. 37-41.
120. Bird, J.J., et al., *Helper T cell differentiation is controlled by the cell cycle.* Immunity, 1998. **9**(2): p. 229-37.
121. Birkett, A.M., et al., *Dietary intake and faecal excretion of carbohydrate by Australians: importance of achieving stool weights greater than 150 g to improve faecal markers relevant to colon cancer risk.* Eur J Clin Nutr, 1997. **51**(9): p. 625-32.
122. Kau, A.L., et al., *Human nutrition, the gut microbiome and the immune system.* Nature, 2011. **474**(7351): p. 327-36.
123. Forman, H.J., F. Ursini, and M. Maiorino, *An overview of mechanisms of redox signaling.* J Mol Cell Cardiol, 2014. **73**: p. 2-9.
124. Campbell, E.L. and S.P. Colgan, *Control and dysregulation of redox signalling in the gastrointestinal tract.* Nat Rev Gastroenterol Hepatol, 2019. **16**(2): p. 106-120.
125. West, A.P., G.S. Shadel, and S. Ghosh, *Mitochondria in innate immune responses.* Nat Rev Immunol, 2011. **11**(6): p. 389-402.
126. Genova, M.L., et al., *The site of production of superoxide radical in mitochondrial Complex I is not a bound ubisemiquinone but presumably iron-sulfur cluster N2.* FEBS Lett, 2001. **505**(3): p. 364-8.
127. Brookes, P.S., et al., *Calcium, ATP, and ROS: a mitochondrial love-hate triangle.* Am J Physiol Cell Physiol, 2004. **287**(4): p. C817-33.
128. Beckman, J.S. and W.H. Koppenol, *Nitric oxide, superoxide, and peroxynitrite: the good, the bad, and ugly.* Am J Physiol, 1996. **271**(5 Pt 1): p. C1424-37.

129. Kulkarni, A.C., P. Kuppusamy, and N. Parinandi, *Oxygen, the lead actor in the pathophysiologic drama: enactment of the trinity of normoxia, hypoxia, and hyperoxia in disease and therapy.* Antioxid Redox Signal, 2007. **9**(10): p. 1717-30.
130. Zoetendal, E.G., et al., *The human small intestinal microbiota is driven by rapid uptake and conversion of simple carbohydrates.* ISME J, 2012. **6**(7): p. 1415-26.
131. Donaldson, G.P., S.M. Lee, and S.K. Mazmanian, *Gut biogeography of the bacterial microbiota.* Nat Rev Microbiol, 2016. **14**(1): p. 20-32.
132. Sundin, O.H., et al., *The human jejunum has an endogenous microbiota that differs from those in the oral cavity and colon.* BMC Microbiol, 2017. **17**(1): p. 160.
133. Tropini, C., et al., *The Gut Microbiome: Connecting Spatial Organization to Function.* Cell Host Microbe, 2017. **21**(4): p. 433-442.
134. Buckel, W., *Energy Conservation in Fermentations of Anaerobic Bacteria.* Front Microbiol, 2021. **12**: p. 703525.
135. Maitra, A. and K.A. Dill, *Bacterial growth laws reflect the evolutionary importance of energy efficiency.* Proc Natl Acad Sci U S A, 2015. **112**(2): p. 406-11.
136. Mukhtar, K., H. Nawaz, and S. Abid, *Functional gastrointestinal disorders and gut-brain axis: What does the future hold?* World J Gastroenterol, 2019. **25**(5): p. 552-566.
137. Drossman, D.A., et al., *Psychosocial aspects of the functional gastrointestinal disorders.* Gut, 1999. **45 Suppl 2**(Suppl 2): p. II25-30.
138. Xavier, R.J. and H.J. Thomas, *Gastrointestinal diseases*, in *Hunter's Tropical Medicine Emerging Infectious Disease*, A.J. Mgaill, et al., Editors. 2012, Saunders. p. 18-27.
139. Banyai, K., et al., *Viral gastroenteritis.* Lancet, 2018. **392**(10142): p. 175-186.
140. Velazquez, F.R., et al., *Rotavirus infection in infants as protection against subsequent infections.* N Engl J Med, 1996. **335**(14): p. 1022-8.
141. Ahmed, S.M., et al., *Global prevalence of norovirus in cases of gastroenteritis: a systematic review and meta-analysis.* Lancet Infect Dis, 2014. **14**(8): p. 725-730.
142. Flynn, T.G., M.P. Olortegui, and M.N. Kosek, *Viral gastroenteritis.* Lancet, 2024. **403**(10429): p. 862-876.
143. Blacklow, N.R. and H.B. Greenberg, *Viral gastroenteritis.* N Engl J Med, 1991. **325**(4): p. 252-64.
144. Lorrot, M. and M. Vasseur, *How do the rotavirus NSP4 and bacterial enterotoxins lead differently to diarrhea?* Virol J, 2007. **4**: p. 31.
145. Ettayebi, K., et al., *Replication of human noroviruses in stem cell-derived human enteroids.* Science, 2016. **353**(6306): p. 1387-1393.
146. Troeger, H., et al., *Structural and functional changes of the duodenum in human norovirus infection.* Gut, 2009. **58**(8): p. 1070-7.
147. Karandikar, U.C., et al., *Detection of human norovirus in intestinal biopsies from immunocompromised transplant patients.* J Gen Virol, 2016. **97**(9): p. 2291-2300.
148. Tam, C.C., et al., *Changes in causes of acute gastroenteritis in the United Kingdom over 15 years: microbiologic findings from 2 prospective, population-based studies of infectious intestinal disease.* Clin Infect Dis, 2012. **54**(9): p. 1275-86.
149. Shah, N., H.L. DuPont, and D.J. Ramsey, *Global etiology of travelers' diarrhea: systematic review from 1973 to the present.* Am J Trop Med Hyg, 2009. **80**(4): p. 609-14.
150. Hodges, K. and R. Gill, *Infectious diarrhea: Cellular and molecular mechanisms.* Gut Microbes, 2010. **1**(1): p. 4-21.

151. Ranasinghe, S. and C.N.J.M. Fhogartaigh, *Bacterial gastroenteritis.* Medicine, 2021. **49**(11): p. 687-693.
152. Bashar, S., et al., *Severe Gastroenteritis From Giardia lamblia and Salmonella Saintpaul Co-Infection Causing Acute Renal Failure.* Cureus, 2022. **14**(5): p. e25288.
153. Naumova, E.N., et al., *The elderly and waterborne Cryptosporidium infection: gastroenteritis hospitalizations before and during the 1993 Milwaukee outbreak.* Emerg Infect Dis, 2003. **9**(4): p. 418-25.
154. Gonzalez-Visiedo, M., M.D. Kulis, and D.M. Markusic, *Manipulating the microbiome to enhance oral tolerance in food allergy.* Cell Immunol, 2022. **382**: p. 104633.
155. Nowak-Wegrzyn, A., H. Szajewska, and G. Lack, *Food allergy and the gut.* Nat Rev Gastroenterol Hepatol, 2017. **14**(4): p. 241-257.
156. Bock, S.A., *Prospective appraisal of complaints of adverse reactions to foods in children during the first 3 years of life.* Pediatrics, 1987. **79**(5): p. 683-8.
157. Kalach, N., et al., *Intestinal permeability in children: variation with age and reliability in the diagnosis of cow's milk allergy.* Acta Paediatr, 2001. **90**(5): p. 499-504.
158. Rona, R.J., et al., *The prevalence of food allergy: a meta-analysis.* J Allergy Clin Immunol, 2007. **120**(3): p. 638-46.
159. Savage, J., S. Sicherer, and R. Wood, *The Natural History of Food Allergy.* J Allergy Clin Immunol Pract, 2016. **4**(2): p. 196-203; quiz 204.
160. Warren, C.M., J. Jiang, and R.S. Gupta, *Epidemiology and Burden of Food Allergy.* Curr Allergy Asthma Rep, 2020. **20**(2): p. 6.
161. Wang, L.J., et al., *Clinical Manifestations of Pediatric Food Allergy: a Contemporary Review.* Clin Rev Allergy Immunol, 2022. **62**(1): p. 180-199.
162. Muraro, A., et al., *EAACI food allergy and anaphylaxis guidelines: diagnosis and management of food allergy.* Allergy, 2014. **69**(8): p. 1008-25.
163. Bartra, J., P.J. Turner, and R.M. Munoz-Cano, *Cofactors in food anaphylaxis in adults.* Ann Allergy Asthma Immunol, 2023. **130**(6): p. 733-740.
164. Maret-Ouda, J., S.R. Markar, and J. Lagergren, *Gastroesophageal Reflux Disease: A Review.* JAMA, 2020. **324**(24): p. 2536-2547.
165. Savarino, E., et al., *Expert consensus document: Advances in the physiological assessment and diagnosis of GERD.* Nat Rev Gastroenterol Hepatol, 2017. **14**(11): p. 665-676.
166. Napierkowski, J. and R.K. Wong, *Extraesophageal manifestations of GERD.* Am J Med Sci, 2003. **326**(5): p. 285-99.
167. Eusebi, L.H., et al., *Global prevalence of, and risk factors for, gastro-oesophageal reflux symptoms: a meta-analysis.* Gut, 2018. **67**(3): p. 430-440.
168. Poddar, U., *Gastroesophageal reflux disease (GERD) in children.* Paediatr Int Child Health, 2019. **39**(1): p. 7-12.
169. Zagari, R.M., et al., *Gastro-oesophageal reflux symptoms, oesophagitis and Barrett's oesophagus in the general population: the Loiano-Monghidoro study.* Gut, 2008. **57**(10): p. 1354-9.
170. Pregun, I., et al., *Peptic esophageal stricture: medical treatment.* Dig Dis, 2009. **27**(1): p. 31-7.
171. Eusebi, L.H., et al., *Global prevalence of Barrett's oesophagus and oesophageal cancer in individuals with gastro-oesophageal reflux: a systematic review and meta-analysis.* Gut, 2021. **70**(3): p. 456-463.

172. Coleman, H.G., S.H. Xie, and J. Lagergren, *The Epidemiology of Esophageal Adenocarcinoma.* Gastroenterology, 2018. **154**(2): p. 390-405.
173. Ness-Jensen, E., et al., *Lifestyle Intervention in Gastroesophageal Reflux Disease.* Clin Gastroenterol Hepatol, 2016. **14**(2): p. 175-82 e1-3.
174. Hamilton, J.W., et al., *Sleeping on a wedge diminishes exposure of the esophagus to refluxed acid.* Dig Dis Sci, 1988. **33**(5): p. 518-22.
175. Zalvan, C.H., et al., *A Comparison of Alkaline Water and Mediterranean Diet vs Proton Pump Inhibition for Treatment of Laryngopharyngeal Reflux.* JAMA Otolaryngol Head Neck Surg, 2017. **143**(10): p. 1023-1029.
176. Pratt, N.L., et al., *Use of proton pump inhibitors among older Australians: national quality improvement programmes have led to sustained practice change.* Int J Qual Health Care, 2017. **29**(1): p. 75-82.
177. Kahrilas, P.J., et al., *American Gastroenterological Association Medical Position Statement on the management of gastroesophageal reflux disease.* Gastroenterology, 2008. **135**(4): p. 1383-1391, 1391 e1-5.
178. Sung, H., et al., *Global Cancer Statistics 2020: GLOBOCAN Estimates of Incidence and Mortality Worldwide for 36 Cancers in 185 Countries.* CA Cancer J Clin, 2021. **71**(3): p. 209-249.
179. Jagadeesan, D., et al., *Comprehensive insights into oral squamous cell carcinoma: Diagnosis, pathogenesis, and therapeutic advances.* Pathol Res Pract, 2024. **261**: p. 155489.
180. Smyth, E.C., et al., *Oesophageal cancer.* Nat Rev Dis Primers, 2017. **3**: p. 17048.
181. He, Y.T., et al., *Trends in incidence of esophageal and gastric cardia cancer in high-risk areas in China.* Eur J Cancer Prev, 2008. **17**(2): p. 71-6.
182. Trivers, K.F., S.A. Sabatino, and S.L. Stewart, *Trends in esophageal cancer incidence by histology, United States, 1998-2003.* Int J Cancer, 2008. **123**(6): p. 1422-8.
183. Freedman, N.D., et al., *A prospective study of tobacco, alcohol, and the risk of esophageal and gastric cancer subtypes.* Am J Epidemiol, 2007. **165**(12): p. 1424-33.
184. Freedman, N.D., et al., *Fruit and vegetable intake and esophageal cancer in a large prospective cohort study.* Int J Cancer, 2007. **121**(12): p. 2753-60.
185. Edgren, G., et al., *A global assessment of the oesophageal adenocarcinoma epidemic.* Gut, 2013. **62**(10): p. 1406-14.
186. Jain, S. and S. Dhingra, *Pathology of esophageal cancer and Barrett's esophagus.* Ann Cardiothorac Surg, 2017. **6**(2): p. 99-109.
187. Cook, M.B., et al., *Gastroesophageal reflux in relation to adenocarcinomas of the esophagus: a pooled analysis from the Barrett's and Esophageal Adenocarcinoma Consortium (BEACON).* PLoS One, 2014. **9**(7): p. e103508.
188. Launoy, G., et al., *Trends in net survival from esophageal cancer in six European Latin countries: results from the SUDCAN population-based study.* Eur J Cancer Prev, 2017. **26 Trends in cancer net survival in six European Latin Countries: the SUDCAN study**: p. S24-S31.
189. Siegel, R., et al., *Cancer statistics, 2014.* CA Cancer J Clin, 2014. **64**(1): p. 9-29.
190. Morita, F.H., et al., *Narrow band imaging versus lugol chromoendoscopy to diagnose squamous cell carcinoma of the esophagus: a systematic review and meta-analysis.* BMC Cancer, 2017. **17**(1): p. 54.

191. Pech, O., et al., *Long-term efficacy and safety of endoscopic resection for patients with mucosal adenocarcinoma of the esophagus.* Gastroenterology, 2014. **146**(3): p. 652-660 e1.
192. Fitzgerald, R.C., et al., *British Society of Gastroenterology guidelines on the diagnosis and management of Barrett's oesophagus.* Gut, 2014. **63**(1): p. 7-42.
193. Bray, F., et al., *Global cancer statistics 2018: GLOBOCAN estimates of incidence and mortality worldwide for 36 cancers in 185 countries.* CA Cancer J Clin, 2018. **68**(6): p. 394-424.
194. Siewert, J.R. and H.J. Stein, *Classification of adenocarcinoma of the oesophagogastric junction.* Br J Surg, 1998. **85**(11): p. 1457-9.
195. Bornschein, J., et al., *H. pylori infection is a key risk factor for proximal gastric cancer.* Dig Dis Sci, 2010. **55**(11): p. 3124-31.
196. Wang, F., et al., *Helicobacter pylori-induced gastric inflammation and gastric cancer.* Cancer Lett, 2014. **345**(2): p. 196-202.
197. Wang, H.H., et al., *Lymphoepithelioma-like carcinoma of the stomach: a subset of gastric carcinoma with distinct clinicopathological features and high prevalence of Epstein-Barr virus infection.* Hepatogastroenterology, 1999. **46**(26): p. 1214-9.
198. Wu, M.S., et al., *Epstein-Barr virus-associated gastric carcinomas: relation to H. pylori infection and genetic alterations.* Gastroenterology, 2000. **118**(6): p. 1031-8.
199. Oliveira, C., et al., *Familial gastric cancer: genetic susceptibility, pathology, and implications for management.* Lancet Oncol, 2015. **16**(2): p. e60-70.
200. Guilford, P., et al., *E-cadherin germline mutations in familial gastric cancer.* Nature, 1998. **392**(6674): p. 402-5.
201. Majewski, I.J., et al., *An alpha-E-catenin (CTNNA1) mutation in hereditary diffuse gastric cancer.* J Pathol, 2013. **229**(4): p. 621-9.
202. Van Cutsem, E., et al., *Gastric cancer.* Lancet, 2016. **388**(10060): p. 2654-2664.
203. Axon, A., *Symptoms and diagnosis of gastric cancer at early curable stage.* Best Pract Res Clin Gastroenterol, 2006. **20**(4): p. 697-708.
204. Van Cutsem, E., et al., *The diagnosis and management of gastric cancer: expert discussion and recommendations from the 12th ESMO/World Congress on Gastrointestinal Cancer, Barcelona, 2010.* Ann Oncol, 2011. **22 Suppl 5**: p. v1-9.
205. Douaiher, J., et al., *Colorectal cancer-global burden, trends, and geographical variations.* J Surg Oncol, 2017. **115**(5): p. 619-630.
206. Arnold, M., et al., *Global patterns and trends in colorectal cancer incidence and mortality.* Gut, 2017. **66**(4): p. 683-691.
207. Morgan, E., et al., *Global burden of colorectal cancer in 2020 and 2040: incidence and mortality estimates from GLOBOCAN.* Gut, 2023. **72**(2): p. 338-344.
208. Grady, W.M. and C.C. Pritchard, *Molecular alterations and biomarkers in colorectal cancer.* Toxicol Pathol, 2014. **42**(1): p. 124-39.
209. Amersi, F., M. Agustin, and C.Y. Ko, *Colorectal cancer: epidemiology, risk factors, and health services.* Clin Colon Rectal Surg, 2005. **18**(3): p. 133-40.
210. Shussman, N. and S.D. Wexner, *Colorectal polyps and polyposis syndromes.* Gastroenterol Rep (Oxf), 2014. **2**(1): p. 1-15.
211. Keller, D.S., et al., *Colorectal cancer in inflammatory bowel disease: review of the evidence.* Tech Coloproctol, 2019. **23**(1): p. 3-13.
212. Ma, Y., et al., *Type 2 diabetes and risk of colorectal cancer in two large U.S. prospective cohorts.* Br J Cancer, 2018. **119**(11): p. 1436-1442.

213. Shao, T. and Y.X. Yang, *Cholecystectomy and the risk of colorectal cancer.* Am J Gastroenterol, 2005. **100**(8): p. 1813-20.
214. Rawla, P., T. Sunkara, and A. Barsouk, *Epidemiology of colorectal cancer: incidence, mortality, survival, and risk factors.* Prz Gastroenterol, 2019. **14**(2): p. 89-103.
215. Keum, N. and E. Giovannucci, *Global burden of colorectal cancer: emerging trends, risk factors and prevention strategies.* Nat Rev Gastroenterol Hepatol, 2019. **16**(12): p. 713-732.
216. Sawicki, T., et al., *A Review of Colorectal Cancer in Terms of Epidemiology, Risk Factors, Development, Symptoms and Diagnosis.* Cancers (Basel), 2021. **13**(9).
217. Chan, D.S., et al., *Red and processed meat and colorectal cancer incidence: meta-analysis of prospective studies.* PLoS One, 2011. **6**(6): p. e20456.
218. Cheng, Y., Z. Ling, and L. Li, *The Intestinal Microbiota and Colorectal Cancer.* Front Immunol, 2020. **11**: p. 615056.
219. Carethers, J.M. and C.A. Doubeni, *Causes of Socioeconomic Disparities in Colorectal Cancer and Intervention Framework and Strategies.* Gastroenterology, 2020. **158**(2): p. 354-367.
220. Tanaka, T., *Colorectal carcinogenesis: Review of human and experimental animal studies.* J Carcinog, 2009. **8**: p. 5.
221. Rosty, C., et al., *Serrated polyps of the large intestine: current understanding of diagnosis, pathogenesis, and clinical management.* J Gastroenterol, 2013. **48**(3): p. 287-302.
222. Brenner, H., et al., *Risk of progression of advanced adenomas to colorectal cancer by age and sex: estimates based on 840,149 screening colonoscopies.* Gut, 2007. **56**(11): p. 1585-9.
223. Kuipers, E.J., et al., *Colorectal cancer.* Nat Rev Dis Primers, 2015. **1**: p. 15065.
224. van de Velde, C.J., et al., *EURECCA colorectal: multidisciplinary management: European consensus conference colon & rectum.* Eur J Cancer, 2014. **50**(1): p. 1 e1-1 e34.
225. Valentini, V., et al., *EURECCA consensus conference highlights about rectal cancer clinical management: the radiation oncologist's expert review.* Radiother Oncol, 2014. **110**(1): p. 195-8.
226. Camilleri, M., *Diagnosis and Treatment of Irritable Bowel Syndrome: A Review.* JAMA, 2021. **325**(9): p. 865-877.
227. Williams, R.E., et al., *Determinants of healthcare-seeking behaviour among subjects with irritable bowel syndrome.* Aliment Pharmacol Ther, 2006. **23**(11): p. 1667-75.
228. Riedl, A., et al., *Somatic comorbidities of irritable bowel syndrome: a systematic analysis.* J Psychosom Res, 2008. **64**(6): p. 573-82.
229. Lovell, R.M. and A.C. Ford, *Prevalence of gastro-esophageal reflux-type symptoms in individuals with irritable bowel syndrome in the community: a meta-analysis.* Am J Gastroenterol, 2012. **107**(12): p. 1793-801; quiz 1802.
230. Fond, G., et al., *Anxiety and depression comorbidities in irritable bowel syndrome (IBS): a systematic review and meta-analysis.* Eur Arch Psychiatry Clin Neurosci, 2014. **264**(8): p. 651-60.
231. Lovell, R.M. and A.C. Ford, *Global prevalence of and risk factors for irritable bowel syndrome: a meta-analysis.* Clin Gastroenterol Hepatol, 2012. **10**(7): p. 712-721 e4.
232. Manning, L.P., C.J. Tuck, and J.R. Biesiekierski, *The lived experience of irritable bowel syndrome: A focus on dietary management.* Aust J Gen Pract, 2022. **51**(6): p. 395-400.

233. Lovell, R.M. and A.C. Ford, *Effect of gender on prevalence of irritable bowel syndrome in the community: systematic review and meta-analysis.* Am J Gastroenterol, 2012. **107**(7): p. 991-1000.
234. Chey, W.D., J. Kurlander, and S. Eswaran, *Irritable bowel syndrome: a clinical review.* JAMA, 2015. **313**(9): p. 949-58.
235. Simren, M., et al., *Intestinal microbiota in functional bowel disorders: a Rome foundation report.* Gut, 2013. **62**(1): p. 159-76.
236. Dupont, H.L., *Review article: evidence for the role of gut microbiota in irritable bowel syndrome and its potential influence on therapeutic targets.* Aliment Pharmacol Ther, 2014. **39**(10): p. 1033-42.
237. Halmos, E.P., et al., *A diet low in FODMAPs reduces symptoms of irritable bowel syndrome.* Gastroenterology, 2014. **146**(1): p. 67-75 e5.
238. Ford, A.C., et al., *Efficacy of antidepressants and psychological therapies in irritable bowel syndrome: systematic review and meta-analysis.* Gut, 2009. **58**(3): p. 367-78.
239. Ford, A.C., et al., *American College of Gastroenterology monograph on the management of irritable bowel syndrome and chronic idiopathic constipation.* Am J Gastroenterol, 2014. **109 Suppl 1**: p. S2-26; quiz S27.
240. Min, Y.W., et al., *Effect of composite yogurt enriched with acacia fiber and Bifidobacterium lactis.* World J Gastroenterol, 2012. **18**(33): p. 4563-9.
241. Fakhoury, M., et al., *Inflammatory bowel disease: clinical aspects and treatments.* J Inflamm Res, 2014. **7**: p. 113-20.
242. Guindi, M. and R.H. Riddell, *Indeterminate colitis.* J Clin Pathol, 2004. **57**(12): p. 1233-44.
243. Yu, Y.R. and J.R. Rodriguez, *Clinical presentation of Crohn's, ulcerative colitis, and indeterminate colitis: Symptoms, extraintestinal manifestations, and disease phenotypes.* Semin Pediatr Surg, 2017. **26**(6): p. 349-355.
244. Agostini, A., et al., *Differential Brain Structural and Functional Patterns in Crohn's Disease Patients are Associated with Different Disease Stages.* Inflamm Bowel Dis, 2023. **29**(8): p. 1297-1305.
245. Kirsner, J.B., *Historical origins of current IBD concepts.* World J Gastroenterol, 2001. **7**(2): p. 175-84.
246. Kobayashi, T., et al., *Ulcerative colitis.* Nat Rev Dis Primers, 2020. **6**(1): p. 74.
247. Kaur, A. and P. Goggolidou, *Ulcerative colitis: understanding its cellular pathology could provide insights into novel therapies.* J Inflamm (Lond), 2020. **17**: p. 15.
248. Uhlig, H.H., et al., *Differential activity of IL-12 and IL-23 in mucosal and systemic innate immune pathology.* Immunity, 2006. **25**(2): p. 309-18.
249. Lissner, D., et al., *Monocyte and M1 Macrophage-induced Barrier Defect Contributes to Chronic Intestinal Inflammation in IBD.* Inflamm Bowel Dis, 2015. **21**(6): p. 1297-305.
250. Harusato, A., et al., *IL-36gamma signaling controls the induced regulatory T cell-Th9 cell balance via NFkappaB activation and STAT transcription factors.* Mucosal Immunol, 2017. **10**(6): p. 1455-1467.
251. Machiels, K., et al., *A decrease of the butyrate-producing species Roseburia hominis and Faecalibacterium prausnitzii defines dysbiosis in patients with ulcerative colitis.* Gut, 2014. **63**(8): p. 1275-83.
252. Van Klinken, B.J., et al., *Sulphation and secretion of the predominant secretory human colonic mucin MUC2 in ulcerative colitis.* Gut, 1999. **44**(3): p. 387-93.

253. Banerjee, A.K. and T.J. Peters, *The history of Crohn's disease.* J R Coll Physicians Lond, 1989. **23**(2): p. 121-4.
254. Roda, G., et al., *Crohn's disease.* Nat Rev Dis Primers, 2020. **6**(1): p. 22.
255. Yamamoto, S. and X. Ma, *Role of Nod2 in the development of Crohn's disease.* Microbes Infect, 2009. **11**(12): p. 912-8.
256. de Souza, H.S. and C. Fiocchi, *Immunopathogenesis of IBD: current state of the art.* Nat Rev Gastroenterol Hepatol, 2016. **13**(1): p. 13-27.
257. Uhlig, H.H. and F. Powrie, *Translating Immunology into Therapeutic Concepts for Inflammatory Bowel Disease.* Annu Rev Immunol, 2018. **36**: p. 755-781.
258. Marotto, D., et al., *Extra-intestinal manifestations of inflammatory bowel diseases.* Pharmacol Res, 2020. **161**: p. 105206.
259. Vavricka, S.R., et al., *Frequency and risk factors for extraintestinal manifestations in the Swiss inflammatory bowel disease cohort.* Am J Gastroenterol, 2011. **106**(1): p. 110-9.
260. Lindstrom, L., et al., *Increased risk of colorectal cancer and dysplasia in patients with Crohn's colitis and primary sclerosing cholangitis.* Dis Colon Rectum, 2011. **54**(11): p. 1392-7.
261. Nikolaus, S. and S. Schreiber, *Diagnostics of inflammatory bowel disease.* Gastroenterology, 2007. **133**(5): p. 1670-89.
262. Feakins, R.M., *Ulcerative colitis or Crohn's disease? Pitfalls and problems.* Histopathology, 2014. **64**(3): p. 317-35.
263. Wolfson, D.M., et al., *Granulomas do not affect postoperative recurrence rates in Crohn's disease.* Gastroenterology, 1982. **83**(2): p. 405-9.
264. Black, S., I. Kushner, and D. Samols, *C-reactive Protein.* J Biol Chem, 2004. **279**(47): p. 48487-90.
265. Iskandar, H.N. and M.A. Ciorba, *Biomarkers in inflammatory bowel disease: current practices and recent advances.* Transl Res, 2012. **159**(4): p. 313-25.
266. Solem, C.A., et al., *Correlation of C-reactive protein with clinical, endoscopic, histologic, and radiographic activity in inflammatory bowel disease.* Inflamm Bowel Dis, 2005. **11**(8): p. 707-12.
267. D'Haens, G., et al., *Fecal calprotectin is a surrogate marker for endoscopic lesions in inflammatory bowel disease.* Inflamm Bowel Dis, 2012. **18**(12): p. 2218-24.
268. Gisbert, J.P., A.G. McNicholl, and F. Gomollon, *Questions and answers on the role of fecal lactoferrin as a biological marker in inflammatory bowel disease.* Inflamm Bowel Dis, 2009. **15**(11): p. 1746-54.
269. Langhorst, J., et al., *Noninvasive markers in the assessment of intestinal inflammation in inflammatory bowel diseases: performance of fecal lactoferrin, calprotectin, and PMN-elastase, CRP, and clinical indices.* Am J Gastroenterol, 2008. **103**(1): p. 162-9.
270. Nancey, S., et al., *Neopterin is a novel reliable fecal marker as accurate as calprotectin for predicting endoscopic disease activity in patients with inflammatory bowel diseases.* Inflamm Bowel Dis, 2013. **19**(5): p. 1043-52.
271. Kaiser, T., et al., *Faecal S100A12 as a non-invasive marker distinguishing inflammatory bowel disease from irritable bowel syndrome.* Gut, 2007. **56**(12): p. 1706-13.
272. Ng, S.C., et al., *Worldwide incidence and prevalence of inflammatory bowel disease in the 21st century: a systematic review of population-based studies.* Lancet, 2017. **390**(10114): p. 2769-2778.

273. Ng, S.C., et al., *Population Density and Risk of Inflammatory Bowel Disease: A Prospective Population-Based Study in 13 Countries or Regions in Asia-Pacific.* Am J Gastroenterol, 2019. **114**(1): p. 107-115.
274. Yen, H.H., et al., *Epidemiological trend in inflammatory bowel disease in Taiwan from 2001 to 2015: a nationwide populationbased study.* Intest Res, 2019. **17**(1): p. 54-62.
275. Perminow, G., et al., *A characterization in childhood inflammatory bowel disease, a new population-based inception cohort from South-Eastern Norway, 2005-07, showing increased incidence in Crohn's disease.* Scand J Gastroenterol, 2009. **44**(4): p. 446-56.
276. Malmborg, P., et al., *Increasing incidence of paediatric inflammatory bowel disease in northern Stockholm County, 2002-2007.* J Pediatr Gastroenterol Nutr, 2013. **57**(1): p. 29-34.
277. Benchimol, E.I., et al., *Trends in Epidemiology of Pediatric Inflammatory Bowel Disease in Canada: Distributed Network Analysis of Multiple Population-Based Provincial Health Administrative Databases.* Am J Gastroenterol, 2017. **112**(7): p. 1120-1134.
278. Shah, S.C., et al., *Sex-Based Differences in Incidence of Inflammatory Bowel Diseases-Pooled Analysis of Population-Based Studies From Western Countries.* Gastroenterology, 2018. **155**(4): p. 1079-1089 e3.
279. Halme, L., et al., *Family and twin studies in inflammatory bowel disease.* World J Gastroenterol, 2006. **12**(23): p. 3668-72.
280. Yang, H., et al., *Familial empirical risks for inflammatory bowel disease: differences between Jews and non-Jews.* Gut, 1993. **34**(4): p. 517-24.
281. Jostins, L., et al., *Host-microbe interactions have shaped the genetic architecture of inflammatory bowel disease.* Nature, 2012. **491**(7422): p. 119-24.
282. Khor, B., A. Gardet, and R.J. Xavier, *Genetics and pathogenesis of inflammatory bowel disease.* Nature, 2011. **474**(7351): p. 307-17.
283. Ogura, Y., et al., *A frameshift mutation in NOD2 associated with susceptibility to Crohn's disease.* Nature, 2001. **411**(6837): p. 603-6.
284. Hampe, J., et al., *A genome-wide association scan of nonsynonymous SNPs identifies a susceptibility variant for Crohn disease in ATG16L1.* Nat Genet, 2007. **39**(2): p. 207-11.
285. Cuthbert, A.P., et al., *The contribution of NOD2 gene mutations to the risk and site of disease in inflammatory bowel disease.* Gastroenterology, 2002. **122**(4): p. 867-74.
286. Anderson, C.A., et al., *Meta-analysis identifies 29 additional ulcerative colitis risk loci, increasing the number of confirmed associations to 47.* Nat Genet, 2011. **43**(3): p. 246-52.
287. Franke, A., et al., *Genome-wide meta-analysis increases to 71 the number of confirmed Crohn's disease susceptibility loci.* Nat Genet, 2010. **42**(12): p. 1118-25.
288. Frank, D.N., et al., *Molecular-phylogenetic characterization of microbial community imbalances in human inflammatory bowel diseases.* Proc Natl Acad Sci U S A, 2007. **104**(34): p. 13780-5.
289. Lepage, P., et al., *Twin study indicates loss of interaction between microbiota and mucosa of patients with ulcerative colitis.* Gastroenterology, 2011. **141**(1): p. 227-36.
290. Martinez, C., et al., *Unstable composition of the fecal microbiota in ulcerative colitis during clinical remission.* Am J Gastroenterol, 2008. **103**(3): p. 643-8.
291. Ott, S.J., et al., *Reduction in diversity of the colonic mucosa associated bacterial microflora in patients with active inflammatory bowel disease.* Gut, 2004. **53**(5): p. 685-93.

292. Kang, S., et al., *Dysbiosis of fecal microbiota in Crohn's disease patients as revealed by a custom phylogenetic microarray.* Inflamm Bowel Dis, 2010. **16**(12): p. 2034-42.
293. Rowan, F., et al., *Desulfovibrio bacterial species are increased in ulcerative colitis.* Dis Colon Rectum, 2010. **53**(11): p. 1530-6.
294. Neut, C., et al., *Changes in the bacterial flora of the neoterminal ileum after ileocolonic resection for Crohn's disease.* Am J Gastroenterol, 2002. **97**(4): p. 939-46.
295. Kotlowski, R., et al., *High prevalence of Escherichia coli belonging to the B2+D phylogenetic group in inflammatory bowel disease.* Gut, 2007. **56**(5): p. 669-75.
296. Varela, E., et al., *Colonisation by Faecalibacterium prausnitzii and maintenance of clinical remission in patients with ulcerative colitis.* Aliment Pharmacol Ther, 2013. **38**(2): p. 151-61.
297. Swidsinski, A., et al., *Active Crohn's disease and ulcerative colitis can be specifically diagnosed and monitored based on the biostructure of the fecal flora.* Inflamm Bowel Dis, 2008. **14**(2): p. 147-61.
298. Mahid, S.S., et al., *Smoking and inflammatory bowel disease: a meta-analysis.* Mayo Clin Proc, 2006. **81**(11): p. 1462-71.
299. Cosnes, J., et al., *Gender differences in the response of colitis to smoking.* Clin Gastroenterol Hepatol, 2004. **2**(1): p. 41-8.
300. Cosnes, J., et al., *Effects of current and former cigarette smoking on the clinical course of Crohn's disease.* Aliment Pharmacol Ther, 1999. **13**(11): p. 1403-11.
301. Cosnes, J., et al., *Effects of cigarette smoking on the long-term course of Crohn's disease.* Gastroenterology, 1996. **110**(2): p. 424-31.
302. Cosnes, J., *Tobacco and IBD: relevance in the understanding of disease mechanisms and clinical practice.* Best Pract Res Clin Gastroenterol, 2004. **18**(3): p. 481-96.
303. Cosnes, J., *What is the link between the use of tobacco and IBD?* Inflamm Bowel Dis, 2008. **14 Suppl 2**: p. S14-5.
304. Higuchi, L.M., et al., *A prospective study of cigarette smoking and the risk of inflammatory bowel disease in women.* Am J Gastroenterol, 2012. **107**(9): p. 1399-406.
305. Mahid, S.S., et al., *Active and passive smoking in childhood is related to the development of inflammatory bowel disease.* Inflamm Bowel Dis, 2007. **13**(4): p. 431-8.
306. Virta, L., et al., *Association of repeated exposure to antibiotics with the development of pediatric Crohn's disease--a nationwide, register-based finnish case-control study.* Am J Epidemiol, 2012. **175**(8): p. 775-84.
307. Shaw, S.Y., J.F. Blanchard, and C.N. Bernstein, *Association between the use of antibiotics in the first year of life and pediatric inflammatory bowel disease.* Am J Gastroenterol, 2010. **105**(12): p. 2687-92.
308. Ananthakrishnan, A.N., et al., *A prospective study of long-term intake of dietary fiber and risk of Crohn's disease and ulcerative colitis.* Gastroenterology, 2013. **145**(5): p. 970-7.
309. Zhang, Z., et al., *Regulatory role of short-chain fatty acids in inflammatory bowel disease.* Cell Commun Signal, 2022. **20**(1): p. 64.
310. Devkota, S., et al., *Dietary-fat-induced taurocholic acid promotes pathobiont expansion and colitis in Il10-/- mice.* Nature, 2012. **487**(7405): p. 104-8.
311. Hart, A.R., et al., *Diet in the aetiology of ulcerative colitis: a European prospective cohort study.* Digestion, 2008. **77**(1): p. 57-64.

312. Sonnenberg, A., *Occupational distribution of inflammatory bowel disease among German employees.* Gut, 1990. **31**(9): p. 1037-40.
313. Cook, M.D., et al., *Forced treadmill exercise training exacerbates inflammation and causes mortality while voluntary wheel training is protective in a mouse model of colitis.* Brain Behav Immun, 2013. **33**: p. 46-56.
314. Khalili, H., et al., *Physical activity and risk of inflammatory bowel disease: prospective study from the Nurses' Health Study cohorts.* BMJ, 2013. **347**: p. f6633.
315. Kang, L., et al., *Neutrophil-Epithelial Crosstalk During Intestinal Inflammation.* Cell Mol Gastroenterol Hepatol, 2022. **14**(6): p. 1257-1267.
316. Kucharzik, T., et al., *Acute induction of human IL-8 production by intestinal epithelium triggers neutrophil infiltration without mucosal injury.* Gut, 2005. **54**(11): p. 1565-72.
317. Chen, Z., et al., *Intestinal IL-33 promotes platelet activity for neutrophil recruitment during acute inflammation.* Blood, 2022. **139**(12): p. 1878-1891.
318. Keates, S., et al., *Enterocytes are the primary source of the chemokine ENA-78 in normal colon and ulcerative colitis.* Am J Physiol, 1997. **273**(1 Pt 1): p. G75-82.
319. Kruidenier, L., et al., *Myofibroblast matrix metalloproteinases activate the neutrophil chemoattractant CXCL7 from intestinal epithelial cells.* Gastroenterology, 2006. **130**(1): p. 127-36.
320. Chami, B., et al., *The role of CXCR3 in DSS-induced colitis.* PLoS One, 2014. **9**(7): p. e101622.
321. Scapini, P., et al., *Neutrophils produce biologically active macrophage inflammatory protein-3alpha (MIP-3alpha)/CCL20 and MIP-3beta/CCL19.* Eur J Immunol, 2001. **31**(7): p. 1981-8.
322. Danne, C., et al., *Neutrophils: from IBD to the gut microbiota.* Nat Rev Gastroenterol Hepatol, 2024. **21**(3): p. 184-197.
323. Al-Sadi, R., et al., *Matrix Metalloproteinase-9 (MMP-9) induced disruption of intestinal epithelial tight junction barrier is mediated by NF-kappaB activation.* PLoS One, 2021. **16**(4): p. e0249544.
324. Xiao, Y., et al., *Matrix metalloproteinase 7 contributes to intestinal barrier dysfunction by degrading tight junction protein Claudin-7.* Front Immunol, 2022. **13**: p. 1020902.
325. Nighot, P., et al., *Matrix metalloproteinase 9-induced increase in intestinal epithelial tight junction permeability contributes to the severity of experimental DSS colitis.* Am J Physiol Gastrointest Liver Physiol, 2015. **309**(12): p. G988-97.
326. Ginzberg, H.H., et al., *Neutrophil-mediated epithelial injury during transmigration: role of elastase.* Am J Physiol Gastrointest Liver Physiol, 2001. **281**(3): p. G705-17.
327. Raab, Y., et al., *Neutrophil mucosal involvement is accompanied by enhanced local production of interleukin-8 in ulcerative colitis.* Gut, 1993. **34**(9): p. 1203-6.
328. Karmakar, M., et al., *N-GSDMD trafficking to neutrophil organelles facilitates IL-1beta release independently of plasma membrane pores and pyroptosis.* Nat Commun, 2020. **11**(1): p. 2212.
329. Yang, D., et al., *Human neutrophil defensins selectively chemoattract naive T and immature dendritic cells.* J Leukoc Biol, 2000. **68**(1): p. 9-14.
330. Wang, S., et al., *S100A8/A9 in Inflammation.* Front Immunol, 2018. **9**: p. 1298.
331. Gottlieb, Y., et al., *Neutrophil extracellular traps in pediatric inflammatory bowel disease.* Pathol Int, 2018. **68**(9): p. 517-523.
332. Lehmann, T., et al., *Metaproteomics of fecal samples of Crohn's disease and Ulcerative Colitis.* J Proteomics, 2019. **201**: p. 93-103.

333. Li, T., et al., *Neutrophil Extracellular Traps Induce Intestinal Damage and Thrombotic Tendency in Inflammatory Bowel Disease.* J Crohns Colitis, 2020. **14**(2): p. 240-253.
334. Bennike, T.B., et al., *Neutrophil Extracellular Traps in Ulcerative Colitis: A Proteome Analysis of Intestinal Biopsies.* Inflamm Bowel Dis, 2015. **21**(9): p. 2052-67.
335. Drury, B., et al., *Neutrophil Extracellular Traps in Inflammatory Bowel Disease: Pathogenic Mechanisms and Clinical Translation.* Cell Mol Gastroenterol Hepatol, 2021. **12**(1): p. 321-333.
336. Wera, O., P. Lancellotti, and C. Oury, *The Dual Role of Neutrophils in Inflammatory Bowel Diseases.* J Clin Med, 2016. **5**(12).
337. Demir, A.K., et al., *The relationship between the neutrophil-lymphocyte ratio and disease activity in patients with ulcerative colitis.* Kaohsiung J Med Sci, 2015. **31**(11): p. 585-90.
338. Kuno, Y., et al., *Possible involvement of neutrophil elastase in impaired mucosal repair in patients with ulcerative colitis.* J Gastroenterol, 2002. **37 Suppl 14**: p. 22-32.
339. Farkas, K., et al., *The diagnostic value of a new fecal marker, matrix metalloprotease-9, in different types of inflammatory bowel diseases.* J Crohns Colitis, 2015. **9**(3): p. 231-7.
340. Liu, C., et al., *Twist1 contributes to developing and sustaining corticosteroid resistance in ulcerative colitis.* Theranostics, 2021. **11**(16): p. 7797-7812.
341. Lu, H., et al., *Cyclosporine modulates neutrophil functions via the SIRT6-HIF-1alpha-glycolysis axis to alleviate severe ulcerative colitis.* Clin Transl Med, 2021. **11**(2): p. e334.
342. Marks, D.J., et al., *Defective acute inflammation in Crohn's disease: a clinical investigation.* Lancet, 2006. **367**(9511): p. 668-78.
343. Hayee, B., et al., *The neutrophil respiratory burst and bacterial digestion in Crohn's disease.* Dig Dis Sci, 2011. **56**(5): p. 1482-8.
344. Smith, A.M., et al., *Disordered macrophage cytokine secretion underlies impaired acute inflammation and bacterial clearance in Crohn's disease.* J Exp Med, 2009. **206**(9): p. 1883-97.
345. Walls, A.F., et al., *Roles of the mast cell and basophil in asthma.* Clinical & Experimental Allergy Reviews, 2001. **1**(2): p. 68-72.
346. Guo, Y., et al., *Insights into the Characteristics and Functions of Mast Cells in the Gut.* Gastroenterology Insights, 2023. **14**(4): p. 637-652.
347. Kurashima, Y., et al., *Extracellular ATP mediates mast cell-dependent intestinal inflammation through P2X7 purinoceptors.* Nat Commun, 2012. **3**: p. 1034.
348. Vuerich, M., et al., *Control of Gut Inflammation by Modulation of Purinergic Signaling.* Front Immunol, 2020. **11**: p. 1882.
349. Gelbmann, C.M., et al., *Strictures in Crohn's disease are characterised by an accumulation of mast cells colocalised with laminin but not with fibronectin or vitronectin.* Gut, 1999. **45**(2): p. 210-7.
350. Andoh, A., et al., *Immunohistochemical study of chymase-positive mast cells in inflammatory bowel disease.* Oncol Rep, 2006. **16**(1): p. 103-7.
351. Raithel, M., H.T. Schneider, and E.G. Hahn, *Effect of substance P on histamine secretion from gut mucosa in inflammatory bowel disease.* Scand J Gastroenterol, 1999. **34**(5): p. 496-503.
352. Raithel, M., et al., *Release of mast cell tryptase from human colorectal mucosa in inflammatory bowel disease.* Scand J Gastroenterol, 2001. **36**(2): p. 174-9.

353. Winterkamp, S., et al., *Urinary excretion of N-methylhistamine as a marker of disease activity in inflammatory bowel disease.* Am J Gastroenterol, 2002. **97**(12): p. 3071-7.
354. Vivinus-Nebot, M., et al., *Functional bowel symptoms in quiescent inflammatory bowel diseases: role of epithelial barrier disruption and low-grade inflammation.* Gut, 2014. **63**(5): p. 744-52.
355. Bernstein, C.N., et al., *A prospective population-based study of triggers of symptomatic flares in IBD.* Am J Gastroenterol, 2010. **105**(9): p. 1994-2002.
356. Zheng, P.Y., et al., *Psychological stress induces eosinophils to produce corticotrophin releasing hormone in the intestine.* Gut, 2009. **58**(11): p. 1473-9.
357. Bain, C.C., et al., *Resident and pro-inflammatory macrophages in the colon represent alternative context-dependent fates of the same Ly6Chi monocyte precursors.* Mucosal Immunol, 2013. **6**(3): p. 498-510.
358. Thiesen, S., et al., *CD14(hi)HLA-DR(dim) macrophages, with a resemblance to classical blood monocytes, dominate inflamed mucosa in Crohn's disease.* J Leukoc Biol, 2014. **95**(3): p. 531-41.
359. Kamada, N., et al., *Unique CD14 intestinal macrophages contribute to the pathogenesis of Crohn disease via IL-23/IFN-gamma axis.* J Clin Invest, 2008. **118**(6): p. 2269-80.
360. Hegarty, L.M., G.R. Jones, and C.C. Bain, *Macrophages in intestinal homeostasis and inflammatory bowel disease.* Nat Rev Gastroenterol Hepatol, 2023. **20**(8): p. 538-553.
361. Heresbach, D., et al., *Frequency and significance of granulomas in a cohort of incident cases of Crohn's disease.* Gut, 2005. **54**(2): p. 215-22.
362. Nayar, S., et al., *A myeloid-stromal niche and gp130 rescue in NOD2-driven Crohn's disease.* Nature, 2021. **593**(7858): p. 275-281.
363. Shouval, D.S., et al., *Interleukin-10 receptor signaling in innate immune cells regulates mucosal immune tolerance and anti-inflammatory macrophage function.* Immunity, 2014. **40**(5): p. 706-19.
364. Lapaquette, P., et al., *Crohn's disease-associated adherent-invasive E. coli are selectively favoured by impaired autophagy to replicate intracellularly.* Cell Microbiol, 2010. **12**(1): p. 99-113.
365. Lesage, S., et al., *CARD15/NOD2 mutational analysis and genotype-phenotype correlation in 612 patients with inflammatory bowel disease.* Am J Hum Genet, 2002. **70**(4): p. 845-57.
366. Watanabe, T., A. Kitani, and W. Strober, *NOD2 regulation of Toll-like receptor responses and the pathogenesis of Crohn's disease.* Gut, 2005. **54**(11): p. 1515-8.
367. Vos, A.C., et al., *Anti-tumor necrosis factor-alpha antibodies induce regulatory macrophages in an Fc region-dependent manner.* Gastroenterology, 2011. **140**(1): p. 221-30.
368. Dige, A., et al., *Soluble CD163, a specific macrophage activation marker, is decreased by anti-TNF-alpha antibody treatment in active inflammatory bowel disease.* Scand J Immunol, 2014. **80**(6): p. 417-23.
369. Sands, B.E., et al., *A randomised, double-blind, sham-controlled study of granulocyte/monocyte apheresis for moderate to severe Crohn's disease.* Gut, 2013. **62**(9): p. 1288-94.
370. Sands, B.E., et al., *A randomized, double-blind, sham-controlled study of granulocyte/monocyte apheresis for active ulcerative colitis.* Gastroenterology, 2008. **135**(2): p. 400-9.

371. Selby, W.S., et al., *Intestinal lymphocyte subpopulations in inflammatory bowel disease: an analysis by immunohistological and cell isolation techniques.* Gut, 1984. **25**(1): p. 32-40.
372. Schreiber, S., et al., *Increased activation of isolated intestinal lamina propria mononuclear cells in inflammatory bowel disease.* Gastroenterology, 1991. **101**(4): p. 1020-30.
373. Villarino, A.V., et al., *Helper T cell IL-2 production is limited by negative feedback and STAT-dependent cytokine signals.* J Exp Med, 2007. **204**(1): p. 65-71.
374. Toumi, R., et al., *Autocrine and paracrine IL-2 signals collaborate to regulate distinct phases of CD8 T cell memory.* Cell Rep, 2022. **39**(2): p. 110632.
375. Choy, M.Y., et al., *Differential expression of CD25 (interleukin-2 receptor) on lamina propria T cells and macrophages in the intestinal lesions in Crohn's disease and ulcerative colitis.* Gut, 1990. **31**(12): p. 1365-70.
376. Allez, M., et al., *CD4+NKG2D+ T cells in Crohn's disease mediate inflammatory and cytotoxic responses through MICA interactions.* Gastroenterology, 2007. **132**(7): p. 2346-58.
377. Pariente, B., et al., *Activation of the receptor NKG2D leads to production of Th17 cytokines in CD4+ T cells of patients with Crohn's disease.* Gastroenterology, 2011. **141**(1): p. 217-26, 226 e1-2.
378. Monteleone, G., et al., *Interleukin 12 is expressed and actively released by Crohn's disease intestinal lamina propria mononuclear cells.* Gastroenterology, 1997. **112**(4): p. 1169-78.
379. Monteleone, G., et al., *Bioactive IL-18 Expression Is Up-Regulated in Crohn's Disease1.* The Journal of Immunology, 1999. **163**(1): p. 143-147.
380. Heller, F., et al., *Interleukin-13 is the key effector Th2 cytokine in ulcerative colitis that affects epithelial tight junctions, apoptosis, and cell restitution.* Gastroenterology, 2005. **129**(2): p. 550-64.
381. Fuss, I.J., et al., *Disparate CD4+ lamina propria (LP) lymphokine secretion profiles in inflammatory bowel disease. Crohn's disease LP cells manifest increased secretion of IFN-gamma, whereas ulcerative colitis LP cells manifest increased secretion of IL-5.* J Immunol, 1996. **157**(3): p. 1261-70.
382. Kobayashi, T., et al., *IL23 differentially regulates the Th1/Th17 balance in ulcerative colitis and Crohn's disease.* Gut, 2008. **57**(12): p. 1682-9.
383. Eastaff-Leung, N., et al., *Foxp3+ regulatory T cells, Th17 effector cells, and cytokine environment in inflammatory bowel disease.* J Clin Immunol, 2010. **30**(1): p. 80-9.
384. Ishimaru, N., et al., *Development of inflammatory bowel disease in Long-Evans Cinnamon rats based on CD4+CD25+Foxp3+ regulatory T cell dysfunction.* J Immunol, 2008. **180**(10): p. 6997-7008.
385. Pereira, C., et al., *Oxidative Stress and DNA Damage: Implications in Inflammatory Bowel Disease.* Inflamm Bowel Dis, 2015. **21**(10): p. 2403-17.
386. Kruidenier, L., et al., *Intestinal oxidative damage in inflammatory bowel disease: semi-quantification, localization, and association with mucosal antioxidants.* J Pathol, 2003. **201**(1): p. 28-36.
387. Alzoghaibi, M.A., I.A. Al Mofleh, and A.M. Al-Jebreen, *Lipid peroxides in patients with inflammatory bowel disease.* Saudi J Gastroenterol, 2007. **13**(4): p. 187-90.

388. Beltran, B., et al., *Mitochondrial dysfunction, persistent oxidative damage, and catalase inhibition in immune cells of naive and treated Crohn's disease.* Inflamm Bowel Dis, 2010. **16**(1): p. 76-86.
389. Canbakan, B., et al., *P389 Reactive oxygen metabolites and antioxidants as biomarkers of disease severity in ulcerative colitis.* Journal of Crohn's and Colitis, 2013. **7**(Supplement_1): p. S165-S165.
390. Bourgonje, A.R., et al., *Oxidative Stress and Redox-Modulating Therapeutics in Inflammatory Bowel Disease.* Trends Mol Med, 2020. **26**(11): p. 1034-1046.
391. Liang, X., et al., *Reactive oxygen species trigger NF-kappaB-mediated NLRP3 inflammasome activation induced by zinc oxide nanoparticles in A549 cells.* Toxicol Ind Health, 2017. **33**(10): p. 737-745.
392. Akman, T., et al., *Erythrocyte deformability and oxidative stress in inflammatory bowel disease.* Dig Dis Sci, 2012. **57**(2): p. 458-64.
393. Sido, B., et al., *Impairment of intestinal glutathione synthesis in patients with inflammatory bowel disease.* Gut, 1998. **42**(4): p. 485-92.
394. Piotrowska, M., et al., *The Nrf2 in the pathophysiology of the intestine: Molecular mechanisms and therapeutic implications for inflammatory bowel diseases.* Pharmacol Res, 2021. **163**: p. 105243.
395. Li, J., et al., *Mkp-1 cross-talks with Nrf2/Ho-1 pathway protecting against intestinal inflammation.* Free Radic Biol Med, 2018. **124**: p. 541-549.
396. Wang, L. and J. Wang, *Honokiol Ameliorates DSS-Induced Mouse Colitis by Inhibiting Inflammation and Oxidative Stress and Improving the Intestinal Barrier.* Oxid Med Cell Longev, 2022. **2022**: p. 1755608.
397. Yuan, Z., et al., *Huang-Lian-Jie-Du Decoction Ameliorates Acute Ulcerative Colitis in Mice via Regulating NF-kappaB and Nrf2 Signaling Pathways and Enhancing Intestinal Barrier Function.* Front Pharmacol, 2019. **10**: p. 1354.
398. Myers, J.N., et al., *Implications of the colonic deposition of free hemoglobin-alpha chain: a previously unknown tissue by-product in inflammatory bowel disease.* Inflamm Bowel Dis, 2014. **20**(9): p. 1530-47.
399. Sabzevary-Ghahfarokhi, M., et al., *The regulatory role of Nrf2 in antioxidants phase2 enzymes and IL-17A expression in patients with ulcerative colitis.* Pathol Res Pract, 2018. **214**(8): p. 1149-1155.
400. Amarante-Mendes, G.P., et al., *Pattern Recognition Receptors and the Host Cell Death Molecular Machinery.* Front Immunol, 2018. **9**: p. 2379.
401. Man, S.M. and T.D. Kanneganti, *Regulation of inflammasome activation.* Immunol Rev, 2015. **265**(1): p. 6-21.
402. Sharif, H., et al., *Structural mechanism for NEK7-licensed activation of NLRP3 inflammasome.* Nature, 2019. **570**(7761): p. 338-343.
403. Jin, T., et al., *Structure of the NLRP1 caspase recruitment domain suggests potential mechanisms for its association with procaspase-1.* Proteins, 2013. **81**(7): p. 1266-70.
404. Levy, M., et al., *NLRP6: A Multifaceted Innate Immune Sensor.* Trends Immunol, 2017. **38**(4): p. 248-260.
405. Zhang, L., et al., *Cryo-EM structure of the activated NAIP2-NLRC4 inflammasome reveals nucleated polymerization.* Science, 2015. **350**(6259): p. 404-9.
406. Fernandes-Alnemri, T., et al., *AIM2 activates the inflammasome and cell death in response to cytoplasmic DNA.* Nature, 2009. **458**(7237): p. 509-13.

407. Nordlander, S., J. Pott, and K.J. Maloy, *NLRC4 expression in intestinal epithelial cells mediates protection against an enteric pathogen.* Mucosal Immunol, 2014. **7**(4): p. 775-85.
408. Allen, I.C., et al., *The NLRP3 inflammasome functions as a negative regulator of tumorigenesis during colitis-associated cancer.* J Exp Med, 2010. **207**(5): p. 1045-56.
409. Zaki, M.H., et al., *The NLRP3 inflammasome protects against loss of epithelial integrity and mortality during experimental colitis.* Immunity, 2010. **32**(3): p. 379-91.
410. Hirota, S.A., et al., *NLRP3 inflammasome plays a key role in the regulation of intestinal homeostasis.* Inflamm Bowel Dis, 2011. **17**(6): p. 1359-72.
411. Inoue, Y., et al., *NLRP3 regulates neutrophil functions and contributes to hepatic ischemia-reperfusion injury independently of inflammasomes.* J Immunol, 2014. **192**(9): p. 4342-51.
412. Elinav, E., et al., *NLRP6 inflammasome regulates colonic microbial ecology and risk for colitis.* Cell, 2011. **145**(5): p. 745-57.
413. Liu, Z., et al., *Role of inflammasomes in host defense against Citrobacter rodentium infection.* J Biol Chem, 2012. **287**(20): p. 16955-64.
414. Hasegawa, M., et al., *Protective role of commensals against Clostridium difficile infection via an IL-1beta-mediated positive-feedback loop.* J Immunol, 2012. **189**(6): p. 3085-91.
415. Seregin, S.S., et al., *NLRP6 Protects Il10(-/-) Mice from Colitis by Limiting Colonization of Akkermansia muciniphila.* Cell Rep, 2017. **19**(4): p. 733-745.
416. Lazaridis, L.D., et al., *Activation of NLRP3 Inflammasome in Inflammatory Bowel Disease: Differences Between Crohn's Disease and Ulcerative Colitis.* Dig Dis Sci, 2017. **62**(9): p. 2348-2356.
417. Ranson, N., et al., *NLRP3-Dependent and -Independent Processing of Interleukin (IL)-1beta in Active Ulcerative Colitis.* Int J Mol Sci, 2018. **20**(1).
418. Ranson, N., et al., *Nod-Like Receptor Pyrin-Containing Protein 6 (NLRP6) Is Up-regulated in Ileal Crohn's Disease and Differentially Expressed in Goblet Cells.* Cell Mol Gastroenterol Hepatol, 2018. **6**(1): p. 110-112 e8.
419. Steiner, A., et al., *Recessive NLRC4-Autoinflammatory Disease Reveals an Ulcerative Colitis Locus.* J Clin Immunol, 2022. **42**(2): p. 325-335.
420. Boets, E., et al., *Systemic availability and metabolism of colonic-derived short-chain fatty acids in healthy subjects: a stable isotope study.* J Physiol, 2017. **595**(2): p. 541-555.
421. Roediger, W.E., et al., *Luminal ions and short chain fatty acids as markers of functional activity of the mucosa in ulcerative colitis.* J Clin Pathol, 1982. **35**(3): p. 323-6.
422. van Nuenen, M.H., et al., *The metabolic activity of fecal microbiota from healthy individuals and patients with inflammatory bowel disease.* Dig Dis Sci, 2004. **49**(3): p. 485-91.
423. Takaishi, H., et al., *Imbalance in intestinal microflora constitution could be involved in the pathogenesis of inflammatory bowel disease.* Int J Med Microbiol, 2008. **298**(5-6): p. 463-72.
424. Zhuang, X., et al., *Systematic Review and Meta-analysis: Short-Chain Fatty Acid Characterization in Patients With Inflammatory Bowel Disease.* Inflamm Bowel Dis, 2019. **25**(11): p. 1751-1763.

425. Thangaraju, M., et al., *GPR109A is a G-protein-coupled receptor for the bacterial fermentation product butyrate and functions as a tumor suppressor in colon.* Cancer Res, 2009. **69**(7): p. 2826-32.
426. Cai, Z., S. Wang, and J. Li, *Treatment of Inflammatory Bowel Disease: A Comprehensive Review.* Front Med (Lausanne), 2021. **8**: p. 765474.
427. Pithadia, A.B. and S. Jain, *Treatment of inflammatory bowel disease (IBD).* Pharmacol Rep, 2011. **63**(3): p. 629-42.
428. Jin, J.J., et al., *Simultaneous Treatment of 5-Aminosalicylic Acid and Treadmill Exercise More Effectively Improves Ulcerative Colitis in Mice.* Int J Mol Sci, 2024. **25**(10).
429. Lauritsen, K., et al., *Effects of sulphasalazine and disodium azodisalicylate on colonic PGE2 concentrations determined by equilibrium in vivo dialysis of faeces in patients with ulcerative colitis and healthy controls.* Gut, 1984. **25**(11): p. 1271-8.
430. Ligumsky, M., et al., *Enhanced thromboxane A2 and prostacyclin production by cultured rectal mucosa in ulcerative colitis and its inhibition by steroids and sulfasalazine.* Gastroenterology, 1981. **81**(3): p. 444-9.
431. Sandoval, M., et al., *Peroxynitrite-induced apoptosis in human intestinal epithelial cells is attenuated by mesalamine.* Gastroenterology, 1997. **113**(5): p. 1480-8.
432. Shanahan, F., et al., *Sulfasalazine inhibits the binding of TNF alpha to its receptor.* Immunopharmacology, 1990. **20**(3): p. 217-24.
433. Mahida, Y.R., et al., *5-Aminosalicylic acid is a potent inhibitor of interleukin 1 beta production in organ culture of colonic biopsy specimens from patients with inflammatory bowel disease.* Gut, 1991. **32**(1): p. 50-4.
434. Oh-Oka, K., et al., *Induction of Colonic Regulatory T Cells by Mesalamine by Activating the Aryl Hydrocarbon Receptor.* Cell Mol Gastroenterol Hepatol, 2017. **4**(1): p. 135-151.
435. Prantera, C., et al., *Mesalamine in the treatment of mild to moderate active Crohn's ileitis: results of a randomized, multicenter trial.* Gastroenterology, 1999. **116**(3): p. 521-6.
436. Eaden, J., et al., *Colorectal cancer prevention in ulcerative colitis: a case-control study.* Aliment Pharmacol Ther, 2000. **14**(2): p. 145-53.
437. Hart, A., et al., *The use of 5-aminosalicylates in Crohn's disease: a retrospective study using the UK Clinical Practice Research Datalink.* Ann Gastroenterol, 2020. **33**(5): p. 500-507.
438. Gjuladin-Hellon, T., et al., *Oral 5-aminosalicylic acid for maintenance of surgically-induced remission in Crohn's disease.* Cochrane Database Syst Rev, 2019. **6**(6): p. CD008414.
439. Akobeng, A.K., et al., *Oral 5-aminosalicylic acid for maintenance of medically-induced remission in Crohn's disease.* Cochrane Database Syst Rev, 2016. **9**(9): p. CD003715.
440. Gisbert, J.P., Y. Gonzalez-Lama, and J. Mate, *5-Aminosalicylates and renal function in inflammatory bowel disease: a systematic review.* Inflamm Bowel Dis, 2007. **13**(5): p. 629-38.
441. Loftus, E.V., Jr., S.V. Kane, and D. Bjorkman, *Systematic review: short-term adverse effects of 5-aminosalicylic acid agents in the treatment of ulcerative colitis.* Aliment Pharmacol Ther, 2004. **19**(2): p. 179-89.
442. Taffet, S.L. and K.M. Das, *Sulfasalazine. Adverse effects and desensitization.* Dig Dis Sci, 1983. **28**(9): p. 833-42.
443. Truelove, S.C. and L.J. Witts, *Cortisone in ulcerative colitis; final report on a therapeutic trial.* Br Med J, 1955. **2**(4947): p. 1041-8.

444. Katz, J.A., *Treatment of inflammatory bowel disease with corticosteroids.* Gastroenterol Clin North Am, 2004. **33**(2): p. 171-89, vii.
445. De Bosscher, K., W. Vanden Berghe, and G. Haegeman, *The interplay between the glucocorticoid receptor and nuclear factor-kappaB or activator protein-1: molecular mechanisms for gene repression.* Endocr Rev, 2003. **24**(4): p. 488-522.
446. Rhen, T. and J.A. Cidlowski, *Antiinflammatory action of glucocorticoids--new mechanisms for old drugs.* N Engl J Med, 2005. **353**(16): p. 1711-23.
447. Barrett, K., S. Saxena, and R. Pollok, *Using corticosteroids appropriately in inflammatory bowel disease: a guide for primary care.* Br J Gen Pract, 2018. **68**(675): p. 497-498.
448. Ford, A.C., et al., *Glucocorticosteroid therapy in inflammatory bowel disease: systematic review and meta-analysis.* Am J Gastroenterol, 2011. **106**(4): p. 590-9; quiz 600.
449. Turner, D., et al., *Response to corticosteroids in severe ulcerative colitis: a systematic review of the literature and a meta-regression.* Clin Gastroenterol Hepatol, 2007. **5**(1): p. 103-10.
450. Dorrington, A.M., et al., *The Historical Role and Contemporary Use of Corticosteroids in Inflammatory Bowel Disease.* J Crohns Colitis, 2020. **14**(9): p. 1316-1329.
451. Waljee, A.K., et al., *Corticosteroid Use and Complications in a US Inflammatory Bowel Disease Cohort.* PLoS One, 2016. **11**(6): p. e0158017.
452. Brunner, M., et al., *Gastrointestinal transit, release and plasma pharmacokinetics of a new oral budesonide formulation.* Br J Clin Pharmacol, 2006. **61**(1): p. 31-8.
453. Sherlock, M.E., et al., *Oral budesonide for induction of remission in ulcerative colitis.* Cochrane Database Syst Rev, 2015. **2015**(10): p. CD007698.
454. Rubin, D.T., et al., *Budesonide Multimatrix Is Efficacious for Mesalamine-refractory, Mild to Moderate Ulcerative Colitis: A Randomised, Placebo-controlled Trial.* J Crohns Colitis, 2017. **11**(7): p. 785-791.
455. Kuenzig, M.E., et al., *Budesonide for maintenance of remission in Crohn's disease.* Cochrane Database Syst Rev, 2014. **2014**(8): p. CD002913.
456. Kuenzig, M.E., et al., *Budesonide for the Induction and Maintenance of Remission in Crohn's Disease: Systematic Review and Meta-Analysis for the Cochrane Collaboration.* J Can Assoc Gastroenterol, 2018. **1**(4): p. 159-173.
457. Truelove, S.C. and L.J. Witts, *Cortisone and corticotrophin in ulcerative colitis.* Br Med J, 1959. **1**(5119): p. 387-94.
458. Derijks, L.J., et al., *Review article: thiopurines in inflammatory bowel disease.* Aliment Pharmacol Ther, 2006. **24**(5): p. 715-29.
459. Shin, J.Y., et al., *Thiopurine Prodrugs Mediate Immunosuppressive Effects by Interfering with Rac1 Protein Function.* J Biol Chem, 2016. **291**(26): p. 13699-714.
460. Jharap, B., et al., *Thiopurine therapy in inflammatory bowel disease patients: analyses of two 8-year intercept cohorts.* Inflamm Bowel Dis, 2010. **16**(9): p. 1541-9.
461. Gisbert, J.P., et al., *Comparative effectiveness of azathioprine in Crohn's disease and ulcerative colitis: prospective, long-term, follow-up study of 394 patients.* Aliment Pharmacol Ther, 2008. **28**(2): p. 228-38.
462. Yamada, S., et al., *Efficacy and Safety of Long-Term Thiopurine Maintenance Treatment in Japanese Patients With Ulcerative Colitis.* Intest Res, 2015. **13**(3): p. 250-8.
463. Connell, W.R., et al., *Bone marrow toxicity caused by azathioprine in inflammatory bowel disease: 27 years of experience.* Gut, 1993. **34**(8): p. 1081-5.

464. Dubinsky, M.C., et al., *6-thioguanine can cause serious liver injury in inflammatory bowel disease patients.* Gastroenterology, 2003. **125**(2): p. 298-303.
465. Wang, Y., et al., *Patients With IBD Receiving Methotrexate Are at Higher Risk of Liver Injury Compared With Patients With Non-IBD Diseases: A Meta-Analysis and Systematic Review.* Front Med (Lausanne), 2021. **8**: p. 774824.
466. van Dieren, J.M., et al., *Revisiting the immunomodulators tacrolimus, methotrexate, and mycophenolate mofetil: their mechanisms of action and role in the treatment of IBD.* Inflamm Bowel Dis, 2006. **12**(4): p. 311-27.
467. Yamaki, K., et al., *Effect of methotrexate on Th1 and Th2 immune responses in mice.* J Pharm Pharmacol, 2003. **55**(12): p. 1661-6.
468. Strauss, G., W. Osen, and K.M. Debatin, *Induction of apoptosis and modulation of activation and effector function in T cells by immunosuppressive drugs.* Clin Exp Immunol, 2002. **128**(2): p. 255-66.
469. Izeradjene, K., J.P. Revillard, and L. Genestier, *Inhibition of thymidine synthesis by folate analogues induces a Fas-Fas ligand-independent deletion of superantigen-reactive peripheral T cells.* Int Immunol, 2001. **13**(1): p. 85-93.
470. Fairbanks, L.D., et al., *Methotrexate inhibits the first committed step of purine biosynthesis in mitogen-stimulated human T-lymphocytes: a metabolic basis for efficacy in rheumatoid arthritis?* Biochem J, 1999. **342 (Pt 1)**(Pt 1): p. 143-52.
471. Lemann, M., et al., *Methotrexate for the treatment of refractory Crohn's disease.* Aliment Pharmacol Ther, 1996. **10**(3): p. 309-14.
472. Chande, N., et al., *Methotrexate for induction of remission in ulcerative colitis.* Cochrane Database Syst Rev, 2014. **2014**(8): p. CD006618.
473. Naganuma, M., T. Fujii, and M. Watanabe, *The use of traditional and newer calcineurin inhibitors in inflammatory bowel disease.* J Gastroenterol, 2011. **46**(2): p. 129-37.
474. Nakase, H., T. Yoshino, and M. Matsuura, *Role in calcineurin inhibitors for inflammatory bowel disease in the biologics era: when and how to use.* Inflamm Bowel Dis, 2014. **20**(11): p. 2151-6.
475. Lichtiger, S., et al., *Cyclosporine in severe ulcerative colitis refractory to steroid therapy.* N Engl J Med, 1994. **330**(26): p. 1841-5.
476. Stange, E.F., et al., *European trial of cyclosporine in chronic active Crohn's disease: a 12-month study. The European Study Group.* Gastroenterology, 1995. **109**(3): p. 774-82.
477. Yoshino, T., et al., *Immunosuppressive effects of tacrolimus on macrophages ameliorate experimental colitis.* Inflamm Bowel Dis, 2010. **16**(12): p. 2022-33.
478. Kino, T., et al., *FK-506, a novel immunosuppressant isolated from a Streptomyces. II. Immunosuppressive effect of FK-506 in vitro.* J Antibiot (Tokyo), 1987. **40**(9): p. 1256-65.
479. Ogata, H., et al., *A randomised dose finding study of oral tacrolimus (FK506) therapy in refractory ulcerative colitis.* Gut, 2006. **55**(9): p. 1255-62.
480. Yamamoto, S., et al., *Long-term effect of tacrolimus therapy in patients with refractory ulcerative colitis.* Aliment Pharmacol Ther, 2008. **28**(5): p. 589-97.
481. Sandborn, W.J. and S.R. Targan, *Biologic therapy of inflammatory bowel disease.* Gastroenterology, 2002. **122**(6): p. 1592-608.
482. Sokic-Milutinovic, A. and T. Milosavljevic, *Inflammatory Bowel Disease: From Conventional Immunosuppression to Biologic Therapy.* Dig Dis, 2024. **42**(4): p. 325-335.

483. Present, D.H., et al., *Infliximab for the treatment of fistulas in patients with Crohn's disease.* N Engl J Med, 1999. **340**(18): p. 1398-405.
484. Sandborn, W.J., et al., *Colectomy rate comparison after treatment of ulcerative colitis with placebo or infliximab.* Gastroenterology, 2009. **137**(4): p. 1250-60; quiz 1520.
485. Hanauer, S.B., et al., *Human anti-tumor necrosis factor monoclonal antibody (adalimumab) in Crohn's disease: the CLASSIC-I trial.* Gastroenterology, 2006. **130**(2): p. 323-33; quiz 591.
486. Sandborn, W.J., et al., *Subcutaneous golimumab induces clinical response and remission in patients with moderate-to-severe ulcerative colitis.* Gastroenterology, 2014. **146**(1): p. 85-95; quiz e14-5.
487. Ben-Horin, S., U. Kopylov, and Y. Chowers, *Optimizing anti-TNF treatments in inflammatory bowel disease.* Autoimmun Rev, 2014. **13**(1): p. 24-30.
488. Mattoo, V.Y., et al., *Systematic review: efficacy of escalated maintenance anti-tumour necrosis factor therapy in Crohn's disease.* Aliment Pharmacol Ther, 2021. **54**(3): p. 249-266.
489. Cheifetz, A., et al., *The incidence and management of infusion reactions to infliximab: a large center experience.* Am J Gastroenterol, 2003. **98**(6): p. 1315-24.
490. Hastings, R., et al., *Neutropenia in patients receiving anti-tumor necrosis factor therapy.* Arthritis Care Res (Hoboken), 2010. **62**(6): p. 764-9.
491. Shivaji, U.N., et al., *Review article: managing the adverse events caused by anti-TNF therapy in inflammatory bowel disease.* Aliment Pharmacol Ther, 2019. **49**(6): p. 664-680.
492. Williams, E.L., S. Gadola, and C.J. Edwards, *Anti-TNF-induced lupus.* Rheumatology (Oxford), 2009. **48**(7): p. 716-20.
493. Chung, E.S., et al., *Randomized, double-blind, placebo-controlled, pilot trial of infliximab, a chimeric monoclonal antibody to tumor necrosis factor-alpha, in patients with moderate-to-severe heart failure: results of the anti-TNF Therapy Against Congestive Heart Failure (ATTACH) trial.* Circulation, 2003. **107**(25): p. 3133-40.
494. Deepak, P., et al., *Neurological events with tumour necrosis factor alpha inhibitors reported to the Food and Drug Administration Adverse Event Reporting System.* Aliment Pharmacol Ther, 2013. **38**(4): p. 388-96.
495. Askling, J., et al., *Cancer risk with tumor necrosis factor alpha (TNF) inhibitors: meta-analysis of randomized controlled trials of adalimumab, etanercept, and infliximab using patient level data.* Pharmacoepidemiol Drug Saf, 2011. **20**(2): p. 119-30.
496. Almradi, A., et al., *Clinical Trials of IL-12/IL-23 Inhibitors in Inflammatory Bowel Disease.* BioDrugs, 2020. **34**(6): p. 713-721.
497. Feagan, B.G., et al., *Induction therapy with the selective interleukin-23 inhibitor risankizumab in patients with moderate-to-severe Crohn's disease: a randomised, double-blind, placebo-controlled phase 2 study.* Lancet, 2017. **389**(10080): p. 1699-1709.
498. Yoshimura, N., et al., *Safety and Efficacy of AJM300, an Oral Antagonist of alpha4 Integrin, in Induction Therapy for Patients With Active Ulcerative Colitis.* Gastroenterology, 2015. **149**(7): p. 1775-1783 e2.
499. Lowe, S.C., et al., *Declining Rates of Surgery for Inflammatory Bowel Disease in the Era of Biologic Therapy.* J Gastrointest Surg, 2021. **25**(1): p. 211-219.

500. Lamb, C.A., et al., *British Society of Gastroenterology consensus guidelines on the management of inflammatory bowel disease in adults.* Gut, 2019. **68**(Suppl 3): p. s1-s106.
501. Rutgeerts, P., et al., *Predictability of the postoperative course of Crohn's disease.* Gastroenterology, 1990. **99**(4): p. 956-63.
502. Gan, S.I. and P.L. Beck, *A new look at toxic megacolon: an update and review of incidence, etiology, pathogenesis, and management.* Am J Gastroenterol, 2003. **98**(11): p. 2363-71.
503. Grieco, M.B., et al., *Toxic megacolon complicating Crohn's colitis.* Ann Surg, 1980. **191**(1): p. 75-80.
504. Greenstein, A.J., et al., *Outcome of toxic dilatation in ulcerative and Crohn's colitis.* J Clin Gastroenterol, 1985. **7**(2): p. 137-43.
505. Jalan, K.N., et al., *An experience of ulcerative colitis. I. Toxic dilation in 55 cases.* Gastroenterology, 1969. **57**(1): p. 68-82.
506. Moulin, V., et al., *Toxic megacolon in patients with severe acute colitis: computed tomographic features.* Clin Imaging, 2011. **35**(6): p. 431-6.
507. Wen, C., et al., *Animal models of inflammatory bowel disease: category and evaluation indexes.* Gastroenterol Rep (Oxf), 2024. **12**: p. goae021.
508. Low, D., D.D. Nguyen, and E. Mizoguchi, *Animal models of ulcerative colitis and their application in drug research.* Drug Des Devel Ther, 2013. **7**: p. 1341-57.
509. Eichele, D.D. and K.K. Kharbanda, *Dextran sodium sulfate colitis murine model: An indispensable tool for advancing our understanding of inflammatory bowel diseases pathogenesis.* World J Gastroenterol, 2017. **23**(33): p. 6016-6029.
510. Kim, J.J., et al., *Investigating intestinal inflammation in DSS-induced model of IBD.* J Vis Exp, 2012(60).
511. Heller, F., et al., *Oxazolone colitis, a Th2 colitis model resembling ulcerative colitis, is mediated by IL-13-producing NK-T cells.* Immunity, 2002. **17**(5): p. 629-38.
512. Nguyen, D.D., et al., *Wiskott-Aldrich syndrome protein deficiency in innate immune cells leads to mucosal immune dysregulation and colitis in mice.* Gastroenterology, 2012. **143**(3): p. 719-729 e2.
513. Bhan, A.K., et al., *Colitis in transgenic and knockout animals as models of human inflammatory bowel disease.* Immunol Rev, 1999. **169**: p. 195-207.
514. Watanabe, M., et al., *Mucosal IL-7-mediated immune responses in chronic colitis-IL-7 transgenic mouse model.* Immunol Res, 1999. **20**(3): p. 251-9.
515. Sadlack, B., et al., *Ulcerative colitis-like disease in mice with a disrupted interleukin-2 gene.* Cell, 1993. **75**(2): p. 253-61.
516. Antoniou, E., et al., *The TNBS-induced colitis animal model: An overview.* Ann Med Surg (Lond), 2016. **11**: p. 9-15.
517. Baydi, Z., et al., *An Update of Research Animal Models of Inflammatory Bowel Disease.* ScientificWorldJournal, 2021. **2021**: p. 7479540.
518. Matsumoto, T., et al., *An animal model of longitudinal ulcers in the small intestine induced by intracolonically administered indomethacin in rats.* Gastroenterol Jpn, 1993. **28**(1): p. 10-7.
519. Pizarro, T.T., et al., *SAMP1/YitFc mouse strain: a spontaneous model of Crohn's disease-like ileitis.* Inflamm Bowel Dis, 2011. **17**(12): p. 2566-84.

520. Kontoyiannis, D., et al., *Impaired on/off regulation of TNF biosynthesis in mice lacking TNF AU-rich elements: implications for joint and gut-associated immunopathologies.* Immunity, 1999. **10**(3): p. 387-98.
521. Steiner, C.A., et al., *The TNF(DeltaARE) Mouse as a Model of Intestinal Fibrosis.* Am J Pathol, 2023. **193**(8): p. 1013-1028.
522. Sandborn, W.J., et al., *Tofacitinib as Induction and Maintenance Therapy for Ulcerative Colitis.* N Engl J Med, 2017. **376**(18): p. 1723-1736.
523. Dhillon, S. and S.J. Keam, *Filgotinib: First Approval.* Drugs, 2020. **80**(18): p. 1987-1997.
524. Feagan, B.G., et al., *Filgotinib as induction and maintenance therapy for ulcerative colitis (SELECTION): a phase 2b/3 double-blind, randomised, placebo-controlled trial.* Lancet, 2021. **397**(10292): p. 2372-2384.
525. Vermeire, S., et al., *Clinical remission in patients with moderate-to-severe Crohn's disease treated with filgotinib (the FITZROY study): results from a phase 2, double-blind, randomised, placebo-controlled trial.* Lancet, 2017. **389**(10066): p. 266-275.
526. Loftus, E.V., Jr., et al., *Upadacitinib Induction and Maintenance Therapy for Crohn's Disease.* N Engl J Med, 2023. **388**(21): p. 1966-1980.
527. Jaszewski, R., et al., *Increased colonic mucosal angiotensin I and II concentrations in Crohn's colitis.* Gastroenterology, 1990. **98**(6): p. 1543-8.
528. Wildhaber, B.E., et al., *Intestinal intraepithelial lymphocyte derived angiotensin converting enzyme modulates epithelial cell apoptosis.* Apoptosis, 2005. **10**(6): p. 1305-15.
529. Wengrower, D., et al., *Prevention of fibrosis in experimental colitis by captopril: the role of tgf-beta1.* Inflamm Bowel Dis, 2004. **10**(5): p. 536-45.
530. Jahovic, N., et al., *The effect of angiotensin-converting enzyme inhibitors on experimental colitis in rats.* Regul Pept, 2005. **130**(1-2): p. 67-74.
531. Inokuchi, Y., et al., *Amelioration of 2,4,6-trinitrobenzene sulphonic acid induced colitis in angiotensinogen gene knockout mice.* Gut, 2005. **54**(3): p. 349-56.
532. Sueyoshi, R., et al., *Angiotensin converting enzyme-inhibitor reduces colitis severity in an IL-10 knockout model.* Dig Dis Sci, 2013. **58**(11): p. 3165-77.
533. Karime, C., et al., *The Effect of Renin-Angiotensin-Aldosterone System Blocking Agents on the Long-term Disease Course of Patients With Crohn's Disease.* J Clin Gastroenterol, 2024. **58**(5): p. 454-463.
534. Perera, A.P., et al., *MCC950, a specific small molecule inhibitor of NLRP3 inflammasome attenuates colonic inflammation in spontaneous colitis mice.* Sci Rep, 2018. **8**(1): p. 8618.
535. Saber, S. and E.M.A. El-Kader, *Novel complementary coloprotective effects of metformin and MCC950 by modulating HSP90/NLRP3 interaction and inducing autophagy in rats.* Inflammopharmacology, 2021. **29**(1): p. 237-251.
536. Caseley, E.A., et al., *Inflammasome inhibition under physiological and pharmacological conditions.* Genes Immun, 2020. **21**(4): p. 211-223.
537. Marchetti, C., et al., *OLT1177, a beta-sulfonyl nitrile compound, safe in humans, inhibits the NLRP3 inflammasome and reverses the metabolic cost of inflammation.* Proc Natl Acad Sci U S A, 2018. **115**(7): p. E1530-E1539.
538. Huang, Y., et al., *Tranilast directly targets NLRP3 to treat inflammasome-driven diseases.* EMBO Mol Med, 2018. **10**(4).
539. Morohoshi, Y., et al., *Inhibition of neutrophil elastase prevents the development of murine dextran sulfate sodium-induced colitis.* J Gastroenterol, 2006. **41**(4): p. 318-24.

540. Ahmad, G., et al., *The Synthetic Myeloperoxidase Inhibitor AZD3241 Ameliorates Dextran Sodium Sulfate Stimulated Experimental Colitis.* Front Pharmacol, 2020. **11**: p. 556020.
541. Tang, W., et al., *Berbamine ameliorates DSS-induced colitis by inhibiting peptidyl-arginine deiminase 4-dependent neutrophil extracellular traps formation.* Eur J Pharmacol, 2024. **975**: p. 176634.
542. Wang, P., et al., *The role of protein arginine deiminase 4-dependent neutrophil extracellular traps formation in ulcerative colitis.* Front Immunol, 2023. **14**: p. 1144976.
543. Karimi, M., et al., *Safety and efficacy of fecal microbiota transplantation (FMT) as a modern adjuvant therapy in various diseases and disorders: a comprehensive literature review.* Front Immunol, 2024. **15**: p. 1439176.
544. Zhang, F., et al., *Should we standardize the 1,700-year-old fecal microbiota transplantation?* Am J Gastroenterol, 2012. **107**(11): p. 1755; author reply p 1755-6.
545. Perez, E., C.H. Lee, and E.O. Petrof, *A Practical Method for Preparation of Fecal Microbiota Transplantation.* Methods Mol Biol, 2016. **1476**: p. 259-67.
546. Nicco, C., et al., *From Donor to Patient: Collection, Preparation and Cryopreservation of Fecal Samples for Fecal Microbiota Transplantation.* Diseases, 2020. **8**(2).
547. Andary, C.M., et al., *Dissecting mechanisms of fecal microbiota transplantation efficacy in disease.* Trends Mol Med, 2024. **30**(3): p. 209-222.
548. Zhu, F., et al., *Effects of Different Treatment of Fecal Microbiota Transplantation Techniques on Treatment of Ulcerative Colitis in Rats.* Front Microbiol, 2021. **12**: p. 683234.
549. Chen, Q., et al., *Capsulized Fecal Microbiota Transplantation Induces Remission in Patients with Ulcerative Colitis by Gut Microbial Colonization and Metabolite Regulation.* Microbiol Spectr, 2023. **11**(3): p. e0415222.
550. Qian, X., et al., *Fecal microbiota transplantation combined with prebiotics ameliorates ulcerative colitis in mice.* Future Microbiol, 2023. **18**: p. 1251-1263.
551. El Hage Chehade, N., et al., *Efficacy of Fecal Microbiota Transplantation in the Treatment of Active Ulcerative Colitis: A Systematic Review and Meta-Analysis of Double-Blind Randomized Controlled Trials.* Inflamm Bowel Dis, 2023. **29**(5): p. 808-817.
552. Sokol, H., et al., *Fecal microbiota transplantation to maintain remission in Crohn's disease: a pilot randomized controlled study.* Microbiome, 2020. **8**(1): p. 12.
553. Fehily, S.R., et al., *Fecal microbiota transplantation therapy in Crohn's disease: Systematic review.* J Gastroenterol Hepatol, 2021. **36**(10): p. 2672-2686.
554. Luhrs, H., et al., *Butyrate inhibits NF-kappaB activation in lamina propria macrophages of patients with ulcerative colitis.* Scand J Gastroenterol, 2002. **37**(4): p. 458-66.
555. Facchin, S., et al., *Microbiota changes induced by microencapsulated sodium butyrate in patients with inflammatory bowel disease.* Neurogastroenterol Motil, 2020. **32**(10): p. e13914.
556. Hamer, H.M., et al., *Effect of butyrate enemas on inflammation and antioxidant status in the colonic mucosa of patients with ulcerative colitis in remission.* Clin Nutr, 2010. **29**(6): p. 738-44.
557. Marzocco, S., et al., *Supplementation of Short-Chain Fatty Acid, Sodium Propionate, in Patients on Maintenance Hemodialysis: Beneficial Effects on Inflammatory Parameters and Gut-Derived Uremic Toxins, A Pilot Study (PLAN Study).* J Clin Med, 2018. **7**(10).

558. He, H., et al., *Oridonin is a covalent NLRP3 inhibitor with strong anti-inflammasome activity.* Nat Commun, 2018. **9**(1): p. 2550.
559. Liu, Q.Q., et al., *Oridonin derivative ameliorates experimental colitis by inhibiting activated T-cells and translocation of nuclear factor-kappa B.* J Dig Dis, 2016. **17**(2): p. 104-12.
560. Ortiz-Cerda, T., et al., *Effects of polyphenolic maqui (Aristotelia chilensis) extract on the inhibition of NLRP3 inflammasome and activation of mast cells in a mouse model of Crohn's disease-like colitis.* Front Immunol, 2023. **14**: p. 1229767.
561. Langmead, L., et al., *Randomized, double-blind, placebo-controlled trial of oral aloe vera gel for active ulcerative colitis.* Aliment Pharmacol Ther, 2004. **19**(7): p. 739-47.
562. Vecchi Brumatti, L., et al., *Curcumin and inflammatory bowel disease: potential and limits of innovative treatments.* Molecules, 2014. **19**(12): p. 21127-53.
563. Hanai, H., et al., *Curcumin maintenance therapy for ulcerative colitis: randomized, multicenter, double-blind, placebo-controlled trial.* Clin Gastroenterol Hepatol, 2006. **4**(12): p. 1502-6.
564. Singla, V., et al., *Induction with NCB-02 (curcumin) enema for mild-to-moderate distal ulcerative colitis - a randomized, placebo-controlled, pilot study.* J Crohns Colitis, 2014. **8**(3): p. 208-14.
565. Lang, A., et al., *Curcumin in Combination With Mesalamine Induces Remission in Patients With Mild-to-Moderate Ulcerative Colitis in a Randomized Controlled Trial.* Clin Gastroenterol Hepatol, 2015. **13**(8): p. 1444-9 e1.
566. Hung, H.Y., et al., *Chemical Constituents of Hedyotis diffusa and Their Anti-Inflammatory Bioactivities.* Antioxidants (Basel), 2022. **11**(2).
567. Huo, J., et al., *Structural characterization and anticomplement activity of an acidic polysaccharide from Hedyotis diffusa.* Int J Biol Macromol, 2020. **155**: p. 1553-1560.
568. Yoshida, Y., et al., *Immunomodulating activity of Chinese medicinal herbs and Oldenlandia diffusa in particular.* Int J Immunopharmacol, 1997. **19**(7): p. 359-70.
569. Kim, S.J., et al., *Oldenlandia diffusa Ameliorates Dextran Sulphate Sodium-Induced Colitis Through Inhibition of NF-kappaB Activation.* Am J Chin Med, 2011. **39**(5): p. 957-69.
570. Lim, D.W., et al., *Activation of the Nrf2/HO-1 Pathway by Amomum villosum Extract Suppresses LPS-Induced Oxidative Stress In Vitro and Ex Vivo.* Evid Based Complement Alternat Med, 2020. **2020**: p. 2837853.
571. Blackwell, J., et al., *Prevalence and duration of gastrointestinal symptoms before diagnosis of Inflammatory Bowel Disease and predictors of timely specialist review: a population-based study.* J Crohns Colitis, 2020.
572. Ananthakrishnan, A.N., *Epidemiology and risk factors for IBD.* Nat Rev Gastroenterol Hepatol, 2015. **12**(4): p. 205-17.
573. Rozich, J.J., A. Holmer, and S. Singh, *Effect of Lifestyle Factors on Outcomes in Patients With Inflammatory Bowel Diseases.* Am J Gastroenterol, 2020. **115**(6): p. 832-840.
574. Australia, C.s.C., *State of the Nation in Inflammatory Bowel Disease in Australia*. 2024: Online. p. 1-202.
575. Leppkes, M., et al., *Neutrophils prevent rectal bleeding in ulcerative colitis by peptidyl-arginine deiminase-4-dependent immunothrombosis.* Gut, 2022. **71**(12): p. 2414-2429.
576. Yang, K., et al., *Myocardial reperfusion injury exacerbation due to ALDH2 deficiency is mediated by neutrophil extracellular traps and prevented by leukotriene C4 inhibition.* Eur Heart J, 2024. **45**(18): p. 1662-1680.

577. Gri, G., et al., *CD4+CD25+ regulatory T cells suppress mast cell degranulation and allergic responses through OX40-OX40L interaction.* Immunity, 2008. **29**(5): p. 771-81.
578. Kashyap, M., et al., *Cutting edge: CD4 T cell-mast cell interactions alter IgE receptor expression and signaling.* J Immunol, 2008. **180**(4): p. 2039-43.
579. Suto, H., et al., *Mast cell-associated TNF promotes dendritic cell migration.* J Immunol, 2006. **176**(7): p. 4102-12.
580. Sayed, B.A., et al., *The master switch: the role of mast cells in autoimmunity and tolerance.* Annu Rev Immunol, 2008. **26**: p. 705-39.
581. Dalile, B., et al., *The role of short-chain fatty acids in microbiota-gut-brain communication.* Nat Rev Gastroenterol Hepatol, 2019. **16**(8): p. 461-478.
582. Cummings, J.H., et al., *Short chain fatty acids in human large intestine, portal, hepatic and venous blood.* Gut, 1987. **28**(10): p. 1221-7.
583. Thibault, R., et al., *Butyrate utilization by the colonic mucosa in inflammatory bowel diseases: a transport deficiency.* Inflamm Bowel Dis, 2010. **16**(4): p. 684-95.
584. Chang, C.J., et al., *Ganoderma lucidum reduces obesity in mice by modulating the composition of the gut microbiota.* Nat Commun, 2015. **6**: p. 7489.
585. Shao, S., et al., *A unique polysaccharide from Hericium erinaceus mycelium ameliorates acetic acid-induced ulcerative colitis rats by modulating the composition of the gut microbiota, short chain fatty acids levels and GPR41/43 respectors.* Int Immunopharmacol, 2019. **71**: p. 411-422.
586. Sun, J., et al., *Curcumin protects mice with myasthenia gravis by regulating the gut microbiota, short-chain fatty acids, and the Th17/Treg balance.* Heliyon, 2024. **10**(4): p. e26030.
587. Chassaing, B., et al., *Dextran sulfate sodium (DSS)-induced colitis in mice.* Curr Protoc Immunol, 2014. **104**: p. 15 25 1-15 25 14.
588. Silva, I., et al., *Chronic Experimental Model of TNBS-Induced Colitis to Study Inflammatory Bowel Disease.* Int J Mol Sci, 2022. **23**(9).
589. Dieleman, L.A., et al., *Chronic experimental colitis induced by dextran sulphate sodium (DSS) is characterized by Th1 and Th2 cytokines.* Clin Exp Immunol, 1998. **114**(3): p. 385-91.
590. Peng, S., et al., *Poly(ADP-ribose) polymerase-1 inhibitor ameliorates dextran sulfate sodium-induced colitis in mice by regulating the balance of Th17/Treg cells and inhibiting the NF-kappaB signaling pathway.* Exp Ther Med, 2021. **21**(2): p. 134.
591. Kang, C., et al., *Colon-Targeted Poly(ADP-ribose) Polymerase Inhibitors Synergize Therapeutic Effects of Mesalazine Against Rat Colitis Induced by 2,4-Dinitrobenzenesulfonic Acid.* Pharmaceutics, 2024. **16**(12).
592. Mostafapour, A., et al., *The evaluation of synergistic effects of combination therapy with sulfasalazine and angiotensin-converting enzyme inhibitor in the treatment of experimental colitis in mice %J Physiology and Pharmacology.* 2024. **28**(2): p. 169-179.
593. Rehman, H. and M.I. Ahmad, *COVID-19: quarantine, isolation, and lifestyle diseases.* Arch Physiol Biochem, 2023. **129**(2): p. 434-438.
594. Birimoglu Okuyan, C. and M.A. Begen, *Working from home during the COVID-19 pandemic, its effects on health, and recommendations: The pandemic and beyond.* Perspect Psychiatr Care, 2022. **58**(1): p. 173-179.
595. Pinto, A.J., et al., *Combating physical inactivity during the COVID-19 pandemic.* Nat Rev Rheumatol, 2020. **16**(7): p. 347-348.